Regulation of angiogenic processes in omental endothelial cells during metastasis of epithelial ovarian cancer

Submitted by Md Zahidul Islam Pranjol to the University of Exeter as a thesis for the degree of Doctor of Philosophy in Medical Studies, June 2017

I certify that all material in this thesis which is not my own work has been identified and that no material has previously been submitted and approved for the award of a degree by this or any other University.

Signature: ……

Md Zahidul Islam Pranjol

Abstract

Epithelial ovarian cancer frequently metastasizes to the omentum, a process that requires pro-angiogenic activation of local microvascular endothelial cells (ECs) by tumour-secreted factors. We have previously shown that ovarian cancer cells secrete factors, other than vascular endothelial growth factor (VEGF), with possible roles in metastatic angiogenesis including the lysosomal proteases cathepsin L (CathL) and cathepsin D (CathD), and insulin-like growth factor binding protein 7 (IGFBP7). However, the mechanisms by which these factors may contribute to omental endothelial angiogenic changes are unknown.

Therefore the aims of this thesis were a) to examine disease relevant human omental microvascular endothelial cell (HOMEC) proliferation, migration and angiogenesis tube-formation induced by CathL, CathD and IGFBP7; b) to investigate whether CathL and CathD act via a proteolytic or non-proteolytic mechanism; c) to identify activated downstream intracellular signalling cascades in HOMECs and their activation in proliferation and migration; and finally d) to identify activated cell surface receptors by these factors.

CathL, CathD and IGFBP7 significantly induced proliferation and migration in HOMECs, with CathL and CathD acting in a non-proteolytic manner. Proteome-profiler and ELISA data identified increased phosphorylation of the ERK1/2 and AKT (protein kinase B) pathways in HOMECs in response to these factors. CathL induced HOMEC proliferation and migration via the ERK1/2 pathway, whereas, although CathD-induced proliferation was mediated by activation of ERK1/2, its migratory effect was dependent on both ERK1/2 and AKT pathways. Interestingly, CathL induced secretion of galectin-1 (Gal1) from HOMECs which in turn significantly induced HOMEC proliferation via ERK1/2. However, none of the ERK1/2 or AKT pathways was observed to be active in Gal1-induced HOMEC migration. Interestingly, Gal1-induced proliferation and migration were significantly inhibited by L-glucose, suggesting a role for a receptor with extracellular sugar moieties. IGFBP7-induced migration was shown to be mediated via activation of the ERK1/2 pathway only. CathL, Gal1 and IGFBP7 significantly induced angiogenesis tube-formation in HOMECs which was not observed in CathD-treated cells. Receptor tyrosine kinase array revealed

activation of Tie-1 and VEGF receptor type 2 (VEGFR2) in CathL and IGFBP7-treated HOMECs respectively.

In conclusion, all CathL, CathD, Gal1 and IGFBP7 have the potential to act as proangiogenic factors in the metastasis of ovarian cancer to the omentum. These *in vitro* data suggest all four factors activate intracellular pathways which are involved in well-known angiogenesis models.

CONTENTS

Acknowledgement

I would like to express my deepest gratitude and appreciation to both my supervisors. Sincere thanks to my lead supervisor Dr Jacqueline Whatmore, for her patience, encouragement and intellectual input, without which the completion of this thesis would not have been possible. You have continually conveyed a spirit of adventure in regard to research as a whole. Thank you for encouraging me to keep up with the work with much optimism.

I am extremely grateful to my second supervisor, Dr Nicholas Gutowski, for his insight and opinions on my hypotheses and results over the years. His encouragement, patience and extensive scientific and clinical knowledge has been truly inspirational.

I would also like to extend my appreciation to Mr Michael Hannemann and his surgical team at the Royal Devon and Exeter hospital, who helped with tissue collection, as well as the patients who kindly donated omental tissue, without which the project would not have been possible.

A massive thank you to FORCE Cancer Charity for funding in this research. Their continued funding of medical research makes a vital difference to patients and the public, here in the UK and around the world.

I would also like to thank all my IBCS colleagues and friends for your kindness, friendship and support. Your smiles and spontaneous humour kept me going throughout the research process. Thank you for all the dairy-free baked goods over the years.

Finally, I would to thank my family, particularly my parents and siblings who have given me their unequivocal support throughout, as always, for which my mere expression of thanks cannot equal. Thank you for your patience, positivity and optimism during this endeavour.

List of figures

List of tables

Abbreviations

2D	Two dimensional
3D	Three dimensional
ABC	ATP binding cassette
AGM	Angiomodulin
AKT	Protein kinase B
ALCL	Anaplastic large cell lymphomas
ALK	Anaplastic lymphoma kinase
AMPK	Adenosine monophosphate kinase
Ang	Angiotensin
APE	Girdin/AKT phosphorylation enhancer
ATP	Adenosine trisphosphate
Bad	BCL2-associated agonist of cell death
BCA	Bicinchoninic acid assay
BCL2	B-cell lymphoma 2
BFA	Brefeldin A
bFGF	Basic fibroblast growth factor
BH3	BCL2 homology domain 3
Bid	BH3-interacting domain
BM	Basement membrane
BrdU	Bromodeoxyuridine
BSA	Bovine serum albumin
BTK	Burton's tyrosine kinase
CA125	Ovarian cancer biomarker
CAA	Cancer-associated adipocyte
CAF	Cancer-associated fibroblast
Calcein AM	Calcein acetoxymethyl
CAM	Chick chorioallantoic membrane
CathB	Cathepsin B
CathD	Cathepsin D
CathL	Cathepsin L
CathS	Cathepsin S
CCL	Chemokine (C-C motif) ligand
CD	Cluster of differentiation
CD31	Platelet endothelial cell adhesion molecule
CD105	Endoglin
CD141	Thrombomodulin
CDK	Cyclin-dependant kinase
cDNA	Complementary DNA
CEP	Circulating endothelial precursors
CNS	Central nervous system
COX-2	Cyclooxygenase-2
CRD	Carbohydrate recognition domain
DEPC	Diethyl pyrocarbonate

DMSO	Dimethyl sulfoxide
DSS	Disease-specific survival
DTT	Dithiothreitol
ECM	Extracellular matrix
EC	Endothelial cell
EDTA	Ethylenediaminetetraacetic acid
EE	Early endosome
EGF	Epidermal growth factor
EGFR	Epidermal growth factor receptor
EHS	Engelbreth-Holm-Swarm
ELISA	Enzyme-linked immunosorbent assay
EMT	Epithelial mesenchymal transition
EOC	Epithelial ovarian cancer
EPC	Endothelial progenitor cell
ER	Endoplasmic reticulum
ERK	Extracellular signal–regulated kinases
Ex/Em	Excitation/Emission
FAK	Focal adhesion kinase
FCS	Foetal calf serum
FGF	Fibroblast growth factor
g	Gravitational force
Gal1	Galectin-1
GAPDH	Glyceraldehyde 3-phosphate dehydrogenase
Gas6	Growth arrest-specific protein 6
GBM	Glioblastoma
GDNF	Glial cell line-derived neurotrophic factor
GFLs	GDNF family of ligands
GFP	Green fluorescent protein
GFRα	GDNF family receptor-α
GFs	Growth factors
GIST	Gastrointestinal stromal tumour
GPCRs	G-protein coupled receptors
Grb2	Growth factor receptor bound protein 2
GTPases	Guanosine triphosphatase
HAECs	Human aortic endothelial cells
HBSS	Hank’s balanced salt solution
HCMECs	Human cerebral microvascular endothelial cells
HEPES	4-(2-hydroxyethyl)-1-piperazineethanesulfonic acid
HGF	Hepatocyte growth factor
HIF-1	Hypoxia-inducible factor-1
HMGB1	high mobility group box 1
HOMECs	Human omental microvascular endothelial cells
HRT	Hormone replacement therapy
HUVECs	Human umbilical vein endothelial cells
ICAM1	Intercellular Adhesion Molecule 1
IFN	Interferon

IGF1	Insulin-like growth factor 1
IGFBP	Insulin-like growth factor binding protein
IGFBP-rp1	IGFBP-related protein 1
IgG	Immunoglobulin G
IL	Interleukin
JAK	Janus Kinase
JAM-A	Junctional adhesion molecule-A
JNK	c-Jun N-terminal kinases
LDL	Low-density lipoprotein
LE	Late endosome
LFA1	Lymphocyte function-associated antigen 1
L-glu	L-gluocose
LPA	Lipoprotein A
M6P	Mannose-6-phosphate
M6PR	Mannose-6-phosphate receptor
MAPK	Mitogen-activated protein kinase
MCP1	Monocyte chemotactic protein 1
MEK	mitogen-activated protein kinase kinase
MHC	Major histocompatibility complex
MIP	Macrophage Inflammatory Proteins
MLC	Myosin light-chain
MLCK	Myosin light-chain kinase
MMP	Matrix metalloproteinases
mTOR	Mechanistic target of rapamycin
mTORC2	Mechanistic target of rapamycin protein complex 2
Na_2HPO_4	Sodium phosphate dibasic
ND	Not determined
NFκB	Nuclear factor kappa-light-chain-enhancer of activated B cell
NRP1	Neuropilin 1
PAS	periodic acid-Schiff
PBMCs	Peripheral blood mononuclear cells
PBS	Phosphate-buffered saline
pCathD	Pro-cathepsin D
pCathL	Pro-cathepsin L
PDGF	Platelet-derived growth factor
PDK1	Phosphoinositide-dependent kinase-1
PECAM1, CD31	Platelet endothelial cell adhesion molecule1
pepA	Pepstatin A
PFS	Progression-free survival
PI3K	Phosphatidylinositol-4,5-bisphosphate 3-kinase
PKCα	Protein kinase C alpha
PLCγ	Phospholipase C, gamma
ppCathL	Preprocathepsin L
PSF	Prostacyclin-stimulating factor
PtdIns	Phosphatidylinositol

qRT-PCR	Real-time reverse transcription polymerase chain reaction
RCC	Renal cell carcinoma
rER	Rough endoplasmic reticulum
RSK	Ribosomal s6 kinase
RT2 mice	RIP1-Tag2 mice
RTK	Receptor tyrosine kinase
S473	Serine 743
S536	Serine 536
SD	Standard deviation
SGK3	Serum- and glucocorticoid- inducible protein kinase 3
SLC	Secondary lymphoid tissue chemokine
SMC	Smooth muscle cells
SOS	Son of Sevenless
STAT	Signal transducer and activator of transcription
T185	Tyrosine 185
T202	Tyrosine 202
TAMRA	6-carboxytetramethylrhodamine
tBid	Truncated BH3-interacting domain
TCF	Ternary complex factor
TGF- β1	Transforming growth factor- beta 1
TGN	*Trans* Golgi network
TIMP2	Tissue inhibitor of metalloproteinases
TKIs	Tyrosine kinase inhibitors
TNF-α	Tumour necrosis factor-alpha
TRAIL	TNF-related apoptosis-inducing ligand
VCAM1	Vascular cell adhesion protein 1
VEGF	Vascular endothelial growth factor
VEGFR	Vascular endothelial growth factor receptor
VLA-4	Very late antigen-4
vWF	Von Willebrand factor
WB	Western blot
WST-1	Water soluble tetrazolium salt 1
β2M	Beta 2 microglobulin

Chapter 1 Introduction

1.1 The vasculature

The vascular network consists of three major types of vessels – arteries, veins and capillaries, which are specifically designed to accommodate varying levels of blood flow and pressure. The walls of larger vessels i.e. arteries and veins have three layers: an outer layer (tunica externa) composed of connective tissue, a middle layer (tunica media) composed of smooth muscle and elastic fibres and an innermost layer (tunica intima) composed of endothelial cells (ECs), which rest on a thin sheet of extracellular matrix called the basement membrane (BM) and an internal elastic lamina (absent in veins). The walls of capillaries, the smallest of the blood vessels connecting the arteries and veins, consists of only a single layer of ECs surrounded by a BM (Figure: 1.1).

1.1.1 Microvasculature

Microvasculature refers to the narrowest of blood vessels that distribute blood within tissues. The microcirculation is comprised of arterioles, metarterioles, capillaries and post capillary venules as shown in Figure: 1.2. Capillaries are the smallest blood vessels (8-10 μm diameter) consisting only of tunica intima which, depending on the location, differently regulates permeability. Specialised capillaries in the body include continuous (fenestrated and unfenestrated), and sinusoidal capillaries (Figure: 1.2). Unfenestrated capillaries are found in organs such as the brain where they form an essential component of the blood brain barrier. Continuous, fenestrated capillaries found in exocrine and endocrine glands, gastric and intestinal mucosa, choriocapillaris, and renal glomeruli have fenestrations in ECs that allow greater permeability to water and small solutes but similar permeability to albumin and larger macromolecules compared with unfenestrated capillaries. Discontinuous, sinusoidal capillaries are characterised by fenestrae without diaphragms and poorly organised basement membrane that allow passage of large molecules. These ‘leaky capillaries’ are found in liver, spleen and bone marrow (Aird, 2007a, Aird, 2007b).

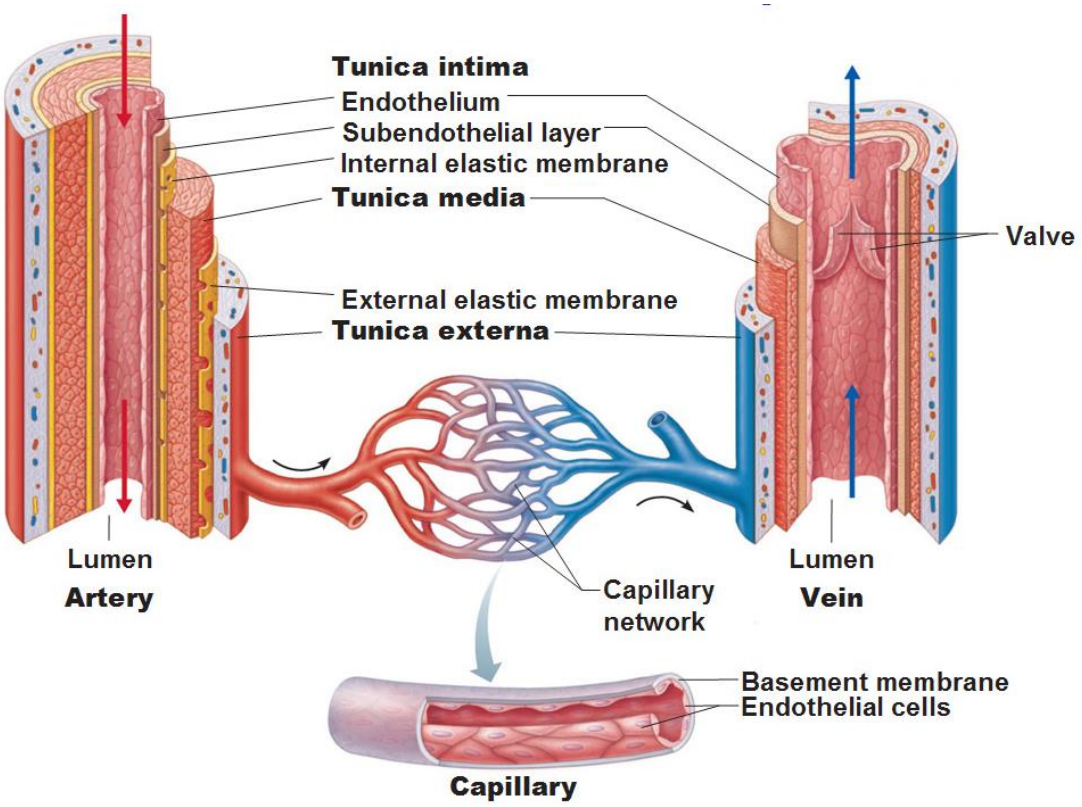

Figure 1.1: **Structural layers of the three main blood vessels**: arteries, veins and capillaries. The walls of arteries and veins consist of an outer layer of connective tissue, a middle layer of smooth muscle and an innermost layer of endothelial cells, while the capillary wall is a one-layer endothelium. Taken from (Mescher, 2010).

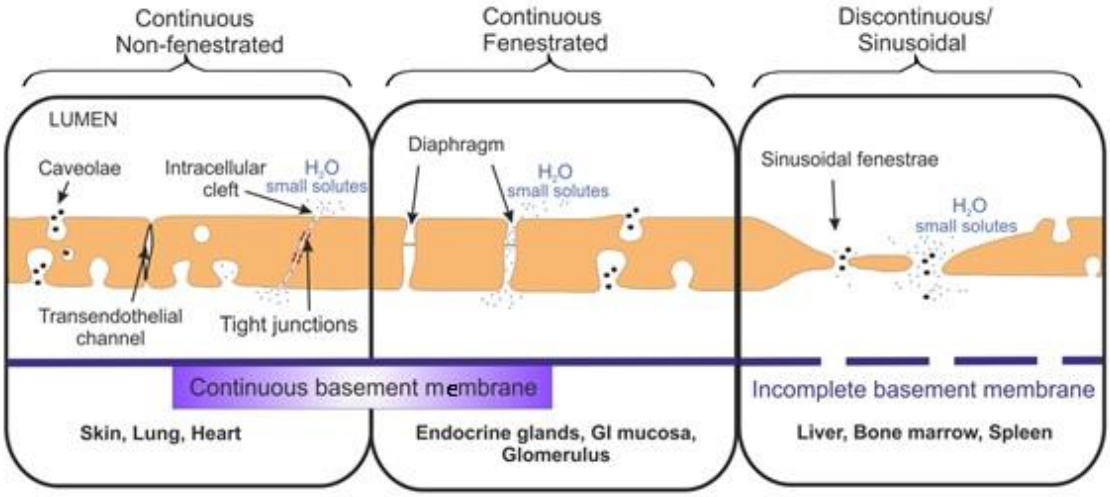

Figure 1.2: **Types of specialised capillaries and their role in regulation of permeability.** Continuous nonfenestrated endothelium is permeable to water and small solutes (molecular radius <3 nm), whereas larger solutes (illustrated as black dots) pass through ECs either via transendothelial channels or transcytosis (mediated mainly by caveolae, typical for capillaries in the heart and skeletal muscle but rare in blood–brain barrier). Continuous fenestrated endothelium is more permeable to water and small solutes with similar permeability to albumin and larger macromolecules compared with its nonfenestrated counterpart (the diaphragms of the fenestrae act as molecular filters). Discontinuous endothelium is highly permeable to water and both small and larger solutes (fenestrae without diaphragms, incomplete basement membrane). Taken from (Aird, 2007a).

1.1.2 Endothelium

An endothelium lines the interior surface of the entire vascular and lymphatic system and is composed of a monolayer of ECs. It is now well-known that vascular ECs are highly metabolically active and play critical roles in physiology and most pathological conditions. Some common functions of ECs are regulation of vascular growth, modulation of leukocyte interactions with the vessel wall at sites of inflammation, maintenance of selective permeability, regulation of vascular tone, production of signalling molecules upon activation and maintenance of thromboresistance (Yang et al., 2008). These functions are organ/tissue specific, giving rise to the concept of heterogeneity. For example, brain capillary ECs create a tight blood-brain barrier in order to selectively regulate entry of macromolecules, antibodies, non-specific drugs and other toxic products. On the other hand, glomerular ECs form a semi-permeable barrier, enabling filtration of components to be excreted. In disease states the microvascular ECs play critical roles. For instance, in inflammatory conditions, activated ECs in post-capillary venules express specific adhesion molecules that aid rolling/tethering of leukocytes to facilitate their entry to the inflamed tissue via transcellular/paracellular migration pathways. Also, during tumour growth, pro-angiogenic and pro-inflammatory factors activate ECs to rapidly proliferate and form new blood vessels from the existing ones, in a process called neo-angiogenesis. This process alters the normal EC physiology which is a quiescent and proliferatively inactive state with a long life span (0.1% replications per day) (Cines et al., 1998).

1.1.2.1 Microvascular EC function

Regulation of vascular tone and growth

Vascular ECs play an important role in regulating vascular tone. Endothelium-derived nitric oxide and prostacyclin are released in response to physical stimuli, hormones, and platelet-derived substances. These stimuli have several effects on the vascular tone such as vasorelaxation, hyperpolarisation of smooth muscle cells and inhibition of platelet function (Rajendran et al., 2013). In addition, ECs can release several contraction-inducing factors (e.g., endothelin, thromboxane

A2, angiotensin (Ang) II, superoxide, and unidentified endothelium-derived contraction-inducing factors), at least under certain conditions. ECs are also a source of growth inhibitors and promoters, such as heparin and heparin sulphates, platelet-derived growth factor, and thrombospondin (Rajendran et al., 2013). Several vasoactive substances are also produced by the endothelium, such as nitric oxide, endothelin, and angiopoetin-2 (Ang2) that may also play a role in the regulation of vascular growth. Thus, the endothelial layer can regulate vascular tone and growth. Dysfunction of these endothelium-dependent regulatory mechanisms may contribute to cardiovascular diseases, such as hypertension and atherosclerosis (Barton et al., 2012).

Thrombosis, thrombolysis and coagulant mechanism

The endothelium serves an integral role in the haemostatic system. Depending on specific tissue needs and local stresses, ECs are capable of evoking either antithrombotic or prothrombotic events. Under normal physiological conditions, ECs prevent thrombosis by means of different anticoagulant and antiplatelet mechanisms (Stern et al., 1991). These cells are involved in all main haemostatic pathways triggered upon vascular injury and limit clot formation to the areas where haemostasis is needed to restore vascular integrity. One important way in which ECs control the clotting system is by regulating the expression of binding sites for anticoagulant and procoagulant factors on the cell surface. In a quiescent state, ECs maintain blood fluidity by promoting the activity of numerous anticoagulant pathways, including the protein C/protein S pathway (Rajendran et al., 2013). Once activated (discussed below) by cytokines, the balance of EC properties can be tipped in favour for clot formation through a coordinated and regulated induction of procoagulant and suppression of anticoagulant mechanisms. For example, tumour necrosis factor-α (TNF-α) suppresses the formation of thrombomodulin, an endothelial anticoagulant cofactor, and induces the expression of tissue factor (procoagulant cofactor) (Yau et al., 2015). This coordinated mechanism can allow fibrin formation to proceed in an inflamed focus whilst maintaining blood fluidity in the surrounding area of normal vasculature. However, a dysfunctional endothelium can induce a disturbance in the complex balance of pro- and anti-coagulation mechanism, resulting in atherogenesis and

predisposition to arterial thrombosis (Rajendran et al., 2013). Thus, ECs play a significant role in the haemostatic and coagulation system.

Platelet and leukocyte interaction

The concept of “rolling” of blood cells along the endothelium surface was first described more than 160 years ago, when leukocytes were shown to adhere to blood vessel walls- a key interaction during a pro-inflammatory response (de Gaetano et al., 2003). Platelet adhesion to and leukocyte rolling on the endothelium represent the initial stage of a multistep process leading to extravasation of white blood cells to sites of inflammation or infection, to platelet-leukocyte interaction and aggregation on a thrombogenic surface, and finally to vascular occlusion (Rajendran et al., 2013). During inflammation, leukocytes are recruited from the vasculature to a site of tissue injury through a sequence of adhesion and activation events. On arrival, leukocytes transiently adhere to the EC surface, which is mediated by the rapid and reversible interactions of selectins such as E- and P-selectin (present on ECs) with their corresponding carbohydrate ligands such as α, β-integrins and L-selectins (found on leukocytes) (Gout et al., 2008). The flow of blood in the vessels pushes along the loosely tethered leukocytes, causing them to roll along the endothelium. The rolling movement stimulates the leukocytes by eliciting the release of chemokines. This induces the expression of other adhesion molecules such as integrins and immunoglobulins, whose interactions consequently lead to the reinforcement and stabilisation of the initial adhesive bonds (Brooks et al., 2010). For instance, an increased expression of intercellular adhesion molecule 1 (ICAM1) and vascular cell adhesion molecule 1 (VCAM1) on the EC surface which interact with lymphocyte function-associated antigen 1 (LFA1) and very late antigen 4 (VLA-4) respectively, which are expressed on leukocytes. This firm adhesion is followed by transendothelial migration via a number of cell adhesion molecules, allowing entry of leukocytes to the site of inflammation or infection (Muller, 2011).

Angiogenesis

The endothelium is also involved in blood vessel formation. The production and development of new functional blood vessels from existing ones is known as

angiogenesis (discussed below). The development of a functional vascular network requires a remarkable degree of coordination between different cell types undergoing complex changes and is exquisitely dependent upon signals exchanged between these cell types. Growth factors such as vascular endothelial growth factor (VEGF), Ang, platelet-derived growth factors (PDGF) and basic fibroblast growth factor (bFGF) are some key proangiogenic factors (Apte et al., 2004). Angiogenesis is a key phenomenon in embryogenesis and also plays important role in disease progression, such as tumour metastasis.

1.1.2.2 Vascular EC heterogeneity

It is now widely accepted that ECs vary functionally, proteomically and morphologically. This heterogeneity (specialised to a particular site arises from the variations in the biochemical and biomechanical properties of their local microenvironment. Therefore, it is important to use disease-site specific ECs when investigating their role in pathogenesis. This section briefly describes the level of heterogeneity that exists in ECs from different vascular beds and their physiological and pathological relevance.

Markers

Although anatomically ECs represent the inner layer of the vessels, their characteristic ultrastructural features such as Weibel-Palade bodies or fenestrae, vary. ECs arise from the same precursor as haemapoetic cells, a blast-like bipotential cell, the haemangioblast, and hence share frequent molecular markers. However, other cell lineages may transdifferentiate into ECs, and ECs into other lineages. The expression of EC markers is determined by the local microenvironment and the location of activated vascular beds. Furthermore, this heterogeneity is also observed between different organs, vessels of differing sizes (macro- and micro-vascular) and between ECs of various vascular beds within the same organ, as well as within the same vessel (Muller et al., 2002).

Despite this enormous variance, there are few protein/mRNA markers that are both specifically and uniformly expressed on all human vascular endothelium, such as platelet endothelial cell adhesion molecule 1 (PECAM1, CD31), vascular

endothelial cadherin (VE-cadherin), thrombomodulin (CD141) and vascular endothelial growth factor receptor 2 (VEGFR2). Other markers (e.g. VCAM1, ICAM1, Tie-2 and eNOS) are differentially expressed and their expression solely depends on pathogenesis, tumour angiogenesis, site and type of organs and also, varying sizes of vessels.

Morphology

ECs display differing morphologies depending on the tissue –specific vascular beds, shear stress and direction of blood flow and requirements of the underlying tissues. A typical EC is characterised by a flat morphology; however, they are plump or cuboidal in high endothelial venules. Their thickness also varies from less than 0.1µm in capillaries and veins to 1µm in the aorta. In the arteries (not at the branch points) the cells and their nuclei are aligned in straight segments in the direction of the blood flow, representing a reversible endothelial structural remodelling in response to haemodynamic shear stress, reviewed in (Aird, 2007a).

Tight junctions and adhesive proteins

There are highly specialised cellular structures such as intracellular junctions in the endothelium that regulate transfer of molecules from luminal to abluminal space and vice-versa, and also maintain different functions of vascular homeostasis. These dynamic structures can be divided into tight junctions, adherens junctions and gap junctions (Aird, 2007a).

Tight junctions: A unique structure mainly composed of junctional adhesion molecule A (JAM-A), occludin and claudins forming a transport barrier between ECs to regulate paracellular permeability and to maintain cell polarity between luminal and abluminal side of the endothelium, reviewed in (Bazzoni and Dejana, 2004, van Buul et al., 2004).

Adherens junctions: These are key structures in ECs for the maintenance of cell-specific properties, such as permeability to solutes or circulating inflammatory cells (leukocytes), contact inhibition of cell growth, and apoptosis. The molecular

organisation of adherens junctions are complex and include both adhesive and signalling molecules. The predominant transmembrane protein is VE-cadherin that is found in all ECs in all types of vascular beds. VE-cadherin has been shown to interact with endothelial-specific signalling proteins by binding to VEGFR2 and aid modulation of signalling cascade through phosphatidylinositol 3-kinase (PI3K), reviewed in (Bazzoni and Dejana, 2004).

Gap junctions: These structures consist of tightly packed clusters of channels at the plasma membrane of one cell that interacts with a matched set of channels in an opposing cell, effectively connecting the cytoplasms of the two cells. The sets of proteins that make up gap junctions are called connexins, which allow transfer of ions, simple sugars, amino acids, nucleotides, short polypeptides, and second messengers between cells. Phosphorylation of specific connexins such as Cx43, has been shown to affect endothelial biology through both gap-junction dependent and independent means, reviewed in (Marquez-Rosado et al., 2012).

The endothelial junctions are organised in a diverse manner along the vascular tree depending on tissue-specific requirements. The brain, for instance, is a very immune privileged organ that requires a strict control of permeability between blood and the nervous system. Hence, the junctions are well developed and are rich in tight junctions. In large arteries, where maintenance of permeability during high pressure and pulsatile blood flow is required, the tight junctions are well developed. In contrast, post-capillary venules, which are involved in trafficking of leukocytes and plasma proteins to the site of inflammation (discussed above), display poorly organised tight junctions. This morphology may account for the high sensitivity of post-capillary venules to permeability-increasing agents such as histamine and bradykinin, which are pathologically relevant in causing septic shock.

1.1.2.3 Activation of ECs

Although vascular ECs vary functionally, proteomically and morphologically, activation of these cells is essential for eliciting a response within the local microenvironment. ECs remain proliferatively quiescent in normal physiology.

However, in some conditions these cells are activated, which may contribute to a number of pathogenic states, including tumour development and metastasis.
Activation of ECs is necessary to initiate the process of angiogenesis. As described above EC activation can take place during the inflammatory response and tumour angiogenesis. It is well established that tumours interact with neighbouring vasculature, tissues and cells by secreting molecules that encourage tumour growth and metastasis. When a tumour reaches 2-3 mm^3, it requires an increased supply of oxygen and essential nutrients. This induces an angiogenic switch in order to initiate new blood vessels and progress into the angiogenic stage, allowing the tumour to grow and effectively establish secondary foci and further metastases. Secretion of pro-angiogenic factors, such as VEGF, bFGF, PDGF and interleukin 8 (IL8) by cancer cells activates cognate receptors on ECs transducing multiple signals downstream. For instance, VEGF increases vascular permeability that leads to extravasation of plasma proteins (fibrinogen and other clotting factors), which in turn activate tissue factor (procoagulant expressed by many cells, including tumour cells) generating thrombin and contributing to the stromal matrix creation found in tumours, healing wounds and inflammation, reviewed in (Dvorak, 2005). Local degradation of the vascular basement membrane, necessary to capillary formation, is achieved by VEGF-induced activity of endothelial proteases, reviewed in (Brown et al., 1997, Ferrara, 2002). The breakdown of extracellular matrix is followed with EC migration and proliferation, and homing of newly sprouting vessels.

Angiogenesis plays a key role in tumour metastasis. It has been shown that patients with highly angiogenic tumours, such as bladder cancer, are associated with poor prognosis (Papadopoulos et al., 2004). Although angiogenesis is a common phenomenon in both physiology (embryology) and pathology, the development of new blood vessels vary depending on the type of organ and disease. Therefore, it is important to recognise the different types of angiogenesis in the body.

1.2 Different types of angiogenesis

In tumours the angiogenic switch is initiated by the tumour resulting in EC activation (mediated by interactions of secreted potent angiogenic factors on

ECs) leading to new vessel formation. For many years, tumour angiogenesis (sprouting angiogenesis) was considered to be the main mechanism of tumour vascularisation (Figure 1.3). Briefly, the process of sprouting angiogenesis consists of enzymatic degradation of capillary basement membrane containing extracellular matrix (ECM), EC proliferation and directed migrations, tube formation, vessel fusion, vessel pruning, and pericyte stabilisation. Specifically, in poorly perfused tissues, hypoxia is induced which results in an increased demand for new blood vessel formation to meet the metabolic requirements of local cells (Hanahan and Weinberg, 2000). Tumour secreted factors such as VEGF activate endothelial tip cells that guide the developing capillary sprout through the ECM towards an angiogenic stimulus (Gerhardt, 2008). Long, thin cellular processes on tip cells called filopodia secrete large amounts of proteolytic enzymes, which digest a pathway through the ECM for the developing sprout (Small et al., 2002). The filopodia of tip cells are heavily endowed with VEGFR2, allowing them to "sense" differences in VEGF-A concentrations and causing them to align with the VEGF-A gradient (van Hinsbergh and Koolwijk, 2008). Meanwhile, endothelial stalk cells proliferate as they follow behind a tip cell causing elongation of the capillary sprout (Blanco and Gerhardt, 2013). Vacuoles develop and coalesce, forming a lumen within a series of stalk cells. These stalk cells become the trunk of the newly formed capillary (Adair and Montani, 2010). When the tip cells of two or more capillary sprouts converge at the source of VEGF-A secretion, the tip cells fuse together creating a continuous lumen through which oxygenated blood can flow. When the local tissues receive adequate amounts of oxygen, VEGF-A levels return to near normal (Adair and Montani, 2010). Pericytes surrounding the ECs induce maturation and stabilisation of the capillary. These process are also accompanied by deposition of ECM along with shear stress and other mechanical signals (Chien, 2007).

Although sprouting angiogenesis is well-known in tumour progression, recently, additional mechanisms have been recognised that strengthen the number of possible ways that a tumour can achieve survival (Figure 1.3). These include intussusceptive angiogenesis, angioblast recruitment, cooption, mosaic vessels and vasculogenic mimicry, reviewed in (Auguste et al., 2005), which are described below in greater detail.

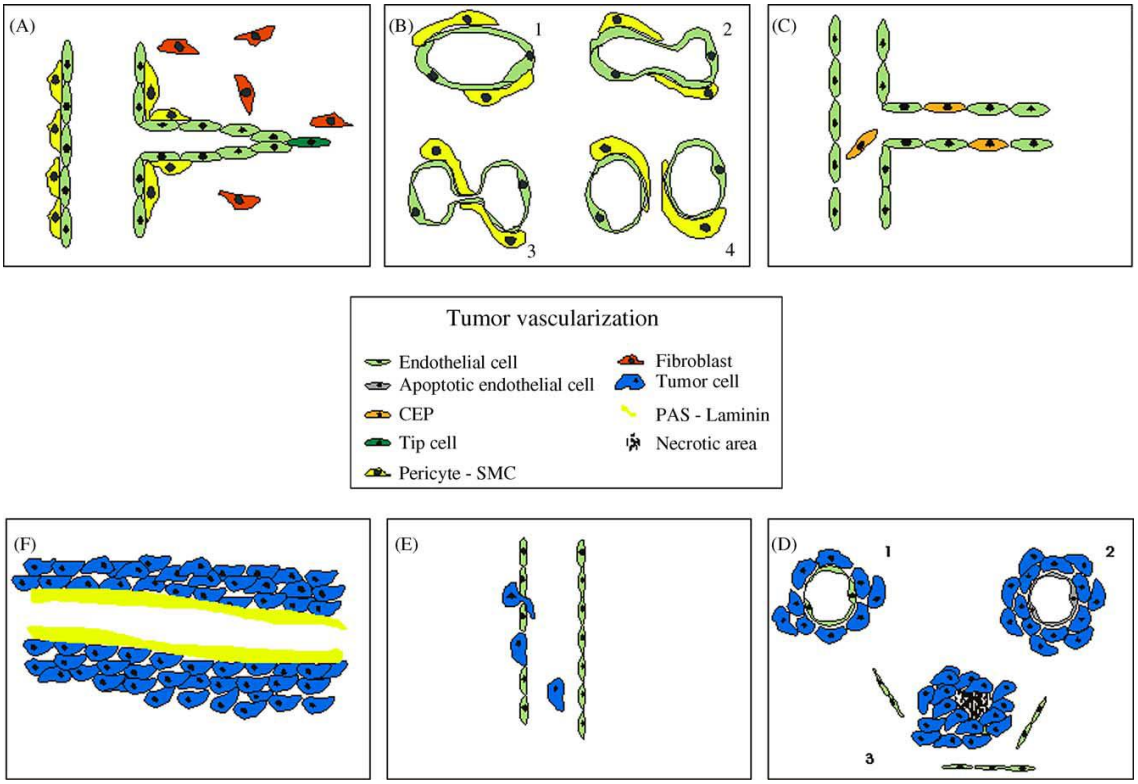

Figure 1.3: **Mechanisms of tumour vascularisation**. The different mechanisms of tumour vascularisation are depicted. These include: (A) sprouting angiogenesis; (B) intussusception; (C) recruitment of circulating endothelial precursors (CEP); (D) cooption; (E) mosaic vessels; (F) vascular mimicry-periodic acid-Schiff (PAS) and laminin network development. Taken from (Auguste et al., 2005)

Intussusceptive angiogenesis occurs when interstitial tissue folding in from the vessel wall induces the partition of the vessel lumen. The intussusception incorporates the process of EC membrane “kissing”, during which intra-EC junctions are created, allowing two membranes to be thinned and finally two separated vessels to be formed (Burri et al., 2004). This mechanism was firstly described as occurring primarily during lung development, and has now been found in most organs, and also occurs in tissue repair and tumour angiogenesis.

Angioblasts, multipotent progenitor cells found in adults with characteristics close to both the hematopoietic and EC lineage, can be stimulated by VEGF-A to differentiate into ECs *in vitro*, reviewed in (Moore, 2002). It has been shown that VEGF responsive hematopoietic stem and progenitor cells are recruited to the tumour vasculature and may act as endothelial precursors and become incorporated into the endothelium (Lyden et al., 2001).

Cooption was first described by Holash *et al.* in brain tumours, where cancer cells surrounding the host vasculature create coopted vessels (Holash et al., 1999). In these vessels ECs produce both Ang2 and its receptor Tie2, inhibiting angiostatin-1 and inducing EC apoptosis. Therefore, the number of vessels is reduced with time. In surviving vessels the diameter is enlarged and the progressing hypoxia upregulates VEGF-A secretion that causes robust angiogenesis at the tumour margin (Holash et al., 1999).

The process of mosaic blood vessel creation was described by Chang *et al.* and depends on intravasation of cancer cells into the capillary vessel wall, where they temporarily stay (with preservation of the vascular function) (Holash et al., 1999, Chang et al., 2000).

Vasculogenic mimicry has been primarily described in aggressive uveal melanoma (Maniotis et al., 1999). It has been shown that an absence of ECs within the tumour is compensated for by a system of “vascular channels” created by cancer cells laid on a thin basal lamina with circulating blood cells inside. Vasculogenic mimicry has also been observed in other cancer types, including ovarian cancer (Sood et al., 2001, Passalidou et al., 2002). Mechanisms of

tumour vascularisation together with factors regulating these mechanisms are shown in Figure 1.3.

One tumour type where metastasis significantly impacts on survival of patients is epithelial ovarian cancer (EOC). The nature of its aggressiveness while metastasising to secondary organs and the lack of availability and efficiency of anti-tumour therapy has highlighted an importance for development of novel treatment targets. Hence, understanding this process in the metastasis of EOC, specifically angiogenesis, is the main focus of this study. Below are sections where the epidemiology and risk factors, along with the metastatic cascade of this disease is discussed.

1.3 Epidemiology of epithelial ovarian cancer (EOC)

EOC is the fifth most common cancer among women and the leading cause of gynaecological cancer death in the UK. Globally, incidence of this disease is highest in the developed countries of Europe and North America with decreasing trends in Africa and Asia. Each year more than 6,500 women are diagnosed with ovarian cancer in the UK and about 4,400 women die of the disease (Doufekas and Olaitan, 2014). Incidence in England and Wales has increased gradually since the early 1970s, especially in older women (Coleman et al., 1993), whereas the ascending trend in younger women reached its peak by the late 1990s. In most cases (80%-90%), ovarian cancer occurs after the age of 40 with a plateau at the age of 60. However, this type of carcinoma remains relatively rare in premenopausal women with only 10% of cases arising under the age of 45. Although the ideal therapy of primary cytoreductive surgery and combination chemotherapy with platinum has improved the prognosis of patients with malignant ovarian cancer, the 5-year survival rate remains ~45%. It is the most lethal of all gynaecological cancers due to non-specific initial symptoms, and as a result, around 75% women present with advanced stage of the disease at diagnosis.

1.3.1 Risk factors

The exact aetiology of ovarian cancer remains uncertain and is the subject of current research. Some geographical and race variation exists (Ushijima, 2009, Ferlay et al., 2010). However, tumour types appear to share major common risk factors irrespective of geographical or racial factors (Purdie et al., 2003). Theories about causes focus on continual ovulation, excessive gonadotropin secretion, and oestrogen and progestogen imbalance (Riman et al., 2004b). But none are certain and no effective screening tools are currently available in clinical practice. However, the most current theories associated with EOC pathogenesis are as follows:

Hereditary

A significant family history, where two or more cases of ovarian or breast cancer have been diagnosed at an early stage in first-degree relatives, has been linked to the development of hereditary ovarian malignancy (Whittemore et al., 2004, Kauff et al., 2008). Approximately 5–15% of ovarian carcinomas occur in women known to carry mutations of the tumour suppressant genes BRCA1 and BRCA2 (breast cancer genes) (Gayther and Pharoah, 2010). Women with a family history of either breast or ovarian cancer, and a known BRCA mutation, are estimated to have a lifetime risk of developing ovarian cancer of approximately 40–50%, compared with a 2% risk in the general UK population (Kauff et al., 2008, Watson et al., 2008). However, not all women with known BRCA mutations go on to develop malignant disease. Equally, BRCA mutations do not account for all ovarian cancers diagnosed in women with a known family history (McLaughlin et al., 2007). Further research into the role of gene mutations may benefit women at risk of hereditary ovarian cancer and facilitate informed choice for women considering prophylactic oophorectomy (surgical ovary removal) to prevent ovarian disease. Genetic mutations contributing to the development of ovarian tumours can also be acquired throughout life. Known as somatic mutations, these have been observed in epithelial ovarian tumours and include mutations in other tumour suppressor genes and cell-signalling genes, which lead to chromosomal instability (Hennessy et al., 2009).

Reproductive factors

Reproductive history influences ovarian cancer risk and is related to factors that affect a woman's exposure to oestrogen and progesterone, the hormones produced by the ovaries (Riman et al., 2004b, Sueblinvong and Carney, 2009). Early age at menarche and late age at menopause increase the risk of ovarian cancer only modestly, so that it can be assumed that the length of menstrual life plays no crucial role in the pathogenesis of this disease. However, factors that reduce ovulation such as increasing parity, oral contraceptives and breastfeeding are associated with lower ovarian cancer risk (Salehi et al., 2008, Hennessy et al., 2009). Pregnancy appears to have a protective effect, with an associated risk reduction with each birth (Kurian et al., 2005, Pasalich et al., 2013). Conversely, factors associated with increased ovarian activity, such as null parity (never having children) or infertility, appear to increase the risk (Tworoger et al., 2007) (Jensen et al., 2009).

Oral contraceptives

Women taking oral contraceptives for five or more years appear to have a 50% reduction in ovarian cancer risk compared with women who have never used this method of contraception (Riman et al., 2004a, Pasalich et al., 2013). The risk reduction is already apparent after a few months of use and persists for years after discontinuation. However, insufficient evidence exists to determine whether oral contraception influences risk in women who are carriers of BRCA1 or BRCA2 mutations (Whittemore et al., 2004).

Hormone replacement therapy (HRT)

The evidence that HRT may increase risk of this disease remains inconsistent. Several recent studies revealed a small increase of the risk, especially for long-term users of oestrogen replacement therapies (Daniilidis and Karagiannis, 2007). However, short-term and past use of HRT for the relief of menopausal symptoms appears unlikely to increase ovarian cancer risk (Beral et al., 2007). Intermittent rather than continuously added progestins might further increase the risk (Cramer et al., 2001). However, other studies have recorded an increased

risk of approximately 50% in HRT users compared with non-HRT users, with risks increasing further in long-term use of five years or more (Riman et al., 2004b).

1.4 Introduction to EOC metastasis

The potential sites of origin of high grade serous carcinomas (high mitotic grade) are the ovarian surface epithelium, the fallopian tube epithelium and the mesothelium covering the surface of the peritoneal cavity. As this thesis investigates factors secreted by ovarian epithelial cancer cells and their effects on omental microvascular ECs, the metastasis cascades from the ovarian surface to the omentum will be discussed in the following sections.

The metastasis process starts at the primary tumour- from detachment of tumour cells to their arrival and establishment in the secondary site, usually the omentum or other organs within the peritoneum. Thus, the omentum, its structure and the establishment of the secondary tumour foci and further tumour invasion process will be discussed in the following section.

1.4.1 Omentum: Structure, physiology/pathology

The omentum is a flap of adipose tissue that forms a sac within the peritoneum. It has two sections- greater omentum and lesser omentum. Anatomically the greater omentum hangs from the greater curvature of the stomach like an apron, covering the intestines. The lesser omentum extends from the liver to the lesser curvature of the stomach and the first part of the duodenum (Platell et al., 2000). It is the greater omentum, also commonly referred to as the omentum, which homes ovarian cancer cells and allows invasion and further metastasis.

Metastases of primary epithelial tumours of the ovaries as well as the stomach and colon are known to spread to the omentum very extensively. Direct seeding of epithelial ovarian malignant cells onto the highly vascularised omentum characterises metastatic disease (advanced) and is associated with a poor survival prognosis. The ultrastructure of the omentum comprises two mesothelial layers surrounding the adipose tissue and loose connective tissue. The adipose region of the omentum contains so-called “milky spots”, which contain a dense

capillary network accompanied by an accumulation of immune cells (macrophages, B and T cells). These sites (in mice) are characterised by a discontinuous layer of mesothelium allowing direct contact of the vascular beds with the peritoneal cavity (Cui et al., 2002).

The omental “milky spots” play a role in the clearance of bacteria and debris, and provide a niche for the origination and maturation of peritoneal macrophages (Mandache et al., 1985, Van Vugt et al., 1996). In response to external stimuli (such as inflammation, foreign material) the omental tissue in these areas can adhere to and enclose the pathological insult. This induces local activation of omental tissue, with increased local omental blood flow, production of multipotent stem cells and secretion of various inflammatory and growth factors, such as VEGF and bFGF (Zhang et al., 1997, Bikfalvi et al., 1990). Indeed, in an experimental wound model it has been shown that the expression of bFGF (macrophages, fibroblasts, and ECs) and transforming growth factor beta 1 (TGF-β1) (macrophages) from the omentum promoted wound healing (gastric ulcers) by inducing bFGF mediated angiogenesis and TGF-β1 mediated collagen production (Matoba et al., 1996). Interestingly, although milky spots are filled with active immune cells, it is not known how tumour cells escape the potent immune response. It was thought that, tumour cells undergo differentiation at the milky spots, expressing a variation of antigens on their cell surface membranes (Dunn et al., 2002). Already differentiated and activated immune cells target only a specific variant or a group of variants of antigens on tumour cells, killing a small number of tumour cells. However, newly differentiated tumour cells retain the potency to proliferate, and therefore, these cells form micro-metastases within the milky spots and evade the immune response (Oosterling et al., 2006). This allows the tumour cells to metastasise further in the omentum.

It is important to note that, these immune cells secrete both pro- and anti-inflammatory factors, where the balance is “tipped” towards a pro-inflammatory reservoir. Interestingly, immune cell-secreted growth factors VEGF and bFGF have also been shown to be highly proangiogenic, which explains the highly vascularised milky spots, aiding active metastasis via angiogenesis. The metastatic cascade is discussed below in two phases- early phase and late phase metastasis.

1.4.2 Early phase metastasis

The ovarian surface epithelium is a single layer of cells covering the ovary, derived from the coelomic epithelium. Approximately 90% of human ovarian cancers are thought to originate from the epithelium (Ahmed et al., 2007). Before ovarian cancer cells detach and initiate the metastasis cascade, they gain resistance to anoikis (a process of apoptosis when cells lose their cell-to-matrix interactions), followed by an epithelium-to-mesenchymal (EMT) transition (Lengyel, 2010). This weakens the attachment of epithelial cells to the basement membrane and loosens the intercellular adhesions between the cancer cells. During EMT, cancerous epithelial cells lose E-cadherin-mediated-cell-cell interactions, and upregulate other cadherins such as N-cadherin and P-cadherin, as part of a global “cadherin switch” (Lengyel, 2010). E-cadherin, a membrane glycoprotein located at cell adherens junctions, connects through α and β-catenin to the actin microfilaments within the cytoplasm, thereby anchoring epithelial cells to each other. In cancerous cells, E-cadherin is cleaved off by matrix metalloproteinase (MMP)-9, induced by cancer cells, contributing to the loosening of cell-cell adhesion and allowing the transformed cells to shed as single cells or spheroids into ascites (abnormal accumulation of fluid within the peritoneum). Also, active MMP1, a transmembrane protease, cleaves α3-integrin, contributing to the detachment of the spheroid from the primary tumour, reviewed in (van Zijl et al., 2011, Pranjol et al., 2015).

With reduced levels of E-cadherins, the transformed cells appear as fibroblasts, acquiring an invasive phenotype with enhanced cellular proliferation (Lengyel, 2010). It has been shown that EOC cells with low E-cadherin expression are more invasive and the absence of E-cadherin expression in ovarian cancer predicts poor patient survival (Lengyel, 2010). Detached cancer cells, with a decrease in expressed E-cadherin, increase upregulation of the fibronectin receptor, α5β1 integrin, α6β1 integrin (binds laminin) and α2β1 integrin (binds type IV collagen), facilitating the adhesion of ovarian cancer cells to the secondary site. These cells spread to the secondary sites within the peritoneum, including the omentum, carried by the physiological movement of peritoneal fluid, reviewed in (Lengyel, 2010). A schematic diagram of omental metastasis is shown in figure 1.4.

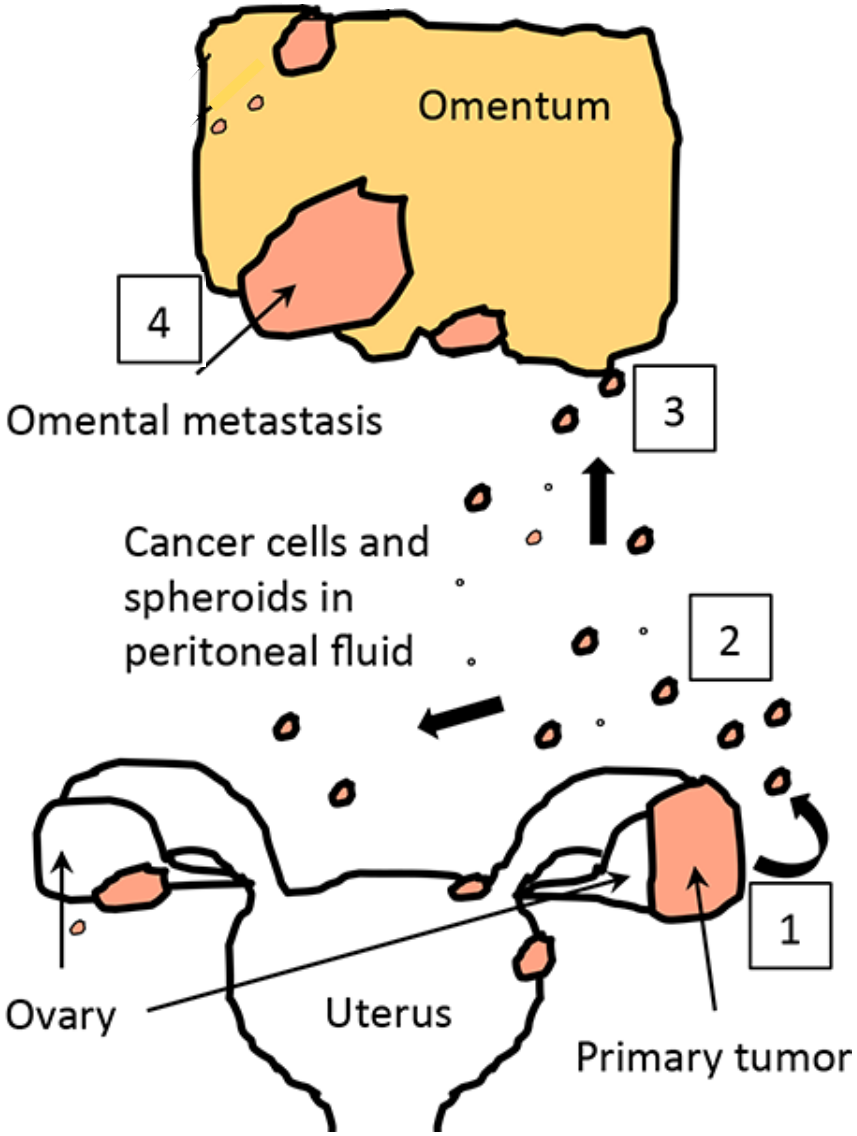

Figure 1.4: **Mechanisms of ovarian cancer metastasis**: Transcoelomic dissemination. (1) The cancer cells loose cell–cell contact and exfoliate into the peritoneal cavity. (2) They float in the peritoneal fluid and are carried all over the peritoneal cavity. (3) Attachment to the peritoneal organs such as the omentum. (4) Formation of the metastatic tumour.

Once at the secondary site (the omentum), disseminated cancer cells interact with the mesothelial cells covering the basement membrane. β1 integrins have been identified as important mediators of this adhesion to the mesothelium. This integrin has been shown to dimerise with different types of α integrin subunits, thus aiding this attachment (Lengyel, 2010). Another important adhesion receptor VCAM1 is present on mesothelial cells and binds to α4β1 integrin on ovarian cancer cells. Neutralising antibodies directed against VCAM1 and β1 integrin blocked this migration and metastasis in a xenograft model (Lengyel, 2010). Other lesser characterised adhesion factors that may influence this attachment between ovarian cancer cells and the mesothelium are the vitronectin receptor (αvβ3 integrin) and CD44 (surface receptor for hyaluronic acid). These factors are currently under investigation for their roles in ovarian cancer metastasis, reviewed in (Lengyel, 2010).

Once attached to mesothelial cells, migrant cancer cells upregulate MMP2, promoting cleavage of the extracellular matrix proteins fibronectin and vitronectin into smaller fragments. The cancer cells adhere more strongly to these smaller fragments, using the fibronectin (α5β1) and vitronectin (αvβ3) receptors. Interestingly, MMP9 also plays a key role in the metastatic process by aiding angiogenesis and tumour growth as shown in mice lacking the MMP9 gene which had impaired angiogenesis and reduced tumour growth, reviewed in (Pranjol et al., 2015, Lengyel, 2010).

1.4.3 Late phase metastasis

Early metastasis is well-coordinated via adhesion and proteolysis, which provides a niche for EOCs to establish secondary foci in the omentum by invading the basement membrane- initiating late phase of the metastatic cascade. Although early metastasis is very well studied because of the availability of appropriate models, less is known about what happens after the ovarian cancer cells have implanted. In order for the secondary tumour to grow and survive, a microenvironment is created by cancer and surrounding cells such as fibroblasts, mesothelial cells, adipocytes and monocytes. A number of factors are secreted by these cells into the microenvironment which influence tumour cell implantation, proliferation and chemoresistance acquisition, are briefly discussed below.

Fibroblasts

Ovarian cancer cells stimulate the secretion of urokinase-type plasminogen activator in fibroblasts, by releasing fibroblast growth factor 2 (FGF2), heparin-binding EGF-like growth factor, hepatocyte growth factor (HGF), insulin-like growth factor 1 (IGF1), IL1α, pro-matrix metalloproteinases 2 (pro-MMP2) and tissue inhibitor of metalloproteinase 2 (TIMP2) (Noskova et al., 2009). proMMP-2 is activated by a membrane bound metalloproteinase which then results in the degradation of ECM, allowing the invasion of ovarian cancer cells. Fibroblasts in the omentum are able to enhance ovarian cancer cell adhesion and invasion into the omentum by cell-cell contact through a complex cross talk between the expressions of the aforementioned secreted factors and activation of MMP2, reviewed in (Thibault et al., 2014).

Mesothelial cells

Mesothelial cells line the peritoneal cavity and its organs including the omentum. The major known role of these cells is to express ECM proteins and adhesion molecules such as hyaluronan which promotes ovarian cancer cell adhesion to the omentum via CD44 (Thibault et al., 2014). Mesothelial cells are also able to secrete pro-tumoural factor IL6, and pro-proliferative and proangiogenic factor bFGF. In addition, mesothelial cells constitutively produce lysophosphatidic acid (LPA) that enhances adhesion, migration and invasion of ovarian cancer cells, reviewed in (Thibault et al., 2014).

Adipocytes

Role of adipocytes in the ovarian tumoural microenvironment is poorly studied. The omentum is principally composed of adipocytes (as previously described) and is a major site of advanced ovarian cancer metastasis that results in transformation of this soft pad of tissue, primarily composed of adipocytes, to a solid tumour histologically devoid of adipocytes. If metastasis was a random event, all organs in contact with peritoneal fluid would have an equal distribution of metastases. However, both primary and recurrent high-grade serous ovarian carcinomas preferentially metastasise to adipose tissue (Nieman et al., 2011).

Thus, it is believed that the adipocytes play a major role in cancer cell migration and invasion, although the molecular mechanisms underlying this predilection are unknown. Interestingly, these cells are known to induce the homing of ovarian cancer cells by secreting cytokines such as IL6, 8, monocyte chemotactic protein 1 (MCP1) and adiponectin (Thibault et al., 2014, Nieman et al., 2011). Omental adipocytes significantly promoted invasion of ovarian cancer cells when compared with subcutaneous adipocytes, suggesting that adipocytes promote the early steps of ovarian cancer metastasis to the omentum, although a mechanistic explanation for the prevalence of omental metastatic tumours in women with ovarian cancer remained elusive (Nieman et al., 2011).

1.5 Tumour cells- secreted factors

Ovarian tumour cells secrete a number of cytokines, growth factors, pro- and anti-angiogenic factors. These factors create a niche for cancer cells to establish secondary foci, grow and metastasise further from the omentum. As the focus of this thesis is tumour-angiogenesis, only the secreted proangiogenic factors that have been identified in EOC are described in the following table 1.1:

Although these aforementioned cells and their secreted factors enhance ovarian cancer cell invasion into the omentum, their survival as secondary tumour foci is vastly dependent on angiogenesis. As EOC cells metastasise to the omentum where angiogenesis occurs, it is important to discuss the omentum and its suitability as a niche for secondary tumour foci.

Table 1.1: Proangiogenic factors secreted by ovarian cancer cells- an exhaustive list.

Activators	**Function**	**References**
Vascular endothelial growth factor (VEGF)	Stimulates angiogenesis, permeability	(Banerjee and Kaye, 2011)
Angiopoietin-1 (Ang1) and Tie2 receptor	Ang1: stabilises vessels by strengthening endothelial-smooth muscle interactions; Tie2R: inhibits permeability	(Lin et al., 2011)
Fibroblast growth factor (FGF)	Stimulate angiogenesis and arteriogenesis	(Tebben et al., 2005)
Transforming growth factor (TGF-β1)	Stabilises vessels by stimulating ECM production	(Toutirais et al., 2003)
Heparin-binding epidermal growth factor-like growth factor	Binds to epidermal growth factor receptor (EGFR) and promote angiogenesis	(Tanaka et al., 2005)
IL6	Induces migration of ECs in the mesentery in EOC	(Toutirais et al., 2003, Nilsson et al., 2005)
IL8	Stimulates VEGF expression and the autocrine activation of VEGFR2 in ECs	(Lokshin et al., 2006, Toutirais et al., 2003)

1.6 Angiogenesis – an overview in EOC

The development of new blood vessels from the existing ones in response to tumour-cell secreted proangiogenic factors is known as tumour-angiogenesis. Without angiogenesis tumour expansion cannot proceed beyond 1–2 mm because tumour proliferation is severely limited by nutrient supply to, and waste removal from the tumour (Bamberger and Perrett, 2002). Therefore, it is a crucial factor in secondary solid tumour formation and metastases, including EOC. Vascularisation is also a prerequisite for tumour cells to spread by shedding into the circulation; the newly formed, immature, and leaky capillaries aid the process of metastasis because their basement membranes are fenestrated, allowing greater accessibility for stray tumour cells, reviewed in (Bamberger and Perrett, 2002).

In the growing secondary tumour, hypoxia induces hypoxia inducible factor 1 (HIF-1) expression and the consequent release of proangiogenic factors such as VEGF, which activate ECs within these microvessels (Hu et al., 2001, Lee et al., 2006). In the tumour microenvironment the balance between pro- and anti-angiogenic factors favours the proangiogenic process. This hypoxic microenvironment containing VEGF also triggers ECs to secrete proteases such as matrix metalloproteinases initiating degradation of the ECM (basement membrane), followed by induction of EC migration along angiogenic factor gradient towards the tumour site. These ECs are differentiated into highly proliferative stalk cells which make up the main body of the new blood vessels-tube formation (Blanco and Gerhardt, 2013). This increased blood supply stimulates further tumour growth, invasion and metastasis (Bamberger and Perrett, 2002).

VEGF plays a key role in vascular maturation and patterning. There is fine-tuning in the activity of proaniogenic and promaturation factors that results in vascular remodelling and maturation. For instance, VEGF and Ang2 cooperatively promote EC sprouting and pericyte detachment (Brudno et al., 2013). Pro-maturation factors platelet-derived growth factor B (PDGF) and Ang1 inhibit the early stages of VEGF- and Ang2-mediated angiogenesis if present

simultaneously with VEGF and Ang2, but promote these behaviours if added subsequently to the pro-angiogenesis factors (Brudno et al., 2013). VEGF and Ang2 were also found to additively enhance microvessel density in a subcutaneous model of blood vessel formation, while simultaneously administered PDGF/Ang1 inhibit microvessel formation (Brudno et al., 2013). However, a temporally controlled scaffold that released PDGF and Ang1 at a delay relative to VEGF/Ang2, promoting both vessel maturation and vascular remodeling without inhibiting sprouting angiogenesis. This also ensures correct vascular patterning in physiological antiogenesis. However, in pathology, due to increased secretion of pro-angiogenic factors (e.g. VEGF) into the tumour microenvironment, local microvascular ECs become overactive and as a compensatory mechanisms, these cells express an increased amount of VEGFR2 (Nagy et al., 2009). This results in a disrupted vascular patterning where immature blood vessels are formed with increased pearmeability to solutes, proteins and migrating tumour cells, aiding metastasis to distant organ through circulation.

In advanced EOC, angiogenesis plays a significant role in disease prognosis and patient survival. Although debulking surgery and chemotherapy offer some clinical benefits to patients, chemoresistance portrays a massive challenge. Therefore, targeting angiogenesis for therapeutic purposes holds a promising clinical outcome. The following sections explore anti-tumour and anti-angiogenic therapies in place and/or are undergoing clinical trials.

1.6.1 Anti-tumour/angiogenic therapies

General assessment of patients with EOC

As discussed earlier, patients are often diagnosed with advanced stage disease. This is primarily due to having non-specific symptoms such as pain and abdominal swelling (that may refer to primary ovarian mass, epigastric omental plaques, ascites or a combination of these), gastroenterological manifestations (vomiting, dyspepsia and alternations of bowel) and less common urinary symptoms (pressure on the bladder).

A definitive diagnosis of EOC requires histopathological assessment, using a surgical specimen which is often obtained during staging laparotomy. The type of treatment for EOC depends on the cancer stage and histotype. Early stages of disease may involve surgery including abdominal hysterectomy and omentectomy. In patients with advanced EOC, primary debulking surgery (maximal surgical cytoreduction) has been shown to have a survival advantage (Griffiths, 1975). This is carried out to remove as much malignant tissue as possible. Depending on the remaining cancerous tissue, chemotherapies are given to patients intravenously. However, if the cancer reoccurs (recurrent ovarian cancer), a combination of chemotherapeutic drugs are often used such as carboplatin with gemcitabine or paclitaxel, although chemotherapy cannot usually cure the disease at this stage. This lack of treatment efficacy meant development of therapies targeting other steps of pathogenesis of EOC metastasis, such as antiangiogenic therapies.

1.6.1.1 Antiangiogenic therapies

Angiogenesis plays a major role in solid tumour progression, including in EOC. It is well established that the degree of angiogenesis, measured as microvessel density, in omental metastases of ovarian cancer and in primary ovarian tumours is an independent prognostic indicator of the overall survival of patients with advanced EOC (Hollingsworth et al., 1995, Abulafia et al., 1997). Due to limited treatment options for advanced stage EOC and the risk of recurrence and gaining chemoresistance, much enthusiasm has been shown for novel therapeutic strategies for ovarian cancer, particularly developing anti-angiogenesis agents. Since vascular endothelial growth factor (VEGF) has been extensively shown to be involved in the progression of other cancers, an anti-VEGF monoclonal antibody, bevacizumab, was approved for the treatment of advanced stage EOC.

Bevacizumab (avastin) is an IgG1 anti-VEGF monoclonal antibody that targets VEGFA by binding to it and thereby inhibiting its ability to bind to VEGFR1 and VEGRF2. A phase III trial conducted by Perren *et al.* with 1528 patients reported that 7.5mg/kg bevacizumab taken intravenously with chemotherapy increased the progression free period by a mean of 1.5 months against the patients treated with chemotherapy alone (Perren et al., 2011). Another phase III study conducted

by Aghajanian *et al.* involved 484 ovarian cancer patients who had experienced a recurrence more than 6 months after a prior chemotherapy treatment (Aghajanian et al., 2012). The results concluded there was a 52% increase in the progression free period in those who were treated with bevacizumab and chemotherapy compared to those who were treated with chemotherapy alone. Tumour shrinkage was also greater in the group treated with bevacizumab (79% versus 57% respectively), and hence bevacizumab (despite showing relatively modest benefits) in combination with paclitaxel and carboplatin has been prescribed for first-line treatment in advanced ovarian cancer.

Many other studies have indicated the therapeutic benefits of bevacizumab in ovarian angiogenesis but despite this, the clinical significance still remains unknown due to its toxicity. It has been reported in 16 clinical studies with over 600 patients that 21% of those treated with bevacizumab alone were later diagnosed with grade 3 – 4 hypertension (Stone et al., 2010). Further to this, bevacizumab treatment in clinical trials has been found to be linked to a proteinuria diagnosis in patients when used alongside aflibercept (Stone et al., 2010), which is a recombinant fusion protein consisting of VEGF-binding portions from the extracellular domains of human VEGF receptors 1 and 2 that are able to “trap” soluble VEGF (Rodriguez, 2013).

Although bevacizumab combined with chemotherapy has been prescribed to be the first-line treatment for advanced EOC, it has been found to be associated with increased arterial thromboembolic events in various metastatic cancers against chemotherapy treatment alone (Scappaticci et al., 2007). The links between the side effects and ovarian cancer are not well characterised as arterial thromboembolic events are relatively rare in ovarian cancer. However, Tateo *et al.* found of 253 patients there was a 16.6% incidence of vascular thromboembolic events in ovarian cancer malignancies (Tateo et al., 2005). Stone *et al.* reported a total of 30 vascular thromboembolic events including 2 deaths resulting from bevacizumab treatment (Stone et al., 2010). Due to the mechanism of VEGF antagonism, bleeding can also be a common side effect due to the decreased ability of ECs to renew although life threatening haemorrhages are most commonly linked to tumours situated close to major blood vessels. 10 – 90% of

ovarian malignancies treated with bevacizumab have reported mild bleeding present as grade 1 or 2 mucosal bleeding (Stone et al., 2010).

1.6.1.2 Tyrosine kinase inhibitors

Besides antibody-dependent antiangiogenic therapies, several tyrosine kinase inhibitors such as sorafenib, cediranib, vatalanib, sunitinib and panzopanib, are being investigated that inhibit the VEGFRs directly rather than the binding of the VEGF ligand (Table 1.2). These inhibitors have been developed to inhibit activation of tyrosine residues present on the intracellular domain of cell surface receptors which in turn leads to the activation of downstream cell signalling pathways such as RAS/Raf/MEK, PI3K/AKT/mTOR, JAK/STAT and p38, mediating cellular proliferation, survival, migration and altered cell permeability. Despite high specificity and efficacy, these inhibitors have been shown to be very toxic in completed clinical trials. For example, it was recently been shown that sorafenib, when added to standard therapy of advanced ovarian cancer, did not induce any benefit but rather increased severe toxicity (Hainsworth et al., 2015). The investigators suggested that sorafenib is not the angiogenesis inhibitor of choice in the treatment of patients with advanced ovarian cancer.

The other drugs stated in table 1.2 are undergoing clinical trials. However, data from completed clinical trials show severe side effects associated with using these inhibitors such as leukopenia (reduction of leukocytes), lymphopenia (low levels of lymphocytes), hypertension, diarrhoea and prolonged irregular heartbeat (that can lead to life threatening arrhythmia) (reviewed in (Morotti et al., 2013). These reports promise very little in treating the advanced disease, suggesting an urgent need for the identification of new targets in the development of anti-angiogenic therapies in the treatment of advanced EOC.

Table 1.2: A table displaying a brief summary of clinical trials for tyrosine kinase inhibitors (TKIs) for ovarian cancer, including route of administration, molecular target and observed response.

Key: RCC - renal cell carcinoma; GIST – gastrointestinal stromal tumour; PFS – progression free survival.

Drug	**Administration**	**Target**	**Response**
Sorafenib	Oral	VEGFR 2 and 3, and elements of the signal transduction pathway	FDA approved for RCC. 20% ovarian cancer patients showed 6 months PFS (Matei et al., 2008).
Cediranib	Oral	VEGFRs (1-3)	Significant tumour response / non-progression for up to 16 weeks in ovarian cancer (Matulonis et al., 2009).
Vatalanib	Oral	VEGFRs (1-3) but most selective towards VEGFR2	Significantly reduced tumour growth for ovarian cancer patients (Xu et al., 2000).
Sunitinib	Oral	VEGFRs (1-3)	FDA approved for GIST and RCC (Wen et al., 2013).
Panzopanib	Oral	VEGFRs (1-3)	Significant CA-125 response (Friedlander et al., 2007).

It should be of concern that antiangiogenic therapy is currently only aimed at inhibiting VEGF/VEGFRs axis. Winiarski *et al.* showed that proangiogenic changes in human omental microvascular ECs (HOMECs) were not solely due to VEGF and identified other potential pro-angiogenic factors secreted by EOC cells (Winiarski et al., 2013). Therefore, this thesis hypothesises that non-VEGF proteins play significant roles in inducing or enhancing continuous development of tumour angiogenesis in the omental tissue, supporting metastasis of the cancer.

1.7 Potential proangiogenic factors in ovarian cancer metastasis

Recently, Winiarski *et al.* suggested that omental metastasis of EOC may primarily occur via non-VEGF dependent pathways and reported the presence of potential proangiogenic factors cathepsin L (CathL), cathepsin D (CathD) and insulin-like growth factor binding protein 7 (IGFBP7) in tumour (EOC) conditioned media and ascites of EOC patients (Winiarski et al., 2013). Previously, these proteins have been studied in other cancer models. All three proteins are usually highly expressed or over-secreted or only secreted in cancer models (discussed later). However, their involvement in inducing metastatic angiogenesis in secondary locations such as the omentum is not fully understood, and therefore it is important to review the biological and clinical significance knowledge of these tumour secreted factors in tumour progression, particularly in EOC.

1.7.1 Cathepsin L

CathL is a lysosomal ubiquitous cysteine proteinase that plays an important role in degrading endocytosed proteins as well as intracellular proteins (Kirschke et al., 1977, Kominami et al., 1991). CathL is translated as preprocathepsin L (ppCathL) and processed into procathepsin L (pCathL) in the rough endoplasmic reticulum with a molecular mass of 30kDa and a two-chain form with molecular masses 25kDa and 5kDa (Kominami et al., 1988, Nishimura et al., 1988). It is then transported to endosome/lysosomes via the mannose-6-phosphate/receptor

(M6P/M6PR) pathway (Dong and Sahagian, 1990). CathL contains covalently N-linked oligosaccharides including a mannose moiety that is phosphorylated by phosphodiesterases in the *cis* Golgi (Lang et al., 1984). These M6P groups are recognised by an M6PR protein in the *trans* Golgi network (TGN), and facilitate the delivery of the protein to lysosomes (via endosomes) (Kornfeld, 1986). The cathepsins dissociate from the receptors at low lysosomal pH, and the phosphate group is removed from the M6P moiety by a lysosomal acid phosphatase (Samie and Xu, 2014). However, CathL has also been shown to be secreted out of the cell (discussed later).

It has been reported that 1, 10-phenanthrolin and pepstatin partially inhibited the processing of the proenzyme form of CathL to the mature enzyme and it was speculated that metallo-proteinases or an aspartic protease such as CathD are involved in the proteolysis-mediated activation of CathL in the lysosome (Ishidoh et al., 1991, Ritonja et al., 1988). CathL can also be activated by autocatalysis of pCathL at pH 3 as shown in *in vitro* study of pCathL collected from conditioned media of murine fibroblast cultures (Mason et al., 1987). However, CathL is highly active at physiological pH 5.5 in lysosomes as shown in several studies (Mason et al., 1987, Mason and Massey, 1992).

1.7.1.1 Main role and tight regulation

The main role of CathL is to degrade proteins in the acidic pH of lysosomes (Mason et al., 1987, Mason and Massey, 1992). However, it is also known that CathL is secreted in different forms into the extracellular space in both physiological and pathological conditions, and retains its function as a protease. In physiology, CathL has been shown to degrade the Ii peptide of MHC II complex that in turn allows peptides derived from the proteolytic degradation of foreign or self-proteins to then bind to class II molecules and appear on the cell surface (Nakagawa et al., 1998). Studies showed that CathL is essential for MHC II mediated antigen presentation in cortical thymic epithelial cells but not in bone marrow-derived antigen-presenting cells *in vivo* (Hsieh et al., 2002). This was reflected in CathL deficient mice with a reduction in CD4+ T cells. CathL has also been shown to degrade and process foreign antigens which are then presented

on the MHC II molecule to elicit a CD4+ T-cell dependent immune response (Hsieh et al., 2002). Intracellular CathL is essential for epidermal homeostasis and regular hair follicle morphogenesis and cycling. It was found that CathL-deficient mice develop periodic hair loss and epidermal hyperplasia, acanthosis, and hyperkeratosis (Roth et al., 2000).

In another study, CathL null mice showed reduced bone mass compared to wild type mice suggesting a role for CathL in bone remodelling. CathL null mice showed significant decrease in bone volume in trabecular bone, but not cortical, bone compared to wild type. Bone loss was exacerbated in null mice (compared to wild type) following overiectomy suggesting that CathL is stimulated by external stimuli (e.g. oestrogen) and is likely to play a role in controlling bone turnover during normal development and in pathological states (Potts et al., 2004).

1.7.1.2 CathL secretion

CathL was first identified as a major secreted protein from a transformed murine fibroblast cell line (Mason et al., 1987). However, the mechanism of secretion of CathL remains a mystery. It has been shown that CathL has only one M6P residue, and hence its lower affinity for M6PR, as opposed to enzymes with two M6P residues such as CathD (von Figura and Hasilik, 1986, Dahms et al., 1989, Dong et al., 1989). This observation suggested that not all CathL binds to M6PR and therefore some is secreted out of the cell by default protein trafficking (Dong and Sahagian, 1990). M6PR saturation, downregulation or redistribution to the plasma membrane has also been suggested (Prence et al., 1990, Achkar et al., 1990). Interestingly, hypoxia also induced CathL secretion from the murine fibrosarcoma cell line KHT-LP1 which may accelerate the metastatic process in these cells (Cuvier et al., 1997). Secreted CathL has also been shown to be protective against bacterial infection in airways of mice (Xu et al., 2013).

1.7.1.3 CathL in cancer

In the field of cancer, CathL is less well studied than other cathepsins such as cathepsins B (CathB) and S (CathS). A role for CathL has been linked to tumour

invasion and metastasis, particularly by degrading several ECM components such as proteoglycan, aggrecan, elastin, laminin, fibronectin and collagens: I, II, IX, XI (Maciewicz and Wotton, 1991, Maciewicz et al., 1990, Nguyen et al., 1990, Nosaka et al., 1999, Mason et al., 1986, Ishidoh and Kominami, 1995). Over-expression of CathL was linked to metastasis following ras transformation of NIH/3T3 cells *in vitro* (Chambers et al., 1992). Additionally, non-metastatic melanoma cells were converted to a metastatic state by over-expressing CathL *in vitro* (Frade et al., 1998). An extra-lysosomal role for CathL has been suggested in human and murine melanoma cells in the context of metastasis (Ishidoh and Kominami, 1998). Recently, it was shown that CathL is involved in B16F10 melanoma cell invasion (*in vitro*), particularly through cell migratory influences (Yang and Cox, 2007). There was approximately 70% reduction in CathL anti-sense clone invasion and migration compared to control after 24 hours. However, testing for CathL-induced proliferation in these cells revealed that there was no difference between the rate of proliferation of antisense cell and control cell colonies (Yang and Cox, 2007). Effect of secreted CathL was also investigated where intracellular expression of an antibody to CathL has been shown to block CathL secretion, which resulted in a dramatic inhibition of melanoma metastasis (Rousselet et al., 2004). Although this study did not investigate migratory effects of exogenous CathL, Yang and Cox demonstrated a direct effect of secreted CathL on cell motility where CathL contributes its proteolytic action to the active invasion of melanoma cells (Yang and Cox, 2007). CathL-induced pancreatic cancer cell invasion was also observed in mice. CathL-null mice had a significant reduction in tumour volume and invasion, suggesting a role for its extracellular proteolytic activity in wild-type mice. In contrast to the melanoma cell study discussed above, the latter work demonstrated significant proliferative effects of CathL on pancreatic cancer cells, with a 58% decrease in proliferation in CathL knockout cells, although the mechanism of action, i.e. proteolytic or non-proteolytic, was not investigated (Gocheva et al., 2006).

An increased level of secreted CathL has been observed in the sera of malignant epithelial ovarian cancer patients (Nishida et al., 1995, Zhang et al., 2014b). These studies showed that there was significant increase in the expression of CathL mRNA levels in tumours which correlated with its protein level in serum. These authors also reported that increased level of secreted CathL was higher in

the sera of malignant EOC patient than those with benign or normal ovarian tissue. The levels of CathL mRNA expression and secreted protein in sera samples were higher than benign ovarian tumour and normal ovarian tissue. CathL was later shown to be involved in the invasion and metastasis of EOC, and hence was suggested to be a marker of advanced staged ovarian cancer (Zhang et al., 2014b). This was supported by data demonstrating that the endothelium of vessels within omentum hosting metastatic ovarian high-grade serous carcinoma expressed significantly increased CathL *in vivo* compared with omentum from control patients with benign ovarian cystadenoma (Winiarski et al., 2014). However, CathL-induced cell proliferation produced contradictory data. CathL had less influence on cell growth and proliferation of the A2780 ovarian cancer cell line (Zhang et al., 2014b), whereas downregulation of CathL-gene expression significantly inhibited the proliferative and invasive capability of SKOV3 ovarian cancer cells (Zhang et al., 2015).

1.7.1.4 CathL in angiogenesis

A role for CathL in angiogenesis is a relatively new observation and interestingly evidence from different models suggests that CathL may be both pro-and anti-angiogenic. For instance, recently, CathL derived from skeletal muscle cells transfected with bFGF was shown to promote migration of human umbilical vascular ECs (HUVECs) *in vitro* (Chung et al., 2011). Cell migration, a key component of angiogenesis, was tested in the presence of a cell impermeable CathL-proteolytic inhibitor Z-Phe-Tyr-Cho and CathL for 12 hours. The data revealed a significant reduction in HUVEC migration, suggesting that CathL influences cell migration via its proteolytic-dependent mechanism. Subsequently, CathL was found to activate c-Jun N-terminal kinase (JNK) in migratory HUVECs. However, the exact role of CathL in activating the JNK pathway has not been elucidated (Chung et al., 2011). Interestingly, CathL was found to be secreted by SKOV3 and A2780 EOC cells. Addition of exogenous CathL induced migration and *in vitro* angiogenesis of HOMECs (Winiarski et al., 2013). Together, these data suggest that CathL may trigger a proangiogenic phenotype in these ECs.

In contrast, both secreted and intracellular CathL has been shown to release endostatin, a potent inhibitor of angiogenesis, by cleaving ECM collagen (Felbor

et al., 2000). Since the tumour microenvironment provides a slightly acidic milieu, CathL can efficiently cleave collagen even outside the cells. However, in other studies, CathL had no effect on angiogenesis. For example, Gocheva *et al.* demonstrated that CathL had no significant effects in altering microvascular density in pancreatic cancer in mice (Gocheva et al., 2006). When evaluating the role of CathL in angiogenic switching in homozygous cathepsin knockout RT2 mice compared to control mice, no significant effect on the development of these precursor lesions was observed, suggesting that CathL does not contribute to angiogenic switching. However, other cathepsins such as CathB and CathS were found to be very important in inducing angiogenesis in the same study (Gocheva et al., 2006).

Intriguingly, endothelial progenitor cells (EPCs) have been reported to produce CathL which in turn induces angiogenesis. Urbich *et al.* showed that EPCs are able to stimulate neovascularisation and blood flow in the ischaemic murine hind leg after injection in the affected leg (Urbich et al., 2005). These EPCs significantly enhanced expression of CathL which was revealed in mRNA array analysis. It was suggested that in the neovascularisation process CathL activity may be extra- or pericellular. Mature CathL was shown to remain proteolytically active extracellularly at neutral pH by the chaperone action of a p41 splice variant of the MHC class II-associated invariant chain (Fiebiger et al., 2002), which indeed is strongly expressed in EPCs (Urbich et al., 2005). Such activity may facilitate EPC invasion and neovascularisation. It was shown that CathL deficient mice suffered from impaired neovascularisation. Furthermore, mice treated with CathL-deficient bone marrow cells demonstrated a significant reduction in angiogenesis (Urbich et al., 2005). Another study also showed that CathL expressed in EPCs cells plays a critical role in intraocular angiogenesis (Shimada et al., 2010). However, although CathL has been suggested to induce angiogenesis in these studies, its mechanism of action has not been elucidated.

1.7.2 Cathepsin D

CathD is a soluble lysosomal aspartic endopeptidase primarily involved in degrading unfolded or non-functional proteins intracellularly. The protein is synthesised in rough endoplasmic reticulum as inactive preprocathepsin D (43

kDa), which is in turn cleaved and glycosylated to form 52 kDa procathepsin D (pCathD) containing two N-linked oligosaccharides modified with mannose 6-phosphate (M6P) residues. pCathD is then targeted to intracellular vesicular structures such as lysosomes, endosomes and phagosomes both by M6P receptor (M6PR)-dependent and -independent pathways (reviewed in (Benes et al., 2008)). The latter pathway of targeting is not fully understood; however the sphingolipid activator precursor protein pro-saponin has been suggested to be involved (Gopalakrishnan et al., 2004).

Once pCathD enters the late endosome, the low pH induces its dissociation from M6PR and subsequently the phosphate group is removed. Proteolytic cleavage of propeptide (44aa) of pCathD generates active intermediate enzyme (Laurent-Matha et al., 2006). The propeptide (also known as activation peptide) is essential for the correct folding, activation and delivery of the protein to lysosomes (Takeshima et al., 1995, Yasuda et al., 2005). This peptide, which is expressed in, and secreted from, cancer cells, has also been demonstrated to act as a growth factor for tumour cells (Vetvicka et al., 2000). The intermediate CathD is further processed by cysteine proteases and autocatalysis to generate mature CathD (48 kDa) containing a heavy chain (34 kDa) and a light chain (14 kDa) (Gieselmann et al., 1985). The optimum pH for CathD activity is 3.5 at which it is highly proteolytically active (Yoshinari and Taurog, 1985). However, proteolytic activity has also been reported at neutral pH in the cytosol of apoptotic cells and in neurofibrillary degeneration (Kenessey et al., 1997, Roberg et al., 1999).

1.7.2.1 Physiological roles of CathD as both an intracellular and extracellular protein

CathD has been shown to play a significant role during foetal development. The lysosomal system matures gradually which correlates with increased CathD levels in all tissues (Kageyama et al., 1998). A reduction of CathD expression or its catalytic activity results in neurodegenerative disorders. CathD knockout mice die shortly after birth and display significant neurodegeneration (Kageyama et al., 1998). Congenital mutations in the CathD gene lead to a reduction in expression and subsequent production of enzymatically inactive protein that results in neurodegenerative disease in dogs and humans (Tyynela et al., 2000, Tyynela

et al., 2001, Steinfeld et al., 2006, Fritchie et al., 2009, Siintola et al., 2006, Awano et al., 2006). Recently, it has been shown that CathD deficiency is associated with Parkinson's disease (Cullen et al., 2009). Interestingly, increased CathD expression and activity in cardiac cells induces heart failure in postpartum female mice (Hilfiker-Kleiner et al., 2007). Higher CathD levels have also been suggested to play an important role in the pathogenesis of autism by increasing apoptosis in the cerebellum of autistic subjects (Sheikh et al., 2010).

Several physiological functions of CathD have been suggested based on its proteolytic activity to cleave structural and functional proteins and peptides. These include metabolic degradation of intracellular proteins, activation and degradation of polypeptide hormones and growth factors such as plasminogen, prolactin, endostatin, osteocalcin, thyroglobulin, insulin-like growth factor binding proteins (IGFBP) and secondary lymphoid tissue chemokine (SLC); activation of enzymatic precursors of CathL, CathB and transglutaminase 1; and processing of the enzyme activators and inhibitors prosaposin and cystatin C, reviewed in (Benes et al., 2008).

Although CathD is a lysosomal enzyme and its enzyme activity is usually regulated within the acidic compartment of lysosomes, it has also been shown to be enzymatically active and biologically relevant extra-lysosomally at cytosolic pH, for instance in the control of apoptosis as discussed later.

Unlike other aspartic endopeptidases, under normal physiological conditions, pCathD is sequestered to the lysosome and not secreted extracellularly. However, in some conditions, pCathD/CathD escape the normal targeting pathway and are secreted from cells. Most probably, over-expression of pCathD saturates the limited number of M6PR binding sites available and the protein accumulates in the cytosol, and is subsequently secreted via an as yet unknown mechanism (Mathieu et al., 1991). Indeed pCathD has been found in human, bovine and rat milk and serum and the presence of both pCathD and CathD (34 kDa) was observed in human eccrine sweat and urine (Vetvicka et al., 1993, Larsen and Petersen, 1995, Benes et al., 2002, Zuhlsdorf et al., 1983). CathD in human eccrine sweat was found to be proteolytically active at sweat pH 5.5

(Baechle et al., 2006). Interestingly, there is increasing evidence that extracellular CathD may act via both proteolytic dependent and independent mechanisms.

1.7.2.2 Expression of CathD in ovarian cancer

In many cancer microenvironments, pCathD is a major secreted protein. In the last 2 decades, studies have shown increased overexpression and hypersecretion of CathD in numerous cancer types including ovarian cancer, but also in breast cancer, endometrial cancer, lung cancer, malignant glioma, melanoma and prostate cancer (Table 1.3) (Winiarski et al., 2013, Rochefort, 1992, Ferrandina et al., 1997, Foekens et al., 1999, Briozzo et al., 1991, Chen et al., 2011, Konno et al., 2001, Morikawa et al., 2000, Losch et al., 1996, Zhu et al., 2013, Fukuda et al., 2005, Rochefort et al., 2000, Pruitt et al., 2013, Vetvicka et al., 2004, Nazeer et al., 1992). Early studies investigating ovarian carcinoma suggested that the expression level of CathD was associated with increased cell differentiation and with histological type (Baekelandt et al., 1999, Ferrandina et al., 1998).

Additionally, immunohistochemistry studies have indicated that enhanced CathD expression is an indicator of malignancy in serous ovarian cancer (Henzen-Logmans et al., 1994, Losch et al., 2004, Chai et al., 2012), for instance Losch *et al.* observed that over 70% of invasive ovarian cancers express CathD (Losch et al., 2004). Intriguingly, however, it has also been shown that in ovarian tumours that do express CathD, a high expression level was associated with a favourable survival prognosis (Chai et al., 2012). More recently, in an investigation into omental metastasis of ovarian cancer in our laboratory observed a significantly higher expression of CathD in the omental lesion of serous ovarian carcinoma compared with omentum from patients with benign ovarian cystadenoma and that high omental mesothelial expression of CathD was associated with poor disease-specific survival (DSS) (Winiarski et al., 2014). This stronger expression of CathD in mesothelial cells was observed close to the metastatic tumour, suggesting a paracrine effect for factors secreted from the tumour cells contributing to the increased CathD expression.

Table 1.3. Involvement of CathD in the stages of tumour progression in different cancer types. Taken from (Pranjol et al., 2015)

Cancer Type	Metastasis	Invasion	Angiogenesis	References
Breast	↑	↑	↑	(Rochefort, 1992, Ferrandina et al., 1997, Foekens et al., 1999, Briozzo et al., 1991)
Ovarian	ND	ND	↑	(Winiarski et al., 2013)
Prostate	↑	↑	↓	(Chen et al., 2011, Konno et al., 2001, Morikawa et al., 2000)
Endometrial	ND	↑	ND	(Nazeer et al., 1992)
Melanocytic	↑	↑	ND	(Zhu et al., 2013)
Glioma	↑	↑	ND	(Fukuda et al., 2005)
Lung	ND	↑	ND	(Vetvicka et al., 2004)

↑, increase in effects; ↓, reduction in effects; ND, not determined.

A number of studies have also examined CathD expression in breast cancer. CathD overexpression is correlated with increased risk of clinical metastasis and short survival in breast cancer (Rochefort, 1992, Ferrandina et al., 1997, Foekens et al., 1999) and increased serum pCathD levels were detected in the plasma of patients with metastatic breast carcinoma (Brouillet et al., 1997). Additionally, total CathD concentration in breast cancer tissue was much higher than in other tissues including normal mammary cells (Vetvicka et al., 1994).

1.7.2.3 Role of CathD in tumour progression

It is now recognised that CathD has a potential role in multiple tumour progression steps, both in its intracellular and extracellular form.

As indicated above, a role for intracellular cytosolic CathD has been identified in apoptosis. Here the lysosomal enzyme is translocated to the cytosol due to lysosomal membrane permeabilisation (Roberg et al., 1999, Ollinger, 2000, Kagedal et al., 2001). Subsequently, CathD actively cleaves the BH3-interacting domain (Bid) to form truncated Bid (tBid) which in turn triggers the insertion of Bax into the mitochondrial membrane (Heinrich et al., 2004, Blomgran et al., 2007), and leads to the release of cytochrome c from mitochondria into the cytosol (Johansson et al., 2003). Inhibition of enzymatically-active cytosolic CathD, using the inhibitor pepstatin A (pepA), partially delayed apoptosis induced by IFN-γ or oxidative stress when pepA was co-microinjected with CathD in human foreskin fibroblasts, HeLa cells and neutrophils (Kagedal et al., 2001, Heinrich et al., 2004, Blomgran et al., 2007). The role of CathD in inducing apoptosis has also been shown to be associated with caspases; the pan caspase inhibitor Z-VAD-FMK added in combination with pepA, induced a significant reduction in cell death compared to individual inhibitor treatments. This suggested a strong association between caspases and proteolytically active cytosolic CathD (Zuzarte-Luis et al., 2007b, Zuzarte-Luis et al., 2007a). Additionally, CathD has been shown to cleave tau protein *in vitro* at pH 7 (Kenessey et al., 1997). These studies suggest that, intracellularly, CathD is proteolytically active at cytosolic pH. However, this has been contested by other studies indicating that the effect of a mutant CathD, deprived of its catalytic activity, was indistinguishable from that of the normal enzyme (Beaujouin et al., 2006, Tardy et al., 2003).

Although, a role for intracellular CathD in apoptosis suggests that the protein may be anti-tumourigenic; this is in contrast to the functions observed for extracellular CathD.

For instance CathD is secreted by EOC cancer cell lines (SKOV3 and A2780) (Winiarski et al., 2013), is present in the ascites of patients suffering from ovarian cancer (unpublished data), and exogenous CathD induced migration of human omental microvascular ECs; a key step in angiogenesis during omental metastasis (Winiarski et al., 2013). In a separate study pCathD and CathD have been reported to induce proliferation and migration of breast cancer cells, fibroblasts and ECs in both a proteolytic dependent and independent manner (Ohri et al., 2008) (Figure 1.5). While secreted pCathD is generally considered to be proteolytically inactive, it has been proposed that the acidic pH in the tumour microenvironment promotes the conversion of pCathD into mature, biologically active CathD. This was supported by data indicating that pCathD, collected from tumour-conditioned media, became auto-activated if the pH was lowered and was subsequently able to degrade ECM proteins and release growth factors such as bFGF (Briozzo et al., 1991, Briozzo et al., 1988, Westley and May, 1996), steps important for cancer cells to invade surrounding tissue (Crowe and Shuler, 1999).

There is evidence that CathD may induce mitogenic responses via both proteolytic-dependent and—independent mechanisms. Both the wild type and mutant form of CathD were shown to induce fibroblast proliferation via a mechanism whereby they acted as a protein ligand (Laurent-Matha et al., 2005). In this study, the authors demonstrated an interaction between M6PR and pCathD. Co-incubation with excess M6P partially prevented fibroblast proliferation. Although an unknown receptor molecule was suggested to be involved, the identity of this potential receptor has not yet been resolved.

CathD actions on tumour growth were further reported in studies showing that 3Y1-Ad12 rat tumour cells transfected with human CathD cDNA grew more rapidly *in vitro* and presented an increased experimental metastatic potential *in vivo* (Garcia et al., 1990, Liaudet et al., 1994, Liaudet et al., 1995). Additionally, both wild-type and mutated (Asn 231, proteolytically inactive) CathD stimulated proliferation of 3Y1-Ad12 cells embedded in Matrigel or collagen 1 matrices, colony formation in soft agar and tumour growth in athymic nude mice (Glondu et al., 2001, Berchem et al., 2002). Again, an unknown receptor, other than M6PR,

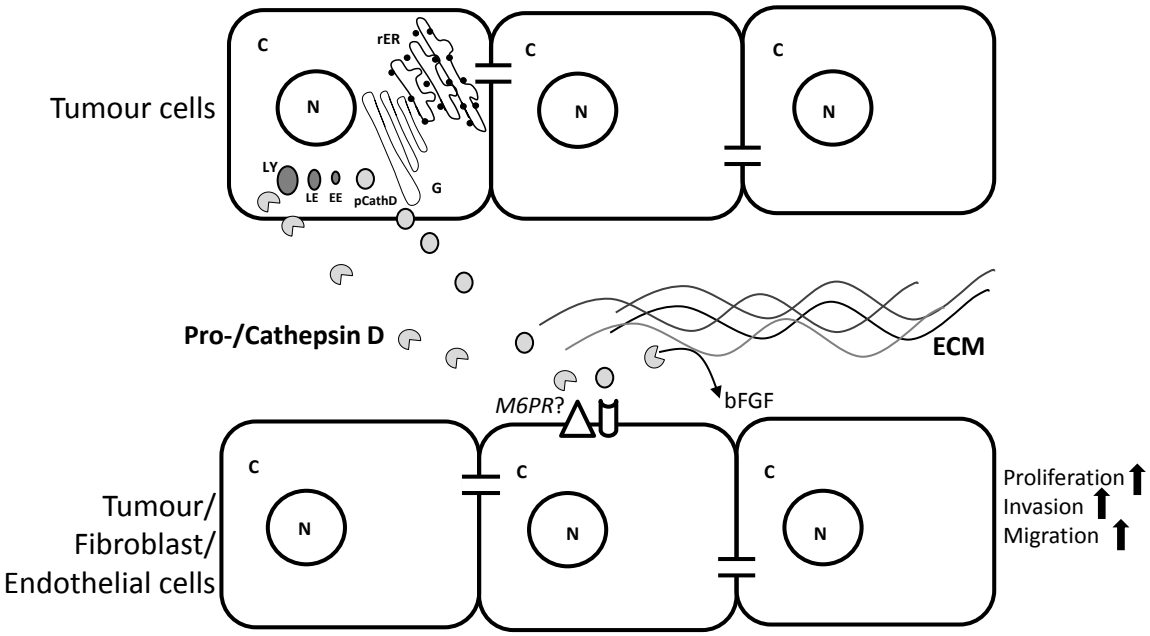

Figure 1.5. **Potential roles of tumour cell-secreted pCathD/CathD on extracellular matrix (ECM), tumour, fibroblast and ECs in the tumour microenvironment.** pCathD is synthesised and processed in the rough endoplasmic reticulum (rER) and Golgi bodies (G), and subsequently transported to early endosome (EE), late endosome (LE) and finally lysosome (LY). Overexpressed pCathD/CathD is secreted into the extracellular space by tumour cells. Mature CathD cleaves ECM and releases basic fibroblast growth factor (bFGF) that may induce angiogenesis. Both pCathD and CathD induce tumour cell proliferation, and hence invasion via an autocrine mechanism. CathD induces proliferation of fibroblasts and migration of ECs. Mannose-6-phosphate receptor (M6PR) may be involved in inducing the proliferative effects. C and N denote cytoplasm and nucleus, respectively. Taken from (Pranjol et al., 2015)

was suggested to be involved in CathD mediated cell growth as no inhibition of cell outgrowth was observed when excess M6P was added, suggesting that M6P did not compete with CathD interacting with M6PR. In the same study the propeptide (27-44aa) of pCathD was found not to be mitogenic, contradicting studies which found otherwise (Vetvicka et al., 2000, Vetvicka et al., 1994, Fusek and Vetvicka, 1994, Vetvicka et al., 1998, Vetvicka et al., 1999, Vetvicka et al., 1997).

The role of CathD has also been extensively studied in human primary breast cancer. Upregulation of CathD expression was observed in oestrogen receptor (ER) positive breast cancer cell lines treated with oestrogen (Rochefort et al., 1987). *In vitro* experiments with the MCF7 cell line supported these data and revealed that pCathD/CathD were overexpressed and hyper-secreted from these cells into the media. Further studies have reported that as a mitogen pCathD acts as a protein ligand rather than enzymatically and that purified pCathD from MCF7 breast cancer cells stimulated MCF7 cell growth on plastic via an autocrine mechanism (Vignon et al., 1986). Intriguingly, CathD has also been shown to selectively degrade macrophage inflammatory protein (MIP)-1α (CCL3), MIP-1β (CCL4), and SLC (CCL21) that, in turn, may affect the generation of the anti-tumoural immune response, the migration of human breast cancer cells, or both processes (Wolf et al., 2003).

In recent years studies have emerged that suggest that CathD can induce angiogenesis *in vivo* and *in vitro. In vivo*, overexpression of CathD in xenografts in an athymic mice model correlated with increased vascular density. The number of microvessels was significantly increased by 1.5-fold and 1.9-fold in the CathD and CathD-Asn 231(proteolytically inactive) groups respectively, suggesting that CathD induces angiogenic effects via an unknown mechanism other than its proteolytic activity (Berchem et al., 2002).

CathD has also been shown to induce blood vessel formation in the chick chorioallantoic membrane (CAM) model (Hu et al., 2008) and a role for CathD in angiogenesis was further illustrated by the observation that migration of HUVECs and *in vitro* angiogenic tube formation were increased when cells were treated with active pure CathD. CathD was proteolytically active in these experiments as complete inhibition of angiogenesis, tube formation and migration was achieved by addition of pepA (Hu et al., 2008). Proteolytically active CathD has also been

suggested to induce angiogenesis in breast cancer by cleaving and releasing ECM-bound pro-angiogenic bFGF (Briozzo et al., 1991). These aforementioned studies suggest that CathD can induce proangiogenic responses via both its proteolytic-dependent mechanism and an unknown mechanism that is not dependent on its proteolytic activity.

In contrast it has also been suggested that CathD activity may be anti-angiogenic For instance, pCathD secreted by prostate cancer cells was shown to have a possible role in generating angiostatin via proteolysis—a specific inhibitor of angiogenesis *in vitro* as well as *in vivo* (Morikawa et al., 2000), suggesting an opposing effect of CathD in angiogenesis. Due to the variability of its mechanisms of action and the opposing effect in angiogenesis, it was important to investigate a specific role for CathD in inducing a proangiogenic response in HOMECs in ovarian cancer metastasis, which was examined in this thesis.

1.7.3 IGFBP7

Insulin-like growth factor-binding protein 7 (IGFBP7), also known as insulin-like growth factor-binding protein-related protein-1 (IGFBP-rp1), tumour adhesion factor, prostacyclin-stimulating factor (PSF), and angiomodulin (AGM), is a secreted protein which is thought to be a vital component of mammalian cell growth, differentiation and proliferation (Chen et al., 2013), particularly in ECs (Akaogi et al., 1996a). IGFBP7 is different from the other IGFBPs in that it has 100-times less affinity for binding to IGF-1 and is the only family member that binds insulin with strong affinity, limiting insulin binding to the insulin receptor (Yamanaka et al., 1997). This difference may suggest that IGFBP7 has unique functions that are primarily IGF1-independent (Hwa et al., 1999).

IGFBP7 is synthesised from the mac25 protein, the propeptide of which has been found to have around a 45% amino acid sequence similarity to human IGFBPs 1-6 (Oh et al., 1996). The mRNA for IGFBP7 has been found in a wide range of healthy tissues including the small intestine, prostate, lungs, skeletal muscle, colon and ovaries (Hwa et al., 1998): this protein is particularly abundant in blood vessels in the mature follicular wall (Wandji et al., 2000), uterus (Kutsukake et al., 2007) and the corpus luteum (Abu-Safieh et al., 2011).

The available data on the role of IGFBP7 in tumour development is conflicting. A negative role for IGFBP7 was first documented when it was identified as a differentially expressed gene in normal leptomeninges compared with meningiomas and in primary prostate epithelial cell lines compared with prostate cancer cell lines (Akiel et al., 2014). A number of studies have reported IGFBP7 downregulation in breast, colorectal and lung cancer (Swisshelm et al., 1995, Hwa et al., 1998, Chen et al., 2007). Moreover, overexpression of IGFBP7 in the breast-cancer cell line MDA-MB-468 abrogated their growth and migration via inhibition of phosphorylation of MAPK extracellular signal-regulated kinase (ERK)-1/2. Treatment of the breast-cancer cell line MDA-MB-231 with recombinant IGFBP7 protein induced G1 cell-cycle arrest and senescence, as indicated by cell-cycle analysis and β-galactosidase staining, respectively. The IGFBP7-induced cell-cycle arrest and senescence was mediated by induction of the p53–p21 axis and the activation of stress-activated p38 MAPK (Akiel et al., 2014). Tail-vein injection of recombinant IGFBP7 for 3–4 days in NOD/SCID mice harbouring xenografted breast-cancer tumours resulted in decreased angiogenesis, as shown by a reduction in cluster of differentiation (CD) 31 and VEGF expression. Recombinant IGFBP7 was able to induce apoptosis as seen by caspase-3 and poly adenosine diphosphate ribose polymerase cleavages (Benatar et al., 2012). Taken together, these results suggest that IGFBP7 could act as a negative regulator of mitogenesis by suppressing ERK-1/2 and activating p38 MAPK and p53-p21 pathways to curb uncontrolled proliferation, induce senescence, and suppress angiogenesis in breast cancer.

Interestingly, a recent study investigating effects of IGFBP7 on angiogenesis demonstrated that VEGF-induced stimulation of tube formation in HUVECs was reduced by treatment with IGFBP7 (Tamura et al., 2009). In the same study it was also found that cell proliferation induced by VEGFA was also inhibited in the presence of IGFBP7. However, IGFBP7 in the absence of VEGFA has not been found to reduce the proliferation or tube formation of vascular ECs (Tamura et al., 2009). This indicates a lack of evidence that IGFBP7 directly affects tumour blood vessels; only in the case of VEGFA-induced angiogenesis (Tamura et al., 2009).

Although the above data suggest that IGFBP7 negatively influences cancer growth by reducing cancer cell proliferation, other data point towards a positive role in tumour development by influencing angiogenesis. Glioblastoma-secreted IGFBP7 has been found to induce capillary formation in human brain ECs, and hence was suggested to be a proangiogenic factor (Pen et al., 2008). In a recent study, Winiarski *et al.* identified secreted-IGFBP7 in EOC tumour conditioned media (Winiarski et al., 2013). IGFBP7 induced omental microvascular EC proliferation, migration and angiogenic tube formation, again suggesting a proangiogenic role for this protein in the metastasis of ovarian cancer to the omentum (Winiarski et al., 2013).

Thus, the role of IGFBP7 in carcinogenesis and angiogenesis remains contradictory across different cancer models. However, since IGFBP7 showed proangiogenic activity in HOMECs and thus may be involved in EOC metastasis, this will be further examined, specifically investigating the activated signalling pathways in these ECs.

1.8 Rationale for this study and aims

EOC is characterised with the highest mortality and the highest post-menopausal morbidity of all gynaecological cancers. Symptoms are vague at the primary stage, and hence early diagnosis is difficult. Therefore, many patients are diagnosed with advance stage of disease that requires a radical surgical intervention such as omentectomy.

Although chemotherapy is applied as second line treatment, the progression-free survival rate has not improved drastically (Fung-Kee-Fung et al., 2007). Unfortunately, due to drug and chemotherapy resistance it is extremely common for a small proportion of the tumour cells in later stages of progression to survive and further proliferate once the chemotherapy schedule is completed. For this reason, it is essential that more permanently effective and targeted treatments are discovered and made available. Since angiogenesis plays a key role in late stage metastasis, numerous anti-angiogenic therapies have been developed targeting the VEGF/VEGFR axis. For example, anti-VEGF monoclonal antibody

bevacizumab, alone or in combination with chemotherapy, demonstrated increased progression-free period. Specifically, progression-free survival at 42 months was 22.4 months without bevacizumab versus 24.1 months with bevacizumab (P=0.04 by log-rank test) (Perren et al., 2011). However, this drug has been observed to be highly toxic, with numerous side-effects as discussed above.

As the tumour microenvironment at the secondary site contains a mixture of growth factors and cytokines released by immune cells, mesothelial cells, ECs, adipocytes, fibroblasts and ovarian cancer cells, targeting only one factor (VEGF) may not be successful in preventing tumour-angiogenesis. Thus, it was essential to investigate tumour-secreted proangiogenic factors, other than VEGF, that may enhance the proangiogenic response in the metastatic cascade of EOC. Indeed Winiarski *et al.* reported that despite blocking the VEGF/VEGFR axis, HOMECs treated with EOC-conditioned media induced significant angiogenic tubule formation, suggesting the presence of potential factors with pro-angiogenic roles (Winiarski et al., 2013). Further studies investigating EOC-secreted factors revealed a number of factors including CathL, CathD and IGFBP7 in the tumour conditioned media, which were shown to be proangiogenic in HOMECs in EOC metastasis. However, their activatory mechanisms in HOMECs have not yet been elucidated.

Interestingly, CathL was shown to induce expression and secretion of Gal1 in HOMECs. Gal1 is a glycoprotein which has been shown to be proangiogenic in several tumour models (discussed later). Thus, Gal1 was investigated in the induction of HOMEC proliferation, migration and angiogenesis, in addition to CathL-induced proangiogenic response in HOMECs.

Therefore, the overall aim of this thesis was to examine possible cross-talk between ovarian cancer cells and omental microvascular ECs in metastasis of ovarian cancer to the omentum, specifically to investigate whether non-VEGF factors secreted from EOC can induce angiogenic changes in the local microvasculature and the signalling pathways activated. Alternative factors examined will be CathL, CathD, Gal1 and IGFBP7. In order to investigate interactions between these cells, the following aims were executed:

- Investigation into the proangiogenic changes induced in HOMECs by CathL (Chapter 3)
- Investigation into the proangiogenic changes induced in HOMECs by Gal1, a glycoprotein secreted by HOMECs in response to CathL (Chapter 4)
- Investigation into the proangiogenic role of CathD in ovarian cancer metastasis to the omentum (Chapter 5)
- Investigation into potential proangiogenic roles of IGFBP7 in HOMECs (chapter 6)

Chapter 2 Materials and methods

2.1 Materials

Abcam, Cambridge, UK: Insulin-like growth factor binding protein-7 (IGFBP-7) protein, goat anti-rabbit IgG-FITC conjugated.

Alphalabs, Hampshire, UK: 300µl tips (autoclavable).

BD Biosciences, Oxford, UK: Syringes, cell strainers (nylon, 40µm and 100µm pore size), cell scrapers.

Biotechne (R&D system, Tocris), Abingdon, UK:

Enzyme-linked immunosorbent assay (ELISAs): Phospho-ERK1 (T202/Y204)/ERK2 (T185/Y187) Cell-Based ELISA, Phospho-Akt (T308) Pan Specific Cell-Based ELISA, Human Galectin-1 Quantikine ELISA Kit, Phospho-RelA/NFκB (nuclear factor κB) p65 (S536) Cell-Based ELISA.

Migration assay kit: Cultrex Cell Migration Assay, 96 well.

Proteome Profiler Antibody Arrays: phosphor-kinase array, phosphor-receptor tyrosine kinase array.

CELLutions Biosystems, Ontario, Canada: Human cerebral microvascular endothelial cell/D3.

eBioscience, Hatfield, UK: Calcein acetoxymethyl (AM) viability dye (ultrapure grade).

Enzo LifeSciences, Exeter, UK: Cathepsin D & E substrate- fluorogenic, Cathepsin L fluorogenic substrate (Z-VVR-AMC), Collagen type 1 (rat tail).

Fisher Scientific, Loughborough, UK: Formaldehyde 16% (Methanol-free), Molecular Probes™ CellLight™ Golgi-GFP- BacMam 2.0, Cyquant NF cell proliferation kit, Corning™ Costar™ Flat Bottom Cell Culture Plates 6 well plate, Corning™ Matrigel™ Membrane Matrix GFR 10ml, GlycoBlue, Gibco™ Collagenase- Type I (powder), Gibco™ Collagenase- Type II (powder), CD31 dynabeads, RNaseZap® RNase decontamination solution, Sodium Chloride, Nuclease-Free water, BCA assay.

Greiner Bio-One Ltd, Gloucestershire, UK: Cell culture plastic-ware.

Lonza, Wokingham, UK: PBS (without/with Ca^{2+}, Mg^{2+}).

Merck Chemicals, Nottingham, UK: Aprotinin, Thrombin (bovine), Cathepsin L (human liver), Pepstatin A, CathL inhibitor Z-Phe-Tyr-CHO (FY-CHO), swinnex filter holders, millex® 0.22 µm filter units, nylon net filters 30 µm, Fibrinogen, Dithiothreitol (DTT).

PeproTech: Human VEGF165, recombinant human galectin 1.

Primerdesign Ltd, Chandler's Ford, UK: Precision DNase kit, PrecisionPLUS master.

Promocell, Heidelberg, Germany: EC growth medium MV2 and supplementation (Foetus calf serum (FCS), EC growth factor kit).

Quanta Biosciences, USA: qScript cDNA Supermix kit.

Roche Diagnostics Ltd, West Sussex, UK: WST-1 reagent.

Santa Cruz Biotechnology (Heidelberg, Germany): Mouse monoclonal anti-human endoglin (CD105) antibody (SN6/N1-3A1).

Sarstedt, Leicester, UK: cell culture plastic-ware.

Stratech Scientifc Ltd (Selleckchem) Newmarket, UK: Kinase inhibitors- U0126, PD98059, LY294002, MK2206; NFκB inhibitor: Sulfasalazine.

Sigma Aldrich, Gillingham, UK: Haemocytometer, Hank's balanced salt solution (HBSS), Trypsin, Cathepsin D from human liver, Bovine Serum Albumin (BSA), L-glucose, D-glucose, Gentamicin (50mg/ml), Dimethyl sulfoxide (DMSO), Gelatin type B (bovine skin), HEPES, TRI Reagent, SU5416, Sodium phosphate dibasic (Na_2HPO_4), Citric Acid, 96 well plates black flat bottom (non-sterile), diethyl pyrocarbonate (DEPC), Tween® 20, Golgi apparatus transportation blocker: Brefeldin A, Calcium chloride ($CaCl_2$) solution (1M), Potassium chloride (KCl), Cytodex 1 bead, Cytodex 3 bead, goat anti-mouse IgG-FITC conjugated, rabbit anti-human von Willebrand Factor (vWF) IgG fraction of antiserum.

Thermo Fischer Scientific, Northumberland, UK: TaqMan® gene expression assays (primers)-LGALS1, GAPDH, B2M (β2-microglobulin), CellLight® Golgi-GFP, BacMam 2.0.

2.2 Buffers and solutions

2.2.1 Cell culture solutions

Complete growth media for HOMECs/HCMECs

Endothelial cell basal medium MV2

FCS (heat inactivated)	5% (v/v)
Gentamicin	50 µg/ml

Endothelial cell growth MV2 kit

$VEGF_{165}$	0.5ng/ml
Human EGF	5ng/ml
Human bFGF	10ng/ml
IGF1	20ng/ml
Ascorbic acid	1µg/ml
Hydrocortisone	0.2µg/ml

Experimental and starvation media for HOMECs/HCMECs (unless otherwise stated)

Endothelial cell basal medium MV2

FBS (heat inactivated)	2% (v/v)
Gentamicin	50µg/ml

Freezing solution for HOMECs

Growth Media	20% (v/v)
FBS	70% (v/v)
DMSO	10% (v/v)

For primary cultures of HOMECs tissue culture plastic ware was coated with gelatin:

Gelatin type B (bovine skin)	2% w/v

Dissolved in ddH_2O and then autoclaved and sterile filtered (while still warm)

For culturing HCMECs tissue culture plastic ware was coated with collagen:

Collagen solution, type I from rat tail	4mg/ml

Diluted stock 1:30 in PBS

HOMEC isolation solutions

Omental samples were collected in medium consisting of:

HBSS	50ml
Amphotericin B	250µg/ml
HEPES solution	10 µM
Gentamicin	50µg/ml

Digest solution 1 (stored at -20C)

The following reagents were dissolved in deionised water by stirring using a magnetic stirrer. The final volume was 100ml.

0.7g NaCl

0.373g KCL

0.09g D-glucose

0.595g HEPES

1.5g BSA

150mg (0.15g) **collagenase type 1**

100µl of 1M $CaCl_2$

Digest solution 2 (stored at -20C)

The following reagents were dissolved in deionised water by stirring using a magnetic stirrer. The final volume was 100ml.

0.7g NaCl

0.373g KCL

0.09g D-glucose

0.595g HEPES

1.5g BSA

150mg (0.15g) **collagenase type 2**

100µl of 1M $CaCl_2$

BSA solution for HOMEC isolation (sterile filtered)

BSA/PBS	10% and 0.1% w/v

2.3 Cell culture

2.3.1 HOMEC isolation

Non-malignant omental tissue samples were collected from non-diabetic female patients undergoing routine abdominal invasive procedures at the Royal Devon and Exeter NHS Foundation Trust (Exeter, United Kingdom) with ethical approval and informed written consent. However, information on tumour or cancer diagnosis of any origin and their ethnicities were not provided by the clinical research facility. HOMECs were isolated and cultured as previously described (Winiarski et al., 2011). Briefly, omental tissue was chopped into approximately 1g segments and digested using digest solution 2. Next, digested tissue was chopped into $6mm^2$ and further digested using digest solution 1. Digested tissue was passed through a sterile gauze to remove undigested tissue and the filtrate was then centrifuged to separate layers of cells, oil and digest solution. After discarding oil and digest solution, the cell pellet was resuspended in ice-cold 10% (w/v) BSA and washed in ice-cold PBS. Next, the cell pellet was resuspended in serum free basal EC growth media MV2 and filtered through a 30 µm nylon swinnex filter. Immunoselection was carried out using anti-CD31 dynabeads to isolate pure HOMECs from the mixture and CD31-bead-bound HOMECs were then cultured and subcultured in complete EC growth media.

2.3.2 HOMEC characterisation

Prior to their use, the HOMECs were characterised by immunocytochemistry techniques to confirm their EC origin (data not shown) as previously described (Winiarski et al., 2011). Briefly, HOMEC monolayer was stained either for cell surface proteins CD31 (mouse monoclonal anti-human) and CD105 (mouse monoclonal anti-human) or for intracellular protein von Willebrand factor (vWF) (rabbit anti-human antibody). A FITC-conjugated secondary antibody (anti-mouse IgG or anti-rabbit IgG) was utilised against corresponding primary antibody staining. Counterstaining of nuclei was performed with DAPI. Cells were washed in PBS (x2) and distilled water and mounted using fluorescence mounting medium with coverslips. To avoid false positives produced by non-specific binding of secondary antibodies, control cells were treated in a similar manner with PBS substituting for primary antibody. The cells were then assessed for fluorescence using an inverted fluorescence microscope (Nikon).

2.3.3 Cell culturing

For all experiments human microvascular omental (HOMECs) and brain (HCMECs) endothelial cells were maintained at 37˚C in a humidified incubator with 5% CO_2.

HOMECs/HCMECs were passaged by trypsinisation when they reached >90% confluency in the tissue culture flasks. The medium was removed and the cells were washed twice with PBS followed by addition of 2 ml trypsin solution (0.2mg/ml). The cells were placed in the incubator at 37˚C for 2-3 minutes. Detachment was monitored by microscope until cells could be seen floating in the trypsin solution. Trypsin was then neutralized by the addition of 8 ml of growth medium (containing 5% (v/v) FCS) and cell suspension was transferred to a tube and centrifuged at 200 *g* for 5 minutes. The supernatant was removed and the cells were resuspended in complete growth medium. Required amount of cells was plated into tissue culture flask (75cm^2 [T75]) and the total volume of medium was filled up to 12ml for T75. The endothelial cells were split at a ratio of 1:2 or 1:3 and fed every 2-3 days. The HOMECs were only used between passage 3 and 7, while the HCMECs were between passages 27 and 35.

It is important to note that, the oxygen concentration in the body is much lower than in the atmospheric air. For instance, oxygen can range from 0.5 to 7% in brain, 4-12% in the liver, heart and kidneys (Ivanovic, 2009). In tumour microenvironment, oxygen concentration can be reduced, known as hypoxia. Therefore, growing ECs in 20% oxygen (atmospheric) may influence the phenotype of the cells in cell culture and, therefore, may not replicate the *in vivo* situation. This can be overcome by using a hypoxic incubator where the oxygen concentration can be lowered to 0.5-1%, making it more physiological. Hence, this was a limitation of this study.

2.3.4 Freezing cells

Cells were trypsinised, centrifuged and resuspended (~$2x10^6$ cells) in 1ml freezing medium. The cell suspension was transferred into sterile labelled vials, which were then placed in a cryocontainer containing isopropanol and stored at -80˚C overnight for slow cooling. Frozen vials were ultimately transferred into liquid nitrogen for long term storage.

2.3.5 Thawing cells

The frozen cells in cryovials were rapidly thawed by placing in a 37˚C water bath. Thereafter, the cells were slowly diluted in 12mls of pre-warmed growth medium and plated in T75 flasks (gelatin-coated for HOMECs and collagen-coated for HCMECs). The medium was replaced after cell attachment (usually 24 hours) in order to remove the DMSO used during freezing.

2.4 Cell viability and proliferation assays

The assessment of cell proliferation and growth (whether as a result of a proliferative response to certain molecules [increased DNA synthesis], or a reduction in cell death) was performed in cell populations using two independent commercially available assays: WST-1 and CyQUANT. WST1 assay is based on cleavage of the tetrazolium salts added to the cell culture media. The tetrazolium salts are cleaved to formazan by the cellular enzymes of metabolically active

cells. The resulting formazan is dissolved to form a colour, which is spectrophotometrically measured. Quantification of the formazan dye corresponds to the number of metabolically active cells.

CyQUANT assay is a highly sensitive fluorescence-based method for quantifying cells and assessing cell proliferation and cytotoxicity. The main component of the Kit is CyQUANT® GR, a proprietary dye that exhibits strong fluorescence enhancement when bound to nucleic acids. The amount of fluorescence detection is a measure of a sample's DNA content i.e. directly quantifying the entire cell population within a broad linear detection range. This method offers improved accuracy over metabolically based cell proliferation or cytotoxicity assays that can be influenced by cell changes that are unrelated to cell number.

2.4.1 WST1 assay

2.4.1.1 Cell seeding and treatments

HOMECs (between passage 3 and 7) were plated onto 2% (w/v) gelatin coated 96-well plates (flat bottom microplates, 10,000cells/well) over-night in 100µl/well MV2 medium supplemented with 2% (v/v) FCS only. Cultures were maintained at 37˚C in a humidified incubator with 5% CO_2. The medium was then aspirated, the plates were washed once with PBS, and fresh medium was applied to the wells (100µl/well). Depending on the experimental procedure, MV2 (containing 2% (v/v) FCS) medium was supplemented with various growth factors and/or compounds, i.e. ± DMSO (vehicle control), inhibitors (Table 2.1) and/or growth factors (positive control 20ng/ml of VEGF, 20-80ng/ml of CathL, 5-125ng/ml of Gal1, 20-80ng/ml of CathD and 10-50 ng/ml of IGFBP7). HOMECs were treated with freshly applied media for 24, 48 and 72 hours as described.

Table 2.1: List of commercially available compounds and their experimental concentrations in µM (unless otherwise stated).

Targets	Compounds	Concentrations (µM)

CathL enzymatic activity	FY-CHO	0.1, 1, 10, 50, 100
CathD enzymatic activity	pepA	0.1, 1, 2.5, 5, 10
ERK1/2	U0126	1, 10, 25
	PD98059	1, 10, 25
PI3K	LY294002	1, 25, 50
AKT	MK2206	1, 3, 5
NFκB	Sulfasalazine	50, 100, 200
Golgi bodies	Brefeldin A	0.025, 0.1, 0.5, 1, 5, 10, 20
Gal1	L-glu	25 mM, 50 mM
VEGFR2	SU5416	10 µM

Cell toxicity induced by compounds was also tested using WST1 assay (Table 2.1). Cell seeding was carried out in an identical manner. However, cell viability was tested over 24 hours after treated with the compounds.

2.4.1.2 WST1 assay procedure

After incubation, pre-warmed (room temperature) WST-1 reagent was added to each sample/blank well (10µl/well) on the cell culture plates. As a blank, serum free MV2 medium was used (100µ/well). WST-1 was incubated with HOMECs for 2 hours at 37˚C in a humidified incubator with 5% CO_2, followed by measurement of the absorbance against the background blank on a microplate reader PHERAstar Plus, (BMG Labtech Ltd, Bucks, UK) (set at 450nm).

2.4.2 CyQUANT assay

2.4.2.1 Cell seeding and treatments

As described in 2.4.1.1 of the WST1 assay.

2.4.2.2 CyQUANT assay procedure

This procedure was performed according the manufacturers instruction. Briefly, after 72 hour treatment, media was removed from each well, followed by addition of the dye binding solution (1X HBSS buffer) containing CyQUANT NF dye reagent. The plates were incubated for 2 hours in a humidified incubator at 37˚C with 5% CO_2. The plates were then read at Ex/Em: 485/530 using a FLUOstar

BMG plate-reader (BMG Labtech Ltd, Bucks, UK) and cell proliferation was assessed based on the fluorescence intensity against the background containing HBSS buffer.

2.5 Cell migration using Cultrex migration assay

The Cultrex migration assay kit is based on the principle of a filter assay (Boyden chamber). It involves a two-compartment system where cells may be induced to migrate from an upper compartment (insert), through a porous membrane, into a lower compartment (plate well). Both chemokinesis and chemotaxis can be assessed using this assay kit. In these studies, a 96-well plate format was used with cell inserts containing an 8 μm pore-size membrane.

2.5.1 Protocol for Cultrex migration assay

HOMECs were seeded into the cell culture inserts ($5x10^4$ cells/insert) in a total volume of 50μl MV2 (supplemented with 0.5% (v/v) FCS ± growth factors/inhibitors) medium. Into the lower compartments MV2 (0.5% (v/v) FCS) medium (150μl/well) was added supplemented with or without various compounds. The final concentrations of the growth factors and inhibitors are shown in tables 2.2 and 2.3**.**

In order to carry out inhibition of migration studies, HOMECs were pre-treated with inhibitors of ERK1/2 or PI3K/AKT inhibitors for 30 minutes to 1 hour. These cells were seeded into the inserts (as described above) and their corresponding treatments were added with or without growth factors, for instance, VEGF ± an inhibitor. The control wells contained MV2 media supplemented with 0.5% (v/v) FCS ± corresponding inhibitor in both compartments. Each condition was carried out in triplicate. All conditions were then incubated for 6 hours at 37˚C in a humidified incubator with 5% CO_2, to allow HOMECs migration.

After 6 hours incubation, the media was aspirated out from both compartments and both upper and lower chambers were washed with pre-warmed PBS. Cell dissociation solution was supplemented with 2 μM calcein AM dye and added to the bottom chamber of the well (100μl/well), and incubated for 1 hour. This allowed dissociation and labelling of migrated cells on the underside of the

inserts. The solution was the transferred to a black opaque 96-well plate and read using a FLUOstar BMG plate reader at Ex/Em: 485/520.

Table 2.2: Experimental concentrations of growth factors used in migration assay.

VEGF	CathL	Gal1	CathD	IGFBP7
20ng/ml	50ng/ml	50ng/ml	50ng/ml	50ng/ml

Table 2.3: Experimental concentrations of inhibitory compounds used in migration assay.

MAPK/ERK1/2 inhibitors		PI3K inhibitor	AKT inhibitor	Gal1 inhibitor
U0126	PD98059	LY294002	MK2206	L-glucose
10 µM	25 µM	25 µM	5 µM	25 mM

2.6 pH studies

The proteolytic activity of CathL and CathD was tested at an array of pHs. This required preparing pH buffer solutions as shown in table 2.4. The pH of cultured media was also measured over time. The pHs of both the cultured media and buffers were measured down to 2 decimal places in 100µl of media/buffer using blood-gas analyser ABL800 FLEX (Radiometer, Akandevej, Denmark). The pH buffer was kept the same for both CathL and CathD experiments.

The stock solutions of both acid and base were prepared as follows:

21.01g citric acid monohydrate to 1 L distilled water

28.40g sodium phosphate dibasic (Na_2HPO_4) in 1 L distilled water

Table 2.4: Preparation of buffer solutions at an array of pHs (derived from buffer reference centre, Sigma-Aldrich). Final volume of each pH buffer was 50ml containing freshly prepared 1 mM DTT (CathL proteolysis assay) or 0.005% (v/v) Tween 20 (CathD proteolysis assay).

pH	Citric acid (ml)		Na_2HPO_4 (ml)
3.0	39.725	+	10.275
3.6	33.900	+	16.100
4.0	30.725	+	19.275
4.6	26.625	+	23.375
5.0	24.250	+	25.750
5.6	21.000	+	29.000
6.0	18.425	+	31.575
6.6	13.625	+	36.375
7.0	8.825	+	41.175
7.6	3.175	+	46.825

2.6.1 CathL proteolytic activity

CathL fluorogenic substrate Z-Val-Val-Arg-AMC (ZVA) 10mg was reconstituted in 150.6µl DMSO to produce a 100 mM stock solution. This was further diluted to a final concentration of 5 µM in individual pH buffer. Substrate and substrate-pH buffer solution were protected from light.

CathL inhibitor Z-Phe-Tyr-CHO (FY-CHO) 2mg was reconstituted in 45µl of DMSO to produce a stock solution of 100 mM. The stock solution was diluted further to final concentration of 10 µM in individual pH buffer solution with or without ZVA.

CathL 336µg/ml (20 mM malonate, pH 5.5, 1 mM EDTA, and 400 mM NaCl) was diluted to produce 300ng/ml in individual pH buffer before dispensing in to the test wells. The experiment was carried out in 96 well black opaque plates. The conditions were as follows (Tables 2.5 and 2.6):

Table 2.5: Experimental conditions for testing CathL proteolytic activity.

	Control wells	Test wells
ZVA	+	+
CathL	-	+

Table 2.6: Experimental conditions for examining inhibition of CathL proteolytic activity:

	Control wells	Test wells
ZVA	+	+
FY-CHO	+	+
CathL	-	+

Procedure:

To test the proteolytic activity of CathL, 100µl of substrate (ZVA) pH buffer solution was dispensed in to both control and test wells. Each condition was run in quadruplets per plate. Finally, 20µl of corresponding pH buffer was added to each control well and 20µl of enzyme solution (300ng/ml) was added to all test wells to obtain a final concentration of 50ng/ml of CathL. Plates were shaken for 2 minutes at room temperature and read immediately using a SpectraMAX plate reader (Molecular Devices, Berkshire, UK) at Ex/Em: 365/440.

In order to test for inhibition of CathL-mediated substrate breakdown, 100µl of solution containing ZVA and FY-CHO was dispensed in both control and test wells. Finally, 20µl of 300ng/ml CathL or 20µl corresponding pH buffer was added to test or control wells respectively, followed by shaking and reading plate as described above.

2.6.2 CathD proteolytic activity

CathD fluorogenic substrate 1mg was reconstituted in 570µl DMSO to produce a 10 mM stock concentration which was further diluted into 100 nM (final concentration) in individual pH buffer. Substrate and substrate-pH buffer solution were protected from light.

Inhibitor of CathD proteolytic activity pepA (5mg) was reconstituted in 363.5µl DMSO, producing a stock solution of 20 mM (stored at -20 ˚C). This was further diluted to produce a final concentration of 1 µM in individual buffer containing CathD substrate. This concentration (1 µM) was recommended by the supplier (Calbiochem, Millipore) to be the effective concentration.

CathD was diluted from its stock solution (50µg/ml) to a working concentration 300ng/ml, which was added (20µl/well) to the wells containing 100µl buffer (substrate + pepA) producing a final concentration 50ng/ml in final volume

120µl/well. The experiment was carried out in 96 well black opaque plates. The conditions were as follows (tables 2.7 and 2.8):

Table 2.7: Experimental conditions for testing CathD proteolytic activity.

	Control wells	Test wells
Substrate	+	+
CathD	-	+

Table 2.8: Experimental conditions for examining inhibition of CathD proteolytic activity:

	Control wells	Test wells
Substrate	+	+
PepA	+	+
CathD	-	+

To test the proteolytic activity of CathD, 100µl of pH buffer solution containing fluorogenic substrate (100 nM) was dispensed into both control and test wells. Each condition was run in quadruplets per plate. Finally, 20µl of corresponding pH buffer or enzyme solution (300ng/ml) was added to control or test wells to obtain a final concentration of 50ng/ml of CathD. Plates were shaken for 2 minutes at room temperature and read immediately using a SpectraMAX plate reader at Ex/Em: 320/393.

Inhibition of CathD-proteolytic activity was examined in the presence of an inhibitor pepA. pH buffer solutions containing CathD-fluorogenic substrate (100 nM) and pepA (1 µM) were dispensed in a 96 well plate, followed by addition of 20µl of the corresponding pH buffer or CathD (50ng/ml) in the control or test wells respectively. The plate was shaken and read as described above.

2.7 Molecular biology

2.7.1 Protein quantification- bicinchoninic acid (BCA) assay

Protein quantification was performed using a colorimetric BCA protein assay kit according to the manufacturer's instruction. Briefly, in a 96-well flat-bottom microtiter plate, 10µl of standard or each lysate sample was added to 200µl of working reagent (50 parts of reagent A to 1 part of reagent B). The plate was incubated at 37 ˚C for 30 minutes and absorbance was measured at 562 nm. Protein concentration calculated using a standard curve of bovine serum albumin (BSA) (Figure 2.1). Final concentration was calculated from the linear regression equation.

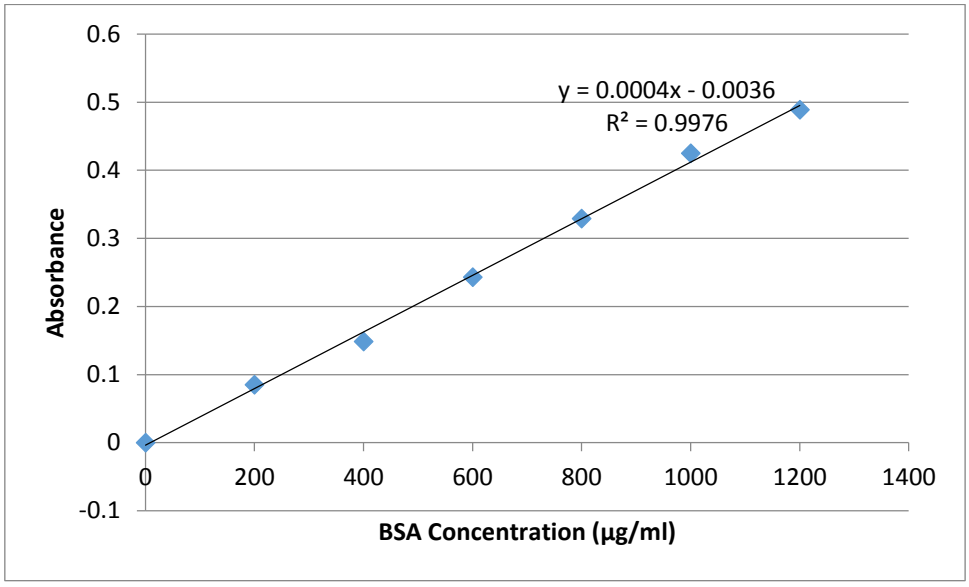

Figure 2.1: **Standard curve derived from BCA protein assay**.

2.7.2 Proteome Profiler Human Phospho-Kinase Array kit

HOMECs were seeded in 10cm^2 dishes and cultured until confluent. Cells were treated with or without CathL, CathD and IGFBP7 supplemented in EC basal media containing 2% (v/v) FCS for 4 minutes, washed once with ice cold PBS and scraped in lysis buffer (provided in kit). Cell lysates were incubated on a rocker at 4˚C for 30 minutes and centrifuged (14,000g) for 5 minutes at 4˚C. Supernatants were collected into fresh microcentrifuge tubes and total protein concentration was determined with the BCA assay. Lysates were stored at -80˚C or experimented immediately according to the manufacturer's instructions. 200µg

cell lysate was added to each membrane. Dot blots were detected via enhanced chemiluminescence using Kodak films (Figure 2.2) Pixel density of the dot blots was analysed using ImageJ software.

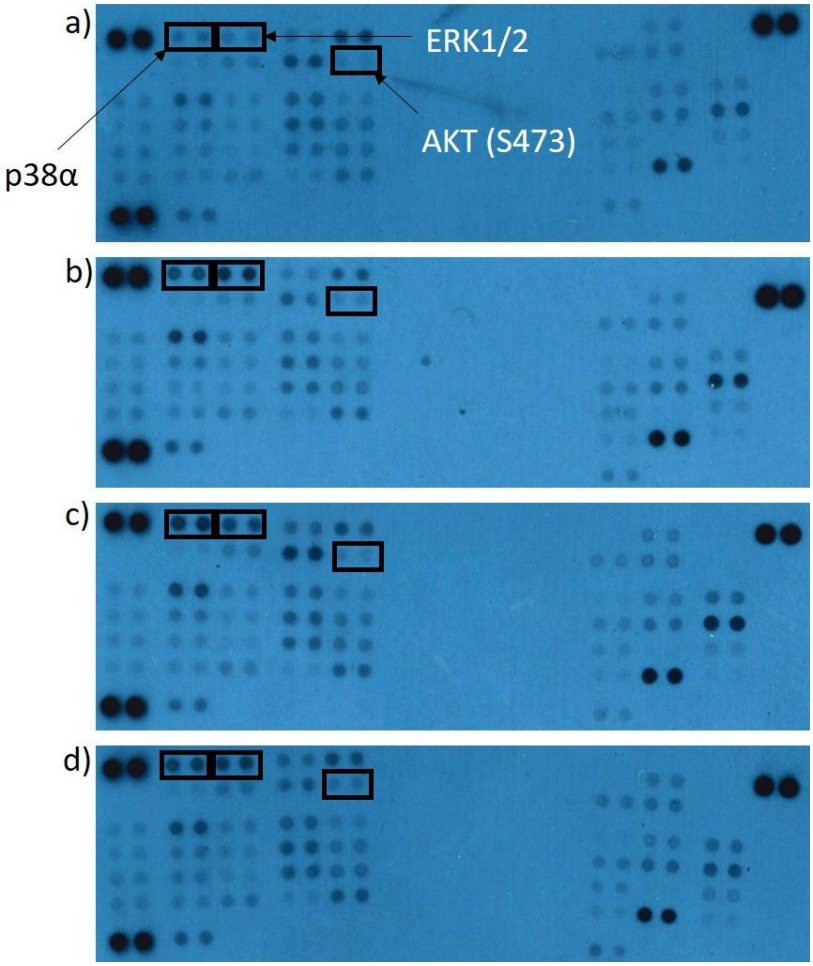

Figure 2.2: **Representation of developed membrane of phosphokinase array data.** a) control (untreated), b) CathL, c) CathD and d) IGFBP7.

2.7.3 Proteome Profiler Human Phospho-Receptor Tyrosine Kinase Array Kit

HOMECs were treated for 10 minutes with or without VEGF, CathL, CathD and IGFBP7, followed by producing cell lysates and total protein quantification (as described in section 2.7.2). The rest of the experiment was performed according to the manufacturer's instructions. The blots were detected via enhanced chemiluminescence using the Azure c600 imaging system. The pixel density of the blots was analysed by AzureSpot.

2.7.4 ELISAs

2.7.4.1 Cell-based ELISAs

Cells were seeded at a density of 10,000 cells per well in a clear bottom black 96 well microplate (provided in the kit). Cells were grown, starved overnight in 2% (v/v) FCS MV2 and treated with various compounds and proteins, followed by fixation with 4% (v/v) methanol free paraformaldehyde (v/v). Fixed cells were permeabilised and levels of phosphorylated and total protein level was determined according to the manufacturer's instructions.

To confirm the inhibitory effect of the inhibitors, HOMECs were pre-incubated with the inhibitors for 20-30 mins (ERK1/2 inhibitors), 1-2 hours (PI3K/AKT inhibitors) and 24 hours (NFκB inhibitor) (Toscano et al., 2011), and then co-treated with or without proangiogenic factors (VEGF, CathL, CathD and IGFBP7) in the absence or presence of the inhibitors for 4 and/or 10 minutes or 4 hours.

The following cell-based ELISAs were performed (Table 2.9):

Table 2.9: Commercially available ELISA kits and their protein targets.

ELISA kit	Treatment time	Target	Source
Phospho-total ERK1/2 (KCB1018)	4 and 10 mins	ERK1(T202/Y204)/2 (T185/Y187)	Biotechne
Phospho-total AKT (KCB887)	4 and 10 mins	AKT(S473)	Biotechne
Phospho-total /NFκB p65 (KCB7226)	4 hours	RelA/NFκB p65 (S536)	Biotechne

2.7.4.2 Human Gal1 Quantikine ELISAs (quantitative sandwich ELISA)

HOMECs were grown, starved overnight and treated with or without CathL for 4 mins, 30 mins, 8 hours and 24 hours. Supernatants were collected, centrifuged at 200 *g* for 10 mins, and transferred into new microfuge tubes which were either stored at -20˚C for future experiments or immediately used to detect levels of Gal1. The assay was carried out according to the manufacturer's instructions.

2.7.4.2.1 Inhibition of Gal1 secretion

HOMECs were pre-treated with the NFκB inhibitor sulfasalazine (100nM) for 24 hours, followed by co-incubation with or without CathL. The cell culture supernatant was collected after 8 hours treatment. Levels of Gal1 was quantified as described in section 2.7.4.2 and according to the manufacturer's instructions.

2.7.5 Reverse transcription and qRT-PCR

2.7.5.1 Prevention of contamination and RNA degradation

For all appropriate steps of the RNA isolation protocol, molecular biology grade chemicals were used and deionised water was pre-treated with 0.1% (v/v) DEPC overnight at room temperature and subsequently autoclaved to deactivate the DEPC. All equipment was thoroughly cleaned with RNaseZap and filtered, nuclease free pipette tips were used to minimise RNA degradation and contamination of the samples with foreign nuclear material.

2.7.5.2 RNA extraction

Cells were grown in a 6 well plate, starved overnight in 2% (v/v) FCS MV2 medium and then treated with CathL (also in 2% (v/v) FCS MV2 medium) for 8 or 24 hours in the presence or absence of sulfasalazine. Total RNA from cell cultures was isolated with TRI Reagent as per manufacturer's protocol. TRI Reagent is a solution of phenol and guanidine isothiocyanate that disrupts cell membrane and dissolves cell components while preserving the integrity of RNA and other nucleic acids. Medium supplemented with or without treatment was removed and TRI Reagent (500µl/well) was added directly onto the surface of culture vessels for cultured cells. Cells were then scraped with a 1ml pipette tip, transferred to a 1.5ml microcentrifuge tube, and treated directly for RNA extraction or stored at -80˚C until needed.

For mRNA extraction, the samples were incubated for 5 minutes at room temperature. 200µl of chloroform per mL TRI Reagent lysate was added, after which the sample was vortexed vigorously and incubated for 10 minutes at room temperature. This incubation allows the formation of an organic phase (containing proteins), an interphase (containing DNA), and an aqueous phase (containing RNA). The tubes were centrifuged at 13000 *g*, 4°C for 15 minutes to firmly

separate the layers. The aqueous phase was removed to a new 1.5 mL tube and combined with 500µl isopropanol (per 1ml TRI Reagent) and 1µl Glycoblue co-precipitant. The addition of 2-propanol changes the solute balance of the solution which causes the RNA to precipitate out of solution. The samples were inverted to mix and incubated at room temperature for 10 minutes to allow full precipitation and spun again at 12000 *g*, 4°C for 12 minutes to pellet the RNA. The supernatants were discarded and the pellets were washed with 500µl of 75% (v/v) ethanol (per 1 ml TRI Reagent), inverted to mix and spun at 10000 *g*, 4°C, for 10 minutes. After the supernatant was removed, the pellets were air dried and dissolved in 10µl nuclease free water.

2.7.5.3 DNase treatment

Contaminating genomic DNA was removed using a Precision DNase kit (according to the manufacturer's instructions). For each sample, 1.2µl 10x reaction buffer (per 10µl sample) and 1µl DNase enzyme were added to the RNA samples. Samples were then incubated at 30°C for 10 minutes followed by 55°C for 5 minutes to deactivate the DNase.

The concentration and purity of the RNA was quantified using a Nanodrop 8000 spectrophotometer (Thermo Scientific, USA). The ratio of the absorbance at 260nm to the absorbance at 280nm (A260/A280) was used as a measure of RNA concentration (ng/µl) of the sample. A ratio of 2 was considered ideal with a range from 1.9 to 2 considered acceptable. These RNA samples were immediately used for c-DNA synthesis, followed by RT-PCR or stored at -80˚C until needed.

2.7.5.4 cDNA synthesis

Total RNA was reverse transcribed into cDNA using the qScript cDNA Supermix kit. As per manufacturer instructions, up to 1µg of RNA was diluted up to a volume of 20 µl containing the following reagents (cDNA synthesis master mix) (Table 2.10).

Table 2.10: List of reagents and their volumes per reaction in cDNA synthesis master mix.

Reagent	Volume per Reaction
qScript 5X Reaction Mix	4.0µl
qScript Reverse Transcriptase	1.0µl
RNA sample	10pg – 1µg total RNA
Nuclease free water	Up to 20.0µl
Total Volume	20.0µl

The samples and mixtures were pulse vortexed. Reverse transcription was then performed under the following conditions: 22°C for 5 minutes, 42°C for 30 minutes, 85°C for 5 minutes with a 4˚C hold. cDNA was produced which can be stored at -80˚C or used immediately.

2.7.5.5 RT-PCR

In order to perform RT-PCR, firstly, 20X TaqMan gene expression (genes of interest and reference genes- GAPDH and β2M), and PrecisionPLUS master mix were defrosted on ice. A RT-PCR master mix (8µl) was made for each well of a 96 well plate with the following constituents (Table 2.11):

Table 2.11: List of reagents and their volume per reaction in RT-PCR master mix.

Reagent	Volume per Reaction
20X TaqMan Primer	0.5 µl
PrecisionPLUS Master mix	5 µl
Nuclease free water	2.5 µl
Total Volume	8.0 µl

2µl of cDNA sample was dispensed into each well containing 8µl of master mix, to make a total volume of 10µl. An optical adhesive seal was applied on the plate to prevent spillage of the sample. This plate was then spun for 1 min in a plate centrifuge to pellet down the mixture. DNA polymerase was activated for 5 minutes at 95°C followed by amplification cycling as shown in Table 2.12. Fluorescence was measured at the end of each 60°C step.

Table 2.12: Stages of cDNA amplification cycles.

Program	Cycles	Step
Preincubation	1	95°C for 120 secs
2 step amplification	40	95°C for 10 secs
		60°C for 30 secs
Cooling	1	37°C for 30 secs

Specificity of the amplification was confirmed by examining a melt curve of the reaction. Following amplification, a melting curve analysis was performed by slowly increasing the temperature from 60°C to 95°C while measuring fluorescence (data not shown). TaqMan probes rely on the 5′– 3′ nuclease activity of *Taq* DNA polymerase to cleave a dual-labelled probe during hybridisation to the complementary target sequence. These fluorogenic hybridisation probes include a re-porter dye i.e. FAM (6-carboxyfluorescein) covalently linked to the 5′ end whose emission spectra is quenched by a second dye i.e. TAMRA (6-carboxytetramethylrhodamine), covalently linked to the 3′ end. During a PCR cycle, the probe specifically hybridises to the corresponding template, cleaves via the 5′ to 3′exonuclease activity of *Taq* DNA polymerase and subsequently increases the FAM fluorescent emission. The increase in fluorescence is proportional to the amount of specific PCR product as the exonuclease activity of *Taq* polymerase acts only if the fluorogenic probe is annealed to the target.

Quantitative differences in mRNA expression between treated and untreated HOMECs were determined using the Cp (crossing point at which the amplification curve crosses the vertical threshold line) value for each target and normalised to the geometric mean of the Cp of at least two commercial housekeeping genes (GAPDH and β2M) (both Primer Design, UK). Fold change in expression was calculated using the standard 2-ΔΔCp method.

2.8 Angiogenesis

2.8.1 Optimising 3D angiogenesis

To investigate the angiogenic potential of EOC secreted factors, an *in vitro* 3D angiogenesis model was utilised. The experimental design of this assay is based on the fibrin matrix gel which was previously published by Nakatsu *et al.* (Nakatsu et al., 2007). Briefly, cytodex 3 (collagen pre-coated) or cytodex 1 (coated with gelatin) beads were coated with approximately 400 HOMECs or HCMECs (per bead). Cell-coated beads were counted and resuspended in fibrinogen (1.82mg/ml)/aprotinin (0, 0.07 or 0.14 U/ml) solution at a concentration of approximately 500 beads/ml. Thrombin solution (0.60 U/ml) was added to each well, followed by addition and careful mixing of the fibrinogen/beads suspension to each well of a 24 well plate. Thrombin converts fibrinogen to fibrin forming a tight matrix. Once the gel was formed, media supplemented with the following treatments were added on top of the 3D matrix (Table 2.13) and media/treatments was replaced every other day up to day 5. Photographs were taken using a Nikon phase-contrast microscope (Nikon UK Limited, Surrey, UK) at 10X magnification.

The protocol was carried out in an identical manner as described above with the exceptions of the following optimisation steps. Due to a lack of responsiveness to the treatments (stage 1; Table 2.13), increasing concentrations of FCS were used to examine HOMEC sprouting (stage 2; Table 2.14). Various concentrations of aprotinin (protease inhibitor), along with a different bead (gelatin-coated cytodex 1) were utilised to test for HOMEC sprouting in the fibrin gel (Table 2.15) in media containing 5% (v/v) FCS with or without supplemented EC growth factors (stage 3).

Table 2.13: Conditions for 3D beads angiogenesis assay using HCMECs and HOMECs

HCMECs and HOMECs			ng/ml in 2% v/v FCS basal medium			
Optimisation stage 1	Control	Positive control	VEGF	CathL	CathD	IGFBP7
	2% v/v FCS	5% v/v FCS	20	50	50	50

Table 2.14: Increasing FCS concentrations to test for HOMEC angiogenesis in 3D assay.

HOMECs	Higher concentrations of FCS

Optimisation stage 2	Control	FCS + Basal or complete EC growth media		
	2% v/v FCS	5% v/v FCS	10% v/v FCS	20% v/v FCS

Table 2.15: Various concentrations used in HOMEC angiogenesis assay.

		(Aprotinin concentrations U/ml)		
Optimisation stage 3	5% v/v FCS basal media	0	0.07	0.14
	5% v/v FCS EC growth media	0	0.07	0.14

2.8.2 2D angiogenesis

2.8.2.1 Fibrin matrix angiogenesis model

An *in* vitro 2D angiogenesis assay was carried out to test for angiogenic tube formation in HOMECs by modifying the protocol from Winiarski *et al.* (Winiarski et al., 2013) To carry out the 2D model, the same fibrin gel was used as above. HOMECs were seeded at 35,000 or 50,000 cells per well in a 48 well plate on top of the gel. After overnight incubation, cells were treated with media supplemented with 2% (v/v) FCS (control media), VEGF (20ng/ml; positive control), CathL (50ng/ml), CathD (50ng/ml) and IGFBP7 (50ng/ml). Photographs were taken at 72 hours after treatment using a Nikon phase contrast microscope camera.

2.8.2.2 Growth factor reduced (GFR) Matrigel model

A commercially available GFR Matrigel was used to examine angiogenic tube formation in HOMECs treated with media supplemented with 2% (v/v) FCS (control media), VEGF (20ng/ml; positive control), CathL (50ng/ml), CathD (50ng/ml) and IGFBP7 (50ng/ml). HOMECs were seeded in 2% (v/v) FCS medium at a density of 50,000 cell per well of a 96 well plate on top of the gel. After a 2 hour incubation, cell culture media was replaced with media supplemented with or without 2% (v/v) FCS (control media), VEGF (20ng/ml; positive control), CathL (50ng/ml), CathD (50ng/ml) and IGFBP7 (50ng/ml) for a further 8 hour incubation at 37°C, 5% CO_2.

Tubular structure formation was analysed at 8 hours after treatment using a Nikon phase contrast microscopy (x4 resolution) and photography (96-well format: 1 photograph taken of the whole well). Quantification of the tube-like structures and nascent tubule-structures was examined using ImageJ grid by two persons. Each point that coincided with a tube-structure or a nascent tubule-structure was recorded. The results were presented as an angiogenic index (AI).

2.9 Staining of the Golgi body

HOMECs were grown in a 6 well plate until 70% confluency. According to the manufacturer's instructions, CellLight® Golgi-GFP, BacMam 2.0 was added to the cultured media and cells were incubated overnight (~16 hours). Next, GFP-transfected cells were treated with BFA (0.025 µM) for 8 hours. Photographs were taken using a Nikon fluoresence microscope (Nikon UK Limited, Surrey, UK) and analysed using ImageJ software.

2.10 Statistical analysis

Statistical analyses were carried out using GraphPad PRISM software 5.04 and Microsoft Office Excel. The Mann Whitney U test was used to test the significance of variables between the two groups. This non-parametric statistical test was chosen over parametric tests due to smaller sample size in these experiments. Also, as the data are presented as percentage of control (100%), there is no normal distribution to perform parametric t-tests. $P<0.05$ was considered statistically significant. The graphical representation of the data was done with mean ± standard deviation (SD).

Chapter 3 Investigation into the proangiogenic changes in HOMECs by Cathepsin L (CathL)

3.1 Introduction

It is well established that tumour-secreted proteins in the tumour microenvironment interact with the host tissue. One of the most significant outcomes of this interaction is enhanced neo-vascularisation of tumours. CathL was previously shown to be secreted by ovarian cancer cell lines SKOV3 and A2780 and to induce proliferation and migration in human omental microvascular endothelial cells (HOMECs), although the mechanisms of action are unknown (Winiarski et al., 2013). Furthermore, CathL has been suggested to be involved in the invasion and metastasis of EOC (Zhang et al., 2014b). Indeed, it was recently shown that the endothelium of vessels within omentum hosting metastatic ovarian high-grade serous carcinoma expressed significantly increased CathL *in vivo* compared with omentum from control patients with benign ovarian cystadenoma (Winiarski et al., 2014).

CathL is a lysosomal protease which is active at an optimum pH of 4.5-5.5. However, CathL has been also shown, in some cases, to be active at neutral pH (Fiebiger et al., 2002). The presence of this protease in the tumour cell secretome and its ability to induce migration and tube-formation in HOMECs (Winiarski et al., 2013) raised important questions (i) does CathL, being a protease, act via its proteolytic activity or a non-proteolytic manner? (ii) what are the signalling pathways activated in inducing cell proliferation and migration?

The literature suggests that CathL can be active as a protease at neutral pH in normal physiological processes and therefore, to answer the former question, CathL-induced HOMEC proliferation was assessed in the presence or absence of an inhibitor of CathL-proteolytic activity. Additionally, in order to address the question of whether CathL is proteolytically active in cell culture media (neutral pH), CathL activity was tested at an array of pHs using a CathL-specific substrate, in the presence or absence of an inhibitor of CathL-proteolytic activity.

The upstream signalling pathways activated during CathL activation of migration and proliferation were examined using several techniques. Initially, a proteome-profiler and cell-based ELISA kits were used to screen and detect activated or phosphorylated levels of intracellular kinases. Kinase-specific inhibitors were then used to investigate whether candidate signalling proteins play a role in CathL-induced proangiogenic effects in HOMECs. Furthermore, tube-structure

formation was assessed when HOMECs were treated with CathL. Finally, receptor targets of CathL was also elucidated in a brief investigation.

3.1.1 Aims

The aims of this chapter are:

- To investigate whether CathL induces HOMEC proliferation in a proteolytic or non-proteolytic manner
- To study potential cell signalling pathways involved in inducing HOMEC proliferation and migration
- To examine angiogenic tube-formation of HOMECs by CathL
- To identify potential receptor targets of CathL in HOMECs

3.2 Methods

HOMEC isolation: HOMECs were isolated according to previously published work (Winiarski et al., 2011) as described in the Method chapter section 2.3.1.

Cell proliferation: HOMEC proliferation was tested using both the WST-1 assay and CyQuant cell proliferation kit as described in the Method chapter sections 2.4.1 and 2.4.2.

CathL-proteolytic activity: The WST-1 assay was used to study CathL-induced HOMEC proliferation in the presence or absence of FY-CHO, a specific inhibitor of CathL-proteolytic activity (Method section 2.4.1). An array of pHs were used to investigate proteolytic activity of CathL in the presence of a CathL-specific fluorogenic substrate and in the presence or absence of FY-CHO, as described in the Method chapter sections 2.6 and 2.6.1. The pH of cultured media was also measured. These pHs were measured down to 2 decimal places in 100µl media/buffer using ABL800 FLEX blood gas analyser.

Activation of intracellular kinases: A commercially available proteome-profiler and cell-based ELISAs were used to detect and assess levels of phosphorylated intracellular kinases as described in the Method chapter sections 2.7.2 and 2.7.4.1.

Cell migration: A commercially available cultrex Boyden chamber kit was used to investigate the underlying mechanisms of CathL-induced HOMEC migration, as described in the Method chapter section 2.5.1.

3D *in vitro* angiogenesis: A 3D angiogenesis model was used to assess HOMEC sprouting as described in the Method chapter section 2.8.1.

2D tube-formation: Angiogenic tube-formation was investigated in HOMECs treated with CathL using both a fibrin matrix assay and commercially available GFR-Matrigel, as described in the Method chapter section 2.8.2.

Identification of potential cell surface receptors: A commercially available human receptor-tyrosine kinase array was used as a screening tool to identify potential receptor as described in the Method chapter section 2.7.3.

3.3 Results

3.3.1 CathL induces HOMEC proliferation

Initially the proliferative effect of CathL in HOMECs was confirmed. A commercially available WST-1 colorimetric assay was used to assess CathL-induced cell proliferation. HOMECs were treated with increasing concentrations of CathL (20, 50 and 80 ng/ml) for 72 hours. CathL significantly increased HOMEC proliferation at 50 and 80ng/ml (167.8± 32.5%, n=50, and 156±40.5%, n=9 vs control (100%) respectively; Figure 3.1), with 50ng/ml being the most effective dose in producing this proangiogenic effect. At 20ng/ml (107.8±38.9%, n=13, vs control (100%); Figure 3.1), CathL did not induce significant HOMEC proliferation compared to control. CathL was not toxic at all concentrations tested. On the basis of this data future experiments were carried out using 50ng/ml of CathL. VEGF was used as a positive control in this assay (Appendix 1, Figure A1.1)

The initial proliferation data was complemented using a CyQUANT kit, which utilises a proprietary green fluorescent dye that exhibits strong fluorescence enhancement when bound to cellular nucleic acids. HOMECs were treated with CathL at 50ng/ml for 72 hours. The data showed an increase in fluorescence intensity which correlates with an escalation of the amount of DNA, and hence demonstrates proliferation of cells (109.1±5.0%, n=20 vs control (100%); Figure

3.2a). VEGF was used as positive control (Appendix 1, Figure A1.2). The data obtained using the CyQUANT kit confirmed the WST-1 proliferation data, and therefore only WST-1 was carried out to investigate cell proliferation/toxicity in the subsequent experiments.

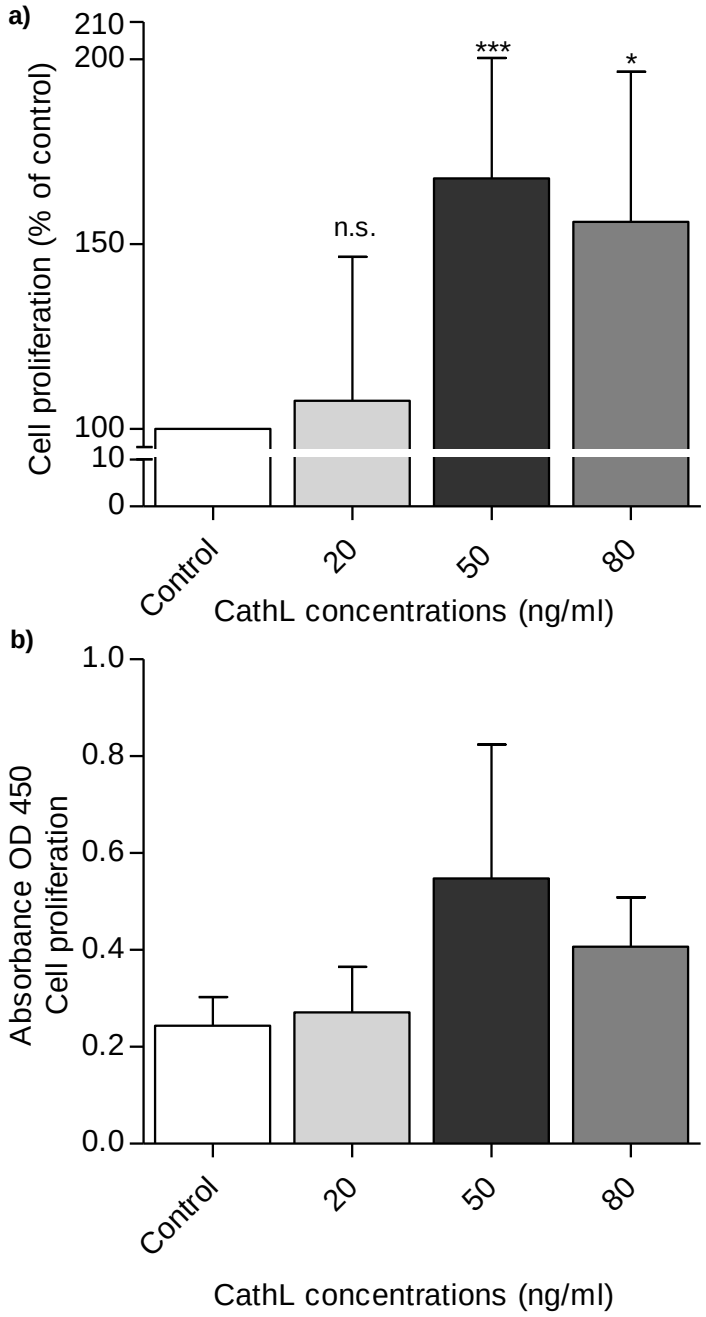

Figure 3.1: **Increased proliferation of HOMECs in media supplemented with CathL (WST-1 assay).** Cells were seeded in 2% gelatin pre-coated 96 well plates at a density of 10,000cells/well in starvation media containing 2% FCS. After overnight incubation, cells were treated with or without various concentrations of CathL and incubated for 72 hours. A commercially available WST-1 kit was used to assess cellular proliferation based on absorbance using PHERAstar BMG plate-reader at 450nm. **a)** Results are mean ±SD and shown as percentage of the control, n.s., *p<0.05, ***p<0.001 vs control (100%), n=9-50. **b)** Raw data from representative experiment. n.s. denotes not significant.

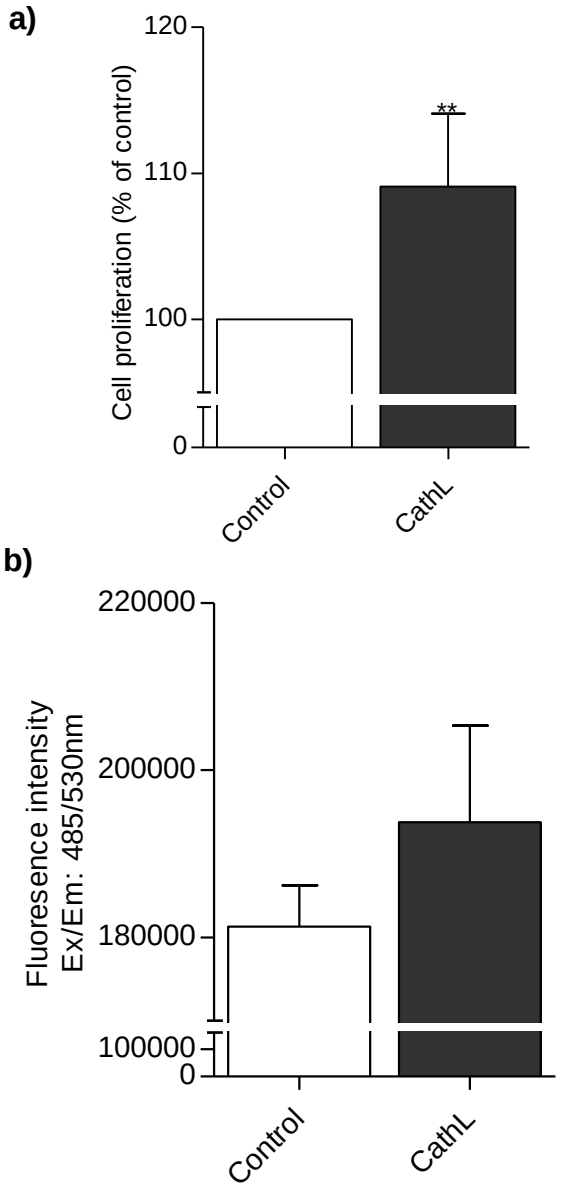

Figure 3.2: **Increased proliferation of HOMECs in media supplemented with CathL (CyQUANT).** Cells were seeded in 2% gelatin pre-coated 96 well plates at a density of 10,000cells/well in starvation media containing 2% FCS. After overnight incubation, cells were treated with or without 50ng/ml of CathL and incubated for 72 hours. A commercially available CyQUANT reagent was used to assess cell proliferation based on fluorescence intensity using FLUOstar BMG plate-reader at Ex/Em: 485/530nm. **a)** Results are mean ±SD and shown as percentage of the control, **p<0.01 vs control (100%), n=20. **b)** Raw data from representative experiment.

3.3.2 CathL induces HOMEC proliferation in a non-proteolytic manner

In normal physiology CathL is active as a lysosomal protease and therefore functions at the pH found in these conditions i.e. pH 4.5-5.5. Since CathL is secreted by EOC cells and has now been shown to induce proliferative changes at neutral pH (from Figures 3.1 and 3.2), it was important to investigate whether CathL is acting in a proteolytic or a non-proteolytic mechanism in HOMECs. Initially, cell proliferation was tested with CathL in the presence or absence of FY-CHO (a specific inhibitor of CathL proteolytic activity) at increasing concentrations over 24, 48 and 72 hours (Figure 3.3a, b), c, d) and e), f) respectively). The data demonstrated that at concentrations up to 10 µM FY-CHO did not inhibit CathL-induced HOMEC proliferation. 50 µM and 100 µM did appear to inhibit CathL-induced proliferation (Figure 3.3 a), c), e); Table 3.1); however, the data shown in figure 3.3 b), d), f) and table 3.1 indicated that FY-CHO was toxic in HOMECs at concentrations higher than 10 µM i.e. at 50 µM and 100 µM at all time points and, hence these concentrations were excluded from further experiments. This set of experiments suggested that CathL is acting in a non-proteolytic manner.

The above data demonstrated that FY-CHO did not inhibit CathL-induced HOMEC proliferation. However, this only means that CathL is not acting in a proteolytic manner if FY-CHO actually inhibits any CathL activity at the pH observed in the tissue culture media (pH 7). Thus, this was investigated further. Initially, the pH of the cell culture media was tested over 24, 48 and 72 hours to confirm that the pH of the media remains unchanged over time. It was found that the pH of the basal media was initially 7.34 and did not reach a lower pH than 7.11 in all conditions tested over time (Table 3.2). It was essential to test for CathL's proteolytic activity at its optimum pH and the ability of the inhibitor to actually inhibit enzyme action. Thus, enzyme activity was tested at a range of pHs using an ionic buffer in the presence of a CathL specific fluorogenic substrate Z-VVR-AMC (5 µM) and in the presence or absence of FY-CHO (10 µM, non—toxic concentration which did not reduce cell proliferation (Table 3.1)). The experiment demonstrated that CathL was active, but with a decreasing trend, from optimum pH 5 to pH 7.6 (Figure 3.4a). This agrees with the current literature which suggests that CathL can be active as a protease at neutral pH. However, the addition of FY-CHO completely abolished CathL-proteolytic activity throughout all pHs (Figure 3.4b), including pH 7. Figure 3.4c) represents a

summary of the proteolytic activity of CathL at pH 5 and pH 7 in the absence or presence of FY-CHO. These combined data suggest that in cell culture media CathL may be proteolytically active but induces HOMEC proliferation by an unknown non-proteolytic mechanism. Since proliferation still occurred in the presence of an inhibitor of CathL-proteolytic activity, it was assumed that CathL was acting as an external ligand, and hence potential downstream signalling pathways were investigated.

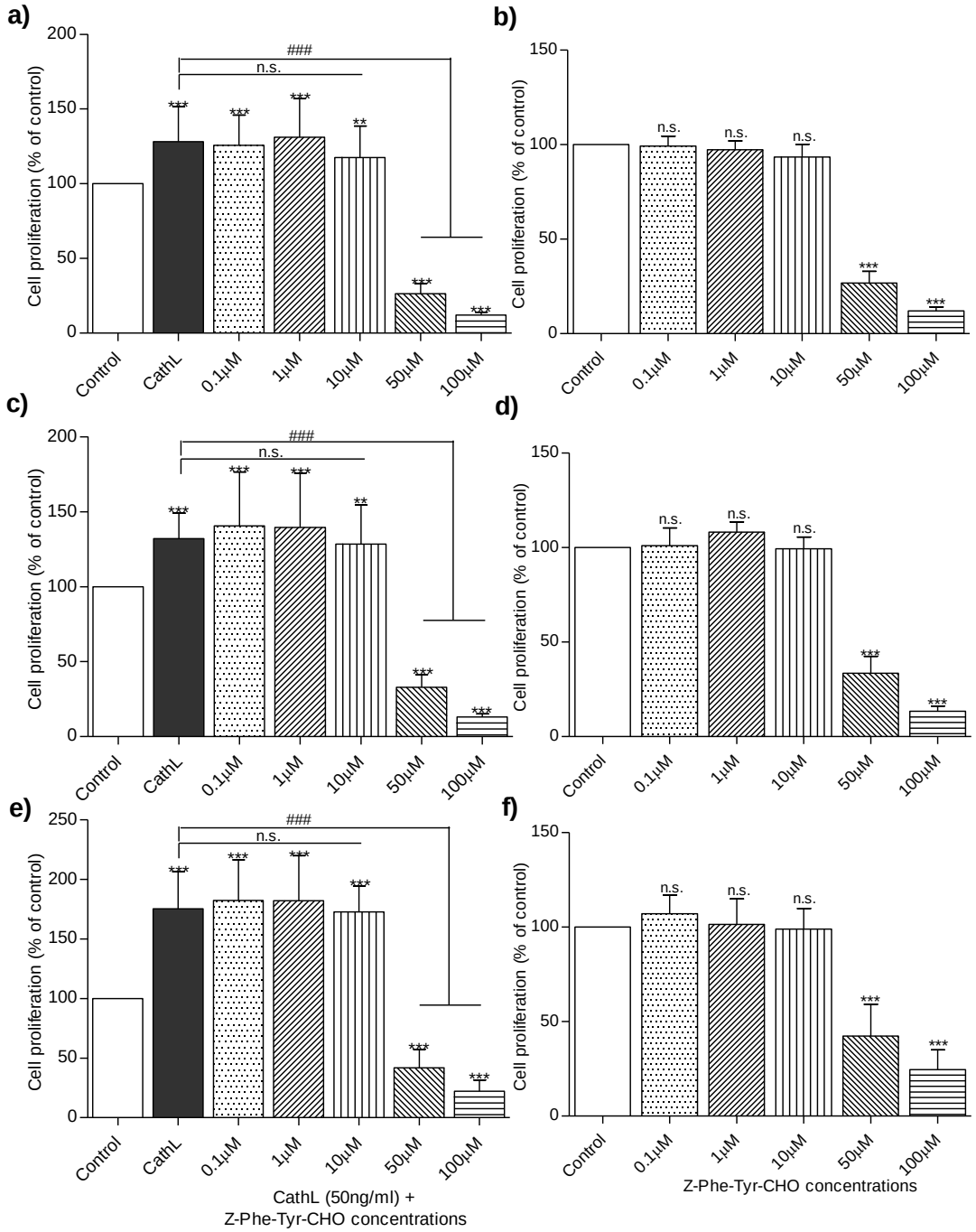

Figure 3.3: **Z-Phe-Tyr-CHO (FY-CHO), an inhibitor of CathL proteolytic activity, does not inhibit CathL-induced HOMEC proliferation.** Cells were seeded in 2% gelatin pre-coated 96 well plates at a density of 10,000cells/well in starvation media containing 2% FCS. After overnight incubation, cells were treated with or without CathL (50ng/ml) in the presence or absence of various concentrations of FY-CHO (as shown above- CathL+ FY-CHO a), c), e) or FY-CHO alone b), d), f)) and incubated for **a), b)** 24, **c), d)** 48 and **e), f)** 72 hours. WST-1 assay was used to assess cellular proliferation based on absorbance using PHERAstar BMG plate-reader at 450nm. Control wells contained 0.1% DMSO (carrier only). Results are mean ±SD and shown as percentage of the control, n.s., **p<0.01, ***p<0.001 vs control (100%); n.s., ###p<0.001 vs CathL (expressed as % of control), n=8-16. n.s. denotes not significant.

Table 3.1: **Summary of effects of FY-CHO on CathL-induced proliferation in HOMECs (shown in figure 3.3).** HOMECs were treated with or without CathL (50ng/ml) and in the presence or absence of increasing concentrations of FY-CHO for 24, 48 and 72 hours. Results are mean ±SD and shown as percentage of control (100%). n.s., ###p<0.001 vs CathL (expressed as % of control), n=8-16. n.s. denotes not significant. Toxic concentrations are highlighted in bold.

			CathL+FY-CHO (% of control)				
	Control (%)	CathL (% of control) (50ng/ml)	0.1 µM (n.s.)	1 µM (n.s.)	10 µM (n.s.)	**50 µM (###)**	**100 µM (###)**
24h	100	128.0±23.4	125.7±20.2	131.1±25.7	117.5±21.1	26.4±6.8	12.0±2.0
48h	100	132.0±17.1	140.5±36.1	139.6±36	128.4±27	32.9±8.5	13.0±2.2
72h	100	175.5±31.3	182.3±34.4	182.1±37.8	172.6±21.9	42.0±15.2	22.1±9.4

Table 3.2: **pH of cell culture media and supernatant overtime.** Cells were seeded in 6 well plates and treated with or without CathL (50ng/ml) for 24, 48 and 72 hours. Media were collected and their pH was measured by using a blood-gas analyser (ABL800 flex). The pH of basal MV2 (starvation media) was analysed at 0 hour. n.d. denotes not determined.

	pH			
	0h	24h	48h	72h
Basal MV2	7.34	n.d.	n.d.	n.d.
Control	n.d.	7.19	7.13	7.12
CathL	n.d.	7.19	7.13	7.11

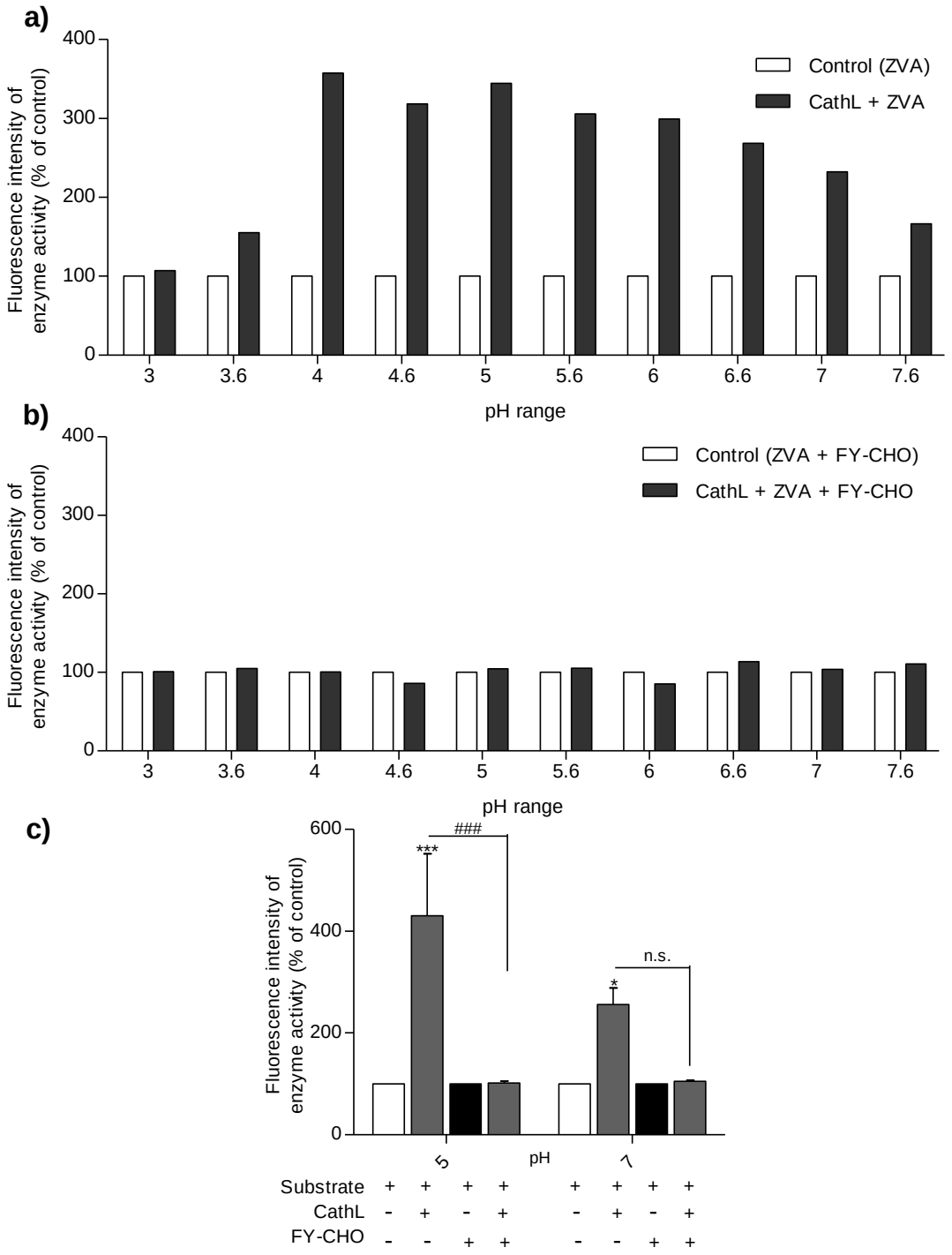

Figure 3.4: **CathL proteolytic activity is inhibited at an array of pHs by FY-CHO, an inhibitor of CathL proteolytic activity.** A specific fluorogenic substrate Z-Val-Val-Arg-AMC (Z-VVR-AMC, ZVA, 5 µM) was incubated with or without CathL (50ng/ml) and in the **a)** absence or **b)** presence of FY-CHO (CathL inhibitor, 10 µM). **c)** A summary of data at pH 5 and 7 with or without CathL and in the presence of the substrate ± FY-CHO. Fluorescence signals were measured immediately using SpectraMax plate reader at Ex/Em: 365/440. Control wells contained pH buffer and substrate and/or inhibitor. The data are represented as percentage of control. *p<0.05, ***p<0.001 vs control (substrate ± FY-CHO) (100%); ###p<0.001 vs CathL + substrate (expressed as % of control), n=3, a) and b) Representative data are from 1 of 3 independent experiments. n.s. denotes not significant.

3.3.3 Activation of intracellular signalling kinases in CathL-treated HOMECs

The induction of cell proliferation is reported to involve activation of several intracellular signalling pathways including MAPK/ERK1/2 and PI3/AKT kinases. Therefore, it was essential to investigate signalling cascades activated in CathL-treated HOMECs. Initially, a commercially available proteome profiler was used to simultaneously screen and detect activation and phosphorylation of 43 kinases. It was revealed that after 4 minutes treatment CathL increases phosphorylation of p38-α, ERK1/2 and AKT (S473) by ~2.5-, 3- and 3-fold respectively, compared to control (Figure 3.5). The spots for ERK1/2 and AKT are shown in figure 2.2 (Chapter 2, Method section 2.7.2). ERK1/2 and AKT were selected for further investigations on HOMECs as these two kinases have been shown to be significantly involved in cell proliferation, survival and cell migration in tumour biology.

The proteome profiler data was confirmed using commercially available cell-based ELISAs. CathL significantly induced ERK1/2 phosphorylation in HOMECs (>2-fold compared to control), similar to positive control VEGF (>2-fold compared to control), after 4 minutes treatment (Figure 3.6a). However, after 10 minutes treatment, levels of phosphorylated ERK1/2 reduced to the basal level (Figure 3.6b). Similar experiments were performed with AKT where AKT phosphorylation was induced (~1.6-fold compared to control) at 4 minutes after treatment (Figure 3.6c) and was reduced to basal level after 10 minutes (Figure 3.6d). VEGF was used as positive control in all cell-based ELISAs.

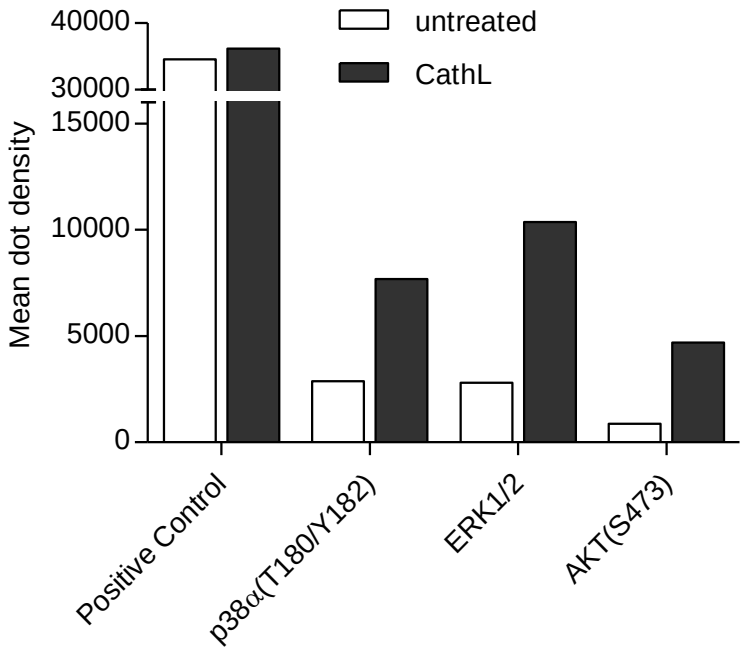

Figure 3.5: **CathL induces phosphorylation of p38α, ERK1/2 and AKT(S473) in HOMECs.** Phosphorylation statuses of intracellular kinases were assessed in cell lysates from cells treated with or without CathL for 4 minutes. The results of 1 minute exposure are expressed as mean dots density (arbitrary units). The relative expression of specific phosphorylated proteins was determined following quantification of scanned images. A combination of 2 cell batches were used in this experiment. n= 2 (n=1).

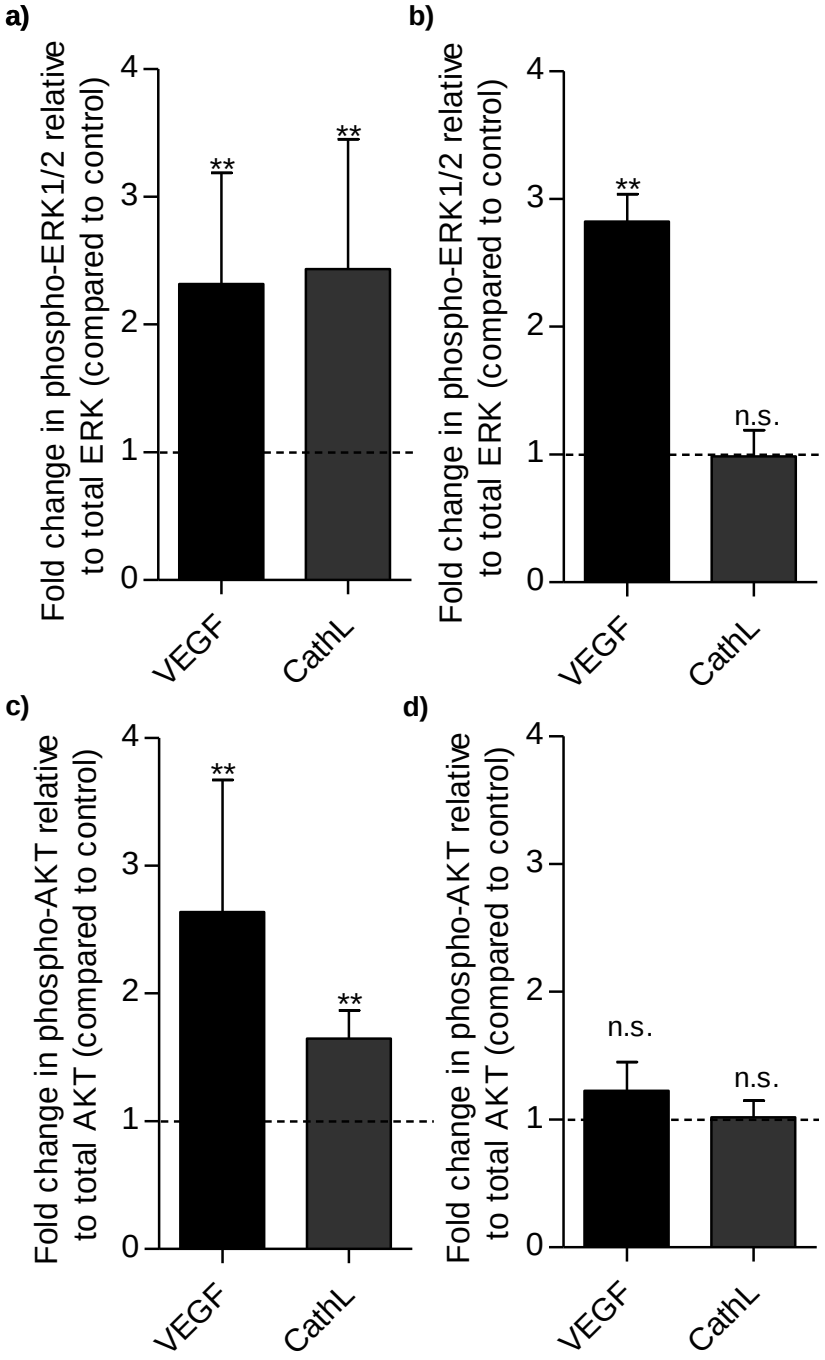

Figure 3.6: **CathL induces phosphorylation of ERK1/2 and AKT in HOMECs.** Cells were seeded in 2% gelatin pre-coated 96 well plates at a density of 10,000cells/well in starvation media containing 2% FCS. After overnight incubation, cells were treated with or without 50ng/ml of CathL or 20ng/ml of VEGF and incubated for 4 or 10 minutes. ERK1/2 (a, b) and AKT (c, d) phosphorylation was examined after 4 minutes (a, c) and 10 minutes (b, d) treatments. Commercially available cell-based ELISAs were used for the determination of ERK1/2 and AKT(S473) phosphorylation level. The ELISA experiments were carried out on two cell batches. The data is represented by fold change in phosho-ERK1/2/AKT relative to total ERK1/2/AKT (compared to control). Results are mean ±SD, n.s., **p<0.01 vs control; n=4-6. n.s. denotes not significant.

3.3.4 CathL-induced HOMEC proliferation is mediated via the ERK1/2 pathway

Since CathL induces activation of the proliferative kinase ERK1/2, it was hypothesised that ERK1/2 might be involved in the downstream signalling cascade in the induction of HOMEC proliferation and experiments were carried out to test this. Firstly, two well-known inhibitors of MEK/ERK1/2 were selected- U0126 and PD98059. Initially toxicity assays were carried out in order to identify their non-toxic concentrations in HOMECs. WST-1 assay was used to test this cytotoxicity 24 hour following inhibitor treatment. It was found that U0126 was not toxic to HOMECs at concentrations of 1 µM (97±6.0%, n=16 vs control (100%)) and 10 µM (96.2±7.1%, n=16 vs control (100%)), although slightly toxic at 25 µM (80.8±10.8%, n=21 vs control (100%)). However, cell viability reduced to less than 20% at 100 µM (7.6±1.3%, n=16 vs control (100); Figure 3.7a), demonstrating that U0126 is toxic at this concentration. On the other hand, PD98059 was not toxic at concentrations of 1 µM (96.4±10.1%, n=10 vs control (100%)), slightly toxic at 10 µM (84.1±12.5%, n=10 vs control (100%)) and 25 µM (63.8±13.3%, n=10 vs control (100%)), and very toxic at 50 µM (54.3±9.3%, n=10 vs control (100%)) (Figure 3.7b). Very toxic concentrations were excluded from further experiments. Non-toxic/slightly toxic concentrations of U0126 (1, 10 and 25 µM) and PD98059 (1, 10 and 25 µM) were used to investigate cell proliferation treated with CathL for 72 hours.

CathL-induced HOMEC proliferation was reduced significantly in the presence of all inhibitor concentrations compared to CathL treatment alone at 72 hour after treatment. For instance, at 1, 10 and 25 µM of U0126 cell proliferation decreased to 84.6±6.2 % (Figure 3.8 a), 88.2±11.4% (Figure 3.8b) and 77.4±4.8% (Figure 3.8c) respectively, compared to CathL (134.8±14.7%) (all expressed as percentage of control). In the case of PD98059, inhibition of proliferation was as follows: 113.6± 3.9% (Figure 3.8d), 73.1± 10.3% (Figure 3.8e) and 64.4± 4.9% (Figure 3.8f) at concentrations 1, 10 and 25 µM respectively, compared to CathL alone (127.0±7.9%) (all expressed as percentages of control).

Although the inhibitors significantly reduced CathL-induced HOMEC proliferation at all concentrations, in consultation with the current literature and data from inhibition of VEGF-induced (positive control, Appendix 1, Figure A1.3) HOMEC

proliferation, a concentration for each drug was selected to carry out further investigations i.e. 10 μM for U0126 and 25 μM for PD98059.

At these concentrations of ERK1/2 inhibitors, CathL-induced HOMEC proliferation was significantly reduced compared to CathL treatment alone. To confirm the validity of the experimental use of the inhibitors it was important to confirm their effect on cellular levels of phosphorylated ERK1/2. Cell-based ELISAs showed that the levels of phosphorylated ERK/2 abolished or reduced in HOMECs to 0.8-fold and 0.25-fold in the presence of U0126 (Figure 3.9a) and PD98059 (Figure 3.9b) respectively when compared with CathL-alone (1.5-fold). These data, along with inhibition of cell proliferation data suggest that CathL induces HOMEC proliferation via activation of ERK1/2.

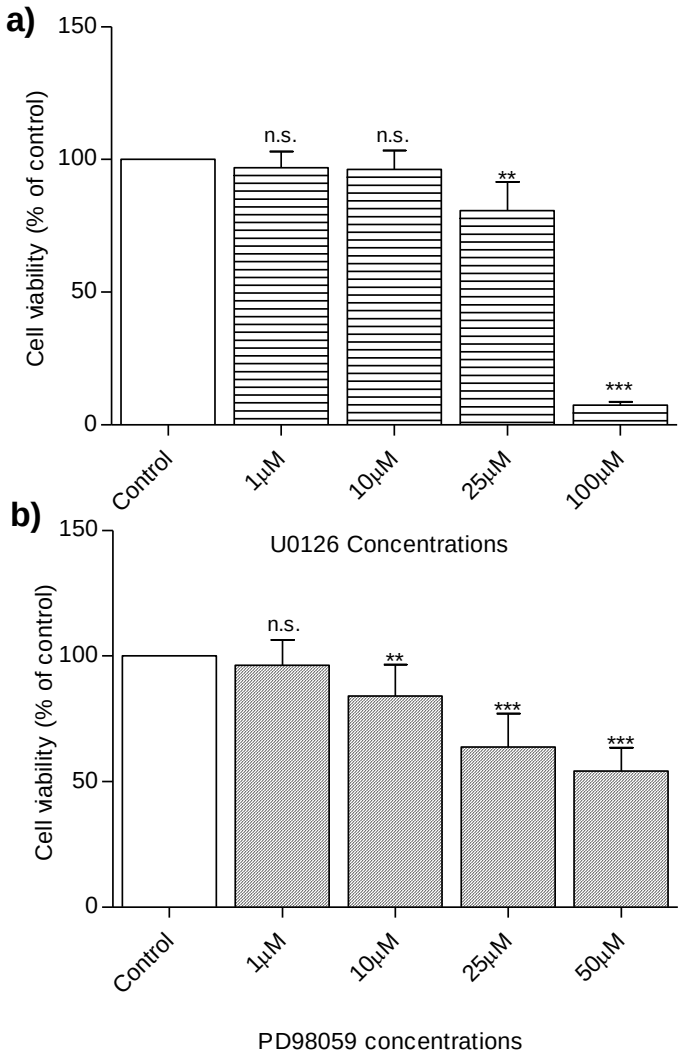

Figure 3.7: **Cytotoxicity (cell viability) induced by ERK1/2 inhibitors.** Cells were seeded in 2% gelatin pre-coated 96 well plates at a density of 10,000cells/well in starvation media containing 2% FCS. After overnight incubation, cells were treated with or without increasing concentrations of a) U0126 and b) PD98059 as indicated above and incubated for 24 hours. WST-1 was used to assess cellular viability. Results are mean ±SD and shown as percentage of the control, n.s., **p<0.01, ***p<0.001 vs control (100%), n=10-21. n.s. denotes not significant.

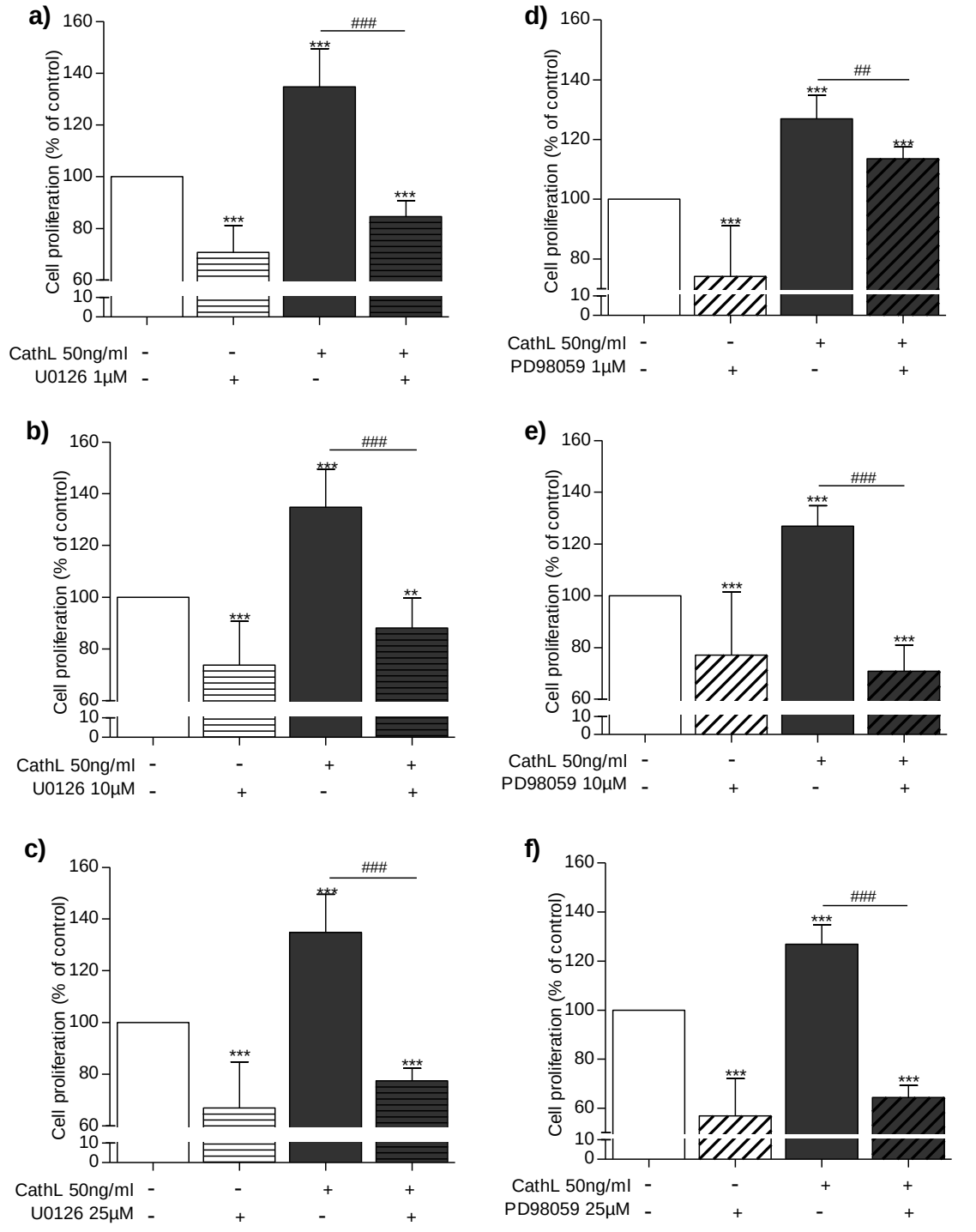

Figure 3.8: **Inhibition of ERK1/2 reduces CathL-induced HOMEC proliferation.** Cells were seeded in 2% gelatin pre-coated 96 well plates at a density of 10,000cells/well in starvation media containing 2% FCS. After overnight incubation, cells were treated with or without CathL (50ng/ml) and in the absence or presence of various concentrations of **a-c)** U0126 and **d-f)** PD98059 as indicated above and incubated for 72 hours. WST-1 assay was used to assess cellular proliferation. Results are mean ±SD and shown as percentage of the control, **p<0.01, ***p<0.001 vs control (100%), ##p<0.01, ###p<0.001 vs CathL (normalised to control 100%), n=7-13.

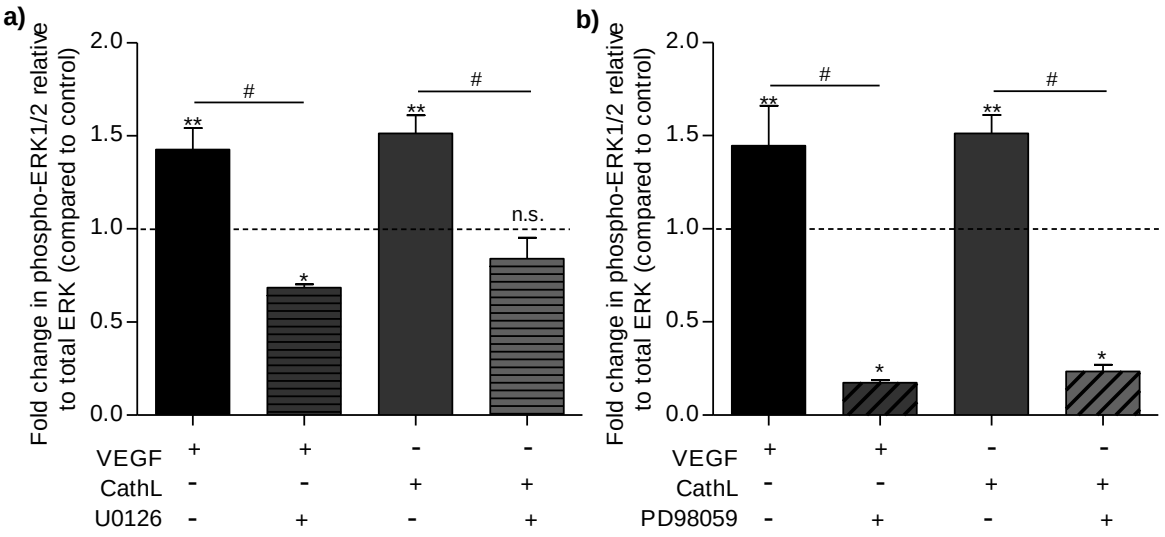

Figure 3.9: **CathL-induced ERK1/2 phosphorylation is inhibited in intact HOMECs treated with ERK1/2 inhibitors a) U0126 (10 µM) and b) PD98059 (25 µM)**. Cells were seeded in 2% gelatin pre-coated 96 well plates at a density of 10,000cells/well in starvation media containing 2% FCS. After overnight incubation, cells were pre-incubated with the inhibitors for 20-30 minutes, and then co-treated with or without 50ng/ml of CathL or 20ng/ml of VEGF in the absence or presence of the inhibitors for 4 minutes. Commercially available cell-based ELISAs were used for determination of ERK1/2 phosphorylation level. The data is represented by fold change in phosho-ERK1/2 relative to total ERK1/2 (compared to control). Results are mean ±SD, n.s., *p<0.05, **p<0.01 vs control (1-fold), #p<0.05 vs VEGF/CathL (normalised to control), n=4. The dotted lines represent basal level (control) of phosphorylation status in untreated HOMECs. n.s. denotes not significant.

3.3.5 CathL-induced HOMEC proliferation is mediated via PI3K but not AKT activation

The PI3K/AKT pathway is also known to promote cell survival and induce proliferation by inhibiting cell cycle arrest (Lawlor and Alessi, 2001). Since CathL induces AKT phosphorylation, it was logical to assess the role of AKT in HOMEC proliferation. In order to address this, two well-known inhibitors of the PI3K/AKT pathway were utilised- PI3K inhibitor LY294002 and AKT inhibitor MK2206. PI3K is upstream of AKT and hence it was necessary to see whether there is a generic role of PI3K in the induction of cell proliferation, and then focus further downstream involving AKT. Initially, a cytotoxic assay was performed to identify their non-toxic concentrations. PI3K inhibitor LY294002 was slightly cytotoxic over 24 hour treatment at concentrations 25 µM (89.0±4.6%, n=8), 50 µM (87.0 ±3.2%, n= 8) and reduced cell viability by approximately 20% at 100 µM (78.6±2.4%, n=8, vs control (100%); Figure 3.10a). With MK2206 the data showed that cells were viable after 24 hours at concentrations 1 µM (100±10.87%, n= 4) and that 5 µM did induce low levels of cytotoxicity (75.7±7.7%, n= 4) (Figure 3.10b). However, 25 µM of MK2206 significantly reduced cell viability to 44.1±1.3% (n= 4) compared to control (100%) (Figure 3.10b), indicating that it is toxic to HOMECs.

Next, proliferation was tested in HOMECs treated with CathL in the absence or presence of LY294002 or MK2206. Based on the data above LY294002 was used at 1, 25 and 50 µM and MK2206 at 1, 3 and 5 µM. Interestingly, LY294002, an inhibitor of PI3K, reduced cell proliferation in a dose-dependent manner. For instance, cell proliferation in the presence of CathL plus at 1 µM, 25 µM and 50 µM of LY294002 were 142.9±6.0% (n= 10; Figure 3.11a), 102.0±5.9% (n= 10; Figure 3.11b) and 74.7±3.7% (n=10; Figure 3.11c), respectively, compared to 50ng/ml CathL alone, 137.3±5.7% (n= 10) (all data expressed as percentage of control). However, cell proliferation was not significantly altered in the presence of MK2206, a selective inhibitor of AKT. For example, cell proliferation in the presence of CathL plus at 1 µM, 3 µM and 5 µM of MK2206 were 128.1±6.4% (n= 9; Figure 3.11d), 127.8±9.7% (n= 8; Figure 3.11e) and 126.7±10.9% (n=10; Figure 3.11f) respectively, compared with CathL-induced proliferation, 125.1±6.7% (n= 9) (all data normalised to control (100%)). Data from control wells for LY294002 demonstrated a significant reduction in cell proliferation over 72

hour period (Figure 3.11 a, b, c). Interestingly, MK2206 did not show any reduction, rather a significant increase in proliferation was observed across all three concentrations (Figure 3.11 d, e, f). These data may suggest that CathL induces HOMEC proliferation by activating the PI3K pathway, but via an AKT-independent mechanism since the AKT-specific inhibitor did not reduce cell growth. A similar observation was made in VEGF-treated HOMECs (Appendix 1, Figure A1.4).

On the basis of the toxicity data, cell proliferation data with LY294002 and MK2206, and current literature (Yang et al., 2015)**,** the concentrations that were chosen to perform further experiments were: 25 µM for LY294002 and 5 µM for MK2206.

The ELISA data with LY294002 (25 µM) and MK2206 (5 µM) confirmed that both drugs do inhibit phosphorylation of AKT in intact HOMECs. In the presence of LY294002, CathL-induced levels of phosphorylated AKT reduced from 1.9-fold to 0.5-fold (Figure 3.12a). In the case of MK2206, levels of phosphorylated AKT decreased from 1.5-fold to 0.5-fold (Figure 3.12b). This suggests that both drugs inhibit the PI3K/AKT pathway in HOMECs. However, a lack of inhibition of cell proliferation suggests that PI3K, but not AKT(S473) is involved in the induction of CathL-mediated HOMEC proliferation.

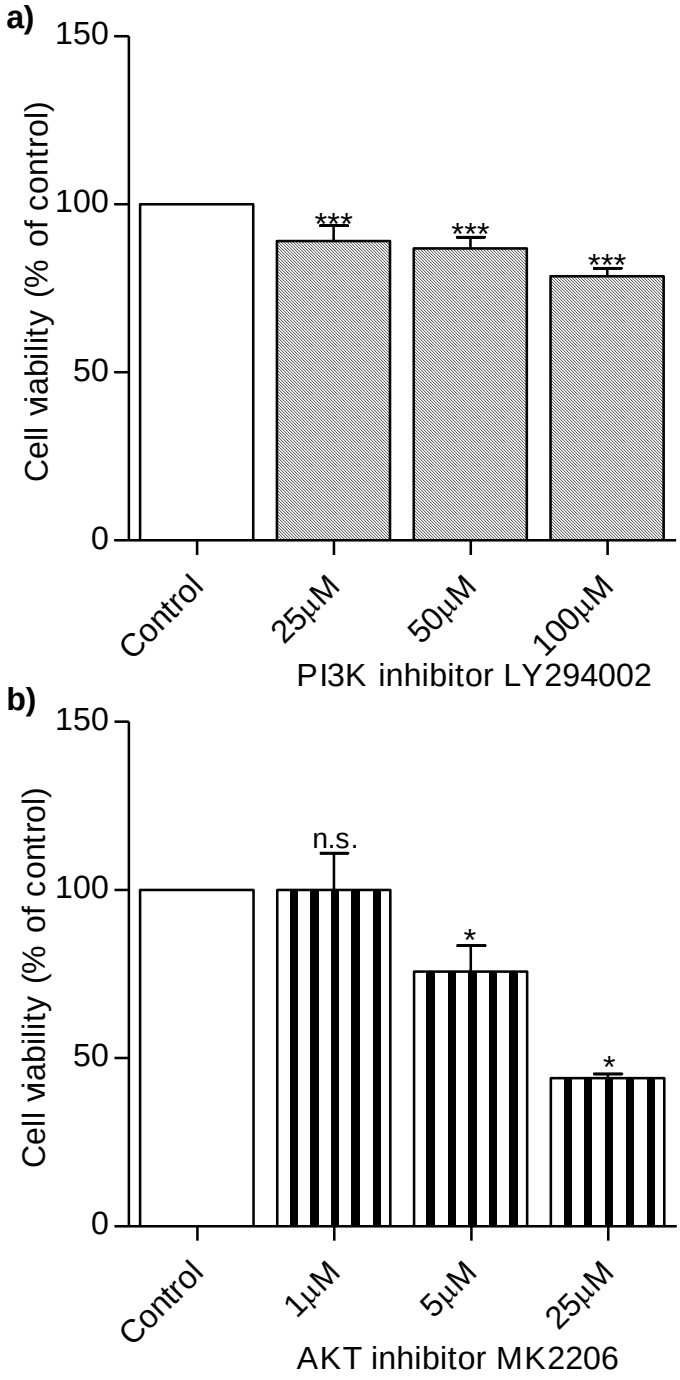

Figure 3.10: **Cytotoxicity (cell viability) induced by PI3K/AKT inhibitors.** Cells were seeded in 2% gelatin pre-coated 96 well plates at a density of 10,000cells/well in starvation media containing 2% FCS. After overnight incubation, cells were treated with or without increasing concentrations of **a)** LY294002 and **b)** MK2206 as indicated above and incubated for 24 hours. WST-1 assay was used to assess cellular viability. Results are mean ±SD and shown as percentage of the control, n.s., *p<0.05, ***p<0.001, vs control (100%), n=4-8. n.s. denotes not significant vs control.

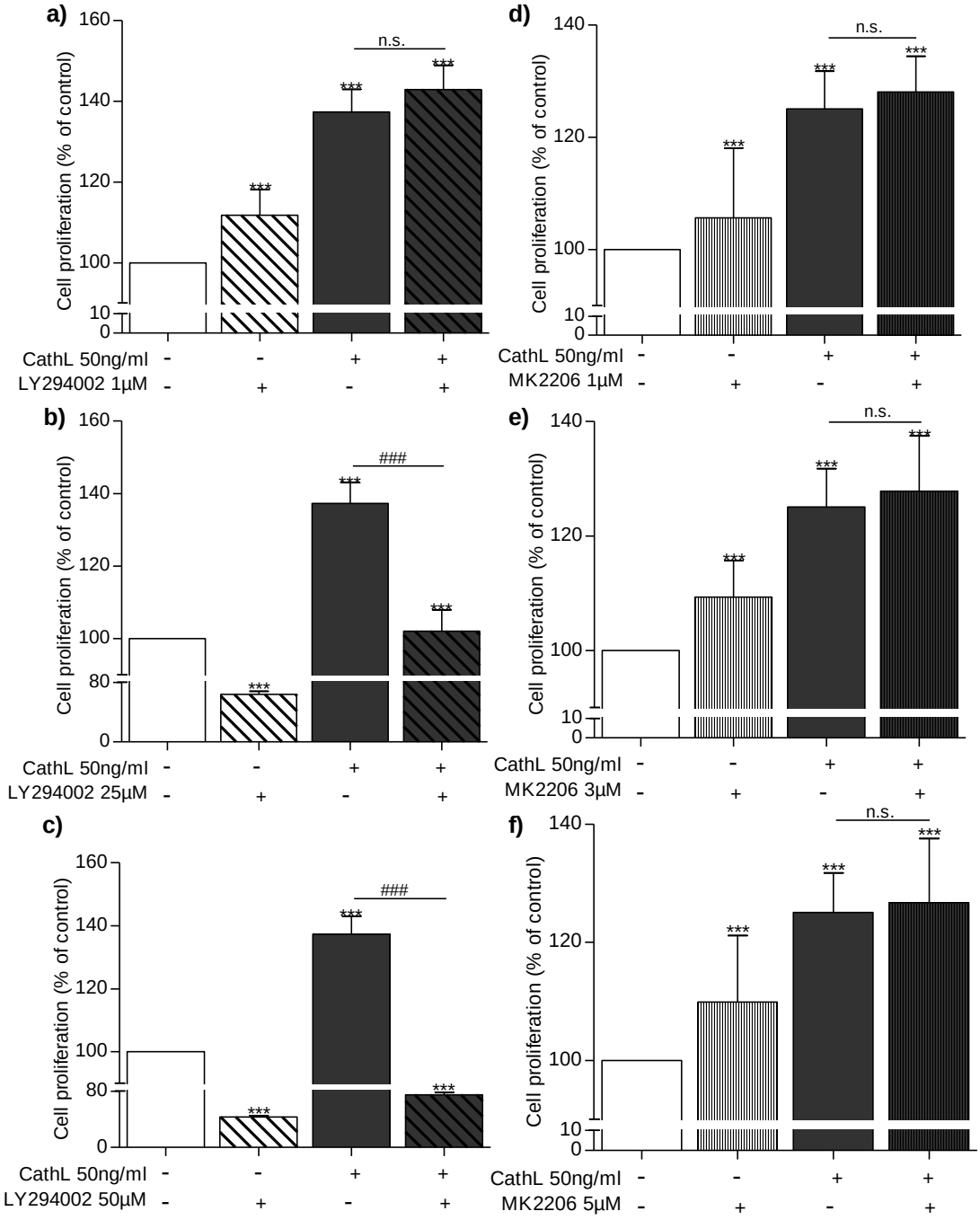

Figure 3.11: **PI3K inhibitor, but not AKT inhibitor, reduces CathL-induced HOMEC proliferation.** Cells were seeded in 2% gelatin pre-coated 96 well plates at a density of 10,000cells/well in starvation media containing 2% FCS. After overnight incubation, cells were treated with or without CathL (50ng/ml) and in the absence or presence of various concentrations of **a-c)** LY294002 (PI3K inhibitor) and **d-f)** MK2206 (AKT inhibitor) as indicated above and incubated for 72 hours. WST-1 assay was used to assess cellular proliferation. Results are mean ±SD and shown as percentage of the control, ***p<0.001 vs control (100%), n.s., ###p<0.001 vs CathL, n=10-15 (normalised to control 100%). n.s. denotes not significant.

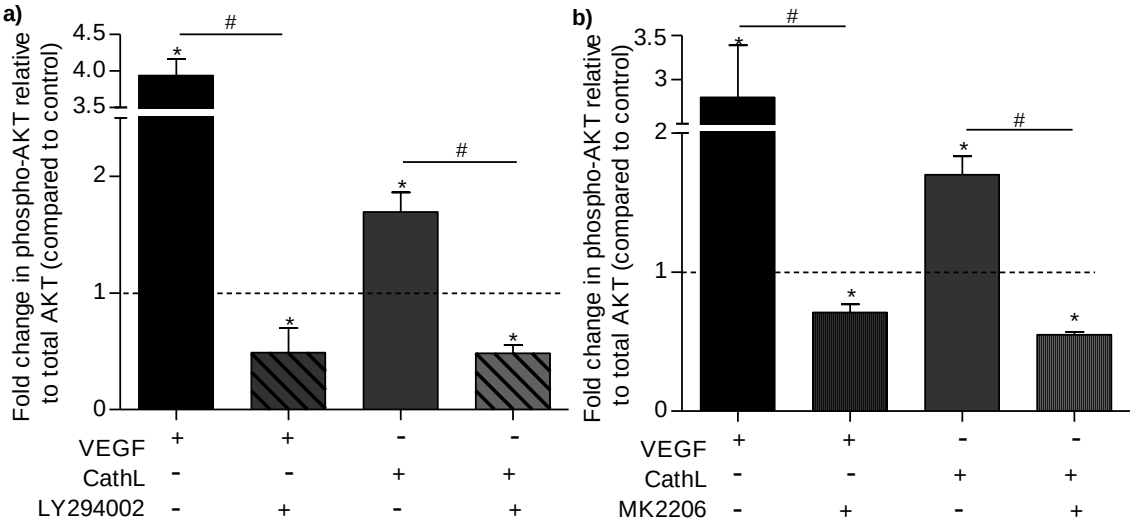

Figure 3.12: **CathL-induced AKT phosphorylation is inhibited in HOMECs treated with PI3K and AKT inhibitors a) LY294002 (25 µM) and b) MK2206 (5 µM)**, respectively. Cells were seeded in 2% gelatin pre-coated 96 well plates at a density of 10,000cells/well in starvation media containing 2% FCS. After overnight incubation, cells were pre-incubated with the inhibitors for 2.5 hours, and then co-treated with or without 50ng/ml of CathL or 20ng/ml of VEGF in the absence or presence of the inhibitors for 4 minutes. Commercially available cell-based ELISAs were used for determination of level of AKT phosphorylation. The ELISA experiments were carried out on two cell batches. The data is represented by fold change in phospho-AKT relative to total AKT (compared to control). Results are mean ±SD, *$p<0.05$ vs control (1-fold), #$p<0.05$ vs VEGF/CathL (normalised to control), n=4. The dotted lines represent basal level (control) of phosphorylation status in untreated HOMECs.

3.3.6 CathL induces migration via ERK1/2, not AKT

In the process of angiogenesis, EC migration is a key step. Cells proliferate and migrate towards the secondary tumour foci and sprout out forming new blood vessels. Since EC migration is vital in angiogenesis, a role for CathL was investigated in HOMECs using a transwell migration Boyden chamber kit (Chapter 2, Section 2.5). Initially, cell migration was tested for 48 hours as was previously tested using the Oris migration kit (Winiarski et al., 2013). However, no significant differences were observed between untreated and CathL-treated HOMECs. Therefore, the incubation time was reduced to 6 hours, and it was revealed that CathL (197.4±49.6%, n= 10; Figure 3.13a) significantly induced HOMEC migration compared to control (100%). VEGF was used as positive control in these experiments. This led to further investigation into the activation of potential downstream signalling cascades.

As previous data showed activation of ERK1/2 and AKT by CathL in HOMECs, cell migration was tested in the presence or absence of the corresponding kinase inhibitors at their chosen concentrations. Initially it was hypothesised that AKT may be involved in the induction of migration in CathL treated cells as AKT has been shown to be activated during cell migration in other models (Zhou et al., 2016, Enomoto et al., 2005, Xue and Hemmings, 2013, Kakinuma et al., 2008, Chin and Toker, 2010, Kawasaki et al., 2003, Goetze et al., 2002, Morales-Ruiz et al., 2000). Therefore, the role of AKT in cell migration was examined in cells pre-treated with or without PI3K and AKT inhibitors for 1 hour and then co-treated with CathL in the absence or presence of the corresponding inhibitor for 6 hours. Neither PI3K inhibitor LY294002 (25 µM) nor AKT inhibitor MK2206 (5 µM) significantly reduced migration of CathL-treated HOMECs. For instance, migration of CathL-treated cells in the presence of LY294002 was 188.8±46.5% (n= 6; Figure 3.14a) with no significant difference compared with CathL-induced migration (199.2±62.2% (n=12) (both expressed as percentage of control (100%)). In the presence of MK2206, cell migration was 175.3±27.0% (n=6; Figure 3.14b), which was not significantly different to CathL-induced migration (199.2±62.2%, n= 12) (both normalised to control 100%). HOMECs treated with only LY294002 and/or MK2206 demonstrated a significant reduction in migration (Figure 3.14 a, b).

Interestingly, a similar observation was made in VEGF-treated HOMECs in the presence of both PI3K/AKT inhibitors, with a non-significant reduction in HOMEC migration compared with corresponding VEGF treatment. VEGF was used as a positive control (Appendix 1, Figure A1.5).

HOMEC migration was then tested using ERK1/2 inhibitors. Cells were pre-treated with U0126 (10 µM) or PD98059 (25 µM) and then were co-treated with CathL in the presence or absence of the inhibitors. After 6 hours incubation, both inhibitors of ERK1/2 abolished HOMEC migration compared to CathL-treated cells. For instance, in the presence of U0126 and PD98059, CathL-induced HOMEC migration was reduced to 75.6±19.1% (n= 7; Figure 3.15a) and 91.5±14.1% (n= 7; Figure 3.15b) respectively, whereas CathL-alone significantly induced migration (146.6±17.3%, n= 9) (all expressed as percentage of control 100%). U0126 treatment alone significantly reduced HOMEC migration (Figure 3.15a), however, although there was a slight reduction in migration by PD98059 alone, it was not significantly different compared to control (Figure 3.15b). These data combined with the ELISA data showing inhibition of ERK1/2 phosphorylation by U0126 and PD98059 (Figure 3.9), suggest that CathL induces HOMEC migration through activation of ERK1/2, but not AKT(S473). A similar observation was made in VEGF-treated HOMECs (Appendix 1, Figure A1.6).

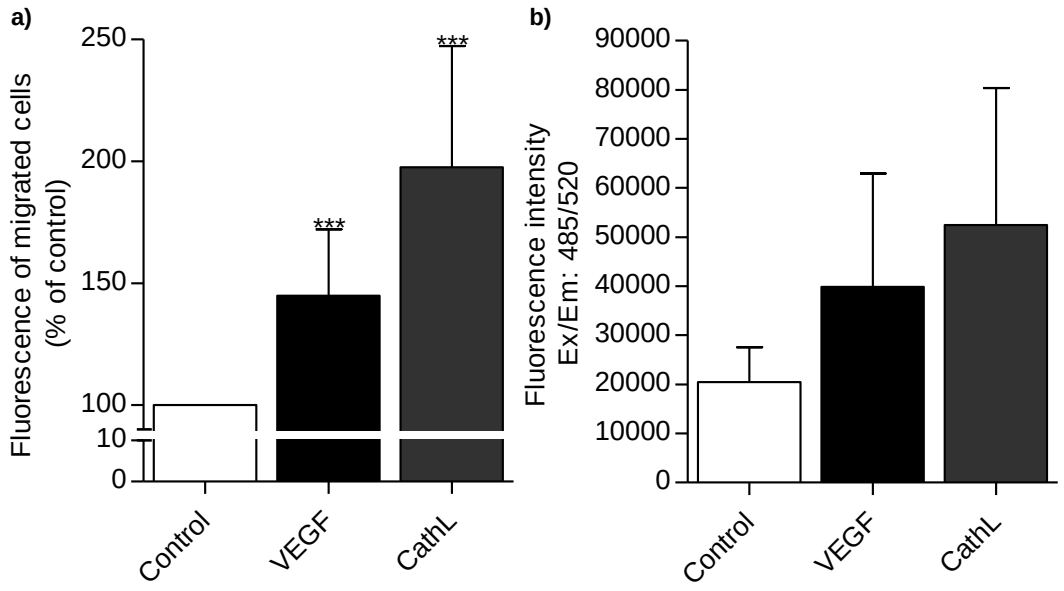

Figure 3.13: **CathL induces HOMEC migration.** HOMECs were seeded on the upper transwell insert and treated with or without CathL (50ng/ml) or VEGF (20ng/ml) supplementation of starvation media containing 0.5% FCS. The lower well contained correspondent treatment i.e. 0.5% FCS media, CathL (50ng/ml) or VEGF (20ng/ml). After 6 hours, migrated cells were stained with calcein AM and fluorescence was quantified using a FLUOstar plate reader at Ex/Em: 485/520. **a)** Results are mean ±SD and shown as percentage of the control, ***p<0.001 vs control (100%), n=10-15, **b)** Raw data from representative experiment.

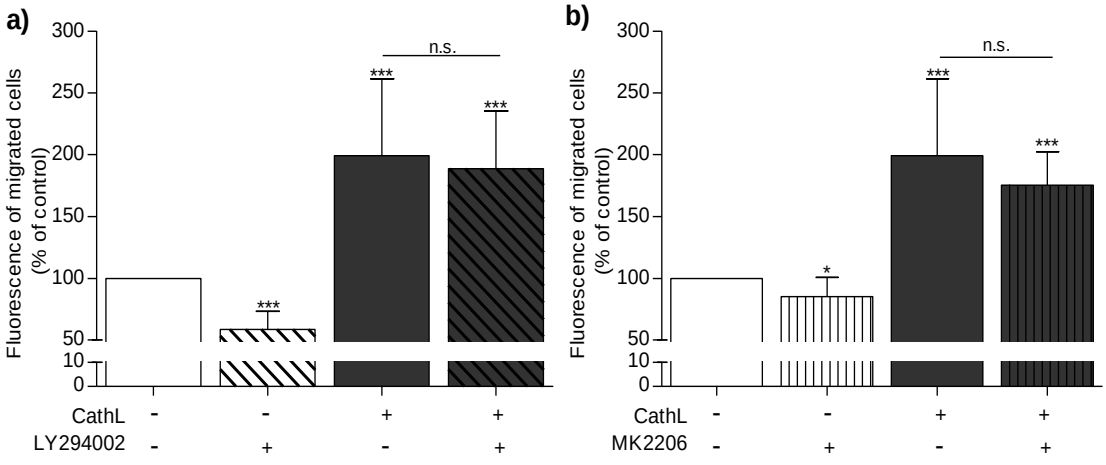

Figure 3.14: **CathL does not induce HOMEC migration via the AKT pathway.** HOMECs were seeded in the upper transwell chamber and treated with or without CathL (50ng/ml) in the absence or presence of PI3K and AKT inhibitors **a)** LY294002 (25 µM) and **b)** MK2206 (5 µM) respectively in media containing 0.5% FCS. The lower well contained correspondent treatments. After 6 hours, migrated cells were stained with calcein AM and fluorescence was quantified using a FLUOstar plate reader at Ex/Em: 485/520. Results are mean ±SD and shown as percentage of the control, *p<0.05, ***p<0.001 vs control (100%), n=6-12. n.s. denotes not significant vs CathL.

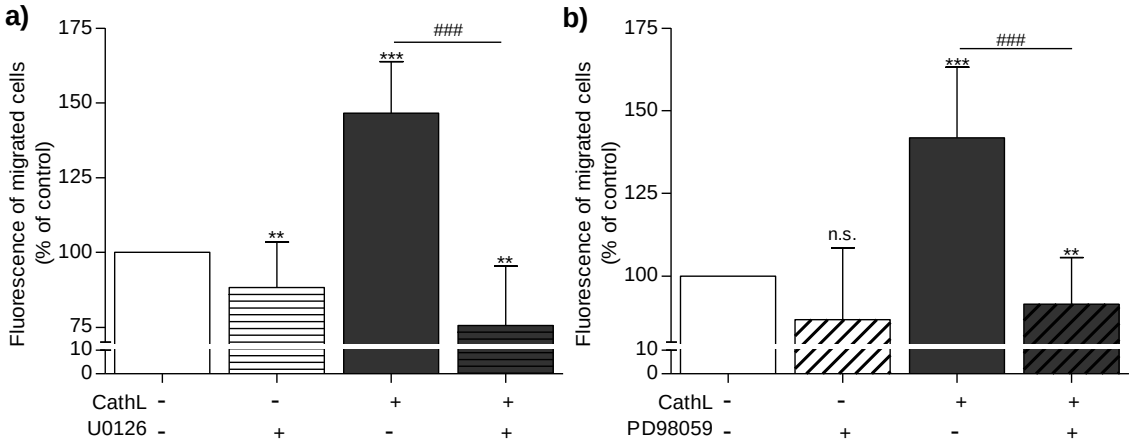

Figure 3.15: **CathL induces HOMEC migration via the ERK1/2 pathway.** HOMECs were seeded in the upper transwell chamber and treated with or without CathL (50ng/ml) in the absence or presence of ERK1/2 inhibitors **a)** U0126 (10 µM) and **b)** PD98059 (25 µM) respectively in media containing 0.5% FCS. The lower well contained correspondent treatments. After 6 hours, migrated cells were stained with calcein AM and fluorescence was quantified using a FLUOstar plate reader at Ex/Em: 485/520. Results are mean ±SD and shown as percentage of the control, n.s., **p< 0.01, ***p<0.001 vs control (100%), ###p<0.001 vs CathL, n=7-9. n.s. denotes not significant.

3.3.7 Optimisation of *in vitro* 3D and 2D angiogenesis

The data previously described indicate that CathL induces cell proliferation and migration, both critical steps in angiogenesis. To examine the ability of CathL to induce angiogenesis in HOMECs, a 3D *in vitro* model of angiogenesis was established according to a protocol described by Nakatsu *et al.* (Nakatsu et al., 2007). This technique studies 3D sprouting of ECs grown on the surface of cytodex beads embedded in a fibrin gel. As described in Chapter 2, Section 2.8.1, HCMECs were primarily used to establish the model due to easy availability. Different conditions were examined: media supplemented with 2% FCS as basal control (Figure 3.16a), media supplemented with 5% FCS and manufacturer-provided growth factors as positive control (complete growth media) (Figure 3.16b), and 2% FCS media supplemented with 20ng/ml of VEGF (a known angiogenic stimulator) (Figure 3.16c) or 50ng/ml of CathL (Figure 3.16d). Cell sprouting was observed in the positive control and in CathL- and VEGF-treated wells, but not in control wells (media with 2% FCS).

However, when the same conditions were applied using HOMECs, the outcome was unsuccessful. No sprouting was observed in any condition, including the positive control after 5 days (Figure 3.17a-d). As ECs show heterogeneity, this may have been due to the requirement for different assay conditions for HOMECs versus HCMECs. Thus, initially alteration of the concentration of serum for HOMECs in the fibrin gel was examined. This may influence access of sufficient FCS to HOMECS for optimal growth. Therefore, higher concentrations of FCS (5%, 10% and 20%) were supplemented with basal media or complete growth media to assess cell survival and sprouting (Figure 3.18 a), b) represent only 20% FCS±GFs data). Visually, it was observed that cells survived across all FCS concentrations in media and therefore, the lowest FCS concentration (5%) was selected to carry out further investigation. Although cells survived across all FCS concentrations, they did not sprout or branch out. This led to a series of experiments to optimise the concentration of the constituents of the fibrin gel. Thrombin-mediated conversion of fibrinogen to fibrin forms a tight network of fibrin monomers which may act as barrier and physically prevent cell proliferation and migration and therefore branching out in HOMECs. In order to address this, a lower thrombin concentration was investigated to reduce the tightened fibrin linkages and to allow flexibility for the cell movement. However, at lower

concentrations of thrombin the gel failed to form fully and so was not used in further experiments (data not shown).

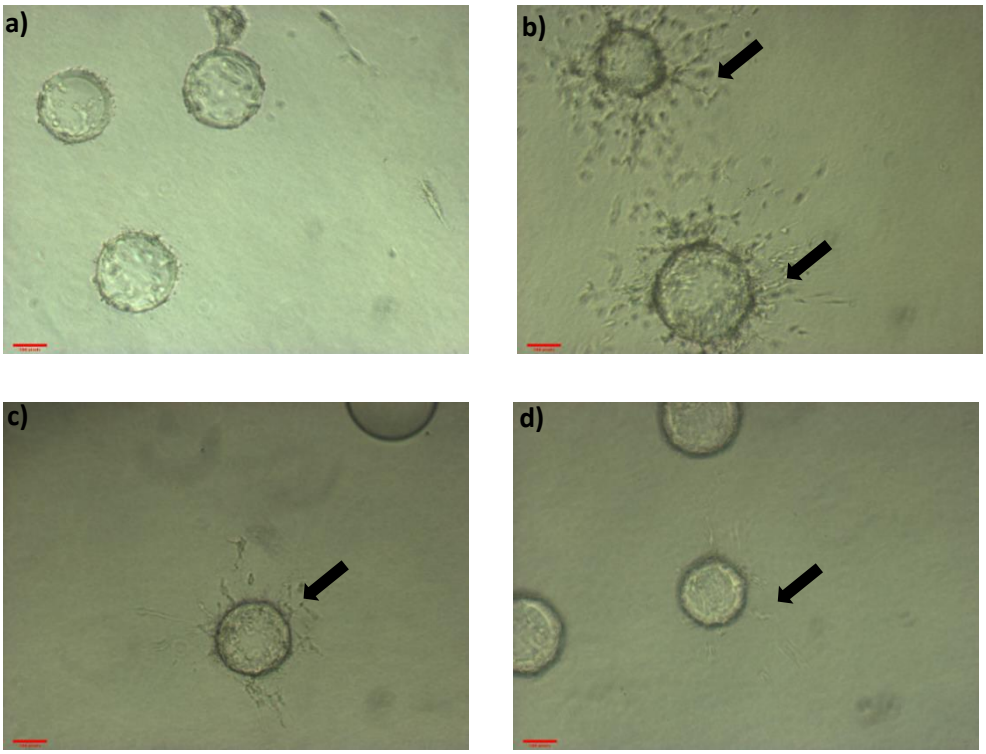

Figure 3.16: **Formation of angiogenic sprouts in human cerebral microvascular endothelial cells (HCMECs) in 3D fibrin gel.** Cells were seeded on cytodex 3 microcarriers and embedded in fibrin gel in media supplemented with 2% FCS **a)** Control, **b)** 5% FCS with added EC growth factors (positive control), **c)** 20ng/ml of VEGF (positive control) or **d)** 50ng/ml of CathL. Media/treatments were replaced every other day up to day 5. Photographs were taken on day 6 post-seeding using a Nikon phase-contrast microscope at 10X magnification. Arrows pointing to cell sprouting. Scale bar =100 μm.

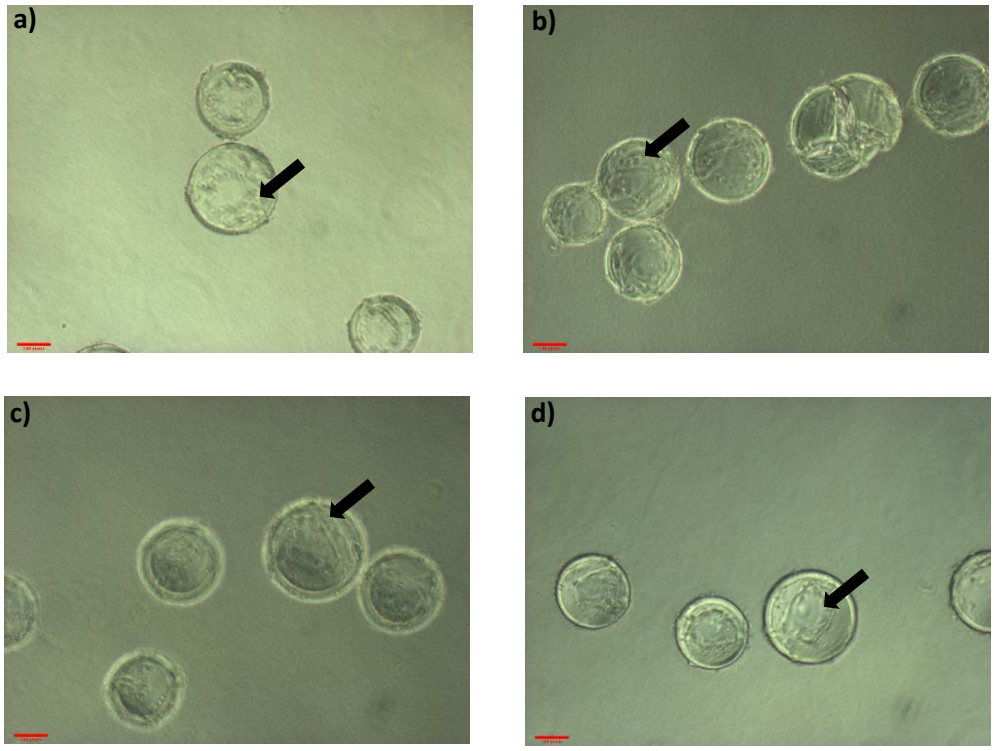

Figure 3.17: **Investigation of angiogenic sprout formation in human omental microvascular endothelial cells (HOMECs) in 3D fibrin gel.** Cells were seeded on cytodex 3 microcarriers and embedded in fibrin gel in media supplemented with 2% FCS **a)** Control, **b)** 5% FCS with added EC growth factors (positive control), **c)** 20ng/ml of VEGF (positive control) or **d)** 50ng/ml of CathL. Media/treatments were replaced every other day up to day 5. Photographs were taken on day 6 post-seeding using a Nikon phase-contrast microscope at 10X magnification. Arrows pointing to live cells on beads. Scale bar =100 µm.

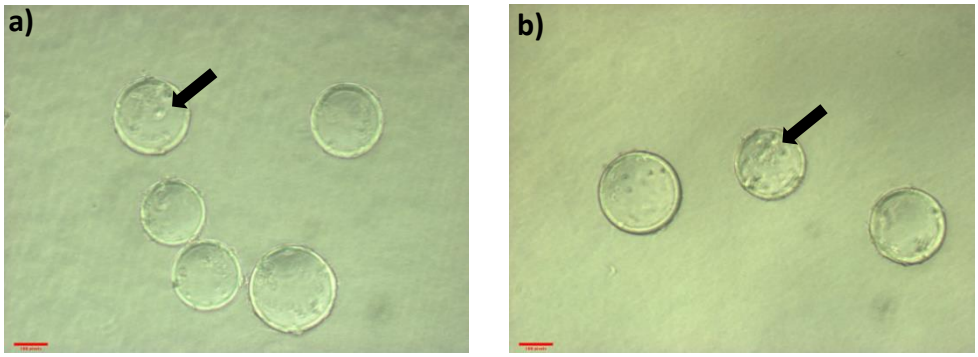

Figure 3.18: **Investigation of effects of higher serum concentrations on angiogenic sprout formation in HOMECs in 3D fibrin gel.** Cells were seeded on cytodex 3 microcarriers and embedded in fibrin gel in media supplemented with 20% FCS **a)** without or **b)** with added EC growth factors (GFs). Media/treatments were replaced every other day up to day 5. Photographs were taken on day 6 post-seeding using a Nikon phase-contrast microscope at 10X magnifications. Arrow pointing to live cells on beads. Scale bar =100 μm.

Aprotinin (0.14 U/ml) is another constituent of this fibrin gel. It is a protease inhibitor which is included to slow down rapid fibrinolysis of the gel (Sacchi et al., 2014). It was hypothesised that aprotinin may inhibit proteases secreted by HOMECs that actively cleave and breakdown fibrin mesh in order for cells to sprout out. Thus, reducing aprotinin concentration may allow more efficient HOMEC sprouting. Three different concentrations of aprotinin were tested- 0, 0.07 and 0.14 U/ml. 0.14U/ml is normally used in the original protocol (Nakatsu et al., 2007). At 0 U/ml of aprotinin, HOMECs supplemented with complete growth media formed a monolayer within the fibrin gel (Figure 3.19b) that was not observed in media without growth factors (Figure 3.19a), suggesting that HOMECs secrete proteases in response to growth factors which then cleave and break down fibrin linkages, allowing EC movement (Figure 3.19). Intriguingly, visually, the fibrin gel remained intact in the absence of aprotinin, indicating durability of fibrin matrix. However, there were no features of sprouting or branching of these ECs at low (0.07 U/ml; Figure 3.19c, d) or recommended (0.14 U/ml; Figure 3.19e, f) concentrations of aprotinin.

The final variable to be studied for optimisation was bead type. Previously, cytodex 3 beads were used to embed cells in the gel. Cytodex 3 beads are pre-coated with collagen. As HOMECs grow on 2% gelatin coated plastic, it was thought that the material might affect cell growth and migration in the gel. Therefore, cytodex 1 beads were used instead of cytodex 3 beads (Figure 3.20). Cytodex 1 beads are pre-coated with gelatin which was thought to be a better option for HOMECs. When tested in fibrin gel containing different concentrations of aprotinin and media supplemented with 5% FCS and with (Figure 3.20b, d, f) or without (Figure 3.20a, c, e) growth factors, there was no difference observed in cell growth between the two beads. At this stage, it was decided that this model may not be suitable to study HOMECs angiogenesis and that angiogenesis of HOMECs should be tested using a 2D fibrin gel model.

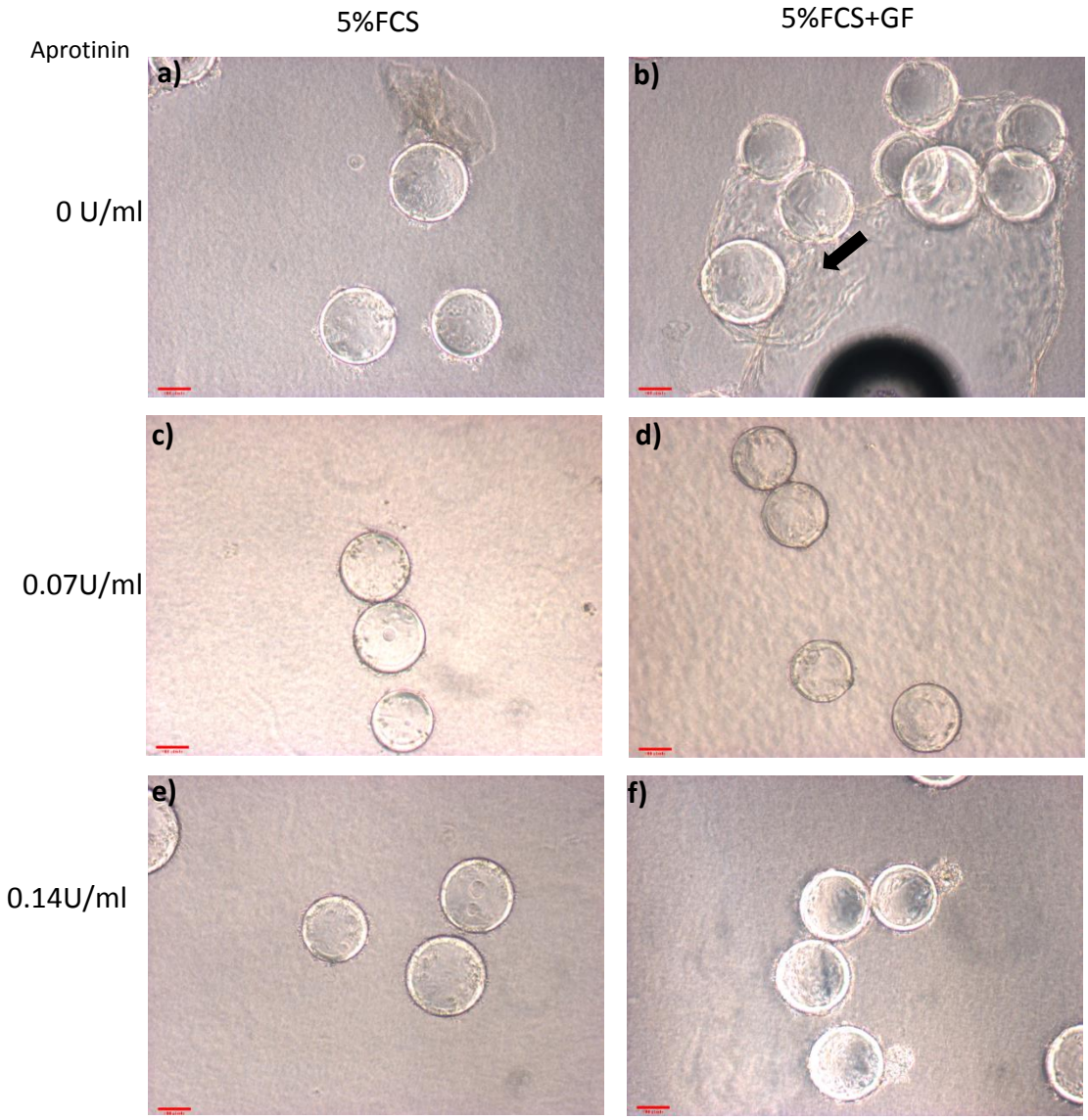

Figure 3.19: **Investigation of effects of different aprotinin concentrations on angiogenic sprout formation in HOMECs in 3D fibrin gel.** Cells were seeded on cytodex 3 microcarriers and embedded in fibrin gel containing 0 **(a, b)**, 0.07 **(c, d)** and 0.14 **(e, f)** U/ml aprotinin as indicated. Next, cells were treated with media supplemented with 5% FCS with **(b, d, f)** or without **(a, c, e)** added EC growth factors (GFs) as shown. Media/treatments were replaced every other day up to day 5. Photographs were taken on day 6 post-seeding using a Nikon phase-contrast microscope at 10X magnifications. Arrow pointing to the monolayer of HOMECs. Scale bar =100 µm.

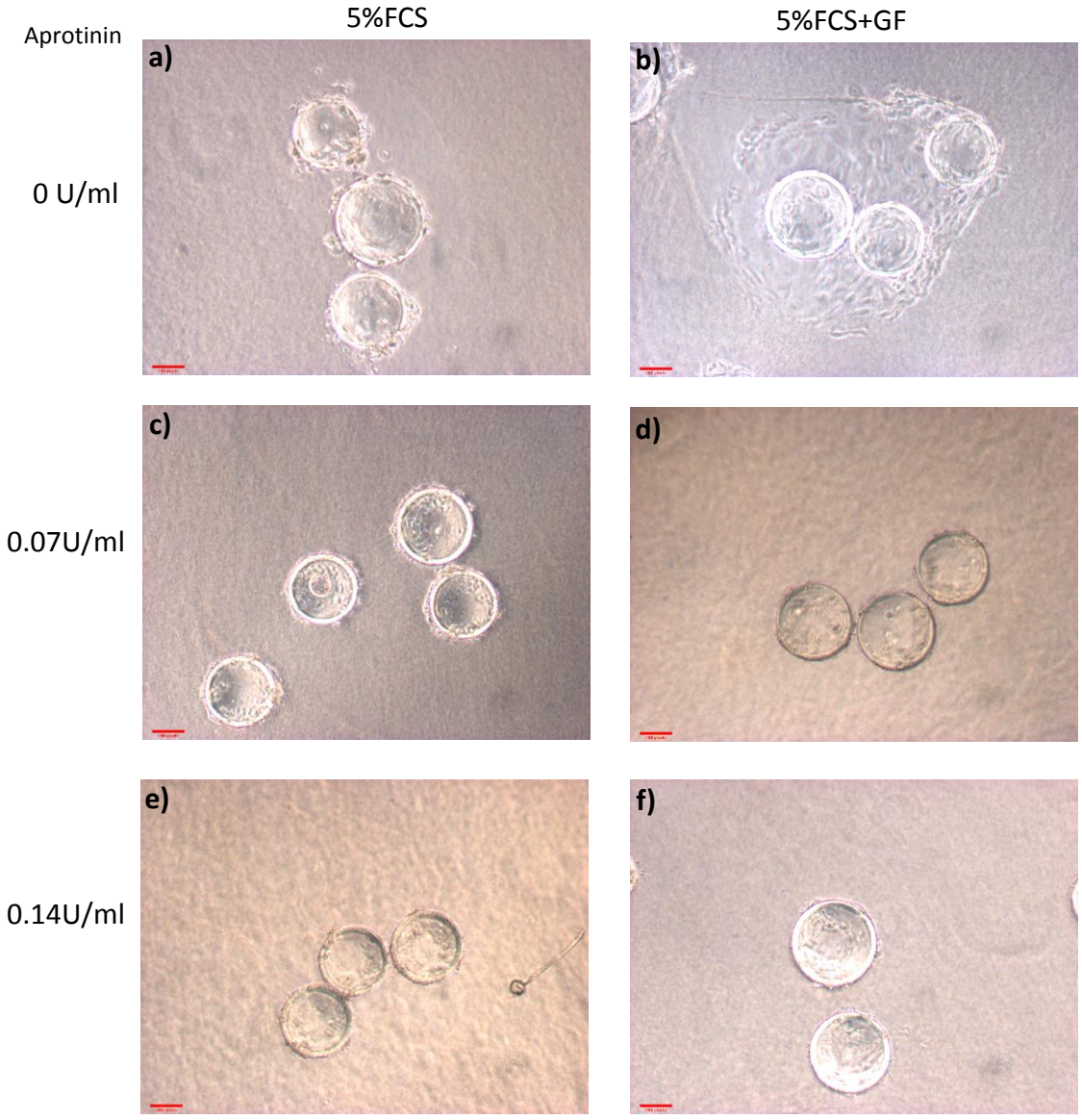

Figure 3.20: **Investigation of effects of seeding HOMECs on cytodex 1 microcarriers on angiogenic sprout formation in HOMECs in 3D fibrin gel.** Cells were seeded on cytodex 1 microcarriers and embedded in fibrin matrix gel containing 0 **(a, b)**, 0.07 **(c, d)** and 0.14 **(e, f)** U/ml aprotinin as indicated. Next, cells were treated with media supplemented with 5% FCS with **(b, d, f)** or without **(a, c, e)** added EC growth factors (GFs) as shown. Media/treatments were replaced every other day up to day 5. Photographs were taken on day 6 post-seeding using a Nikon phase-contrast microscope at 10X magnifications. Scale bar =100 µm.

To carry out the 2D model, the same fibrin gel was used as above, but cells were seeded at 35,000 per well on top of the gel. After overnight incubation, cells were treated with media supplemented with 2% FCS (control media), VEGF (20ng/ml; positive control) or CathL (50ng/ml). At 72 hours after treatment, a complete monolayer formed in the control (Figure 3.21a) and VEGF-treated wells (Figure 3.21b). However, in CathL-treated wells cells did not form a monolayer, rather they loosely organised themselves in a tubule-forming manner (Figure 3.21c). This may have been caused due to seeding cells at a low density. Therefore, this experiment was repeated under the same conditions except with a higher cell density- 50,000 cells per well (Figure 3.22). It was thought that at higher cell density cells will form a confluent monolayer more quickly and after treatment, cells would organise themselves to form tubes. However, after monitoring at 24, 48 and 72 hours incubation no such organisation was observed (Figure 3.22). This may indicate that perhaps fibrin matrix gel is not the ideal model for testing angiogenesis in HOMECs. Therefore, commercially available growth factor-reduced (GFR) Matrigel was chosen to carry out further investigation on HOMECs angiogenesis.

GFR-Matrigel contains a solubilized basement membrane preparation extracted from the Engelbreth-Holm-Swarm (EHS) mouse sarcoma, a tumour rich in extracellular matrix protein, supplemented with low concentrations of growth factors. Although this model is usually used to study inhibition of angiogenesis, at this stage it was the best commercially available model that could be used to test for angiogenesis in HOMECs.

Initially, cells were seeded on the Matrigel and incubated overnight. Interestingly, tube-like structures were formed in this period, halting any further treatment of these cells (Figure 3.23). This indicated the importance of reducing the time between cell seeding and treatment in order to reduce the window of cells forming tubes. Therefore, cells were seeded and treated 2 hours later with or without CathL and positive control VEGF for another 8 hours. A shorter incubation was chosen so that cells do not further proliferate and migrate to form a monolayer after forming tube-like structure. A significant increase in tube formation was observed in CathL treated cells (200±11.1, n=3 (Figure 3.24 c, d) compared to control (145±15) (Figure 3.24 a, d). VEGF also significantly increased tube formation in HOMECs (210.3±22.4, n=3; Figure 3.24 b, d). These data, along

with proliferation and migration data, strongly suggest that CathL plays a proangiogenic role in HOMECs in the metastasis of ovarian cancer.

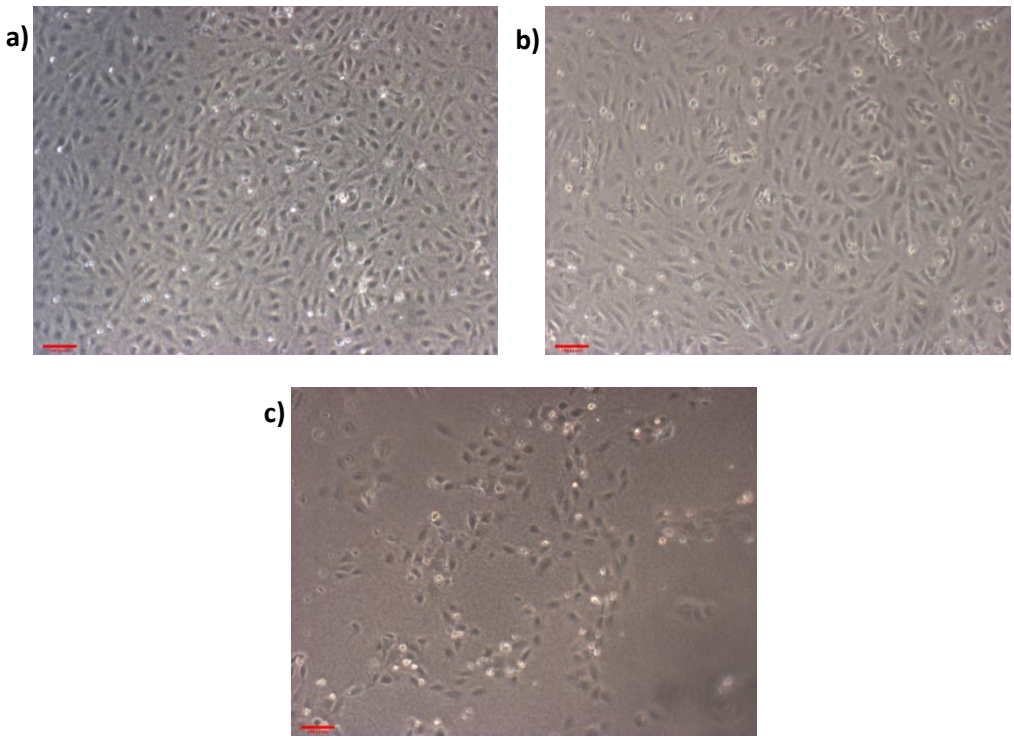

Figure 3.21: **Investigation of tubule structure formation in CathL-treated HOMECs in 2D fibrin gel.** HOMECs were plated onto fibrin matrices and treated with medium containing **a)** 2% FCS (control), **b)** supplemented with VEGF (positive control, 20ng/ml) and/or **c)** CathL (50ng/ml) for 72 hours. Controls contained HOMECs grown in medium containing 2% FCS alone. Photographs were taken at 72 hours after treatment using a Nikon phase contrast microscope camera. Scale bar =40 µm.

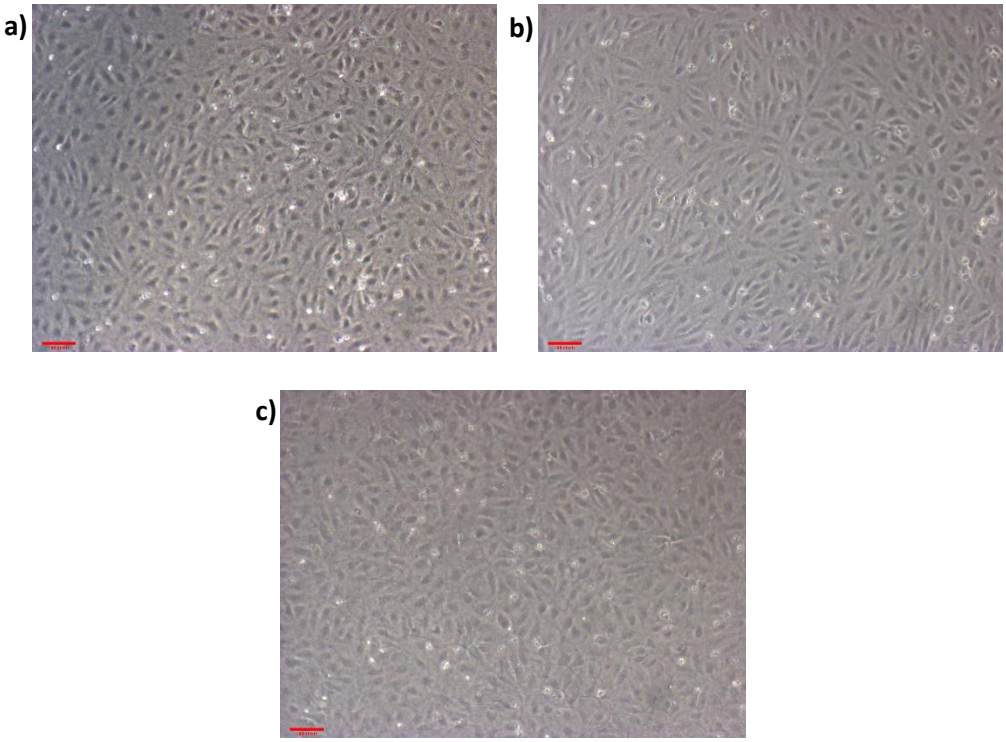

Figure 3.22: **CathL did not induce tubule structure formation in HOMECs in 2D fibrin gel.** HOMECs were plated onto fibrin matrices and treated with medium containing **a)** 2% FCS (control), **b)** supplemented with VEGF (positive control, 20ng/ml) and/or **c)** CathL (50ng/ml) for 72 hours. Controls contained HOMECs grown in medium containing 2% FCS alone. Photographs were taken at 72 hours after treatment using a Nikon phase contrast microscope camera. Scale bar =40 µm.

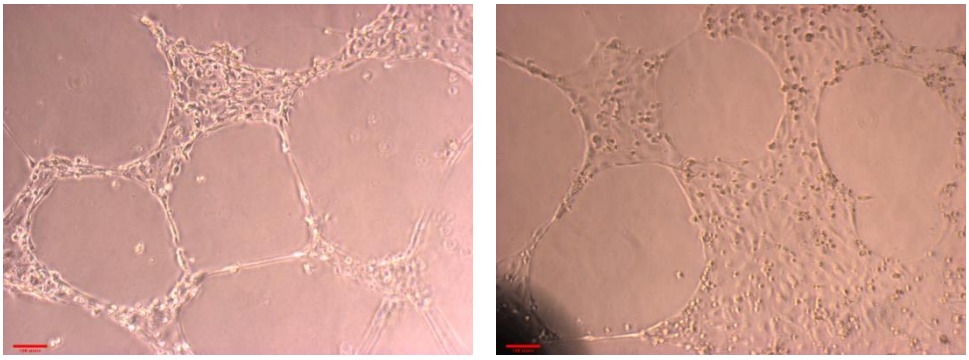

Figure 3.23: **Spontaneous tubule structure formation in HOMECs in 2D Matrigel after 24 hours.** HOMECs were plated onto GFR-Matrigel in medium containing 2% FCS. Photographs were taken at 24 hours after cell seeding using a Nikon phase contrast microscope. Scale bar =75 µm.

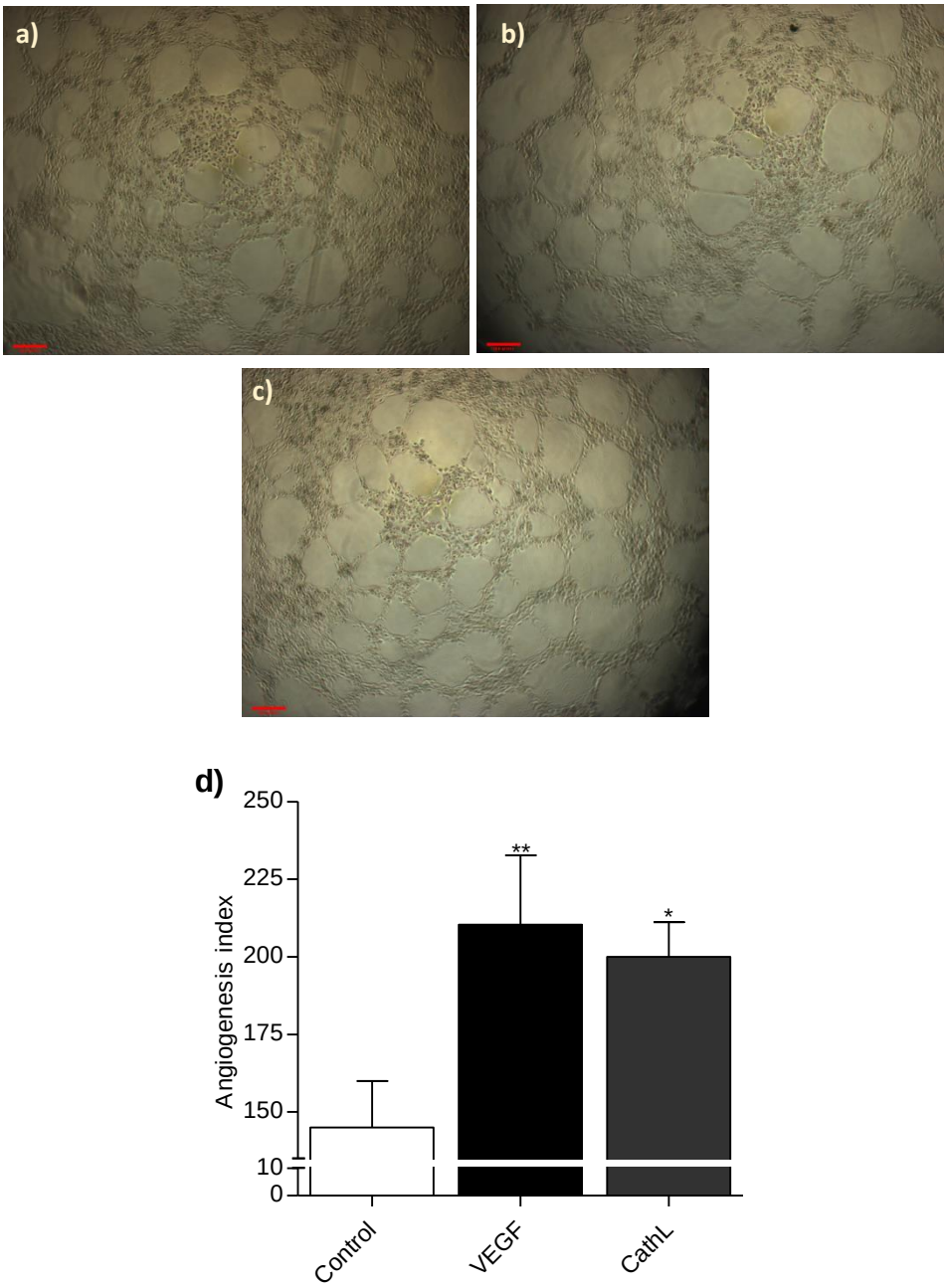

Figure 3.24: **CathL-induced tubule structure formation in HOMECs in a 2D Matrigel- stage 2.** HOMECs were plated onto GFR-Matrigel in medium containing 2% FCS and treated with media supplemented without **a)** control or with **b)** VEGF (20ng/ml) and/or **c)** CathL (50ng/ml) for 8 hours. Controls contained HOMECs grown in medium containing 2% FCS alone. Photographs were taken at 8 hours after treatment using a Nikon phase contrast microscope camera and **d**) tubule-structure formation (including nascent tubule structures) was quantified as described in method section. The results are presented as an angiogenesis index. *p<0.05, **p<0.01 vs control levels, n=4. Scale bars =40 µm.

3.3.8 CathL activates Tie-1 receptor tyrosine kinase

The previous data suggest that CathL plays a role in inducing pro-angiogenic changes via ERK1/2, and activating important intracellular kinases. Since the data also indicate that CathL induces these changes in a manner that is not dependant on its proteolytic activity, it is possible that the protein acts via an extracellular receptor. The possibility that CathL may act via a known tyrosine kinase receptor was investigated using a commercially available kit which simultaneously screens and detects activation of 49 different receptor tyrosine kinases. Cells were treated for 10 minutes with starvation media (2% FCS MV2), media supplemented with CathL (50ng/ml) or VEGF (20ng/ml) (positive control). The experiment was carried out according to the manufacturer's instructions and the membranes containing 49 antibodies were scanned using the Azure system. The data was analysed by Azure software which sets a threshold margin for detecting bands and subtracts any background that may interfere with the actual data. The results revealed that VEGF strongly activated VEGFR2 as expected and slightly activated VEGFR3. Intriguingly, CathL activated Tie-1 receptor kinase which is an orphan receptor and may be involved in angiopoetin/Tie-2 pathways (Ang) (a potent proangiogenic factor (Figure 3.25). Representation of VEGF-induced activation of VEGFR2,3 RTKs are shown in Appendix 1, Figure 1.8.

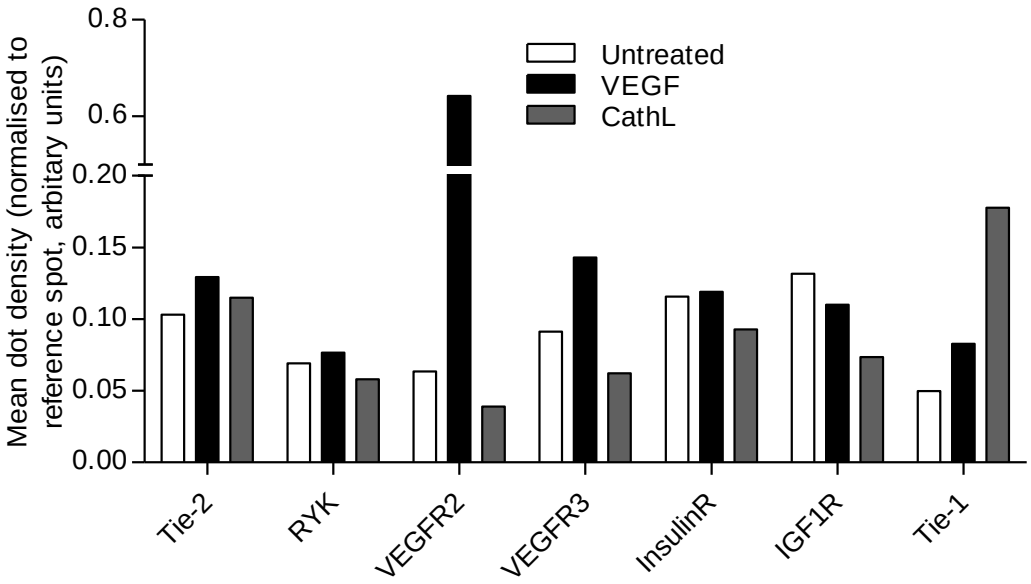

Figure 3.25: **CathL induces phosphorylation and activation of the RTK Tie-1.** Phosphorylation statuses of RTKs were assessed in cell lysates treated with or without CathL or VEGF for 10 minutes. The results of 1 minute exposure are expressed as mean dot density. The relative expression of specific phosphorylated proteins was determined following quantification of scanned images of membrane using Azure software. n=1.

3.4 Discussion

In this chapter, CathL was shown to induce HOMEC proliferation by a non-proteolytic mechanism. In addition, CathL was also observed, for the first time, to induce phosphorylation and activation of ERK1/2, AKT and p38α in HOMECs. Subsequent data suggested that CathL-induced HOMEC proliferation and migration were mediated via activation of the ERK1/2 and PI3K pathways, independent of AKT. Interestingly, CathL was also shown to induce tube formation in HOMECs. In a preliminary investigation, CathL was found to activate receptor tyrosine kinase Tie-1 in HOMECs.

Cells respond to their environment through actions of intracellular pathways. An agent such as a peptide hormone or growth factor typically binds to the extracellular domain of its transmembrane receptor(s), triggering activation of multiple signalling networks which are interconnected and non-linear. In these studies, only the ERK1/2 and AKT pathways have been investigated for their roles in angiogenesis as they have been reported to be involved in several EC models as discussed below.

Role of ERK1/2 and AKT in cellular proliferation and migration

The Raf-mitogen-activated protein kinase kinase- extracellular signal–regulated kinase (Raf-MEK-ERK) pathway represents one of the best characterised MAPK pathways in humans. The stimulation of receptor tyrosine kinases (RTK) by growth factors or cytokines provokes the activation of MAPKs in a multistep process which sequentially activates MEK1 and MEK2 (Mebratu and Tesfaigzi, 2009). The MEKs ultimately phosphorylate p44 MAPK and p42 MAPK, also known as ERK1 and ERK2 respectively, thereby increasing their enzymatic activity. Activated ERK1/2 translocates to the nucleus and transactivates transcription factors, including the ternary complex factor (TCF) - Elk1, serum response factor accessory protein Sap-1a, Ets1, c-Myc, Tal etc, changing gene expression such as the immediate early gene c-fos (Mebratu and Tesfaigzi, 2009). Thus, the ERK1/2 pathway can link G_0/G_1 mitogenic signals to the immediate early response to promote growth, differentiation or mitosis. A summary of the ERK1/2 pathway in cell proliferation is given in figure 3.26.

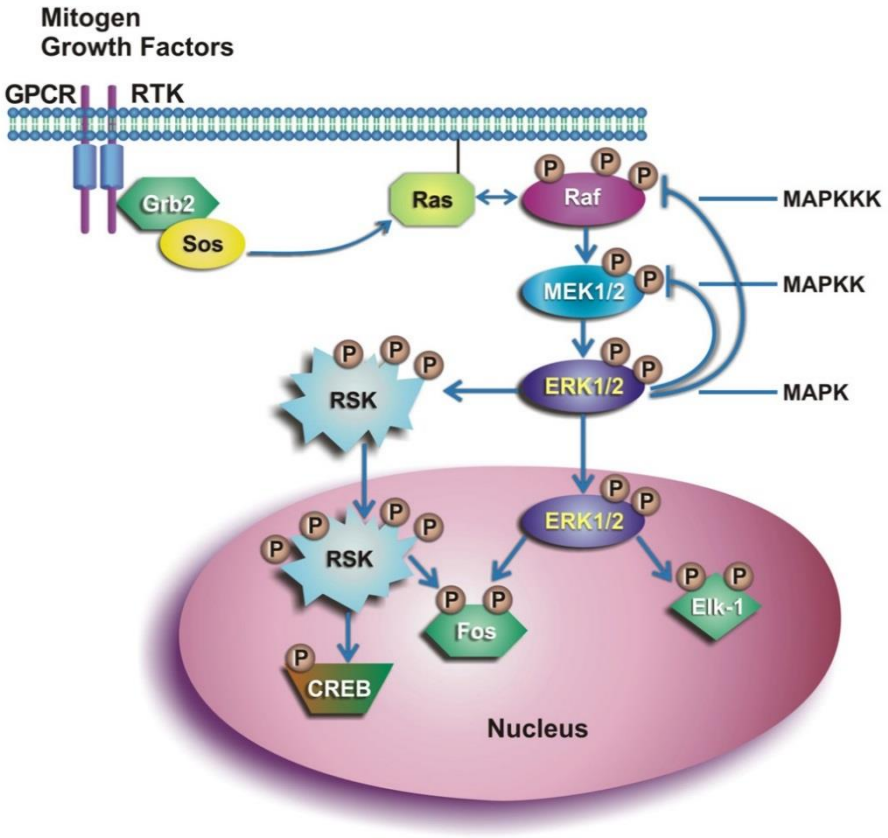

Figure 3.26: **Mechanism of ERK activation and cell proliferation.** Activation of receptor tyrosine kinases (RTKs) or G protein-coupled receptors (GPCRs) by growth factors or mitogens leads to the recruitment of an adaptor protein Grb2 (growth factor receptor bound protein) and the guanine nucleotide exchange factor Son of Sevenless (SOS). SOS activates Ras to recruit and activate Raf at the plasma membrane by phosphorylation at multiple sites. MEK1/2 is then phosphorylated at two serine residues and subsequently phosphorylates ERK1/2 on both threonine and tyrosine. Activated ERK1/2 phosphorylates ribosomal s6 kinase (RSK) and both RSK and ERK translocate to the nucleus where it activates multiple transcription factors, ultimately resulting in effector protein synthesis and causing changes in cell proliferation and survival. ERK phosphorylation of MEK and possibly Raf can inactivate the pathway at those steps creating a negative feedback loop. (Adapted from (Mebratu and Tesfaigzi, 2009)).

A role for activation of ERK1/2 in cell migration is now emerging. It is now known that on receiving extracellular stimuli, active Raf and inactive ERK bind to paxillin, thus mediating ERK activation at focal complexes in HUVECs (Abedi and Zachary, 1997, Ishibe et al., 2003). The paxillin-focal adhesion kinase (FAK) interaction is also involved in ERK activation (Subauste et al., 2004) where ERK phosphorylates paxillin, which in turn enhances paxillin-FAK association (Liu et al., 2002). However, it was also reported that ERK-mediated phosphorylation of FAK at Ser910 blocks the interaction of FAK with paxillin (Hunger-Glaser et al., 2003). These observations suggest a sophisticated regulation of the FAK-paxillin complex, in which ERK might initially promote complex-assembly by phosphorylation of paxillin and then promote disassembly by subsequent phosphorylation of FAK, leading to focal adhesion disassembly, and hence cell motility. Because dynamic integrin activation is required for cell migration (Huttenlocher et al., 1997, Palecek et al., 1997), ERK might regulate integrin activation and induce cell migration. Alternatively, coordinated activation of all these pathways by ERK may be crucial for promoting migration.

There are several other mechanisms that have been suggested by which ERK1/2 may regulate cell migration (Figure 3.27). One possible pathway involves myosin-based contraction via activation of myosin light chain kinase (MLCK) (Huang et al., 2004). In a more recent study, involvement of MLCK was strongly suggested to be a critical component of ERK1/2-mediated cell migration in COS-7 cells (a fibroblast-like cell line derived from monkey kidney tissue), MCF7 human breast cancer cells and HT1080 fibrosarcoma cells whereby ERK1/2 regulates phosphorylation of myosin light chain (MLC), leading to actin-myosin association and cell contraction, and therefore cell motility (Huang et al., 2004). Interestingly, Enomoto *et al.* reported that ERK1/2 is not involved in EGF-induced migration in COS-7 cells (Enomoto et al., 2005). Activated ERK1/2 has also been shown to phosphorylate m-calpain both *in vitro* and *in vivo* (Glading et al., 2004). Calpains are a family of Ca^{2+}-activated proteases that are involved in cell migration (Dourdin et al., 2001, Huttenlocher et al., 1997). Activated m-calpain interacts with FAK and together the complex then associates with the cytoskeleton whereby calpain degrades cytoskeletal proteins and causes adhesion disassembly in mouse embryo fibroblasts (Cuevas et al., 2003).

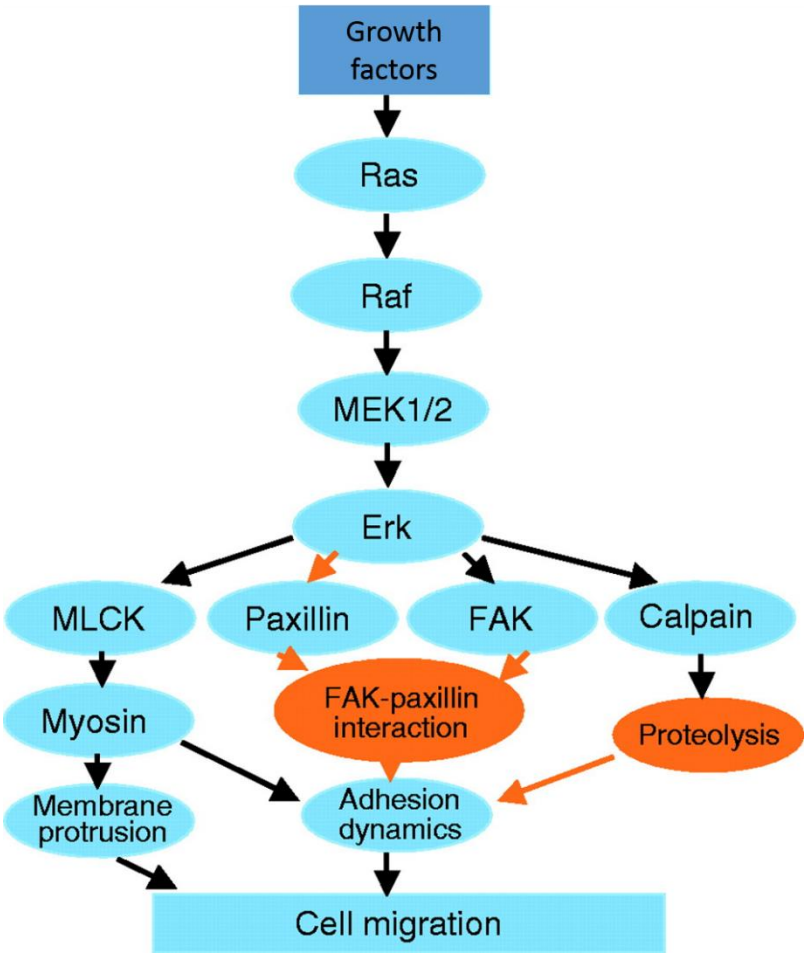

Figure 3.27: **Signalling pathways for cell migration mediated by ERK**. Growth factors, such as PDGF, EGF and FGF, activate ERK through the Ras-Raf-MEK1/2- ERK signalling module. Activated ERK regulates membrane protrusions and focal adhesion turnover via phosphorylating MLCK and promotes focal adhesion disassembly via phosphorylating and activating calpain. Phosphorylation of FAK and paxillin by ERK may regulate focal adhesion dynamics, probably by influencing the paxillin-FAK interaction. Orange lines represent speculative pathways (Adapted from (Huang et al., 2004)).

The AKT kinase is a downstream component of PI3K signalling, which is activated upon autophosphorylation of RTK induced by ligands such as insulin or other growth factors, stimulation of G-protein-coupled receptors, or activation of integrin signalling (Wymann et al., 2003). AKT is translocated to the plasma membrane from the cytoplasm upon activation of PtdIns(3,4,5)P3, a second messenger which is generated by active PI3K. Once recruited to the plasma membrane, AKT is activated by a multistep process that requires phosphorylation of Thr308 and Ser473. Phosphorylation of Ser473 is the key step because it stabilises the active conformation state (Yang et al., 2002). Once activated at the plasma membrane, phosphorylated AKT can translocate to the cytosol or the nucleus (Andjelkovic et al., 1999) and can directly phosphorylate many substrates within several subcellular compartments, including mediators of immediate changes in cell shape, movement and intermediary metabolism, cell viability, division or differentiation (Manning and Cantley, 2007).

In cellular proliferation, AKT is known to regulate cell cycle progression through multiple mechanisms such as by upregulating the expression of cyclin D1 and by regulating the CDK (cyclin –dependent kinase) inhibitor p21 Waf1/Cip1 (Lawlor and Alessi, 2001). Unlike other cyclins that are periodically induced throughout cell cycle progression, cyclin D is regulated by the extracellular mitogenic environment (Lawlor and Alessi, 2001). When the PI3K/AKT pathway was inhibited by LY294002, a marked reduction in cyclin D1 level in HUVECs was observed, suggesting that the PI3K/AKT pathway is involved in the induction of cell proliferation (Chen et al., 2008). Inhibition of AKT was also shown to inhibit cell cycle arrest by phosphorylating p21 which is known to block the cell cycle by reversibly inhibiting several cyclin-CDK complexes in NIH3T3 cells (Zhou et al., 2001). It has been reported that activation of AKT decreases cellular levels of p27, possibly via phosphorylating the forkhead transcription factor which is required for transcription of $p27^{Kip1}$, an enzyme inhibitor that typically causes cell cycle arrest in the G1 phase (Lawlor and Alessi, 2001).

The PI3K/AKT pathway has been shown to be extensively linked to mammalian cell migration. Hawkins *et al.* reported that PI3K activation enhances actin remodelling and generates membrane protrusions through activating Rac1 in porcine aortic ECs, induced by platelet derived growth factor (PDGF) (Hawkins et al., 1995). The PI3K/AKT signals also induce activation of P70S6K (ribosomal

protein S6 kinase β-1) which causes remodelling of actin, leading to cell migration and invasion in chicken embryo fibroblasts (Qian et al., 2004). Girdin/AKT phosphorylation enhancer (APE) is an AKT substrate that upon activation promotes actin organisation and cell motility in COS-7 cells (Enomoto et al., 2005). In human saphenous vein ECs, human aortic ECs and bovine aortic ECs, nitric oxide has also been shown to induce cell migration and angiogenesis via activating PI3K (Kawasaki et al., 2003). Leptin is another factor that also induced human umbilical vein EC migration via activation of AKT (Goetze et al., 2002). Bovine lung microvascular EC and bovine aortic EC migration was also induced by VEGF via activation of the AKT pathway (Morales-Ruiz et al., 2000).

CathL has been linked to tumour invasion and metastasis by its ability to degrade ECM components. As discussed in chapter 1 (section 1.7.1.3), there is considerable evidence that CathL may play a role in the pathogenesis of EOC. The involvement of CathL in the invasion and metastasis of EOC raises the possibility that it may be a marker of advanced stage ovarian cancer. This is supported by data showing a significant increase in CathL expression in the endothelium of vessels within omentum hosting metastatic ovarian high-grade serous carcinoma *in vivo* compared with omentum from control patients with benign ovarian cystadenoma. Recently SKOV3 and A2780 EOC cells were shown to secrete CathL and exogenous addition of CathL to HOMECs used as an *in vitro* model of omental angiogenesis, induced migration and *in vitro* tube structure formation (Winiarski et al., 2013).

CathL in cellular proliferation

The mechanism of CathL-induced cell proliferation, a key step in angiogenesis, had not been explored and therefore, the generic hypothesis of this study was: CathL induces proangiogenic changes in HOMECs in a non-proteolytic mechanism. In order to address the hypothesis, initially, cell proliferation was tested in HOMECs treated with CathL at increasing concentrations using the WST-1 assay, which estimates cell number based on metabolic activity.

Previous published data reported that EOC cell-secreted concentration of CathL into tumour conditioned media was in the ng/ml range. In this current study, three increasing concentrations of CathL (20, 50 and 80ng/ml) were selected to examine proliferation in HOMECs based on the previous findings. CathL at 50ng/ml and 80ng/ml induced significant cell proliferation compared to control, although at the former concentration this rise in cell proliferation was most significant. Therefore, 50ng/ml of CathL was selected to carry out further investigations.

Although WST-1 is an established technique, measuring cell proliferation via metabolic activity may give false positive results as factors other than treatment such as temperature, media conditions, and compounds within the treatment may interfere with the enzymes that generate the metabolically active readout. Therefore, to eliminate the possibility of a false positive, HOMEC proliferation was tested using a second technique the CyQUANT cell proliferation assay which consists of a cell-permeant fluorescently-labelled DNA binding dye that stains nucleic acids within cells and emits a fluorescent measurement. The data from both techniques complemented each other and suggested that CathL significantly induces HOMEC proliferation compared to control.

In normal physiological processes, CathL acts as a lysosomal protease, in which it breaks down unfolded or wrongly folded proteins. Lysosomes have an acidic environment, with a pH ranging from 3-5.5. CathL has an optimum pH of 5.5-6 at which it is proteolytically active (Mason et al., 1987, Mason and Massey, 1992). However, CathL has also been shown to be proteolytic at neutral pH. Since exogenous CathL induces HOMEC proliferation in culture media, it was important to investigate whether CathL is acting via a proteolytic or non-proteolytic mechanism at the prevailing pH. The first set of experiments were designed to examine whether inhibiting proteolytic activity of CathL altered HOMEC proliferation. In the presence of FY-CHO (a potent and selective inhibitor of CathL-proteolytic activity), there was no inhibition of CathL-induced HOMEC proliferation. FY-CHO has been used to prevent secreted CathL-induced bone resorption in unfractionated rat bone cells in the pit formation assay and reduced bone-weight loss in mice in a dose-dependent manner (Woo et al., 1996). Furthermore, it has been extensively used to inhibit CathL mediated *in vitro*

migration and invasion of breast and prostate cancer cells (Sudhan and Siemann, 2013). Here, this inhibitor was primarily chosen over cystatin C, a commonly used CathL inhibitor, because cystatin C elicits non-selective inhibition on all cysteine proteases. The range of concentrations of FY-CHO was selected based around a concentration of 10 μM which strongly inhibited CathL-proteolytic activity against CLN7 membrane glycoprotein in COS-7 cells (Steenhuis et al., 2012). These data initially suggested that CathL induces HOMEC proliferation in a non-proteolytic mechanism.

These data indicate that a CathL inhibitor had no effect in CathL-induced proliferation. Thus, the next set of experiments were designed to examine whether CathL was actually proteolytically active at pH 7.2 (i.e. in culture media) and if so whether FY-CHO would actually inhibit in these conditions. *In vitro* CathL-proteolytic activity at an array of pHs was examined using ZVA, a CathL-specific fluorogenic substrate. Interestingly, CathL was found to be proteolytically active throughout the pH range starting from its optimum pH (4.5) up to pH 7.6, including the pH of cell culture media which was demonstrated to be between 7.11 and 7.34 throughout a typical proliferation experiment. These data coincide with previous findings (Dehrmann et al., 1995), where CathL was also proteolytically active at pH 7 up to pH 8. Thus, CathL is catalytically active at culture media pH. Finally it was important to demonstrate that the inhibitor was active in culture media pH conditions. When FY-CHO was included at the same concentration as in the proliferation experiment (10 μM), CathL proteolytic activity was completely blocked across all pHs. It can be concluded that if CathL was active as a protease in cell culture media, it would have been inhibited by FY-CHO, as was shown in previous studies and in this pH experiment. However, the fact that CathL-induced proliferation was not altered in the presence of the inhibitor suggests that CathL induces HOMEC proliferation via a novel proteolytic-independent mechanism.

CathL-induced activation of intracellular signalling pathways and their role in cellular proliferation

As CathL appeared to induce HOMEC proliferation in a non-proteolytic manner, it was logical to assess the intracellular signalling pathways activated by CathL.

A human phosphokinase array indicated that kinases ERK1/2, AKT(S473) and p38α which are mainly involved in cell survival, proliferation and migration were activated in CathL treated cells compared to untreated cells after 4 minutes treatment. This time point (4 minutes) for CathL was selected because previous reports suggest that MAPK/ERK1/2 and AKT phosphorylation are maximum at 4-5 minutes (Konopatskaya et al., 2005). Out of these three kinases, ERK1/2 and AKT were selected to be investigated in further experiments primarily because both kinases have been shown to be involved in cell proliferation and cell migration, two critical steps of angiogenesis.

Subsequently, cell-based ELISAs were carried out to further confirm the above finding of the proteome profiler. These commercially available ELISA kits use live cells in a 96 well plate which are then fixed and permeabilised. This permeabilsation allows primary and secondary antibodies to enter the cell and bind to corresponding targets. The main benefit of this kit is that there is no need for cell lysis and quantification of protein, and hence it is very efficient and also cost-effective. ELISAs were chosen over western blots (WBs) as WBs only visualise the presence of a particular protein target and quantifying is less sensitive, whereas using these ELISA kits, 96 samples can be analysed and quantified at the same time.

The ELISA was performed at 2 time points, 4 and 10 minutes after CathL treatment. Multiple time points are important to test for phosphorylative statuses of kinases as they vary over time and the activation of intracellular kinases can be transient. Interestingly, CathL induced phosphorylation of both ERK1/2 and AKT 4 minutes after treatment. However, 10 minutes later, the level of phosphorylation reduced back down to their basal level (control). VEGF was used as a positive control in this experiment as it is a well-known activator of ERK1/2 and AKT. As shown for CathL, VEGF also induced ERK1/2 and AKT phosphorylation at 4 minutes after treatment. VEGF-induced AKT phosphorylation was reduced 10 minutes later, although the level of phosphorylated ERK1/2 increased further. This may demonstrate a transient activation and subsequent deactivation of these kinases.

These data demonstrate for the first time that CathL is able to induce ERK1/2 and AKT phosphorylation in ECs. Previously, CathL was shown to induce HUVEC migration via the JNK pathway in a proteolytic manner (Chung et al., 2011).

However, this pathway was not activated by CathL treatment in HOMECs as indicated by proteome profiler (data not shown).

Activation of ERK1/2 has been extensively shown to be involved in cell proliferation (Rubinfeld and Seger, 2005). Therefore, it was hypothesised that ERK1/2 may be involved in the induction of proliferation in CathL-treated HOMECs. Two well-known inhibitors (U0126 and PD98059) of MEK/ERK1/2 were used to examine this. Both inhibitors at different concentrations demonstrated significant inhibition of proliferation in HOMECs compared to CathL-treatment alone, suggesting that ERK1/2 may be involved in CathL-induced HOMEC proliferation. The validity of the use of the inhibitors was established by ELISA data indicating that both inhibitors at their selected concentrations inhibited ERK1/2 phosphorylation.

It is important to note that the concentrations for U0126 and PD98059 were chosen for the above experiments primarily based on their toxicity assay results and also their inhibitory effects on VEGF-induced (positive control, Appendix 1, Figure A1.3) HOMEC proliferation and the current literature. Reported investigations into the cross-reactivity of U0126 and PD9859 showed that the selected concentrations of the ERK1/2 inhibitors in this study do not activate the AMPK pathway, unlike higher concentrations (Dokladda et al., 2005).

The role of activated ERK1/2 in cell proliferation has been reported in other EC types. For instance, Jin *et al.* demonstrated VEGF-induced proliferation of RF/6A cells (rhesus macaque choroid-retinal EC line) mediated by ERK1/2 pathway (Jin et al., 2013). It was reported that hypoxia enhances FGF2- and VEGF-stimulated human placental artery EC proliferation via the MEK/ERK1/2 pathway (Wang et al., 2009). TRAIL, a member of the tumour necrosis factor family of cytokines, was shown to induce HUVEC proliferation via activation of the ERK1/2 pathway but not JNK or p38α pathways (Secchiero et al., 2003). Extracellular VEGF was shown to induce proliferation in HUVECs via activation of the MAPK/ERK1/2 pathway (Kanno et al., 2000). This was further demonstrated by a reduction in DNA synthesis upon PD98059 treatment. Activation of ERK1/2 pathway was observed in FGF2 induced cellular proliferation of murine brain ECs (Klint et al., 1999). Together, these data suggest an important role of ERK1/2 in the induction of cellular proliferation in different EC models. In this study, CathL induced HOMEC proliferation via activation of the ERK1/2 pathway, and this, to my

knowledge, is the first study to report such an observation in mammalian cells to date.

Based on the previously described role for PI3K/AKT in EC proliferation and the fact that CathL induced increased levels of phosphorylated AKT, the involvement of this pathway in HOMEC proliferation stimulated by CathL was also investigated. Initially two well-known inhibitors of this pathway were chosen- PI3K inhibitor LY294002 and selective AKT inhibitor MK2206. As PI3K is upstream of AKT, activation and involvement of this kinase was tested. LY294002 decreased HOMEC proliferation in a dose-dependent manner and ELISA data confirmed that LY294002 inhibited phosphorylation of AKT in HOMECs. This suggested that, like the ERK1/2 pathway, PI3K/AKT pathway is also involved in CathL-induced HOMEC proliferation.

In order to further understand the above findings, a selective inhibitor of AKT was used. Intriguingly, MK2206 did not inhibit cell proliferation induced by CathL, although phosphorylated levels of AKT were maintained at basal level by the inhibitor (Figure 3.12). This may suggest that activated AKT is not responsible for inducing HOMEC proliferation since MK2206 has been shown to be a potent selective inhibitor of AKT, and that PI3K may act via an AKT-independent pathway to induce proliferation. This observation is supported by reports in the literature. An analysis of 547 human breast cancers showed no correlation between AKT phosphorylation and activating PI3K mutations (Stemke-Hale et al., 2008). This was later confirmed in another study that showed that activating mutation of PI3K can markedly reduce AKT phosphorylation (Vasudevan et al., 2009). Additionally, overexpression of PDK1 (phosphoinositide-dependent kinase-1) in human breast cancer cell lines increased anchorage independent growth and tumour formation, which was not prevented by AKT inhibition (Gagliardi et al., 2012). Similarly, no correlation was found between the phosphorylation of AKT and the mutation status of PI3K in colon cancer cell lines (Morrow et al., 2005). It was suggested that a prolonged inhibition of PI3K may fail to block AKT phosphorylation i.e. there are other kinases responsible for AKT activation under chronic PI3K inhibition (Dufour et al., 2013). These reports indicate that to elicit an activated PI3K-mediated cellular response in cancer AKT activation is not essential and that kinases other than AKT may be involved.

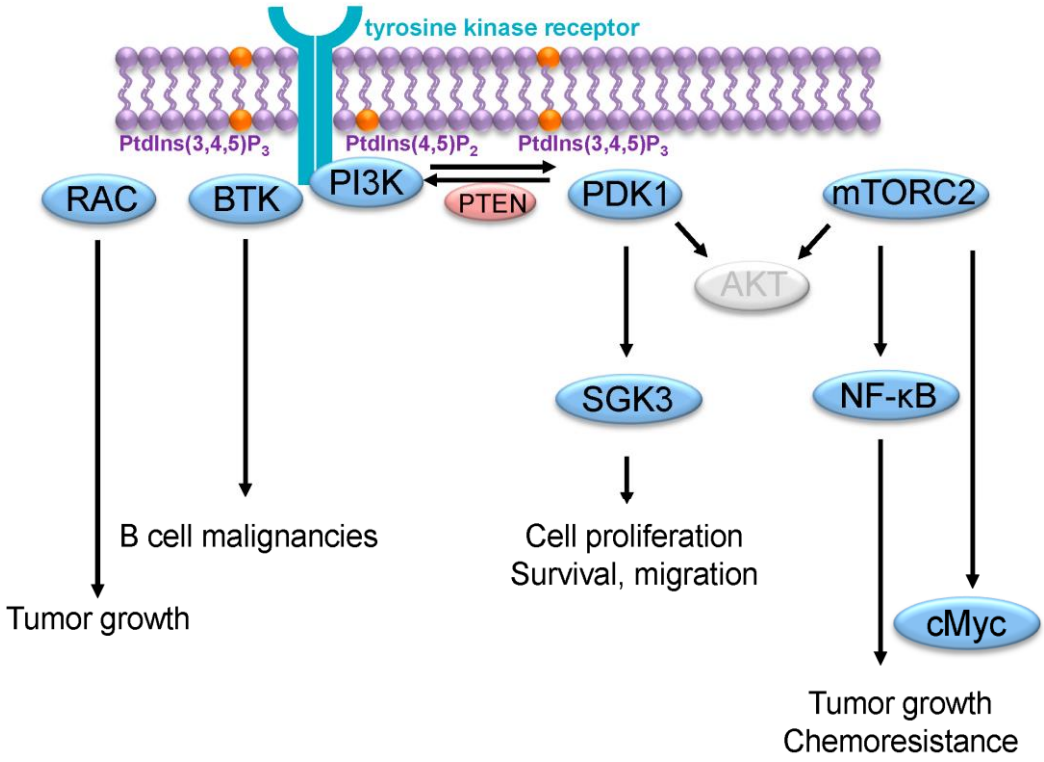

Figure 3.28: **AKT-independent PI3K signalling cascades in cancer.** Several AKT-independent mechanisms used by PI3K to promote cancer growth have been described. They include activation of RAC, Burton's tyrosine kinase (BTK) in B cell malignancies, PDK1/SGK3 and mTORC2/NF-κB; mTORC2/c-Myc. Light grey ovals imply components of the signalling pathway that are not activated or bypassed. Taken from (Faes and Dormond, 2015)

Several kinases downstream of PI3K, other than AKT, have been identified (Figure 3.28). For instance, PDK1 was found to activate MAPK or PKCα (protein kinase C-alpha) pathways (Sato et al., 2004, Zeng et al., 2002). More recent evidence suggests that SGK3 (serum- and glucocorticoid- inducible protein kinase 3) may be involved as a key downstream mediator of PI3K/PDK1 signalling in breast cancer cells (Faes and Dormond, 2015). Activation of mTORC2 has also been identified as another AKT-independent kinase which mediates proliferation of glioblastoma cells (Tanaka et al., 2011). RAC proteins, a subfamily of the Rho family of small GTPases, are also activated by PI3K (Welch et al., 2003). In breast cancer, RAC proteins were shown to activate the MAPK/ERK1/2 pathway which is responsible for mediating cellular proliferation (Ebi et al., 2013). These data strongly indicate that PI3K is able to mediate cellular proliferation via mechanisms independent of AKT. It should be noted that a study investigating cross-reactivity of LY294002 has shown that this inhibitor is able to strongly inhibit ERK1/2 phosphorylation in a dose-dependent manner (1 µM to 30 µM) in Jurkat T cells (Guo et al., 2014). So it is possible that the concentration used in my studies (25 µM) is simply inhibiting ERK1/2 and PI3K is not involved in mediating CathL-induced HOMEC proliferation. This could be examined further by using another PI3K inhibitor or knocking down PI3K in HOMECs using siRNA in future studies.

None of these studies discussed above have used EC models. However, my studies do contradict available reports on ECs in the literature where cell proliferation has been shown to be promoted via activation of the PI3K/AKT pathway. For instance, VEGF-A-induced phosphorylation of PI3K/AKT was suppressed by SMEK1, a tumour suppressor protein, in HUVECs and SKOV3, halting cell proliferation (Kim et al., 2015). Jin *et al.* demonstrated VEGF-induced proliferation of RF/6A (monkey retinal EC) cells mediated by PI3K/AKT pathway (Jin et al., 2013). CD151, a member of the transmembrane 4 superfamily, was shown to significantly induce proliferation of HUVECs by nitric oxide (NO) production via activation of the PI3K/AKT pathway (Zheng and Liu, 2006). Secchiero *et al.* also reported activation of the AKT pathway in TRAIL-induced HUVEC proliferation (Secchiero et al., 2003) which was reduced significantly in the presence of LY294002.

In conclusion, the data presented here agree with the reports described above whereby LY294002 was able to inhibit CathL-induced HOMEC proliferation. However, in contrast to the current literature, CathL did not induce HOMEC proliferation via AKT activation as the selective AKT inhibitor MK2206 did not inhibit this cellular function. It is possible that PI3K elicits its pro-proliferative response in HOMECs via an AKT-independent mechanism as discussed above. Another possibility is that, LY294002 simply inhibits ERK1/2 which was observed to be activated in the proliferative pathway in HOMECs as reported elsewhere (Guo et al., 2014).

CathL-induced HOMEC migration

In angiogenesis, EC migration is another key step. This motile process is directionally regulated by stimuli, usually proangiogenic factors such as VEGF. Previously it was shown that CathL is able to induce HOMEC migration at 48 hour after treatment. This was shown using an Oris migration assay kit which assesses migration of cells in to a cell-free zone. However, ideally, cell migration should be assessed after a shorter incubation time. An incubation of 48 hours with CathL or VEGF, which have been shown to be proliferative, may induce cell proliferation and not just migration. Therefore, in my study, HOMEC migration was not assessed using an Oris migration kit, instead a cultrex transwell Boyden chamber assay kit was used. Also, the incubation period of CathL treatment was brought down to 6 hours which is much shorter than the time required for cells to proceed through a cell cycle (Cary et al., 1996), eliminating any possibility of cell proliferation giving false positive data.

The cultrex cell migration assay kit utilises a simplified Boyden chamber design with an 8 micron polyethylene terephthalate membrane. There are pores in the membrane which allow access of migrating cells to the bottom chamber. With only 6 hour incubation, it allows the active migratory mechanism of cells to be assessed in response to growth factors (Chen, 2005). However, initially, a 48 hour incubation was carried out with VEGF and/or CathL treatment to be consistent with the Oris migration kit data. Interestingly, it was revealed that there were no differences in migration compared to control (data not shown). This might have been because after 48 hours incubation, migratory effects of cells have

plateaued at their maximum level due to induction of cell-cell interaction and a reduction in cell motility and so there was no significant difference between different conditions (Sander et al., 1998, Royal et al., 2000, Ren et al., 2000, Chen et al., 2002). Thus, the incubation period was reduced to 6 hours. At this time point, CathL induced significant migration of HOMECs compared to control.

Role of activated signalling pathways in CathL-induced HOMEC migration

As CathL induces migration in HOMECs, the signalling pathway leading to migration was investigated. Initially, it was hypothesised that the PI3K/AKT pathway was involved in this process since the PI3K/AKT has been shown to be extensively linked to mammalian cell migration. The effects of both the PI3K inhibitor LY294002 and the AKT inhibitor MK2206 were examined. Neither of these inhibitors significantly inhibited CathL-induced HOMEC migration, suggesting that the PI3K/AKT pathway is not involved. This is in contrast to other EC studies previously described in the literature. However, PI3K/AKT independent migration has been observed in primary human fibroblasts stimulated by FGF1 (Marcinkowska and Wiedlocha, 2003). A similar observation was also revealed in VEGF-induced (positive control, Appendix 1, Figure A1.5) HOMEC migration. VEGF is a well-known proangiogenic factor that activates numerous cell signalling cascades. It is possible that VEGF-induced HOMEC migration is not mediated via AKT activation, however, there may be other kinases, such as activated p38-mediated actin polymerisation and ERK1/2 pathway, involved which overcome the inhibitory effects on AKT activation (Rousseau et al., 2000, Chiu et al., 2013).

As AKT phosphorylation was shown not to be involved in the CathL-induced migration of HOMECs, the role of ERK1/2 was investigated. Interestingly, in the presence of ERK1/2 inhibitors, cell migration was completely abolished, suggesting that ERK1/2 plays a significant role in CathL-mediated HOMEC migration. This agrees with the literature where numerous studies have reported the importance of ERK1/2 in cell migration. For instance, human colorectal cancer cell-derived vesicles induced migration in human microvascular ECs and HUVECs via activation of the ERK1/2 pathway (Yoon et al., 2014). It has also been reported that activation of the ERK1/2 pathway plays an important role in

VEGF-induced migration of human aortic ECs, HUVECs and bovine brain ECs (Bellou et al., 2009, Chiu et al., 2013). Ahmad *et al.* reported that activation of ERK1/2 was involved in proliferation of primary human lung microvascular ECs induced by activation of the adenosine A_{2A} receptor (Ahmad et al., 2013). Additionally, activated ERK1/2 plays an important role in mediating human endometrial stromal cell migration induced by platelet derived growth factor BB. In murine brain ECs, activated ERK1/2 within focal adhesions was found to be associated with FGF2-induced chemotaxis (Shono et al., 2001). Zhao *et al.* recently suggested activation of ERK1/2 in conditioned medium-induced migration of human keratinocyte cell line (HaCaT) (Zhao et al., 2016a). Activation of ERK1/2 has also been shown to play an important role in inducing migration of pancreatic carcinoma cells (Cho and Klemke, 2000) and MAPK/ERK1/2 have also been reported to promote EGF-induced migration in human diploid dermal fibroblasts (Xie et al., 1998). Together, these studies strongly suggest that ERK1/2 activation plays an important role in migration in a variety of cell types, however, the exact molecular mechanism remains unknown. At this stage, it is difficult to discern a mechanism that ERK utilises to induce CathL-mediated HOMEC migration, however, MLCK activation and actin-myosin association seems to be a reasonable candidate as it has been confirmed in several cell models, including ECs, as discussed previously (Shono et al., 2001).

CathL-induced angiogenesis in HOMECs

Since CathL is pro-proliferative and pro-migratory in HOMECs, both critical steps in angiogenesis, it was logical to assess angiogenic-tube structure formation in these cells. Previously Winiarski *et al.* showed CathL-induced tube formation in HOMECs using a 2D fibrin matrix model (Winiarski et al., 2013). However, a 3D angiogenesis assay offers a model which is much closer to the actual environment *in vivo* than can be achieved using 2D cultures. Therefore, an *in vitro* 3D model of angiogenesis was initially adopted. Firstly, to verify the technique, HCMEC cells were used. HCMEC proliferated and formed new vessel sprouts in the gel in response to complete growth media (positive control), VEGF and CathL. The assay was thus replicated using HOMECs, under the same conditions. However, HOMECs did not respond to any of the above conditions, i.e. there was no visible cell sprouting.

It was thought that the amount of FCS in culture media may play a role in the spouting of HOMECs. Due to the tight fibrin gel, cells might not have received sufficient quantity of FCS. As EC growth significantly depends on serum concentration (Bala et al., 2011), different concentrations of FCS were supplemented in media with or without EC growth factors. However, there was still no spouting of HOMECs. Also, there was no difference observed between 5% serum and 10 or 20% serum, and hence 5% serum was used for further optimisation.

The next set of experiments investigated the effect of using different concentrations of aprotinin, a potent inhibitor of several serine proteases such as trypsin, chymotrypsin, kallikrein, thrombin, activated protein C and plasmin (Mahdy and Webster, 2004). In the 3D fibrin gel, aprotinin is added to prevent fibrinolysis by proteases in serum such as plasmin. However, since ECs physiologically secrete proteases (matrix metalloproteinases and serine proteases) to break down ECM components during sprouting (Lafleur et al., 2002), it was speculated that aprotinin might be blocking degradation of fibrin matrix by proteases secreted by HOMECs, and hence preventing sprouting. This may not have been observed in HCMEC if they secreted a different profile of proteases. In order to address this, different concentrations of aprotinin were used in the gel. Interestingly, in the absence of aprotinin, HOMECs degraded the fibrin matrix, and instead of forming branches, cells formed a monolayer within the gel. This was not observed in the presence of aprotinin at two different concentrations. This may indicate that HOMEC-secreted proteases are inhibited by aprotinin, and that in order to form branches, the fibrin gel matrix may need significant modifications. For instance, it was thought that the tightened fibrin polymer strands may act as a physical barrier for HOMECs to be mobile within the gel which could be tested by reducing the viscosity of the gel. However, when the rigidity of the gel was reduced by lowering the concentration of thrombin, the gel did not form at all (data not shown), indicating that the thrombin concentration that has been recommended in this protocol is the optimal for this system.

As a future direction, ECM component fibronectin could be incorporated into the fibrin matrices. Fibronectin is an integral part of the ECM and has been shown to play a critical role in angiogenesis by promoting interactions between cell surface integrins and cell-binding domains such as the heparin-binding domain (Kim et

al., 2000). In fibrin gel, fibronectin has been shown to serve as a spacer between fibrin strands, increasing turbidity of the gel (Okada et al., 1985). In another study, fibronectin was shown to promote elongation of sprouting microvessels in 3D collagen gel from rat aorta probably by recruiting migratory ECs, instead of increasing proliferation as no change in DNA was observed (Nicosia et al., 1993). In addition, since ECs secrete proteases to breakdown surrounding ECM, fibronectin may be degraded in 3D culture gel, and fragmented fibronectin has been shown to aid migration of capillary ECs in chemotactic chambers by propelling cells toward areas where the matrix was actively degraded (Ungari et al., 1985). Thus, fibronectin may be a potential candidate, which can be included in the fibrin gel to test for HOMEC sprouting in the 3D environment in future studies.

The assay optimisation process was taken a step further by assessing the effects of the beads that are used to embed cells in the fibrin gel. As recommended in the original protocol, collagen pre-coated cytodex 3 beads were used initially. Since HOMECs grow on 2% gelatin coated surface in culture, it was thought that the absence of gelatin on the beads might have affected growth of these cells. Therefore, gelatin pre-coated cytodex 1 beads were used to embed cells. No difference was observed in the survival or growth between cells embedded on either of the beads.

At this stage of the investigation to produce timely results, it was decided to move on to a 2D fibrin gel assay to assess angiogenic tube-formation in HOMECs. Two-dimensional assays have been popular in assessing angiogenesis. Tubule formation assays are usually performed on matrices consisting of fibrin, collagen or Matrigel (the basement membrane extract of the EHS sarcoma), which stimulate the attachment, migration and differentiation of ECs into tubules in a manner that mirrors the *in vivo* situation (Lawley and Kubota, 1989).

However, as described in result section 3.3.7, developmental studies indicated that Matrigel was the most appropriate matrix for these studies. Matrigel is a solubilised basement membrane preparation extracted from EHS, a tumour rich in ECM proteins and contains large amounts of collagen IV, laminin, heparan sulphate proteoglycans, and entactin/nidogen. It also contains growth factors such as TGF-β, EGF, IGF, FGF, tissue plasminogen activator, and other growth factors already present in the tumour. Lawley and Kubota (1989) demonstrated

that the rate of differentiation of ECs was increased by plating onto Matrigel, with tubules beginning to form in 1 h and completed in 8–12 h (Lawley and Kubota, 1989). This method is extensively used in EC-tubule formation assays, particularly to test for compounds that have anti-angiogenic potential.

Recently, a second form of Matrigel has been developed known as GFR-Matrigel. In this form, the levels of growth factors and cytokines have been markedly reduced. Although extensive tubules can be formed in this GFR-Matrigel, it allows for more selective determination of the efficacy of proangiogenic factors. Thus, GFR-Matrigel was used to study tubule-formation/angiogenesis in HOMECs. Initially, cells were seeded on the Matrigel and incubated for 24 hours in starvation media (supplemented with 2% FCS, no growth factors). Interestingly, HOMECs formed tubules throughout under all conditions after 24 hours, and hence further experiments were not carried out at this time point. In order to overcome this issue, the time between cell seeding and treatment was reduced to two hours to restrict the period in which the cells could spontaneously form tubes. Also, cells were treated only for 6 hours prior to assessment of tubule-formation. It was observed that CathL-induced tubule-structure formation was significantly higher than control (untreated) wells. VEGF was the positive control in this experiment and also induced significant tubule structure formation in HOMECs. Thus, this result, along with the proliferation and migration data, strongly suggests that CathL is a pro-angiogenic growth factor acting on HOMECs and plays a role in metastasis of ovarian cancer to the omentum.

It is important to note that, despite having data that supports the angiogenic properties of CathL in HOMECs, ideally a more robust method should be developed to examine *in vitro* 3D angiogenesis tubule formation. Although Matirgel assay is a very efficient method to visualise *in vitro* angiogenesis, it has significant drawbacks. For instance, it has been shown that the morphology of tubules formed in Matrigel displayed little or no resemblance to capillaries formed *in vivo* (Donovan et al., 2001). Also, tubule length in Matrigel was found to be homogenous and significantly shorter than capillaries formed *in vivo*. This does not replicate the *in vivo* situation as in tumour angiogenesis, ECs form neovessels of various lengths and morphologies (Donovan et al., 2001). Matrigel also displays EC aggregates, which has been suggested to be regulated by growth factors already contained within the Matrigel (Donovan et al., 2001). It is important

to note that, Matrigel assay, due to the presence of numerous growth factors, are able to induce differentiation of non-endothelial cell types such as mesenchymal cells, kidney epithelial cells, blastocytes and colon cancer cells (Donovan et al., 2001), making it less specific. Also, there are some bias in this method of analysing tubule structure formation. For instance, the angiogenic index may vary based on the orientation of the well at which the photograph has been taken. Thus, this method may not be ideal to quantify angiogenesis.

HOMECs are a relatively new cell model that has been extensively used by our group, and so it is crucial to establish a novel way to demonstrate angiogenesis-cell sprouting and tubule-structure formation. This should, in the future, allow in-depth research investigating critical and novel cell signalling pathways that aid the metastatic cascade in ovarian cancer.

CathL induced activation of RTK Tie-1

Since CathL activates intracellular kinases that promote cell survival and growth, it was hypothesised that a receptor tyrosine kinase (RTK) may be involved in mediating such cellular effects. A preliminary investigation was carried out to identify possible RTKs in HOMECs that might be activated by CathL. A commercially available array was used to simultaneously screen activation of 49 RTKs in HOMECs. Intriguingly, it was found that CathL activated Tie-1 (tyrosine kinase with immunoglobulin-like and EGF-like domains 1) in HOMECs. The array was verified by VEGF (positive control) which strongly induced activation of VEGFR2.

Tie-1 is an orphan receptor (an apparent receptor that has similar structure to other identified receptor but whose endogenous ligand has not yet been identified) expressed on activated ECs in vasculogenesis in the early stages of development and in microvessels undergoing angiogenic sprouting (Partanen et al., 1996), and a role has been hypothesised in pathology including tumour angiogenesis and atherosclerosis (Savant et al., 2015). The molecular function of Tie-1 is not completely understood, as it does not directly bind the angiopoietic growth factors, which are the ligands for Tie-2. However, Tie-1 tyrosine phosphorylation is induced by Ang (1 or 4), most likely in a complex with Tie-2 (Marron et al., 2000, Saharinen et al., 2005, Yuan et al., 2007). Ang activates Tie-

2 in a unique manner, which involves the translocation of Tie-2 to EC-cell contacts, with Tie-1 also present in these complexes (Saharinen et al., 2005). Phosphorylation of a chimeric form of Tie-1 has been shown to activate the PI3K/AKT pathway but only in conjunction with Tie-2 activation (Savant et al., 2015). Although CathL induced activation of Tie-1, there was no increased activation of Tie-2 compared to untreated cells. It has been shown that upregulation of Tie-1 in sprouting (tip-like) cells induced downregulation of Tie-2 surface presentation during angiogenic sprouting in HUVECs. This suggests that in spouting ECs, Tie-1, and not Tie-2, plays a significant role (Savant et al., 2015), which might be the case in CathL-treated HOMECs. However, this expression of Tie-1 has been suggested to be transient as it cannot function independently of Tie-2. Tie-1 has also been reported to sustain Ang1-Tie2 signalling, potentially by forming a heteromeric Tie-1-Tie-2 complex, preventing Tie-2 from being rapidly internalised/endocytosed and perpetuating Tie-2 signalling (Savant et al., 2015).

Although CathL induced phosphorylation of ERK1/2, AKT and p38α and activated Tie-1 RTK in HOMECs, it would not be reasonable to speculate at this stage of any association between the two. Tie-1, a receptor for which no growth factor ligands have yet been identified, has been shown to be a potential target for anti-tumour therapy. Lewis lung carcinoma grown in Tie-1-deficient mice had decreased vessel density, vascular perfusion, and tumour-associated EC survival and this was associated with decreased tumour cell survival (D'Amico et al., 2014). Since CathL is a potential proangiogenic factor in omental angiogenesis and has been shown briefly to activate Tie-1, further research should be carried out to investigate the presence of Tie-1 receptor using immunocytochemistry and immunoprecipitation at different time points after CathL treatment, and a role for Tie-1 receptor using function and inhibition studies, and possibly, activation of other novel receptors in HOMECs, which may be targeted in anti-tumour therapies.

A summary of the data from this chapter are described in figure 3.29.

3.5 Conclusion

Taken together, the presented data suggest that ovarian tumour-secreted CathL is a pro-angiogenic factor that induces proliferation, migration and *in vitro* angiogenesis in HOMECs via a non-proteolytic mechanism. These novel findings fit in well with the clinicopathological observations of advanced stage ovarian carcinoma where metastatic ovarian cancer causes extensive vascularisation of omental lesions, increasing the ability of the secondary tumour to survive and spread to other organs. As transcoelomic metastasis requires tumour angiogenesis, CathL, secreted from ovarian cancer cells, in cooperation with other cells present in the omentum may facilitate cellular angiogenesis in HOMECs. This may highlight CathL and its downstream pathways as novel anti-tumourigenic/anti-angiogenic therapeutic targets in the treatment of ovarian cancer.

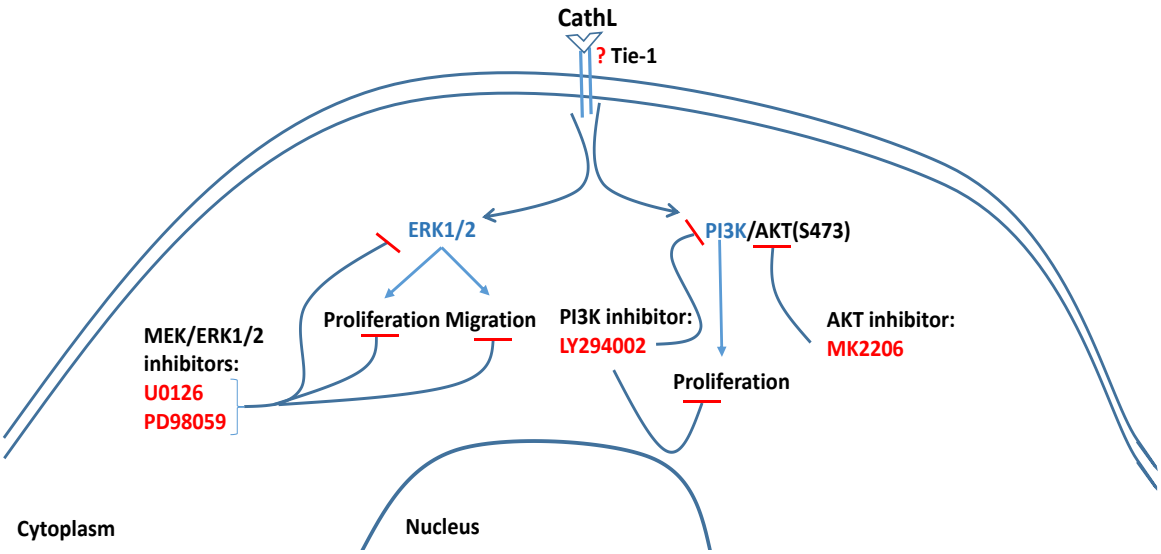

Figure 3.29: **A summary of CathL-induced activation of ERK1/2 and AKT, and their potential role in mediating cellular functions in HOMECs.** CathL possibly activates Tie-1 receptor tyrosine kinase on the cell surface membrane of HOMECs which leads to an increase in phosphorylation of ERK1/2 and AKT. The ERK1/2 activation induces cellular proliferation and migration in HOMECs in response to CathL, since the MEK/ERK1/2 inhibitors U0126 and PD98059 significantly reduce these cellular functions by inhibiting activation of ERK1/2. Both PI3K inhibitor LY294002 and AKT inhibitor MK2206 inhibit phosphorylation of AKT at Ser473 (S473) in CathL-treated HOMECs. However, only LY294002 inhibits CathL-induced HOMEC proliferation, suggesting activation of a pro-proliferative signalling cascade downstream of PI3K that is independent of AKT activation.

Chapter 4 Investigating proangiogenic effects of galectin 1 (Gal1) on HOMECs

4.1 Introduction

Gal1 is the first of 14 members of the gene family of carbohydrate-binding proteins, known as galectins (Barondes et al., 1994a). It has a wide range of roles in physiological and pathological interactions that are both intracellular and extracellular and can be defined by their affinity for β-galactosidase sugars. Such processes may include cell-cell and cell-matrix interactions, as well as the regulation of the immune system (Camby et al., 2006). Defects in Gal1 are thought to be linked to cancer progression, particularly through cancer cell invasion, metastasis formation and angiogenesis (Rek et al., 2009, Hsu et al., 2013) and studies have been carried out to assess the typical up-regulation of this protein in cancers including thyroid carcinoma, prostate, breast and EOC (Chiariotti et al., 1995, van den Brule et al., 2001, Jung et al., 2007, Zhang et al., 2014a).

4.1.1 Synthesis and structure of Gal1

Gal1 is a member of the lectin family (carbohydrate binding proteins) that is a product of the LGALS1 gene. It consists of a chain of approximately 135 amino acids. Gal1 also has two β-galactosidase-binding sites, and therefore, an affinity for β-galactosidase sugars (Cho and Cummings, 1995). Gal-1 occurs as a monomer as well as a non-covalent homodimer consisting of subunits of one carbohydrate recognition domain (CRD) (Gal-1, ~29 kDa) (Barondes et al., 1994b). Human Gal-1 exists as a dimer in solution (Lopez-Lucendo et al., 2004). The integrity of this dimer is maintained principally by interactions between the monomers at the interface and through the well-conserved hydrophobic core, a factor which explains the observed stability of the dimer in molecular terms (Lopez-Lucendo et al., 2004). Nevertheless, homodimeric Gal1 can spontaneously dissociate into monomers which are still able to bind to carbohydrates, but with a lower level of affinity (Cho and Cummings, 1995, Leppanen et al., 2005).

4.1.2 Secretion of Gal1

It is thought that after synthesis, Gal1 is externalised and attached to cell-surface glycoconjugates, staying here for several hours before it is released into the media, simultaneously losing its activity at a rapid rate (Cho and Cummings, 1995). When lectin is newly synthesised, this displaces the surface-bound Gal1 and results in its movement to the media. In Chinese hamster ovary cells specifically, Gal1 is quantitatively secreted at a rate of approximately 4% per hour (Cho and Cummings, 1995).

Most secretory proteins contain an N-terminal or internal signal peptide that direct their sorting to the ER. From the ER, proteins are transported to the extracellular space or the plasma membrane through the classical ER-Golgi pathway. The ER-Golgi pathway is an efficient molecular machine of protein export of eukaryotic cells. Nascent proteins containing signalling peptide are directed to the Golgi where further post-translational modification occurs, leading to the production of mature proteins which are transported to their destination. However, there are cytoplasmic or nuclear secretory proteins which lack these signalling peptides, and hence are exported in an unconventional secretory pathway, independent of the ER-Golgi machine. Such proteins include fibroblast growth factor-2 (FGF2), β-galactoside-specific lectins Gal1 and galectin-3, certain members of the interleukin family and the nuclear proteins high mobility group box 1 (HMGB1) (Seelenmeyer et al., 2005, Seelenmeyer et al., 2008, Lee et al., 2010).

Secretion of Gal1 has been being investigated over the last two decades in several cell models. During differentiation induced with erythropoietin and deprivation of granulocyte-macrophage colony-stimulating factor, the leukaemic cells empty their cytoplasmic content of endogenous galectin 1 into the external medium (Lutomski et al., 1997). Galectin 1 is also secreted quantitatively from C2 mouse myoblasts when induced to form multinucleate fused myotubes (Cooper and Barondes, 1990). Gal1 is also secreted from Chinese hamster ovary cells, although in an unstable denatured form, suggesting an involvement of a folding intermediate in the secretion of Gal1 directly through the plasma membrane (Cho and Cummings, 1995).

Although Gal1 has been shown to be exported from cells, the exact mechanisms have not yet been investigated thoroughly. Several reports suggested an ER-

Golgi-independent pathway, similar to that of FGF2 secretion. FGF2 is a growth factor that lacks an N-terminal signalling peptide which prevents this protein from entering the ER-Golgi pathway (Nickel, 2005). According to Schafer *et al.*, FGF2 translocation through cell membrane is dependent on elevated temperature (37˚C), without requiring ATP as an energy source (Schafer et al., 2004). A two-step process has been suggested that involves FGF2 binding to integral membrane components followed by membrane translocation (Nickel, 2005). The latter process is shown to require cytosolic factors. This secretion was previously shown to be dependent on NA/K-ATPase. FGF2 secretion was also suggested to be mediated by ATP-binding cassette (ABC) transporters (Nickel, 2005), however, no experimental evidence for this model has been established on investigating Gal1 externalisation.

4.1.3 Role of Gal1 in the human body

Gal1 has both extracellular and intracellular functions (Barondes et al., 1994a). In a carbohydrate independent manner, it interacts intracellularly with cytoplasmic proteins, while its extracellular role involves interactions with glycoproteins of the extracellular matrix or those on the cell surface (Camby et al., 2006).

Gal1 plays a role in a variety of processes in the human body, including embryonic development, inflammation, apoptosis, the regulation of cell growth and cell adhesion (Camby et al., 2006). *In vitro* research carried out on vascular ECs from inflamed tissue has shown an increase in the expression of Gal1 (Gil et al., 2006). At sites of inflammation, it has been shown that Gal1 hinders the T-cell migration through the extracellular matrix, while it also prevents the leukocytes from entering these inflamed tissues from the bloodstream (Gil et al., 2006). This has suggested that galectins have a role in the regulation of immune cell migration.

In addition, a recent study has demonstrated selective regulation of dendritic cell migration when Gal1 accumulates in the extracellular matrix and is over-expressed by lymphatic ECs (Norling et al., 2008). In the presence of Gal1, immunogenic dendritic cells exhibit reduced migration through the extracellular matrix. Using a mouse model with lymphoedema, mice with up-regulated Gal1 had a higher number of dendritic cells in draining lymph nodes, indicating that

Gal1 may have contributed to inhibiting dendritic cell emigration (Thiemann et al., 2015).

Furthermore, Gal1 is thought to have a pivotal role in cell growth regulation. It has been suggested that crucial interactions with an α5β1 integrin is necessary for galectin-induced growth inhibition to occur (Fischer et al., 2005). These anti-proliferative effects result from the inhibition of the Ras-MEK-ERK pathway, which is due to the induction of p27 and p21 transcription (Fischer et al., 2005). The promoter of p27 contains two binding sites which have a crucial role in the responsiveness of Gal1. The accumulation of p27 and p21 as mediated by Gal1 results in an inhibition of the activity of CDK2, leading to the cell cycle arrest in G1, and therefore, growth inhibition (Fischer et al., 2005).

4.1.4 Gal1 in cancers and angiogenesis

It has been shown that Gal1 is produced by cancer cells as a tumour promoting protein (Zhang et al., 2014a). Studies have reported that Gal1 is upregulated in the majority of cases of thyroid carcinoma (Chiariotti et al., 1995), while in studies using both melanoma and orthotopic breast cancer, it was found that tumour growth was greatly reduced when Gal1 was “knocked down” (Ito et al., 2011). In a variety of cancers including prostate, colon and thyroid cancers (van den Brule et al., 2001), Gal1 has been found to be highly expressed in cancer-associated stroma, but this over-expression correlates with pathological factors including advanced stages of the disease, tumour invasion and increased rates of disease reoccurrence (Chen et al., 2015). In addition, it has been found that Gal1 regulates cancer cell proliferation and invasion when it accumulates in the peri-tumoural stroma of both breast cancer and ovarian cancer (van den Brule et al., 2003): particularly EOC (Chen et al., 2015).

Gal1 is dysregulated in EOC and has been shown to promote tumour progression (Chen et al., 2015). A recent study has suggested that Gal1 is released from EOC cells and has been detected in the peripheral circulation in patients suffering from the disease. Over-expression of Gal1 has been found to increase tumour cell invasion in the OVCAR-3 cell line (Chen et al., 2015). Moreover, when the levels of Gal1 were compared in patients alongside the most widely used EOC antigen and biomarker CA125, it was found that around 70% of patients were correctly

identified as positive by both proteins (Chen et al., 2015). This provides evidence that Gal1 could potentially be used as a biomarker for EOC progression, as well as outcome.

A study by Seelenmeyer *et al.* has suggested that CA125 is a counter receptor for Gal1 in HeLa cells, with Gal1 levels ten times higher on the surface of CA125-expressing tumour-derived HeLa cells, when compared to Chinese Hamster Ovary cells that are non-tumour derived, with a lack of CA125 (Seelenmeyer et al., 2003). This provides evidence that Gal1 could be regulated by this ovarian cancer antigen, in terms of its dissemination to the cell surface.

Following on from tumour progression, Gal1 has been shown to encourage cell proliferation and migration *in vitro,* using glioblastoma cell lines (Camby et al., 2002). Gal1 is thought to play a role in tumour angiogenesis, acting as a pro-angiogenic factor (Le Mercier et al., 2008). It has been shown that in the presence of elevated Gal1, ECs migrate to form tubules (Thijssen et al., 2006) – a key step in angiogenesis. Furthermore, in Gal1 knockout mice, tumour growth and tubule formation becomes severely implicated (Thijssen et al., 2006), indicating a role for the protein as a pro-angiogenic factor.

Aside from its role as a pro-angiogenic factor, Gal1 has been shown to mediate apoptosis in T-cells, when Gal1 is expressed in HeLa cells (Kovacs-Solyom et al., 2010). A study indicated that Gal1-expressing HeLa cells resulted in apoptosis of T-cells, whereas HeLa cells not expressing the protein led to T-cells surviving (Kovacs-Solyom et al., 2010). This may suggest that Gal1 has a role in the self-defence of tumours, when expressed by tumour cells.

Nevertheless, the exact mechanism for the stimulation of apoptosis has been disputed, with various explanations being put forward in studies involving recombinant Gal1 (Stowell et al., 2008), as well as tumour cell-derived Gal1 (Kovacs-Solyom et al., 2010). Further studies are therefore required to confirm the exact mechanism of cell death.

4.1.5 Rationale of the study

Recent studies have indicated a proangiogenic role for Gal1. Gal1 can be secreted by both tumour cells and EC, aiding EC proliferation, migration and

angiogenic tube-formation. In previous unpublished data, LGALS1, Gal1 mRNA, underwent differential expression when HOMECs were treated with the EOC secreted factor CathL. This raised several questions: (i) does CathL induce secretion of Gal1 in HOMECs? and (ii) what role does Gal1 play in the angiogenic process?

To address these questions, initially secretion of Gal1 from CathL-treated HOMECs was analysed, followed by examination of the level of expressed LGALS1 mRNA. An attempt was also made to dissect the pathway via which CathL may induce expression of Gal1 in these cells. Potential proangiogenic roles of Gal1 and the activated signalling cascades involved in these processes in HOMECs were also investigated. Furthermore, *in vitro* angiogenic tube-structure formation was assessed when HOMECs were treated with Gal1. Finally, Gal1 receptor targets were also elucidated in a preliminary investigation.

4.1.6 Aims

The aims of this chapter are:

- To investigate whether CathL induces secretion of Gal1 and expression of LGALS1 mRNA in HOMECs
- To assess the secretory pathway of Gal1 in HOMECs
- To test whether Gal1 induces HOMEC proliferation and migration
- To study the potential signalling pathways involved in Gal1-induced HOMEC proliferation and migration
- To examine angiogenic tube-formation in HOMECs by Gal1
- To identify potential receptor targets of Gal1 in HOMECs

4.2 Methods

HOMEC isolation: HOMECs were isolated according to (Winiarski et al., 2011) as described in the Method chapter section 2.3.1.

Gal1 quantification: A commercially available solid-phase sandwich ELISA kit was used to measure secreted Gal1 in cell culture supernatant as described in the Method chapter section 2.7.4.2.

Activation of NFκB p65: A commercially available cell-based ELISA was used to detect level of phosphorylated NFκB in CathL-treated HOMECs as described the Method chapter section 2.7.4.1.

Inhibition of the ER/Golgi pathway: HOMECs were grown in a 6 well plate. After 70% confluency reached, cells were transfected with CellLight® Golgi-GFP, BacMam 2.0. GFP-transfected cells were treated with BFA (0.025 μM) for 8 hours, and photographs were analysed as described in Method chapter, section 2.9.

Expression of LGALS1: CathL-treated cells were scraped with TRI reagent and RNA was isolated. After quantification, RNA was amplified in the presence of TaqMan® Gal1 or reference genes (glyceraldehyde-3-phosphate dehydrogenase (GAPDH) and β2-microglobulin (β2M) primers and gene expression was analysed using Roche LightCycler 96 as described in the Method chapter section 2.7.5.

Cell proliferation: HOMEC proliferation was tested using both the WST-1 assay and CyQuant cell proliferation kit as described in the Method chapter sections 2.4.1 and 2.4.2.

Activation of intracellular kinases: Commercially available cell-based ELISAs were used to detect and assess levels of phosphorylated intracellular kinases as described in the Method chapter section 2.7.4.1.

Cell migration: A commercially available cultrex Boyden chamber kit was used to investigate the underlying mechanisms of Gal1-induced HOMEC migration, as described in the Method chapter section 2.5.1.

3D *in vitro* angiogenesis: A 3D angiogenesis model was used to assess HOMEC sprouting as described in the Method chapter section 2.8.1.

2D Tube-formation: Angiogenic tube-formation was investigated in HOMECs treated with Gal1 using both a fibrin matrix assay and commercially available GFR-Matrigel, as described in the Method chapter section 2.8.2

Identification of potential cell surface receptors: A commercially available human receptor-tyrosine kinase array was used as a screening to identify potential receptor as described in the Method section 2.7.3.

4.3 Results

4.3.1 CathL induces secretion of Gal1 from HOMECs

Previously unpublished data from this laboratory suggested that CathL induces differential gene expression of Gal1 mRNA (LGALS1) in HOMECs. Therefore, it was hypothesised that CathL induces production and secretion of Gal1 in these cells. To test this, HOMECs were treated with or without CathL for 4 minutes, 30 minutes, 8 hours and 24 hours and supernates were analysed for Gal1 as described in Method chapter section 2.7.4.1. The results revealed an increase in HOMEC-secreted levels of Gal1 over time at 30 minutes up to 8 hours and then reduced after 24 hours. For example, CathL significantly induced secretion of Gal1 at 30 minutes (2-fold) and 8 hours (5.2-fold) treatment compared to untreated (control) cells (Figure 4.1a). At 24 hours after CathL treatment, a 1.3-fold increase was observed in secreted Gal1 levels compared to control which was not significant and may suggest that the secreted Gal1 was degraded as it has a reported serum half-life of 1.07 hours (Van Ry et al., 2015).

These data suggested that CathL induces secretion of Gal1 from HOMECs. Gal1 secretion at 30 minutes may indicate that there is a rapid release of readily-stored intracellular Gal1 or cleavage of cell surface Gal1. However, the fact that this secretion increases at 8 hours after CathL-treatment raised the possibility of a transcriptional regulation of Gal1 protein levels via altered expression of LGALS1 mRNA in these cells. Thus, this was investigated further. Initially, HOMECs were treated with or without CathL for 6 hours and 24 hours and real-time PCR was performed to quantify expressed levels of LGALS1 mRNA in CathL-treated cells versus untreated cells. It was found that, at 6 hours after CathL-treatment, the level of LGALS1 mRNA expression increased by 1.5-fold ($p<0.05$) compared to control (Figure 4.1b). At 24 hours after treatment, no significant difference was observed between treated and untreated cells. This suggests that CathL may induce a transient increase in LGALS1 mRNA expression, and Gal1 protein production and secretion in HOMECs.

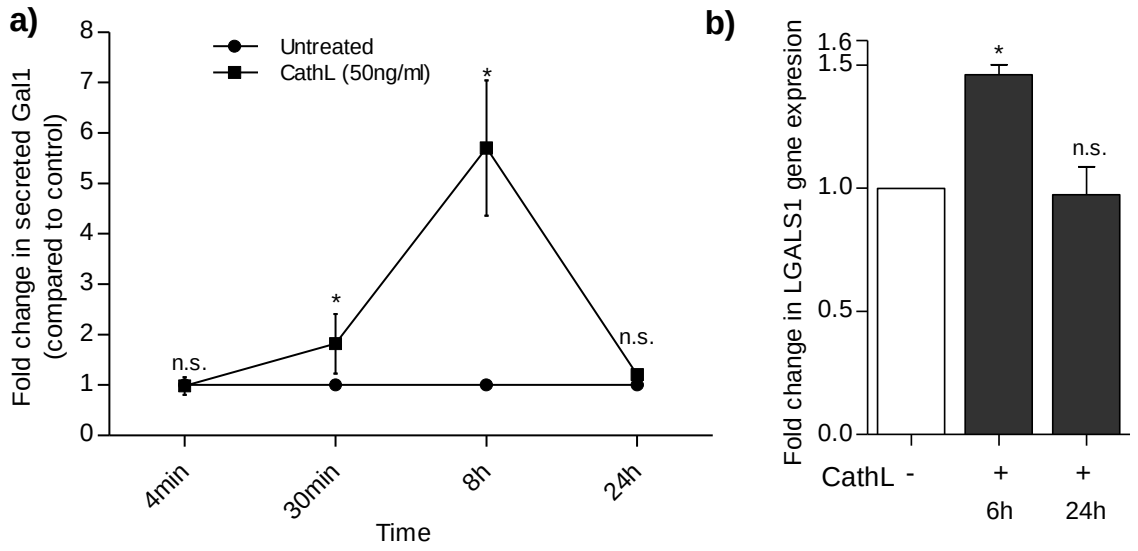

Figure 4.1: **CathL induces transcription and secretion of Gal1 in HOMECs. a)** Cells were seeded in 2% gelatin pre-coated 24-well plates at a density of 35,000 cells/well in starvation media containing 2% FCS. After overnight incubation, cells were treated with or without CathL (50ng/ml) and supernatants were collected after 4 minutes, 30 minutes, 8 hours and 24 hours treatment. A commercially available ELISA kit was used to assess the levels of secreted Gal1 using a SpectraMax plate reader. Results are mean ±SD and represented as fold change in secreted Gal1 vs control. n=4-6.

b) Cells were seeded in 2% gelatin-coated 6-well plates at a density of 250,000 cells/well. At 80-90% confluence, cells were starved in media containing 2% FCS. After overnight incubation, cells were treated with or without CathL (50ng/ml) and lysed after 6 hours or 24 hours treatment. A real-time PCR was performed on extracted RNA using a Roche LightCycler 96 and the data were normalised to GAPDH and β2M. Results are mean ±SD and represented as fold change in LGALS1 gene expression (relative to control). *p<0.05, n= 4. n.s. denotes not significant vs control.

4.3.2 CathL induces increased LGALS1 mRNA expression via activation of NFκB

Since CathL induces secretion of Gal1, the signalling pathway involved in mediating this secretory process was investigated. Initially, the secreted level of Gal1 was quantified in HOMECs treated with or without CathL and in the presence or absence of both ERK1/2 inhibitors (U0126 and PD98059) and PI3K/AKT inhibitors (LY294002/MK2206). This is due to the previously obtained increased activation of these kinases in CathL-treated HOMECs. Interestingly, none of the inhibitors had a consistent effect on Gal1 secretion (data not shown).

However, previous published reports suggested that NFκB is involved in regulating expression of Gal1 in peripheral blood mononuclear cells (PBMCs) (Toscano et al., 2011) and in Kaposi's sarcoma cells (Croci et al., 2012). Since there is no other literature available on this, it was hypothesised that CathL induces activation of NFκB which in turn leads to an increase in the expression of LGALS1 mRNA. To test this, activation of NFκB (p65) was examined in cells treated with or without CathL for 4 hours using a commercially available cell-based ELISA. It was found that CathL significantly induced NFκB activation (1.3-fold) compared to control (untreated cells; Figure 4.2). The treatment time was selected based on previously published study (Takada et al., 2003).

As CathL induced activation of NFκB in HOMECs, the next step was to examine whether inhibiting NFκB-activation reduced LGALS1 expression and Gal1 secretion. A well-known NFκB inhibitor, sulfasalazine, was selected to examine this. Initial toxicity assays (WST-1) were carried out in order to identify non-toxic concentrations of sulfasalazine in HOMECs. It was found that sulfasalazine was not toxic to cells at 50 µM (107.1±4.2%, n=8) or 100 µM (106.1±3.1%, n=8) compared to control (100%; Figure 4.3) over 24 hours. However, cell viability reduced to 91.6±3.1% (n=8) at 200 µM compared to control (100%). Therefore, 100 µM of sulfasalazine was selected to carry out further experiments, which was 20-fold lower than previously published data (Toscano et al., 2011).

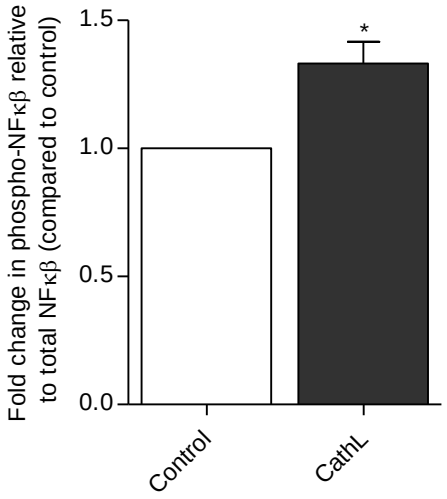

Figure 4.2: **CathL increases phosphorylation of NFκB p65 in HOMECs.** Cells were seeded in 2% gelatin coated 10cm petri dishes and treated with or without CathL (50ng/ml) in starvation media containing 2% FCS. 4 hours after treatment, cells were lysed and concentration of protein was analysed using BCA assay kit. A commercially available NFκB ELISA kit was used to determine NFκB p65 phosphorylation level. Data are represented as fold change in phosphorylated NFκB relative to the total NFκB (normalised to control). Results are mean ±SD, *p<0.05 vs control (1-fold), n=4.

Figure 4.3: **Cytotoxicity (cell viability) induced by the NFκB inhibitor sulfasalazine.** Cells were seeded in 2% gelatin pre-coated 96 well plates at a density of 10,000cells/well in starvation media containing 2% FCS. After overnight incubation, cells were treated with or without various concentrations of sulfasalazine as indicated above and incubated for 24 hours. WST-1 was used to assess cellular viability. Results are mean ±SD and shown as percentage of the control, n.s., *p<0.05 vs control (100%), n=8. n.s. denotes not significant.

Next, secreted level of Gal1 was examined in CathL-treated HOMECs in the presence or absence of 100 μM sulfasalazine. Cells were pre-incubated in the presence or absence of sulfasalazine for 24 hours (as previously described (Toscano et al., 2011) and co-treated with or without CathL for 8 hours (based on Figure 4.1a). It was revealed that the secreted level of Gal1 was significantly reduced in the presence of both the inhibitor and CathL after 8 hours treatment compared to CathL-only treatment (0.9-fold vs 4.8-fold (CathL-treatment), both normalised to control; Figure 4.4a). Although, there was a slight increase in the level of secreted-Gal1 with the inhibitor only treatment, in cells co-treated with CathL and sulfasalazine, the level of secreted Gal1 was abolished to the basal level (Figure 4.4a).

The above data suggested that CathL-induced Gal1 secretion may be mediated by NFκB activation. Since NFκB is a transcription factor and has been shown to be involved in inducing Gal1 protein expression (Toscano et al., 2011), it was important to investigate its role in LGALS1 gene expression in HOMECs. To test this, a qRT-PCR was performed with HOMECs treated with or without CathL and in the absence or presence of sulfasalazine (100 μM). It was found that sulfasalazine significantly inhibited LGALS1 mRNA expression in CathL-treated cells after 6 hours treatment (n=4; Figure 4.4b). Interestingly, there was an increase in the level of LGALS1 mRNA in cells treated with sulfasalazine only compared to control. These results are consistent with the previous data (Figure 3.33a) where the inhibitor abolished levels of secreted Gal1 in CathL-treated HOMECs at 8 hours after treatment.

To confirm the validity of the experimental use of the inhibitor, it was important to confirm its effect on cellular levels of activated NFκB. A cell-based ELISA showed that the level of activated NFκB was significantly reduced in HOMECs in the presence of sulfasalazine when compared with CathL alone (Figure 4.5). These data suggest that CathL induces Gal1 production via activation of NFκB, followed by its secretion.

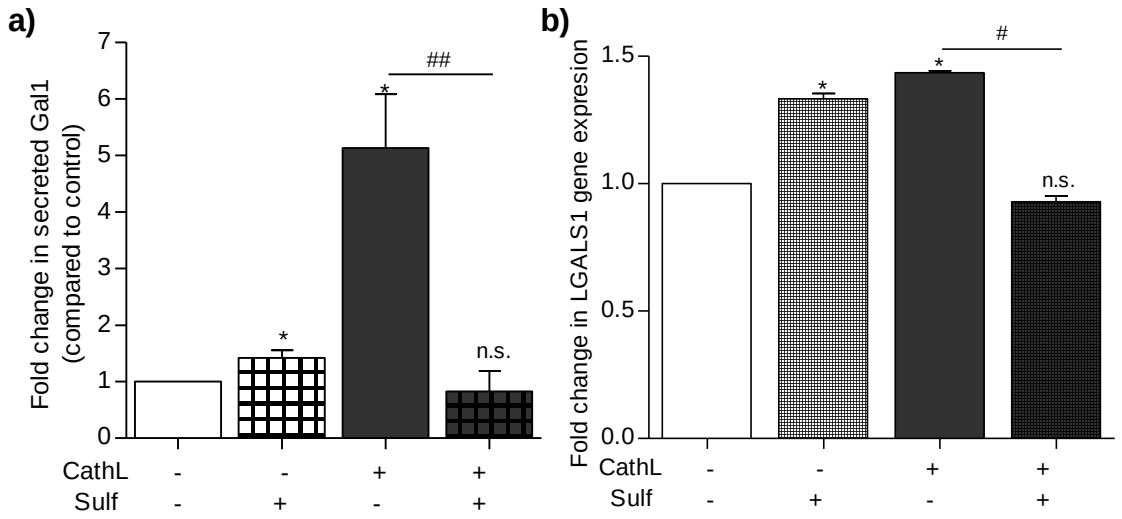

Figure 4.4: **CathL-induced secretion of Gal1 and transcription of LGALS1 mRNA is mediated via NFκB activation.** a) Cells were seeded in 2% gelatin pre-coated 24-well plates at a density of 35,000 cells/well in starvation media containing 2% FCS. After overnight incubation, cells were pre-incubated with or without sulfasalazine (100 μM) for 24 hours, and then co-treated with or without CathL (50ng/ml) and in the absence or presence of the inhibitor. The cell culture supernatant was collected after 8 hours treatment. A commercially available ELISA kit was used to assess the levels of secreted Gal1 using a SpectraMax plate reader. Results are mean ±SD and represented as fold change in secreted Gal1 vs control. *p<0.05 vs control; ##p< 0.01 vs CathL, n=4-6.

b) Cells were seeded in 2% gelatin-coated 6-well plates at a density of 250,000 cells/well. At 80-90% confluence, cells were starved in media containing 2% FCS and pre-treated with or without sulfasalazine (100 μM) for 24 hours. After 24 hours incubation, cells were co-treated with or without CathL (50ng/ml) and in the absence or presence of the inhibitor for 6 hours. A real-time PCR was performed on extracted RNA using a Roche LightCycler 96 and the data were normalised to GAPDH and β2M. Results are mean ±SD and represented as fold change in LGALS1 gene expression (relative to control). n.s., *p<0.05 vs control; #<0.05 vs CathL, n= 4. n.s. denotes not significant.

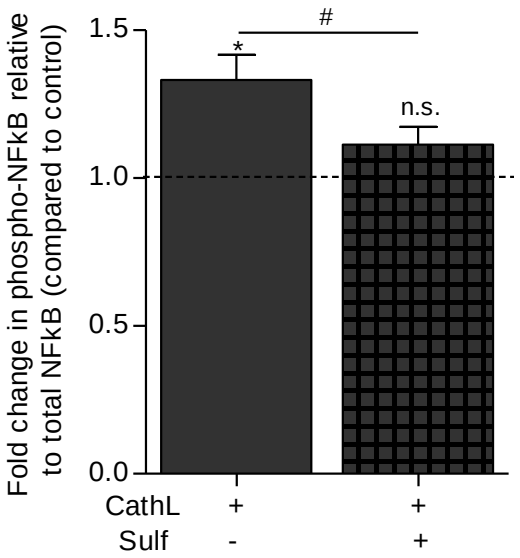

Figure 4.5: **CathL-induced NFκB p65 phosphorylation is inhibited by the NFκB-inhibitor sulfasalazine.** Cells were seeded in 2% gelatin coated 10cm petri dishes in complete growth media. At 80-90% confluence, cells were starved in media containing 2% FCS overnight. After overnight incubation, cells were incubated with sulfasalazine (100 µM) or media alone for 24 hours and then treated with or without CathL (50ng/ml) and in the absence or presence of sulfasalazine (100 µM). After 4 hours, cells were lysed and the concentration of protein was analysed using a BCA assay kit. A commercially available NFκB ELISA kit was used to determine levels of NFκB p65 phosphorylation. Data are represented as fold change in phosphorylated NFκB relative to the total NFκB (normalised to control). Results are mean ±SD, n.s., *p<0.05 vs control (dotted line); #p<0.05 vs CathL, n=4. n.s. denotes not significant.

4.3.3 CathL-induced Gal1 secretion may not be dependent on the ER/Golgi pathway

Protein secretion from cells usually takes place via the ER/Golgi pathway through vesicular membrane fusion followed by exocytosis. However, an ER/Golgi-independent pathway (non-classical route) has also been shown to be important in this process as has been shown for FGF1 and interleukin-1α in NIH3T3 fibroblasts (Prudovsky et al., 2003). There are reports that suggest that Gal1 secretion may be through the non-classical route and since the previous data in this study suggested that CathL induces secretion of Gal1 in HOMECs, it was hypothesised that Gal1 is secreted via an ER/Golgi-independent pathway. To test this, firstly, a well-known inhibitor of intracellular protein transport, brefeldin A (BFA), was selected. Initially toxicity assays were carried out to identify its non-toxic concentrations in HOMECs which was assessed using WST1 after 24 hour inhibitor treatment. It was revealed that BFA was toxic to cells above concentrations of 0.1 µM and therefore, a lower concentration (0.025 µM) was selected to carry out further investigation (Figure 4.6).

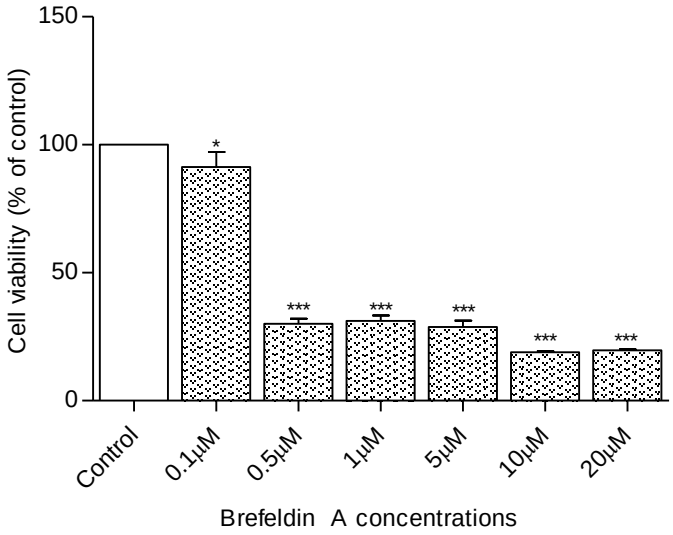

Figure 4.6: **Cytotoxicity (cell viability) induced by brefeldin A (BFA), a specific inhibitor of Golgi body-dependent protein secretion.** Cells were seeded in 2% gelatin pre-coated 96 well plates at a density of 10,000cells/well in starvation media containing 2% FCS. After overnight incubation, cells were treated with or without various concentrations of BFA as indicated above and incubated for 24 hours. WST-1 was used to assess cellular viability. Results are mean ±SD and shown as percentage of the control, *p<0.05, ***p<0.001 vs control (100%), n=10.

Next, the level of Gal1 secretion was tested in CathL-treated cells in the presence of BFA (0.025 µM). There was a partial but a significant decrease in the secreted-Gal1 level (3.9-fold, normalised to control) in the presence of BFA in CathL-treated HOMECs compared to CathL treatment only (4.9-fold, normalised to control; Figure 4.7). BFA-alone treatment had no effect on Gal1-secretion as shown in figure 4.7. These data suggest that the secretory pathway of Gal1 may be partially dependent on the ER/Golgi pathway, although since inhibition is only partial it is possible that an ER/Golgi-independent pathway may also play a role.

To confirm the validity of the experimental use of BFA it was important to demonstrate its effect on the Golgi body. To test this, Golgi-specific green fluorescent protein (GFP)-transfected HOMECs were treated with or without BFA (0.025 µM) for 8 hours. Fluorescence photography confirmed that the Golgi body was fragmented in the presence of BFA (Figure 4.8b) compared to control (untreated) cells (Figure 4.8a). The area of the distorted Golgi body was measured by quantifying the fluorescence intensity which was shown to be significantly higher in BFA-treated cells compared to control (Figure 4.8c). These data suggest that BFA distorts the Golgi in HOMECs supporting at least a partial a role for an ER/Golgi-independent secretory pathway for Gal1.

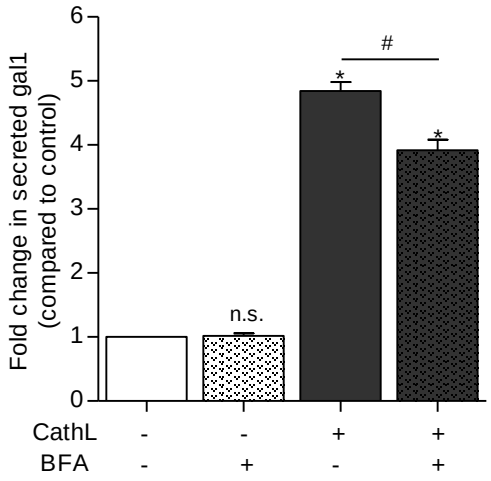

Figure 4.7: **CathL-induced secretion of Gal1 may partially depend on the ER/Golgi pathway.** Cells were seeded in 2% gelatin pre-coated 24-well plates at a density of 35,000 cells/well in starvation media containing 2% FCS. After overnight incubation, cells were pre-incubated with or without BFA (0.025 μM) for 1 hour, and then co-treated with or without CathL (50ng/ml) in the absence or presence of the inhibitor. The cell culture supernatant was collected after 8 hours treatment. A commercially available ELISA kit was used to assess the levels of secreted Gal1 using a SpectraMax plate reader. Results are mean ±SD and represented as fold change in secreted Gal1 vs control. n.s., *$p<0.05$ vs control; #$p<0.01$ vs CathL, n=4. n.s. denotes not significant.

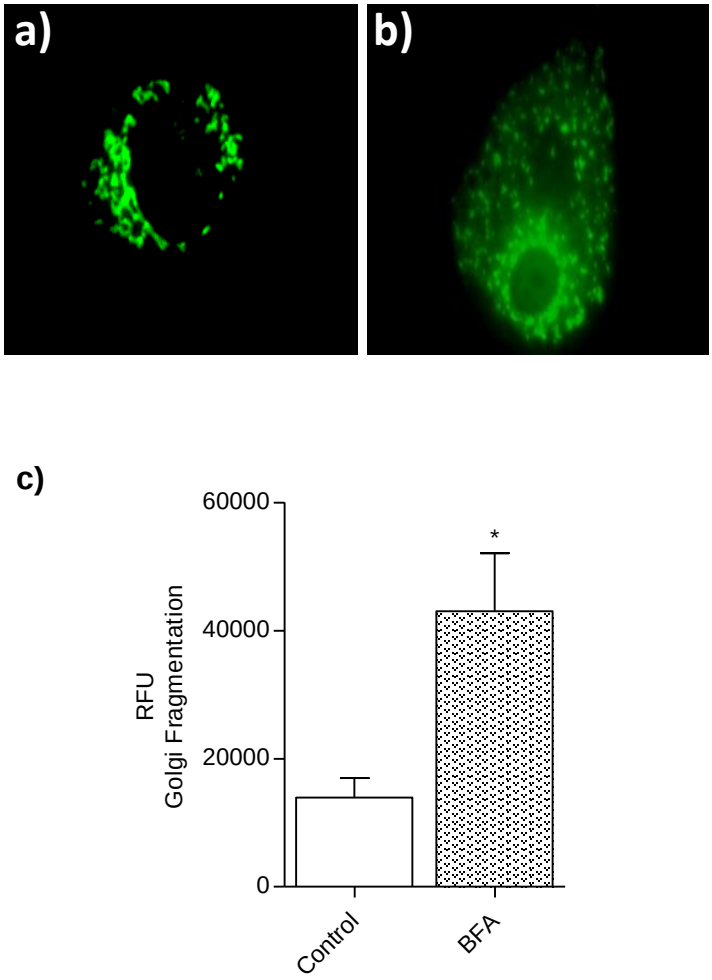

Figure 4.8: **BFA causes fragmentation of the Golgi apparatus in HOMECs.** Cells were seeded in 2% gelatin pre-coated 6 well plates in starvation media containing 2% FCS. At 70% confluence, cells were transfected with CellLight BacMam 2.0 Golgi-GFP construct and incubated overnight. After overnight incubation, transfected cells were treated in the a) absence or b) presence of BFA (0.025 µM) for 8 hours. Photographs were taken using a Nikon fluorescence microscope. c) Quantification of fluorescence intensity of Golgi area indicating Golgi fragmentation. a) and b) show representative images. Golgi fragmentation Relative fluorescence were obtained and analysed by ImageJ. *p<0.05 vs control, n= 3.

4.3.4 Gal1 induces HOMEC proliferation

The observation that Gal1 was secreted into the culture media from HOMECs in response to CathL raised the possibility that CathL-induced proliferation is mediated by Gal1. To examine this further a WST-1 colorimetric assay was initially used to assess proliferation of HOMECs treated with increasing concentrations of Gal1 (1, 5, 25 and 125 ng/ml) for 24 (Figure 4.9a), 48 (Figure 4.9c) and 72 (Figure 4.9e) hours. The range of concentrations was selected based around the secreted concentrations of Gal1 (between 20ng/ml and 80 ng/ml) in the supernatant of CathL-treated cells over 4 minutes, 30 minutes and 8 hours (Appendix 1, Figure A1.7). The data demonstrated that Gal1 significantly induced cell proliferation at all concentrations tested after 48 and 72 hours treatment compared to control (100%) (Figure 4.9c), e); Table 4.1). However, no significant difference in cell proliferation was observed at 24 hours after Gal1 treatment which also confirmed that Gal1 was non-toxic to HOMECs across all the concentrations examined (Figure 4.9a); Table 4.1). On the basis of these results and the levels of secreted Gal1, future experiments were carried out using 50ng/ml.

The initial proliferation data was complemented using a CyQUANT kit. HOMECs were treated with or without Gal1 at 50ng/ml for 72 hours. The data shows an increase in fluorescence intensity confirming proliferation of cells (110.7±6.2%, n=20 vs control (100%); Figure 4.10a) when treated with Gal1. The data obtained using the CyQUANT kit confirmed the WST-1 proliferation data, and therefore only WST-1 was carried out to investigate cell proliferation/toxicity in the subsequent experiments.

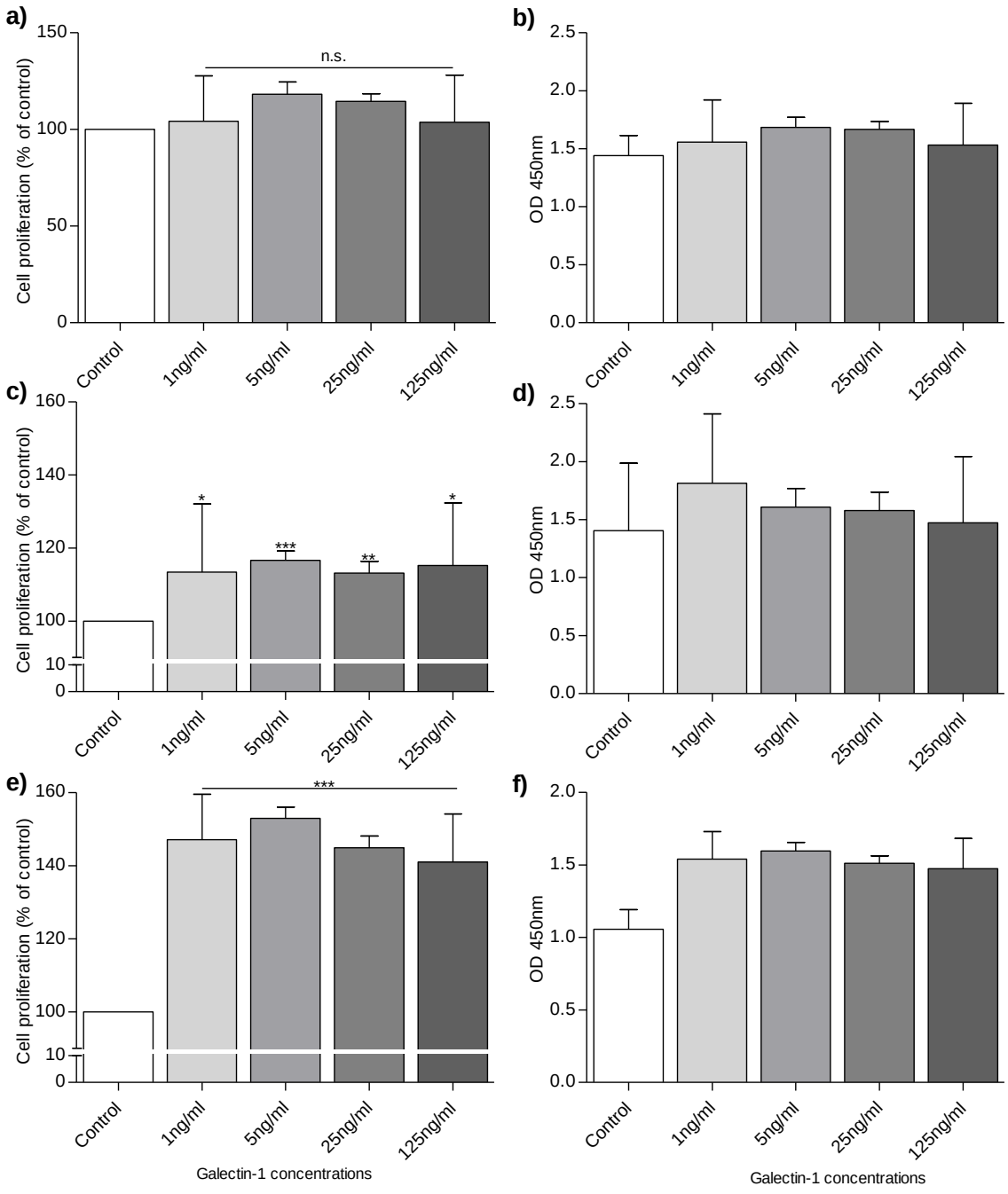

Figure 4.9: **Gal1 induces HOMEC proliferation (WST-1 assay).** Cells were seeded in 2% gelatin pre-coated 96 well plates at a density of 10,000cells/well in starvation media containing 2% FCS. After overnight incubation, cells were treated with or without Gal1 at various concentrations and incubated for **a)** 24, **c)** 48 and **e),** 72 hours. WST-1 assay was used to assess cellular proliferation based on absorbance using a PHERAstar BMG plate-reader at 450nm. Results are mean ±SD and shown as percentage of the control, *p<0.05 **p<0.01, ***p<0.001 vs control (100%); n=11-20. **b)**, **c)** and **d)** are raw data from representative experiments from **a)**, **b)** and **c)** respectively. n.s. denotes not significant vs control.

Table 4.1: **Summary of the pro-proliferative effect of Gal1 on HOMECs at various concentrations (shown in figure 4.9).** HOMECs were treated with or without various concentrations of Gal1 for 24, 48 and 72 hours. Results are mean ±SD and shown as percentage of control (100%). *p<0.05 **p<0.01, ***p<0.001 vs control (100%); n=11-20.

		HOMEC proliferation (as % of control) at each Gal1 concentration			
	Control (%)	**1ng/ml**	**5ng/ml**	**25ng/ml**	**125ng/ml**
24h	100	104.1±23.5	118.2±21.2	114.4±13.9	103.7±24.3
48h	100	113.4±18.7*	116.7±10.1***	113.2±13.7**	115.2±17.1*
72h	100	147.2±12.3***	152.9±13.7***	144.9±14.1***	141.0±13.2***

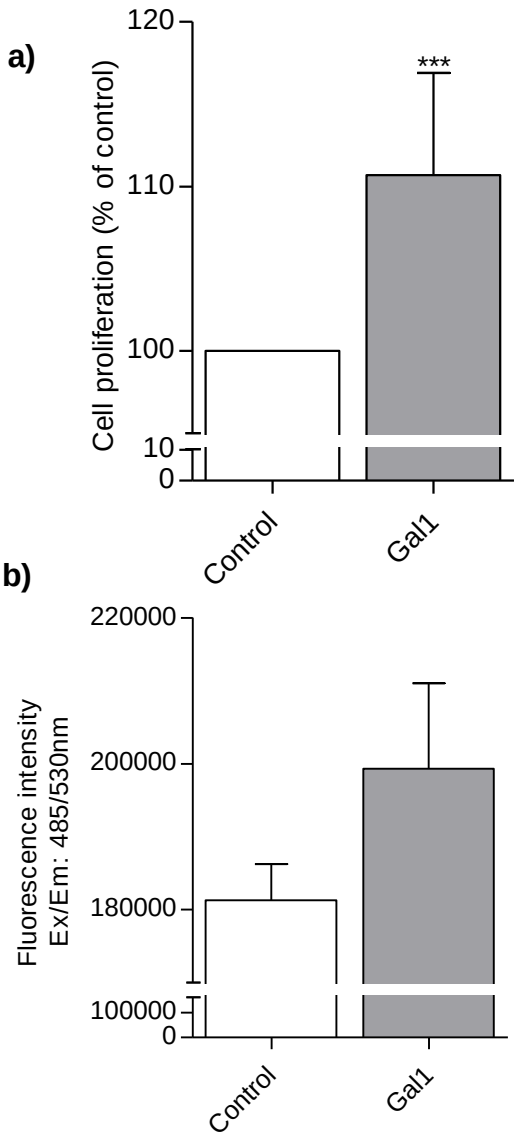

Figure 4.10: **Increased proliferation of HOMECs in media supplemented with Gal1 (CyQUANT).** Cells were seeded in 2% gelatin pre-coated 96 well plates at a density of 10,000cells/well in starvation media containing 2% FCS. After overnight incubation, cells were treated with or without 50ng/ml of Gal1 and incubated for 72 hours. A commercially available CyQUANT reagent was used to assess cell proliferation based on fluorescence intensity using a FLUOstar BMG plate-reader at Ex/Em: 485/530nm. **a)** Results are mean ±SD and shown as percentage of the control, ***p<0.001 vs control (100%), n=20. **b)** Raw data from representative experiment.

4.3.5 CathL-induced HOMEC proliferation is not dependent on Gal1

Data described in figures 3.1. 3.2, 4.9 and 4.10 indicate that both CathL and Gal1 induce HOMEC proliferation. To understand the relationship between the two, experiments were carried out to examine effects of CathL in the presence of an inhibitor of Gal1. Gal1 binds to cell surface sugar residues via its carbohydrate binding domain and since L-glu is a metabolically inert carbohydrate molecule, it was selected to test for its inhibitory effect on Gal1 binding to potential cell surface binding sites. Thus, HOMECs were treated with or without exogenous Gal1 (50ng/ml) and in the presence or absence of 25 mM and 50 mM of L-glucose for 72 hours. The data demonstrated that L-glu significantly reduced Gal1-induced HOMEC proliferation. For example, at 25mM and 50mM of L-glu, cell proliferation was 107.1±9.8% (n=11; Figure 4.11a) and 108.9±4.5% (n=10; Figure 4.11b) respectively, compared to Gal1-treatment (124.7±10.1%, n=9), all data normalised to control (100%).

The above data confirmed that L-glu indeed inhibits Gal1-induced HOMEC proliferation. Thus, CathL-induced HOMEC proliferation was carried out in the presence of L-glu to investigate whether this effect is mediated by Gal1. To test this, cells were treated with CathL (50ng/ml) in the presence or absence of L-glu at 25mM and 50mM for 72 hours and cell proliferation was measured using WST1. It was found that L-glu produced no significant inhibition of CathL-induced HOMEC proliferation. For instance, at 25mM and 50mM of L-glu cell proliferation was 119.3±9.0% (n=11; Figure 4.11c) and 117.8±7.4% (n=10; Figure 4.11d) respectively, compared to CathL-treated HOMECs (120.5±8.7%, n=9), all expressed as percentages of control. A significant increase in cell proliferation was also observed in L-glu only treatments. Together, these data suggest that CathL-induced HOMEC proliferation is not dependent on Gal1.

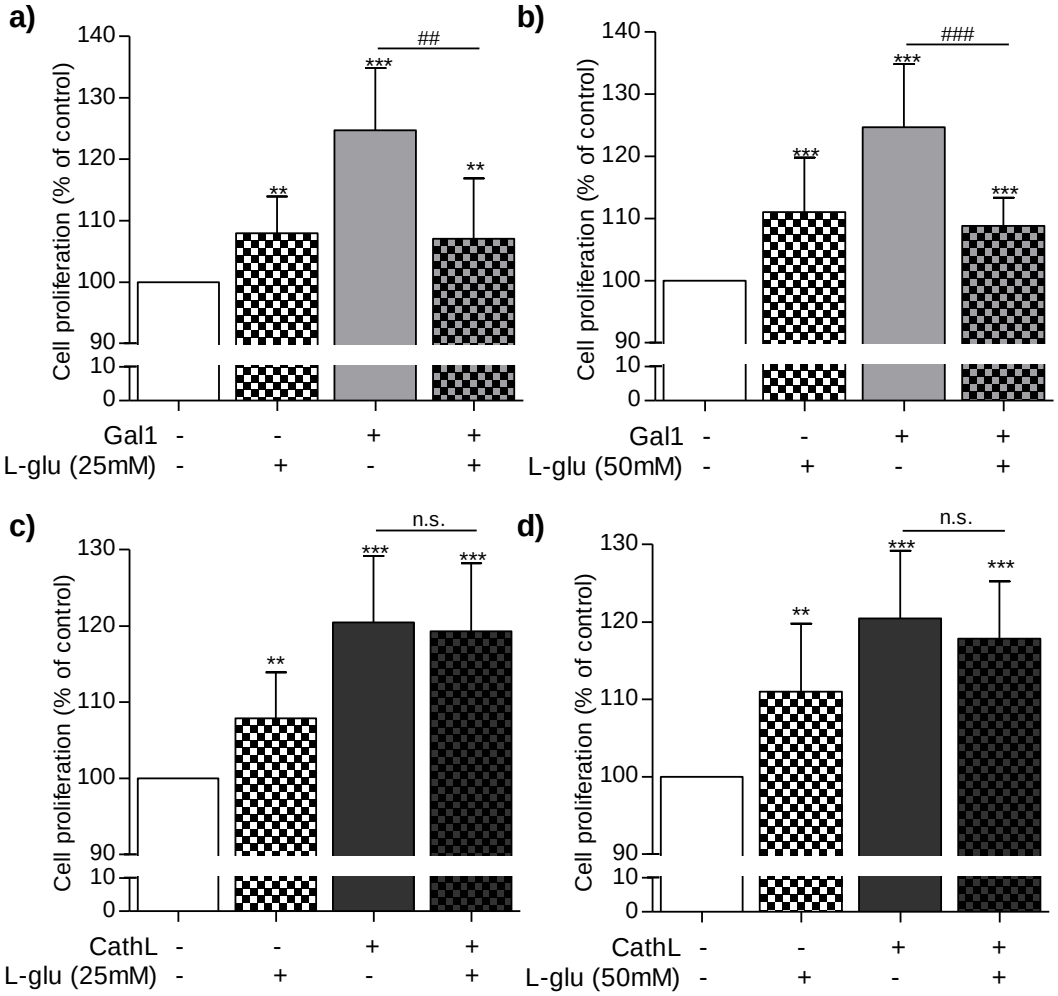

Figure 4.11: **CathL-induced HOMEC proliferation is independent of Gal1-pro-proliferative effect.** Cells were seeded in 2% gelatin pre-coated 96 well plates at a density of 10,000cells/well in starvation media containing 2% FCS. After overnight incubation, cells were treated with or without **a), b)** Gal1 or **c), d)** CathL (50ng/ml) in the presence or absence of L-glucose (L-glu) at **a), c)** 25mM or **b), d)** 50mM for 72 hours. WST-1 assay was used to assess cellular proliferation based on absorbance using a PHERAstar BMG plate-reader at 450nm. Results are mean ±SD and shown as percentage of the control (100%), **p<0.01, ***p<0.001 vs control (100%); ##p<0.01, ###p<0.001 vs Gal1 (expressed as % of control), n=9-11. n.s. denotes not significant vs CathL.

4.3.6 Gal1 induces phosphorylation of ERK1/2 and AKT kinases

According to the above data, although CathL-induced HOMEC proliferation does not require Gal1, Gal1 alone has been shown to be pro-proliferative in HOMECs, indicating that there may be signalling pathways activated downstream of Gal1-cell surface interaction. The induction of cellular proliferation has been reported to involve activation of several intracellular pathways including ERK1/2 and PI3/AKT kinases (discussed in Chapter 3, section 3.4). Since Gal1 induces HOMEC proliferation, the pro-proliferative signalling cascades activated in these cells by Gal1 were investigated. As ERK1/2 and AKT have been shown to be activated in CathL-treated HOMECs in Chapter 3, it was hypothesised that Gal1 also induces phosphorylation of these kinases. To test this, a cell-based ELISA was performed using intact live cells treated with Gal1 or VEGF for 4 minutes and 10 minutes. It was revealed that after 4 minutes treatment Gal1 increased phosphorylation of ERK1/2 (1.8-fold vs control; Figure 4.12a). However, after 10 minutes treatment, levels of phosphorylated ERK1/2 reduced to below the basal level (control; Figure 4.12b). Similar experiments were performed with AKT where AKT phosphorylation was induced (1.7-fold vs control; Figure 4.12c) 4 minutes after treatment and was reduced to basal level after 10 minutes (Figure 4.12d). VEGF was used as positive control in all cell-based ELISAs.

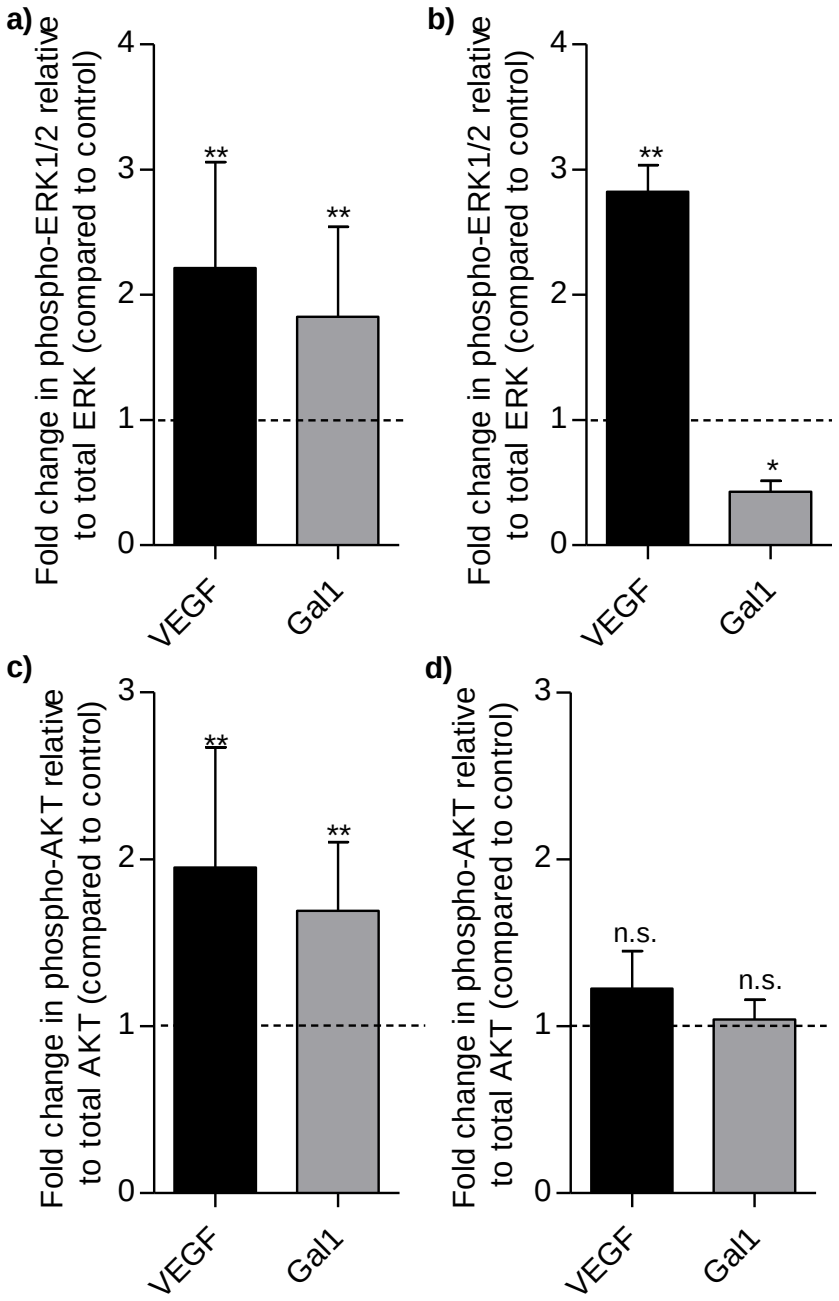

Figure 4.12: **Gal1 induces phosphorylation of ERK1/2 and AKT in HOMECs.** Cells were seeded in 2% gelatin pre-coated 96 well plates at a density of 10,000cells/well in starvation media containing 2% FCS. After overnight incubation, cells were treated with or without 50ng/ml of Gal1 or 20ng/ml of VEGF and incubated for 4 or 10 minutes. ERK1/2 (a, b) and AKT (c, d) phosphorylation was examined after 4 minutes **(a, c)** and 10 minutes **(b, d)** treatments. Commercially available cell-based ELISAs were used for the determination ERK1/2 and AKT(S473) phosphorylation level. The ELISA experiments were carried out in quadruplets on two cell batches. The data is represented by fold change in phosho-ERK1/2/AKT relative to total ERK1/2/AKT (compared to control). Results are mean ±SD, n.s., *p<0.05, **p<0.01 vs control (dotted lines); n=4-6. n.s. denotes not significant vs control.

4.3.7 Gal1-induced HOMEC proliferation is mediated via the ERK1/2 pathway

Since Gal1 induces activation of the pro-proliferative kinase ERK1/2, it was hypothesised that ERK1/2 might be involved in the induction of HOMEC proliferation. Following the toxicity assay using U0126 and PD98059 (Figure 3.7), the concentrations that were selected for further experiments were 1, 10 and 25 µM for both inhibitors. Cell proliferation experiments were carried out to test for any inhibitory effect of these inhibitors on HOMEC proliferation and it was revealed that Gal1-induced HOMEC proliferation was reduced significantly in the presence of both inhibitors at all concentrations. For instance, at 1, 10 and 25 µM of U0126, cell proliferation significantly reduced to 68.9±9.5% (n=15; Figure 4.13a), 63.1±6.9% (n= 15; Figure 4.13b) and 55.9±5.1% (n= 15; Figure 4.13c) respectively compared to Gal1 (133.6±13.1%, n= 14), all data normalised to control (100%). Similarly PD98059 demonstrated a significant reduction in Gal1-induced HOMEC proliferation. Specifically proliferation was: 74.0±6.8% (n= 15; Figure 4.13d), 65.2±4.3% (n= 15; Figure 4.13e) and 47.5±3.4% (n= 15; Figure 4.13f) at concentrations 1, 10 and 25 µM respectively, compared to Gal1 alone (133.6±13.1%, n= 14), all expressed as percentage of control (100%). The inhibitors at all concentrations also prevented HOMEC proliferation at 72 hours in the absence of Gal1 (Figure 4.13).

As discussed in Chapter 3 (section 3.3.4), the concentrations that were selected for further investigations were: 10 µM for U0126 and 25 µM for PD98059. The above data demonstrates that Gal1-induced HOMEC proliferation was significantly reduced at the given concentrations. A cell-based ELISA was performed to confirm such inhibitory effects of these inhibitors at the cellular levels on Gal1-induced phosphorylation of ERK1/2. The data revealed that the levels of phosphorylated ERK1/2 significantly abolished or reduced in HOMECs to 0.4-fold and 0.4-fold in the presence of U0126 (Figure 4.14a) and PD98059 (Figure 4.14b) respectively, compared to Gal1 treatment (1.5-fold). Together, these data suggest that Gal1 may induce proliferation of HOMECs via activation of the ERK1/2 pathway.

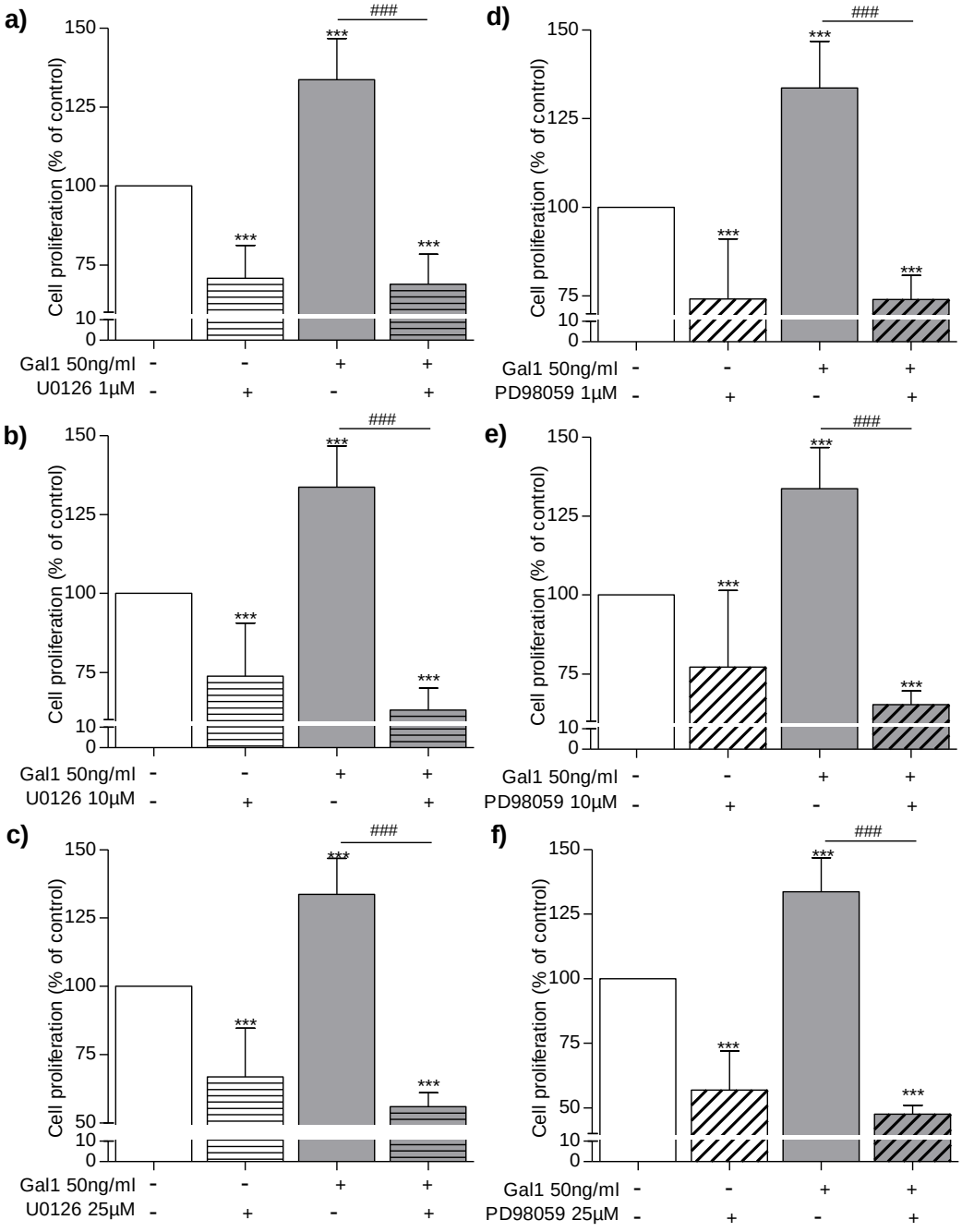

Figure 4.13: **Inhibition of ERK1/2 reduces Gal1-induced HOMEC proliferation.** Cells were seeded in 2% gelatin pre-coated 96 well plates at a density of 10,000cells/well in starvation media containing 2% FCS. After overnight incubation, cells were treated with or without Gal1 (50ng/ml) and in the absence or presence of various concentrations of **a-c)** U0126 and **d-f)** PD98059 as indicated above and incubated for 72 hours. WST-1 assay was used to assess cellular proliferation. Results are mean ±SD and shown as percentage of the control, ***p<0.001 vs control (100%), ###p<0.001 vs Gal1 (normalised to control 100%), n=14-15.

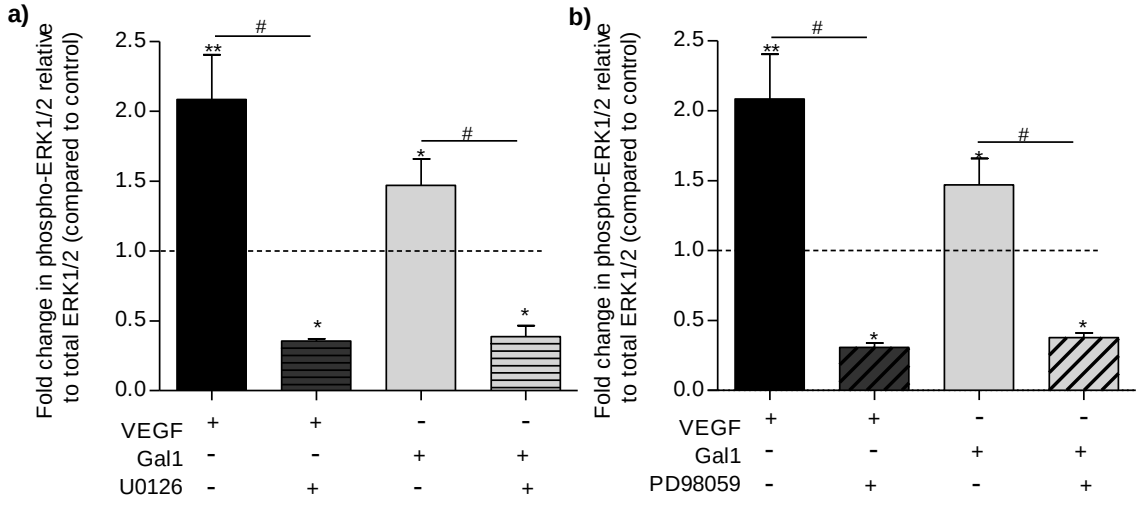

Figure 4.14: **Gal1-induced ERK1/2 phosphorylation is inhibited in intact HOMECs treated with ERK1/2 inhibitors a) U0126 (10 µM) and b) PD98059 (25 µM)**. Cells were seeded in 2% gelatin pre-coated 96 well plates at a density of 10,000cells/well in starvation media containing 2% FCS. After overnight incubation, cells were pre-incubated with the inhibitors for 20-30 minutes, and then co-treated with or without 50ng/ml of Gal1 or 20ng/ml of VEGF in the absence or presence of the inhibitors for 4 minutes. Commercially available cell-based ELISAs were used for determination of ERK1/2 phosphorylation level. The data is represented by fold change in phosho-ERK1/2 relative to total ERK1/2 (compared to control). Results are mean ±SD, *p<0.05, **p<0.01 vs control (1-fold, dotted lines), #p<0.05 vs VEGF/Gal1 (normalised to control), n=4.

4.3.8 Gal1-induced HOMEC proliferation is mediated via PI3K and not AKT activation

It has been reported in several studies that the PI3K/AKT pathway plays a crucial role in mediating survival signals in a wide range of cell models, and thus the involvement of these pathways in Gal1-induced HOMEC proliferation was examined. The role of AKT was assessed in Gal1-induced HOMEC proliferation in the absence or presence of PI3K inhibitor LY294002 (1, 25 and 50 µM) and AKT inhibitor MK2206 (1, 3 and 5 µM), as previously discussed. The data demonstrated that at 1 µM of LY294002 there was no significant reduction in Gal1-induced cell proliferation (131.6±4.9%, n= 10) compared to Gal1 only treatment (124.1±4.8%, n=10; Figure 4.15a). However, a significant reduction in Gal1-induced cell proliferation was observed when HOMECs were co-treated with higher concentrations of LY294002 such as 25 µM (94.3±3.6%, n=10; Figure 4.15b) and 50 µM (67.3±5.9%, n=10; Figure 4.15c), compared to Gal1 treatment (124.1±4.8%), where all data normalised to control (100%). Intriguingly, no significant difference was observed between cells treated with Gal1 and co-treated with three increasing concentrations of MK2206. For example, at 1, 3 and 5 µM of MK2206 cell proliferation was 125.3±3.7% (n=9; Figure 4.15d), 127.8±2.4% (n=7; Figure 4.15e) and 129.0±1.6% (n=7; Figure 4.15f) respectively, compared to Gal1 treatment 125.3±9.2% (n=11), all data normalised to control). The inhibitor only treatment demonstrated that LY294002 abolished HOMEC proliferation, however, MK2206 slightly increased this cellular function (Figure 4.15 d), e), f).

The above data suggested that Gal1 induces HOMEC proliferation via an AKT-independent PI3K pathway. However, this can only be validated if the inhibitors inhibited AKT phosphorylation in Gal1-treated cells. Cell based ELISAs were performed to test this. It was found that both LY294002 (25 µM) and MK2206 (5 µM) inhibited AKT activation in Gal1-treated HOMECs to 1.0-fold (vs 1.6-fold Gal1; Figure 4.16a) and 0.8-fold (vs 1.6-fold Gal1; Figure 4.16b) respectively. This suggested that both drugs inhibited AKT activation. However, a lack of inhibition of cell proliferation suggests that activated PI3K, but not AKT, is involved in the induction of Gal1-induced HOMEC proliferation.

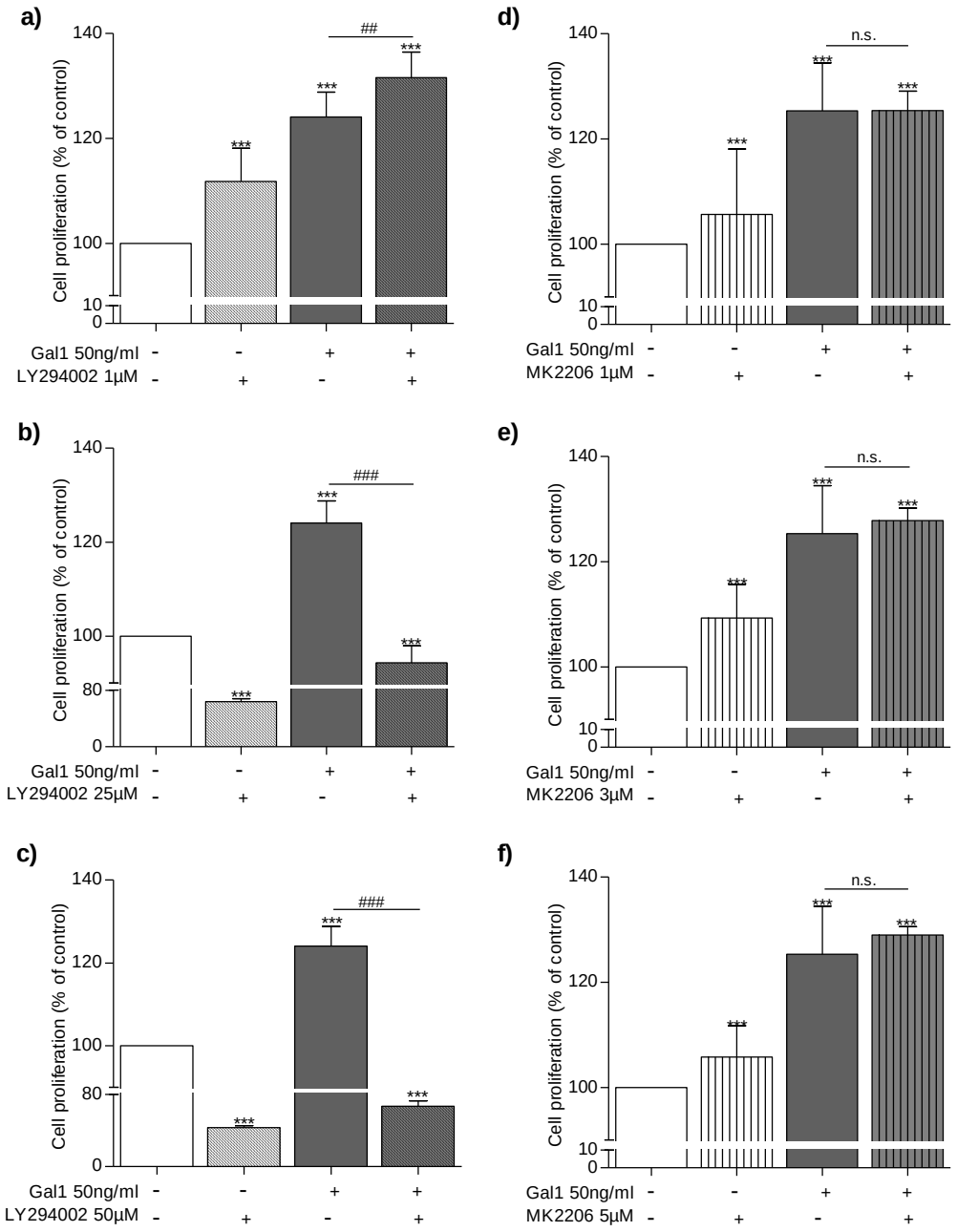

Figure 4.15: **PI3K inhibitor, but not AKT inhibitor, reduces Gal1-induced HOMEC proliferation.** Cells were seeded in 2% gelatin pre-coated 96 well plates at a density of 10,000cells/well in starvation media containing 2% FCS. After overnight incubation, cells were treated with or without Gal1 (50ng/ml) and in the absence or presence of various concentrations of **a-c)** LY294002 (PI3K inhibitor) and **d-f)** MK2206 (AKT inhibitor) as indicated above and incubated for 72 hours. WST-1 assay was used to assess cellular proliferation. Results are mean ±SD and shown as percentage of the control, ***p<0.001 vs control (100%); ###p<0.001 vs Gal1, n=7-11 (normalised to control 100%). n.s. denotes not significant vs Gal1.

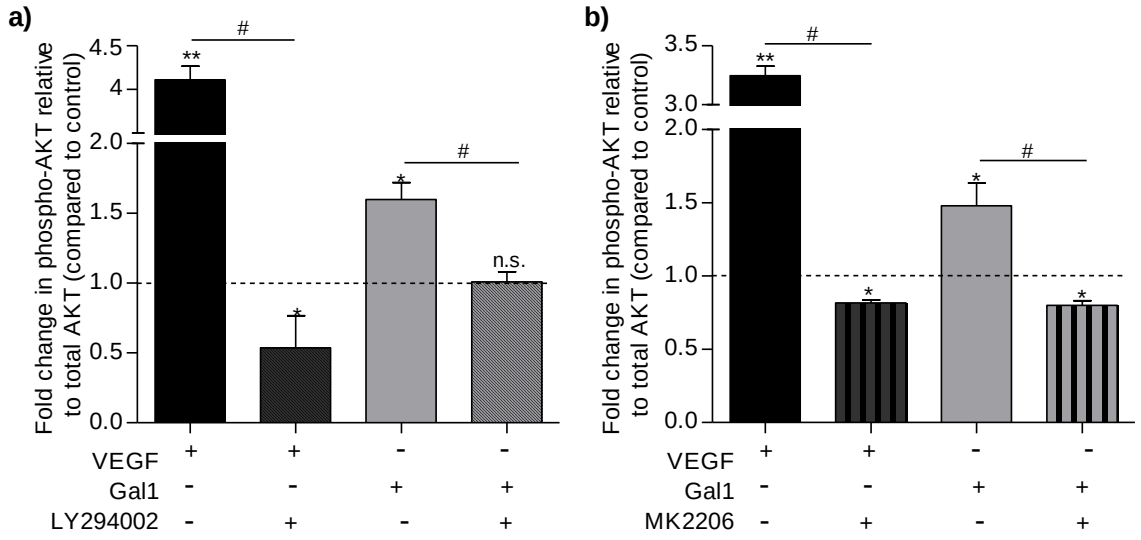

Figure 4.16: **Gal1-induced AKT phosphorylation is inhibited in HOMECs treated with PI3K and AKT inhibitors a) LY294002 (25 μM) and b) MK2206 (5 μM)**, respectively. Cells were seeded in 2% gelatin pre-coated 96 well plates at a density of 10,000cells/well in starvation media containing 2% FCS. After overnight incubation, cells were pre-incubated with the inhibitors for 2.5 hours, and then co-treated with or without 50ng/ml of Gal1 or 20ng/ml of VEGF in the absence or presence of the inhibitors for 4 minutes. Commercially available cell-based ELISAs were used for determination of level of AKT phosphorylation. The data is represented by fold change in phosho-AKT relative to total AKT (compared to control). Results are mean ±SD, n.s., *p<0.05, **p<0.01 vs control (1-fold), #p<0.05 vs VEGF/Gal1 (normalised to control), n=4. n.s. denotes not significant.

4.3.9 Gal1 induces migration in HOMECs

In addition to proliferation, a second key element of angiogenesis is EC migration. Since Gal1 was shown to induce proliferation in HOMECs, its pro-migratory role was also examined in these cells. Initially, cell migration was tested using a transwell Boyden chamber after 6 hours treatment, and it was revealed that Gal1 significantly increased HOMEC migration (161.0±35.5%, n=22; Figure 4.17a) compared to control (100%). VEGF, used as a positive control treatment in the cell migration experiment also induced significant HOMEC migration (144.9±27.3, n=19). This suggested that Gal1 may play a pro-migratory role in HOMECs.

Since Gal1 has been shown to induce phosphorylation of the ERK1/2 and AKT pathways, their role in Gal1-induced HOMEC migration was examined. The AKT pathway has been reported to be involved in the induction of cell migration in several cell models as previously discussed, and therefore the hypothesis was that activated AKT is involved in the induction of HOMEC migration of Gal1. To test this, cells pre-treated with PI3K (LY294002, 25 µM) or AKT (MK2206, 5 µM) inhibitors were co-treated with Gal1 in the presence of the corresponding inhibitors for 6 hours. The data revealed no significant inhibition in Gal1-induced cell migration with inhibitors compared to Gal1 treatment alone. For instance, at 25 µM of LY294002 cell migration was 189.2±48.0% (n=4; Figure 4.18a) compared to Gal1 treatment (158.5±20.2%, n=11), both normalised to control (100%). In the case of MK2206, although cell migration reduced (124.3±43.3%, n=5), it was not significantly different compared to Gal1 treatment (158.5±20.2%, n=11). Interestingly, inhibitor only treatments significantly inhibited cellular migration (Figure 4.18 a, b).

Cell migration was then tested using ERK1/2 inhibitors. HOMECs were pre-treated with U0126 (10 µM) or PD98059 (25 µM) and then co-treated with Gal1 in the presence or absence of the inhibitors for 6 hours. The data revealed that neither of the inhibitors significantly inhibited Gal1-induced HOMEC migration. For instance, Gal1-induced cell migration in the presence of U0126 was 160.7±25.8% (n=6; Figure 4.19a), compared to Gal1-treatment alone (163.4±47.2, n=11), both data normalised to control (100%). In the case of PD98059, there was a reduction in Gal1-induced cell migration (127.4±34.2, n=7; Figure 4.19), although it was not significantly different compared to Gal1

treatment. These data combined with the ELISA data (Figures 4.14, 4.16) suggest that Gal1-induced HOMEC migration may not solely depend on the activation of the ERK1/2 and AKT pathways, and that other kinases may be involved. Intriguingly, ERK1/2 inhibitor U0126-only significantly reduced HOMEC migration (4.19a, b).

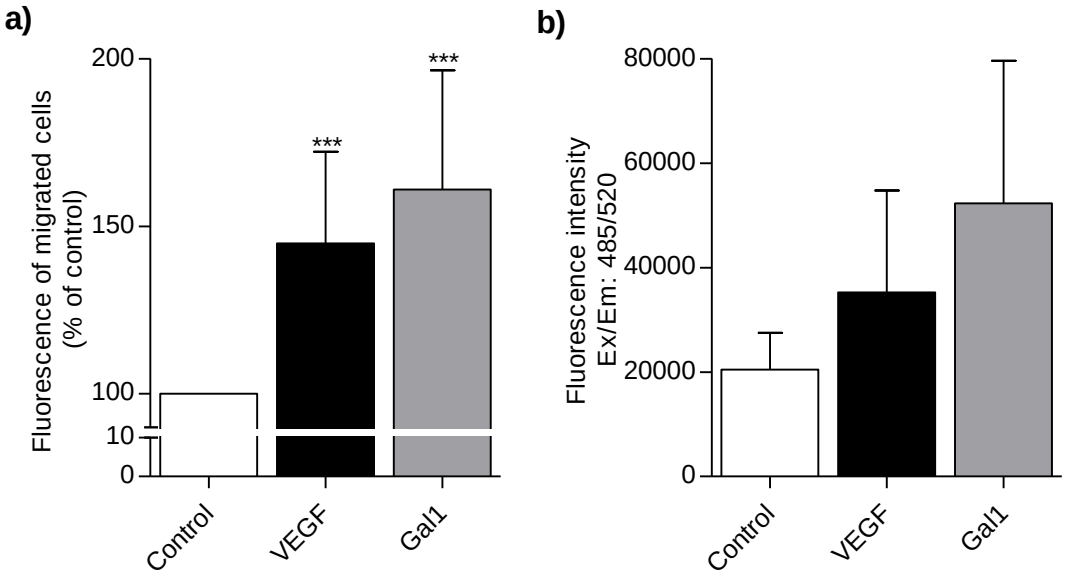

Figure 4.17: **Gal1 induces HOMEC migration.** HOMECs were seeded on the upper transwell insert and treated with or without Gal1 (50ng/ml) or VEGF (20ng/ml) supplementation of starvation media containing 0.5% FCS. The lower well contained correspondent treatment i.e. 0.5% FCS media, Gal1 (50ng/ml) or VEGF (20ng/ml). After 6 hours, migrated cells were stained with calcein AM and fluorescence was quantified by using a FLUOstar plate reader at Ex/Em: 485/520. **a)** Results are mean ±SD and shown as percentage of the control, ***p<0.001 vs control (100%), n=19-22, **b)** Raw data from representative experiment.

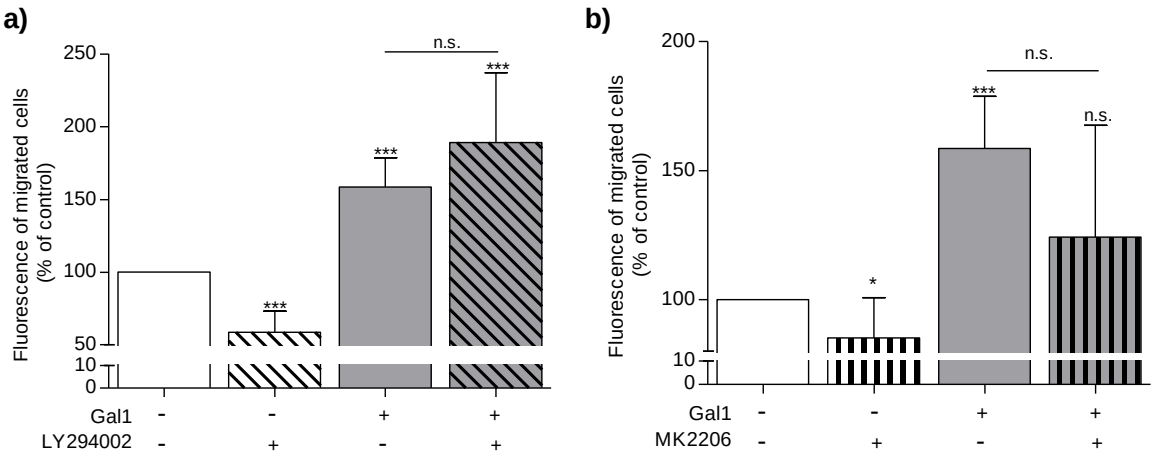

Figure 4.18: **Gal1 does not induce HOMEC migration via the AKT pathway.** HOMECs were seeded in the upper transwell chamber and treated with or without Gal1 (50ng/ml) in the absence or presence of PI3K and AKT inhibitors **a)** LY294002 (25 µM) and **b)** MK2206 (5 µM) respectively in media containing 0.5% FCS. The lower well contained correspondent treatments. After 6 hours, migrated cells were stained with calcein AM and fluorescence was quantified by using a FLUOstar plate reader at Ex/Em: 485/520. Results are mean ±SD and shown as percentage of the control, *p<0.05, ***p<0.001 vs control (100%), p= n.s. vs Gal1 (normalised to control), n=4-11. n.s. denotes not significant.

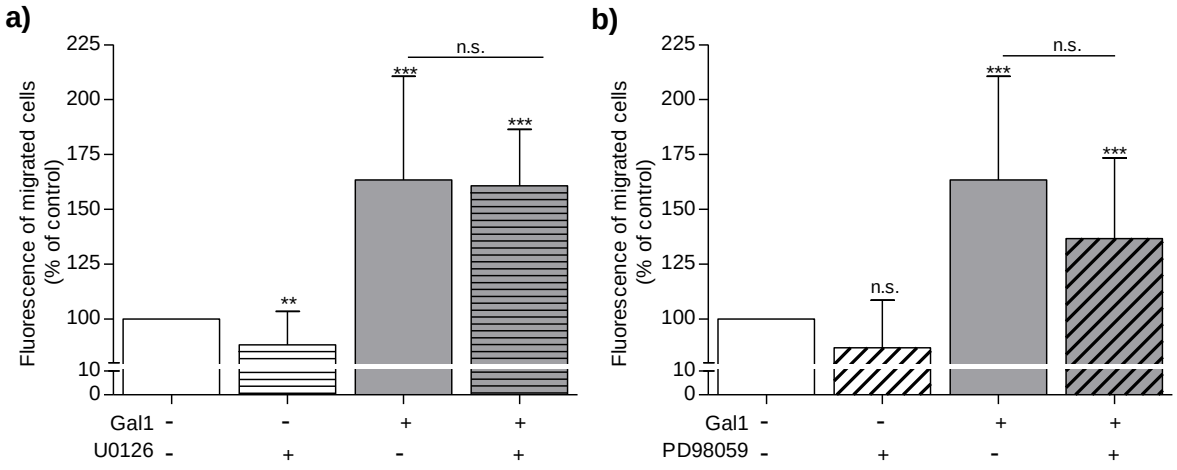

Figure 4.19: **Gal1 does not induce HOMEC migration via the ERK1/2 pathway.** HOMECs were seeded in the upper transwell chamber and treated with or without Gal1 (50ng/ml) in the absence or presence of ERK1/2 inhibitors **a)** U0126 (10 µM) and **b)** PD98059 (25 µM) respectively in media containing 0.5% FCS. The lower well contained correspondent treatments. After 6 hours, migrated cells were stained with calcein AM and fluorescence was quantified a using FLUOstar plate reader at Ex/Em: 485/520. Results are mean ±SD and shown as percentage of the control, **p<0.01, ***p<0.001 vs control (100%); p= n.s. vs Gal1 (normalised to control), n=4-12. n.s. denotes not significant.

4.3.10 Gal1-induced HOMEC migration is inhibited by L-glucose

Since Gal1-induced cell proliferation was inhibited by L-glu co-treatment, it was hypothesised that Gal1 may bind to a cell surface receptor with an extracellular sugar domain. If this was true, L-glu should also block Gal1-induced HOMEC migration. Thus, cellular migration was tested when cells were co-treated with Gal1 and L-glu (25mM) for 6 hours. The data revealed that in the presence of L-glu, Gal1-induced cell migration reduced significantly to 124.8±23.2% (n=6; Figure 4.20) compared to Gal1 treatment (189.3±59.0%, n=5), both data expressed as percentage of control (100%). These data, in combination with the proliferation data (Figure 4.11 a, b), suggest that Gal1 may induce proangiogenic changes in HOMECs via binding with a receptor(s) expressing a sugar moiety on its extracellular domain.

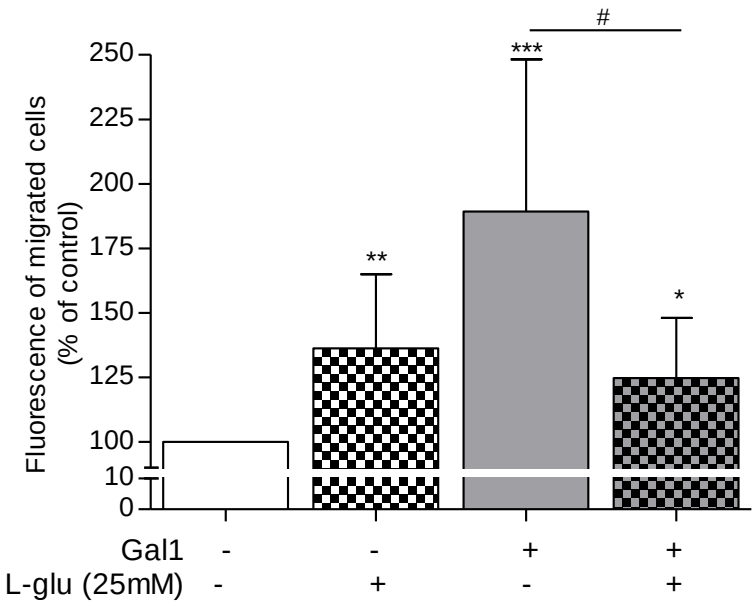

Figure 4.20: **Gal1-induced HOMEC migration is inhibited by L-glucose.** HOMECs were seeded on the upper transwell insert and treated with or without Gal1 (50ng/ml) and in the absence or presence of L-glu (25mM) in media containing 0.5% FCS. The lower well contained correspondent treatment i.e. 0.5% FCS media, Gal1 (50ng/ml) or Gal1±L-glu. After 6 hours, migrated cells were stained with calcein AM and fluorescence was quantified by using a FLUOstar plate reader at Ex/Em: 485/520. Results are mean ±SD and shown as percentage of the control, *p<0.05, **p<0.001, ***p<0.001 vs control (100%); #p<0.01 vs Gal1 (normalised to control), n= 5-6.

4.3.11 Investigation into Gal1 induced angiogenesis in HOMECs

The data described in this chapter indicate that Gal1 has the potential to induce cell proliferation and migration in HOMECs, two key steps of tumour angiogenesis. Thus angiogenesis was tested in HOMECs treated with Gal1 using a 3D *in vitro* model as described in the previous chapter (CathL section). Initially, HCMECs were used to establish the model with different treatments: media supplemented with 2% FCS as basal control (Figure 4.21a), media supplemented with 5% FCS and growth factors as positive control (complete growth media; Figure 4.21b), and 2% FCS media supplemented with 20ng/ml VEGF (Figure 4.21c) or 50ng/ml of Gal1 (Figure 4.21d). Cell sprouting was observed in the positive control, VEGF and Gal1 treated wells, but not in cells containing media with 2% FCS (control).

Interestingly, when the same conditions were applied using HOMECs, no sprouting was observed in any of the wells (data not shown). Therefore, as discussed previously (Chapter 3, section 3.3.7), further optimisation led to the investigation of angiogenesis in 2D growth factor reduced Matrigel (GFR-Matrigel). Initially, cells were seeded and after 2 hours treated for another 6 hours with the following conditions: media with 2% FCS, VEGF (ng/ml) or Gal1 (50ng/ml). It was found that Gal1 induced significant tube-like structures (223.3±18.5, n=3; Figure 4.22) compared to control (145±15, n=3). Positive control VEGF also induced significant tube-structure formation in HOMECs (210.3±22.4, n=3).

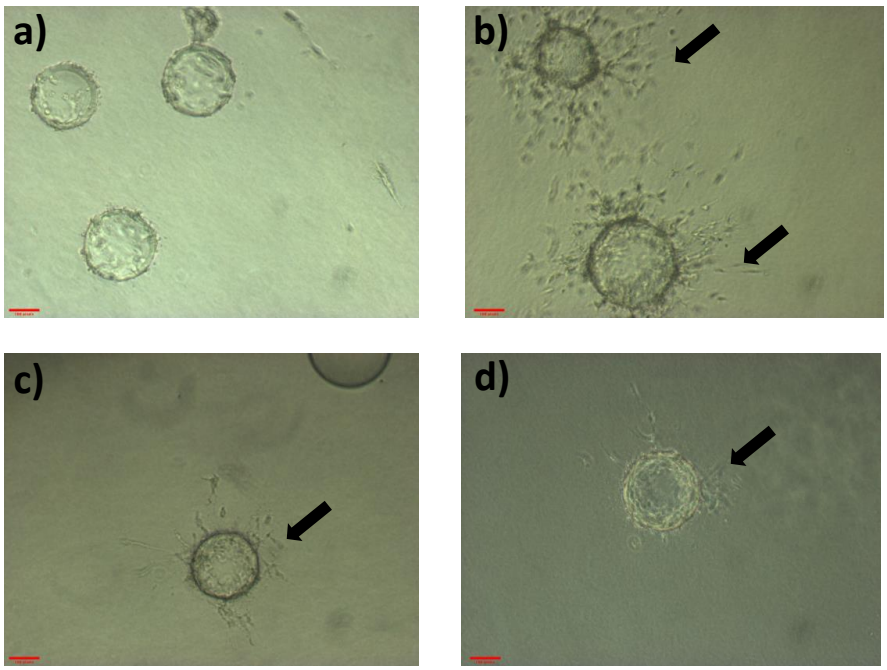

Figure 4.21: **Formation of angiogenic sprout in human cerebral microvascular ECs (HCMECs) in 3D fibrin gel.** Cells were seeded on cytodex 3 microcarriers and embedded in fibrin matrix gel in media supplemented with 2% FCS **a)** Control, **b)** 5% FCS with added ECs growth factors (Positive control), **c)** 20ng/ml of VEGF or **d)** 50ng/ml of Gal1. Media/treatments were replaced every other day up to day 5. Photographs were taken on day 6 post-seeding using a Nikon phase-contrast microscope at 10X magnification. Arrow pointing at cell sprouting. Scale bar =100µM.

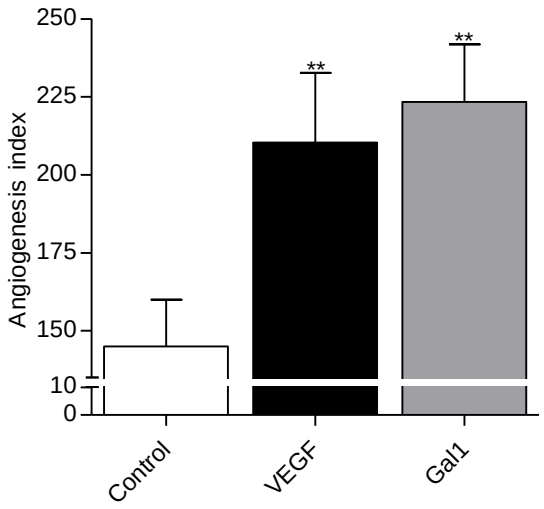

Figure 4.22: **Gal1-induced tubule structure formation in HOMECs in 2D Matrigel.** HOMECs were plated onto growth factor reduced- (GFR) Matrigel in medium containing 2% FCS and treated with media supplemented with or without VEGF (20ng/ml) and/or Gal1 (50ng/ml) for 8 hours. Controls contained HOMECs grown in medium containing 2% FCS alone. Photographs were taken at 8 hours after treatment using a Nikon phase contrast microscope camera and tubule-structure formation (including nascent tubule structures) was quantified as described in method section. The results are presented as an angiogenesis index. **p<0.01 vs control levels, n=4.

4.3.12 Investigating activation of receptor tyrosine kinases (RTKs) by Gal1

Although Gal1 has been shown to interact with cell surface sugar residues, due to its proangiogenic role, it is possible that the glycoprotein acts via an extracellular receptor with intracellular tyrosine kinase activity. Thus, this was tested using RTK array kit. After 10 minutes treatment with or without Gal1 or VEGF, no increase in activity was observed in any of the RTKs (Figure 4.23). The experiment was validated by the positive control VEGF which induced a 12-fold increase in the activation of VEGFR2 and 1.5-fold of VEGFR3.

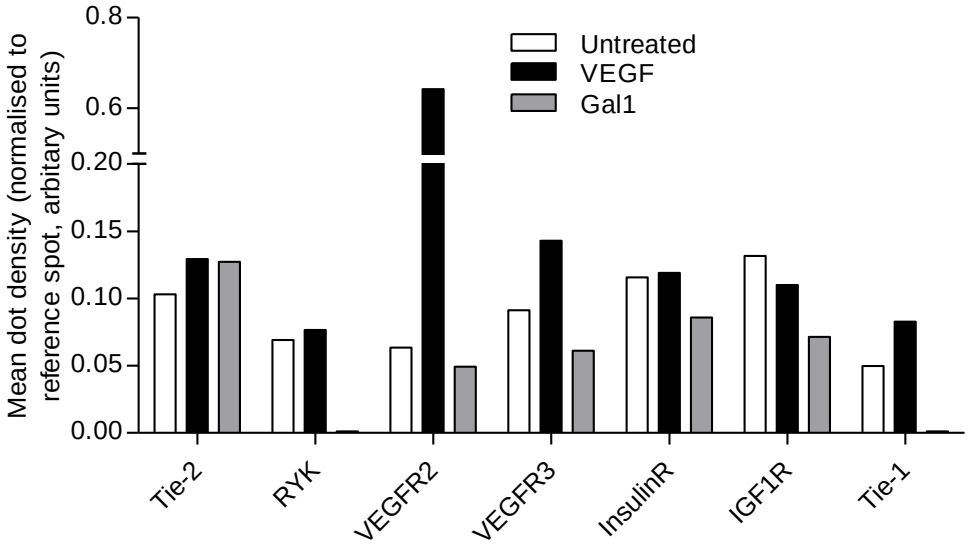

Figure 4.23: **Investigation into activation of potential RTK by Gal1.** Phosphorylation status of RTKs were assessed in cell lysates treated with or without Gal1 or VEGF for 10 minutes. The results of 1 minute exposure are expressed as mean dot density. The relative expression of specific phosphorylated proteins was determined following quantification of scanned images of membrane using Azure software. n=1.

4.4 Discussion

In this chapter, Gal1 was shown to be secreted by HOMECs during CathL treatment. This secretion seems to be transcriptionally regulated and mediated via NFκB activation. Exogenous Gal1 then acted on HOMECs inducing cell proliferation and migration where the former was shown to be mediated via activation of the ERK1/2 and AKT-independent PI3K pathways. Gal1 was also observed to induce angiogenic tube formation in HOMECs. Interestingly, Gal1 was not found to increase activation of any RTKs, although data suggests that Gal1 may be acting on HOMECs by interacting with a cell-surface receptor with a glucose moiety.

CathL induced production and secretion of Gal1 in HOMECs

Gal1 has been shown in the recent years to play a proangiogenic role in several EC models (Thijssen et al., 2006, D'Haene et al., 2013). Previous unpublished data from this laboratory found that CathL (EOC secreted factor) induced differential expression of LGALS1 mRNA in HOMECs. Since Gal1 is shown to be secreted, its presence in the supernatant of CathL-treated HOMECs was examined. Interestingly, a significant increase was observed in the levels of secreted Gal1 in CathL-treated HOMECs after 30 minutes and 8 hours, however it reduced to basal (control) level after 24 hours CathL treatment. Initially, the increased secretion of Gal1 after 30 minutes indicated that Gal1 may have been readily stored in the cytoplasm, possibly associated with unknown intracellular proteins closer to the intracellular side of the cell membrane (Camby et al., 2006). In this study, exogenous CathL triggered a response in HOMECs, and Gal1 was externalised or secreted, and this is the first report to describe this link between these two proteins.

Interestingly, at 8 hours treatment of CathL, the secreted level of Gal1 was even greater, possibly indicating an additional transcriptional regulation of LGALS1 by CathL treatment. Therefore, level of LGALS1 was assessed in HOMECs treated with CathL for 6 hours. The difference in time-points between assaying protein quantity and mRNA expression is to allow a timeframe for protein translation and subsequent secretion from its mRNA (Ben-Ari et al., 2010). The results showed that CathL increases expression of LGALS1, which correlates with the secreted

Gal1 data. Although CathL has never been reported to induce expression of LGALS1 or secretion of Gal1, transcriptional regulation of Gal1 has been reported in ECs. Specifically, minimally oxidised LDL was shown to induce expression of Gal1 in human aortic ECs (HAECs) (Perillo et al., 1995). Interestingly, level of expression of Gal1 mRNA was found to increase at 4 hour onwards in LDL treated HAECs (Baum et al., 1995).

Thijssen *et al.* reported a strong expression of Gal1 in an immunofluorescent study of angiogenically-active EC of human colon carcinoma and breast carcinoma, especially in EC that stained positive for the proliferation marker Ki67 (Thijssen et al., 2006). Interestingly, when HUVECs were activated by a mixture of growth factors, it also resulted in a significant increase in both Gal1 mRNA and protein expression (Thijssen et al., 2006). High LGALS1 mRNA expression and increased secreted levels of Gal1 were also observed in syngeneic tumour models of B16F10 melanoma cells and TC-1 lung carcinoma cells in *Gal1*^{wt} mice, which in turn increased vessel formation and escalated tumour progression *in vivo* (Thijssen et al., 2010). These reports suggest that Gal1 secretion can be induced from both ECs and tumour cells. In the current study, CathL has been shown, for the first time, to increase both LGALS1 expression and Gal1 secretion in HOMECs. There is a possibility that CathL increases LGALS1 expression in HOMECs at a shorter incubation period and that Gal1 level may upsurge at a shorter duration of treatment, which can be tested in future studies. Taken together, these data suggest that CathL increases Gal1 secretion from HOMECs by both a rapid intracellular mobilisation and longer-term transcriptionally-regulated manner.

At 24 hours after treatment, both expression of LGALS1 and secretion of Gal1 reduced to basal level, which contrasted with previous findings where minimally oxidised LDL consistently induced increased expression of LGALS1 mRNA in HAECs from 4 hours and persisted up to 24 hours (Baum et al., 1995). However, in this study the authors only investigated expression of Gal1 on the cell surface membrane and intracellularly, but not the secreted level. As it has been shown that Gal1 can be taken up by cells (Thijssen et al., 2010), it may be that after a certain period, secreted Gal1 was taken up by HOMECs from the culture media. For instance, it has been shown that Gal1 was retaken up by HUVECs and human vascular ECs (EC-RF24) (Thijssen et al., 2006, Thijssen et al., 2010).

However, it is also possible that Gal1 degraded after a certain number of hours as it has a half-life of 1 hour 7 minutes in culture media (Van Ry et al., 2015).

Since CathL was shown to induce LGALS1 expression and subsequent Gal1 secretion, the intracellular pathways that may be activated by CathL upstream of mRNA transcription were investigated. As CathL was shown to activate ERK1/2 and AKT, it was hypothesised that either or both of these kinases may induce LGALS1 transcription. In order to address this hypothesis, both inhibitors of ERK1/2 and AKT were tested. However, due to a lack of consistency in the obtained data on the secreted Gal1 level, no conclusions could be drawn. It would be important to examine this further in future work as signalling pathways upstream of LGALS1 transcription has not been elucidated in any other systems.

It has been reported that in Kaposi's sarcoma cells and T cells hypoxia induces LGALS1 mRNA expression and Gal1 secretion via activation of NFκB. Since the data in this study suggested that CathL induces LGALS1 expression and subsequent Gal1 secretion from HOMECs, it was hypothesised that activation of NFκB may play a role in this. Thus CathL-induced activation of NFκB was tested in HOMECs. Interestingly, it was found that CathL increased NFκB activation and in the presence of sulfasalazine, a selective inhibitor of NFκB, both LGALS1 mRNA expression and Gal1 secretion were significantly reduced. This agrees with the current literature. For instance, Toscano *et al*. demonstrated that the LGALS1 gene is a direct target of NFκB, which initiated the mRNA transcription upon activation in differentiated T cells and the subsequent expression and secretion of Gal1 (Toscano et al., 2011). Another study reported an increase in LGALS1 expression and Gal1 secretion in Kaposi's sarcoma cells in response to hypoxia. It was shown that hypoxia-mediated activation of NFκB subsequently induced LGALS1 mRNA expression and Gal1 secretion (Croci et al., 2012). These phenomena were significantly reduced or completely halted when treated with NFκB inhibitors such as sulfasalazine or Bay11-7082, suggesting that NFκB plays a key role in inducing LGALS1 mRNA expression and subsequently Gal1 secretion.

Secretory pathway for Gal1 in CathL-treated HOMECs

Secretion of Gal1 into the extracellular space as well as on the extracellular side of cell membranes is well accepted. It has been suggested that Gal1 is secreted in a non-ER/Golgi pathway (unconventional protein secretory pathway) since it lacks an N-terminal signalling sequence peptide. However, the exact molecular mechanism of this secretory pathway remains largely unknown. Therefore, it was hypothesised that Gal1 secretion in HOMECs is not mediated through the conventional ER/Golgi pathway. This hypothesis was partially supported by the observation that in the presence of BFA, which destabilises the Golgi, CathL-induced Gal1 secretion was still significantly higher, compared to control. This was despite the observation that BFA appeared to completely disrupt the Golgi integrity. This observation agrees with several studies where Gal1 was shown to be secreted via an unconventional secretory pathway. For example, Toyokawa *et al.* demonstrated that Gal1 secretion was not inhibited in BFA-treated ovine glandular epithelial cells (Toyokawa et al., 2007). There was a slight reduction in Gal1-secretion in the presence of CathL and BFA which is discussed later. Together, these data suggest that Gal1 may be secreted in a non-ER/Golgi pathway in HOMECs treated with CathL.

Proteins such as FGF2, interleukin-1β and Gal1, are thought to be secreted in ER/Golgi-independent pathway, primarily because they lack a signal sequence that is used in the classical secretory pathway to target newly synthesised proteins to the ER. Although the exact molecular mechanism of the secretion of such proteins is unknown, evidence suggests that a plasma membrane resident transporter may play a role in directly translocating FGF2 and Gal1. An ABC transporter has been suggested to mediate this unconventional secretory pathway, although due to a lack of an experimental model with human cells, this has not been tested (Rees et al., 2009). Cleves *et al.* demonstrated release of Gal1 through the peri-plasmic membrane (vesicles) into the external cell wall of transfected yeast expressing rat Gal1 which was reduced in a strain lacking Ste6p, an ABC transporter (Cleves et al., 1996). More recently, the inside-out topology was proposed with the rationale that translocation of a given factor into the lumen of these vesicles would mimic its secretion, as the lumen of these vesicles is topologically equivalent to the extracellular space (Nickel, 2005). Recombinant Gal1 protein, when added, traversed the membrane of these

inside-out vesicles in Chinese hamster epithelial ovarian cells, with an aid of a plasma membrane resident transporter, possibly ABC (Schafer et al., 2004, Nickel, 2005). However, a role for the sodium pump (Na+/K+- ATPase) was also suggested in the Gal1 export pathways as ouabain, a selective inhibitor of the sodium pump, inhibited these export processes (Nickel, 2005). Together, these observations further suggest a secretory pathway for Gal1 that is independent of the classical ER/Golgi pathway.

Interestingly, BFA did slightly reduce Gal1 secretion in CathL-treated HOMECs compared to CathL-only treatment. This may have been due to its effects on other organelles. BFA has been shown to affect other cellular organelles such as ER, lysosomes and endosomes as well as microtubules, actin and other cytoskeleton proteins in normal rat kidney cells (Lippincott-Schwartz et al., 1991, Alvarez and Sztul, 1999). The presence of BFA may have damaged the alternative secretory pathway of Gal1 in HOMECs, reducing its secretion slightly.

Gal1 induced HOMEC proliferation

Since Gal1 is secreted in response to CathL treatment into the cell culture media, it was hypothesised that Gal1 may contribute to the proangiogenic role of CathL in HOMECs. Indeed, it was found that Gal1 increased HOMEC proliferation in a dose-dependent and time-dependent manner, an observation that agrees with other recent findings. For instance, Thijssen *et al.* reported increased proliferation of primary HUVECs and EC-RF24 (human vascular EC line) cells when treated with exogenous Gal1 (Thijssen et al., 2010). Another study demonstrated an increase in proliferation in HUVECs and the human vascular EC line EA.hy 926 when treated with exogenous Gal1 (D'Haene et al., 2013). Interestingly, an additive effect in increased cell proliferation was observed when these cells treated with both Gal1 and Gal3. In an earlier study, exogenous Gal1 was also found to induce proliferation of primary myeloma cells during tumour progression (Abroun et al., 2008). These combined data suggest that Gal1 plays a key pro-proliferative role in different models.

However, there are reports that do not agree with the current findings. For instance, binding of Gal1 to breast cancer cells MCF7 induced apoptosis and also inhibited cellular proliferation (Geiger et al., 2016). In Geiger's study, higher

concentrations of Gal1 (>10 µg/ml) were used which may have induced an anti-proliferative effect. Intriguingly, Adams *et al.* demonstrated a biphasic modulation of growth of human fibroblasts whereby higher concentrations of Gal1 (>20 µg/ml) inhibited cellular proliferation (Adams et al., 1996). These studies suggest that at higher concentrations Gal1 may be anti-proliferative, which was not reflected in the current study as the highest concentration of Gal1 was 125 ng/ml. Interestingly, Gal1 was shown to possess a growth-inhibitory site in its structure, which may be responsible for its anti-proliferative effect (Scott and Zhang, 2002). Taken together, this study and others indicate a biphasic/functional effect of Gal1 in human cells, which should be tested in future studies using HOMECs.

CathL-induced HOMEC proliferation is not mediated by secreted Gal1

Since CathL induced secretion of Gal1 in cultured HOMEC, and both CathL and Gal1 were shown to induce proliferation in HOMECs, the next step was to investigate whether CathL-induced cell proliferation was mediated via Gal1. L-glu was used to examine this hypothesis. Although lactose, a disaccharide of galactose and (D-)glucose with a binding specificity for β-galactosidase binding sites (i.e. on Gal1 CRD), was used in previous studies to block Gal1 binding to both human and mice bone marrow cells (Vas et al., 2005) and to inhibit Gal1-induced proliferation of human dermal fibroblasts (Adams et al 1996), it was not implemented in the current study. Lactose was found to increase HOMEC proliferation (data not shown), possibly by increasing cell metabolism. However, L-glucose, an isomer of (D-)glucose, is metabolically inert (Rudney, 1940) and hence was substituted for lactose.

To test this, initially, HOMECs were treated with Gal1 in the presence of L-glucose and it was found that L-glu inhibited Gal1-induced cell proliferation. However, no inhibition of HOMEC proliferation was observed when L-glu was added in CathL-supplemented media. This suggested that CathL-induced HOMEC proliferation is independent of Gal1-activity.

Gal1-induced activation of intracellular signalling pathways and their role in cellular proliferation

As Gal1 induced HOMEC proliferation, it was logical to assess the intracellular signalling pathways activated. Previously, CathL was shown to induce phosphorylation in ERK and AKT which were found to be activated in the proangiogenic changes in HOMECs (Chapter 3, section 3.3.3). Therefore, only the ERK1/2 and AKT pathways were investigated. Interestingly, both of these kinases were found to be phosphorylated in Gal1-treated HOMECs compared to untreated cells. This agrees with recent evidence indicating that Gal1 induced phosphorylation of ERK1/2 in other human vascular ECs (EA.hy926 and EC-RF24 cell lines) (Thijssen et al., 2010, D'Haene et al., 2013). Chung *et al.* also demonstrated an increase in the level of phosphorylated ERK1/2 in lung cancer cells (A549 cell line; (Chung et al., 2012)). Similar other literature is available regarding the activation of AKT by Gal1. For instance, Hsu *et al.* demonstrated an increase in the levels of phosphorylated AKT in human lung cancer cell lines (A549, CL1-0 and CL1-5; (Hsu et al., 2013)). Gal1 was also reported to induce AKT activation in human hepatocellular carcinoma cells, aiding tumour progression (Zhang et al., 2016). Together, our data suggest that Gal1 induces activation of pro-proliferative and pro-migratory kinases ERK1/2 and AKT in HOMECs.

As previously described, activation of ERK1/2 has been extensively shown to be involved in cell proliferation, including in HOMECs as shown in Chapter 3 (section 3.3.1). Therefore, it was hypothesised that ERK1/2 may play a pro-proliferative role in Gal1-treated HOMECs. The ERK1/2 inhibitors U0126 and PD98059 were used to examine this. Both inhibitors demonstrated significant inhibition of HOMEC proliferation compared to Gal1-treatment alone, suggesting that ERK1/2 may mediate Gal1-induced HOMEC proliferation. This is in agreement with other recent studies. For example, Thijssen *et al.* and D'Haene *et al.* demonstrated that the ERK1/2 activation plays a key role in Gal1-induced proliferation of human vascular EC line (EC-RF24) (Thijssen et al., 2010) and HUVEC proliferation (D'Haene et al., 2013). These reports, along with the current study, suggest that Gal1 induces cell proliferation via activation of ERK1/2.

Interestingly, Fischer *et al.* suggested that at higher concentrations Gal1 induces an anti-proliferative effect in human colonic carcinoma cell lines HT-29 and Caco-2 through an inhibitory effect on ERK1/2 phosphorylation when treated with 200µg/ml of Gal1 (Fischer et al., 2005). As discussed previously, higher concentrations of Gal1 have an anti-proliferative effect in cells, and this may be through inhibiting the pro-proliferative ERK1/2 pathway. Further investigation would be required to confirm this phenomenon in HOMECs, however since levels of Gal1 secreted into the medium were less than 200µg/ml, this phenomenon may not be physiologically relevant in HOMECs.

Based on the previously described role for PI3K/AKT in EC proliferation (Chapter 3, section 3.4) and the fact that Gal1 induced increased levels of phosphorylated AKT, the activation of this pathway in HOMEC proliferation was tested. The PI3K inhibitor LY294002 decreased Gal1-induced HOMEC proliferation in a dose-dependent manner. ELISA data confirmed inhibition of AKT activation in the presence of LY294002, and thus these data suggest that, like ERK1/2, the PI3K/AKT pathway may also be involved in Gal1-induced HOMEC proliferation.

Since PI3K has been shown to induce cellular proliferation independent of AKT activation (discussed in chapter 3, section 3.4), the role for AKT in HOMEC proliferation was investigated. Selective AKT inhibitor MK2206 did not inhibit Gal1-induced HOMEC proliferation at non-toxic concentrations, which was verified by ELISA data. Thus, this data suggested that AKT activation is not required for Gal1-induced HOMEC proliferation.

The role of PI3K and/or AKT in Gal1-induced cellular proliferation is not clear. Indeed, recently, Gal1-induced proliferation has been shown to be mediated via activation of the PI3K/AKT pathway. For instance, Zhang *et al.* demonstrated that inhibiting the PI3K/AKT pathway using LY294002 reduced Gal1-induced proliferation of human hepatocellular carcinoma cell lines (Zhang et al., 2016), indicating a key role for PI3K/AKT pathway in Gal1-induced cellular proliferation. A role for the activated PI3K/AKT pathway was also observed in Gal1-induced proliferation of human renal cell carcinoma cells, which was inhibited in the presence of PI3K inhibitor LY294002 (White et al., 2014). Although activation of AKT was suggested to play a pro-proliferative role in these studies, the authors did not specifically target the AKT kinase (i.e. using a selective inhibitor of AKT) to confirm such findings. However, Lee and colleagues suggested a more direct

role of the AKT pathway in Gal1-induced proliferation of mouse embryonic stem cells (Lee et al., 2009). An unknown inhibitor of AKT was used to test this, which resulted in a decreased Gal1-induced cellular proliferation at S-phase, suggesting a role for AKT activation in this phenomenon. The current study suggests that activation of PI3K, but not AKT, is involved in mediating induction of HOMEC proliferation by Gal1 treatment. Here, selective inhibitors of both PI3K and AKT have been tested, unlike other studies where either PI3K or AKT was inhibited, and hence the results strongly suggest that Gal1-induced HOMEC proliferation may be mediated via an AKT-independent PI3K pathway.

Gal1 induced HOMEC migration

Cellular migration is another key element in tumour progression and angiogenesis. Since Gal1 has been shown to induce HOMEC proliferation, a proangiogenic response, its ability to induce migration was investigated. Interestingly, the data revealed a significant increase in cellular migration by Gal1 compared to control (untreated cells), suggesting a possible role of Gal1 in omental angiogenesis. In support of these data, Gal1 has been shown to be pro-migratory in several cell models. For example, Thijssen *et al.* and Hsieh *et al.* demonstrated an increased migration of HUVECs when treated with Gal1 (Hsieh et al., 2008, Thijssen et al., 2010). This increase in cellular migration was inhibited by adding lactose, suggesting activation of a cell surface receptor with an extracellular sugar moiety. Interestingly, the reported increase in Gal1-induced migration was similar to positive control VEGF-induced HUVEC migration, which was also observed in the current study using HOMECs. Another study revealed Gal1-induced migration of human oral and vulval squamous carcinoma cell lines in an autocrine manner (Rizqiawan et al., 2013). The authors investigated the molecular mechanisms of Gal1-induced cellular migration and observed that Gal1 increased both mRNA and cell surface expression of α2 and β5 integrins via activation of the JNK pathway. A collective migration, a process by which a group of cells move in concert, without completely disrupting their cell-cell contacts, was suggested for wound-healing process which was described by α2-mediated formation of filopodia and subsequent cellular motility (Ilina and Friedl, 2009). Soluble Gal1 has been also demonstrated to induce motility in human glioma cell lines via increasing expression of RhoA, a protein that modulates actin

polymerisation and depolymerisation (Camby et al., 2002). Together, these studies suggest a pro-migratory role for Gal1 which has also been revealed in the current report.

Role of activated signalling pathways in Gal1-induced HOMEC migration

Although the above studies indicated a potential proangiogenic role of Gal1 in angiogenesis, its exact mechanism of action remains largely unknown. Since activated AKT has been shown to mediate cellular migration and Gal1 was found to induce AKT activation in HOMECs, it was hypothesised that AKT may play a key role in the induction of HOMEC migration. Both inhibitors of PI3K and AKT were utilised to test this. Although, none of the inhibitors significantly inhibited Gal1-induced HOMEC migration, a small, but not statistically significant reduction in migration was observed when HOMECs were co-treated with Gal1 and MK2206. This may suggest that AKT activation and subsequent cellular migration is not dependent on PI3K activation (Filippa et al., 1999, Mahajan and Mahajan, 2012). Interestingly, White *et al.* suggested a role for AKT/mTOR in Gal1-induced migration of human renal cell carcinoma cell lines (White et al., 2014). The authors examined this using LY294002, a selective PI3K inhibitor, and demonstrated that when co-treated with Gal1, the inhibitor significantly reduced cellular migration (White et al., 2014). This contradicts the current finding, whereby, PI3K inhibitor did not reduce Gal1-induced HOMEC migration, although significantly inhibited AKT phosphorylation as detected by the ELISA.

This led to investigation of the role of ERK1/2 in Gal1-induced HOMEC migration. Interestingly, neither of the ERK1/2 inhibitors inhibited HOMEC migration when co-treated with Gal1, suggesting that activation of the ERK1/2 kinase may not solely mediate this migratory response. These data contradict the current literature. For instance, Thijssen *et al.* suggested a pro-migratory role of activated ERK1/2 in Gal1-induced HUVEC migration (Thijssen et al., 2010). However, the authors did not verify their finding by attempting to inhibit ERK1/2 activation in Gal1-induced migration. Interestingly, Hsieh *et al.* suggested that activated JNK, a MAP kinase, is responsible for Gal1-induced migration in HUVECs (Hsieh et al., 2008). Although the data revealed an activation of the ERK1/2, the authors did not investigate its role in Gal1-induced migration. Activation of JNK was also observed to be involved in the induction of migration of human vulval and oral squamous carcinoma cells (Rizqiawan et al., 2013), again indicating JNK to be a

potential pro-migratory kinase (Huang et al., 2008, Huang et al., 2003). Together, these data suggest that, there may be multiple intracellular kinases such as AKT, ERK1/2 and JNK that can be activated by Gal1, mediating the pro-migratory response in angiogenesis and tumour progression. This should be investigated further using HOMECs in future studies. For example, Gal1-induced activation of intracellular signalling pathways can be examined using a proteome profiler phosphokinase array (described in Method section 2.7.2) to identify potential kinases such as JNK that may be involved in Gal1-induced HOMEC migration.

L-glu inhibited Gal1-induced HOMEC migration

In these studies, L-glu was shown to inhibit Gal1-induced HOMEC proliferation. This was further investigated in Gal1-induced HOMEC migration. When tested, L-glu significantly reduced Gal-induced cellular migration, suggesting a physical blocking of Gal1 from binding to cell surface receptors. In the literature, Gal1-induced HUVEC migration was significantly reduced in the presence of lactose (Hsieh et al., 2008). A similar observation was revealed in human glioma cell lines, whereby, addition of lactose inhibited Gal1-induced cellular motility (Camby et al., 2002). Taken together, the current report suggests that Gal1 induces HOMEC migration via acting upon a cell surface receptor with an extracellular sugar moiety.

Gal1 induced angiogenic tube formation in HOMEC

Since Gal1 has been shown to be pro-proliferative and pro-migratory in HOMECs, its role in angiogenesis was examined in these cells. As discussed in Chapter 3 (section 3.3.7), initially HCMECs were utilised in a 3D angiogenesis *in vitro* model. Interestingly, Gal1 was shown to induce branching of HCMECs compared to control. However, when tested in HOMECs, no sprouting was observed (data not shown). After a number of optimisation steps, growth factor-reduced Matrigel was used to examine Gal1-induced tube-formation. Intriguingly, the results revealed a significant increase in tubule-structure formation compared to control. This agrees with the current literature where evidence also suggests a proangiogenic role for Gal1 in angiogenic tube formation. For instance,

exogenous Gal1 was observed to induce tube formation in HUVECs and EA.hy296 (human vascular EC) cells (Croci et al., 2012, D'Haene et al., 2013), which was inhibited by addition of lactose or specific anti-Gal1 monoclonal antibody (Croci et al., 2012). Additionally, Thijssen and colleagues reported an increase in the mean vascular density in a wild-type mice model ($Gal1^{+/+}$) compared to knock-out ($Gal1^{-/-}$) models (Thijssen et al., 2006). This phenomenon was also observed *in vitro* using HUVECs and CAM models, suggesting a proangiogenic role for Gal1 in tumour angiogenesis (Thijssen et al., 2006).

Examining RTK activation in Gal1-treated HOMECs

As previous data suggested that Gal1 promotes cell survival and growth via activation of intracellular kinases, it was hypothesised that an RTK may be involved. A brief investigation was carried out to identify possible RTKs in HOMECs that may be activated by Gal1. The data revealed no relative activation of RTKs by Gal1 in HOMECs. Interestingly, Gal1 has been shown to induce activation of neuropilin 1 (NRP1), a co-receptor for VEGFR1/2, in the proangiogenic responses in HUVECs (Hsieh et al., 2008, D'Haene et al., 2013). NRP1 is a transmembrane glycoprotein (i.e. contains sugar residues on the cell surface) that has been shown to be bound by VEGF-A, leading to activation of VEGFR2 and downstream signalling pathways (Herzog et al., 2011). Gal1 is believed to act in a similar manner in EC models (Hsieh et al., 2008, D'Haene et al., 2013), although in the current study VEGFRs was found not to be activated by Gal1. Previously, several binding partners of Gal1 were identified in a variety cell types, eliciting a number of responses. Interestingly, all of these Gal1-targeting cell surface receptors consist of glucose moieties, which may be the case in HOMECs in inducing cell proliferation and migration (Table 4.2), as indicated in the current study. Perhaps, activation of NRP1/VEGFR2 and involvement of other transmembrane glycoproteins should be examined further in Gal1-treated HOMECs.

A summary of the data from this chapter are described in figure 4.24.

4.5 Conclusion

The data from the current study suggest, for the first time, that CathL induces expression of LGALS1 and subsequent secretion of Gal1 in HOMECs. Exogenous Gal1 induces proangiogenic changes in HOMECs such as proliferation, migration and angiogenic-tube formation. These findings shed light in the pathogenesis process of EOC metastasis to the omentum which fits in well with the clinical observations of advanced stage of the disease. Since extensive vascularisation is required for the tumour to survive, Gal1, with its potent proangiogenic response, may facilitate cellular angiogenesis in HOMECs and secondary tumour progression. This may, for the first time, highlight Gal1 as a novel anti-angiogenic therapeutic target in EOC metastasis.

Table 4.2: Binding partners of Gal1 (taken from (Astorgues-Xerri et al., 2014)).

Binding partner	Biological functions	Cell type	Refs.
Integrins a5b1	Inhibition of cell growth, Apoptosis induction	Epithelial tumour, Hepatocarcinoma	(Fischer et al., 2005, Sanchez-Ruderisch et al., 2011)
Integrins α2β5	Induce motility	Human oral and vulval squamous carcinoma	(Rizqiawan et al., 2013)
Ganglioside GM1	Inhibition of cell growth	Neuroblastoma	(Kopitz et al., 2001, Kopitz et al., 1998)
CD44 and CD326	Metastasis development	Colon cancer	(Ito and Ralph, 2012)
CD146	Anti-apoptotic effect	Endothelial	(Jouve et al., 2013)
Neuropilin-1	Proliferation, migration and adhesion induction	Endothelial	(Hsieh et al., 2008)
Glycoprotein 90 K	Homotypic cell aggregation	Melanoma	(Tinari et al., 2001)

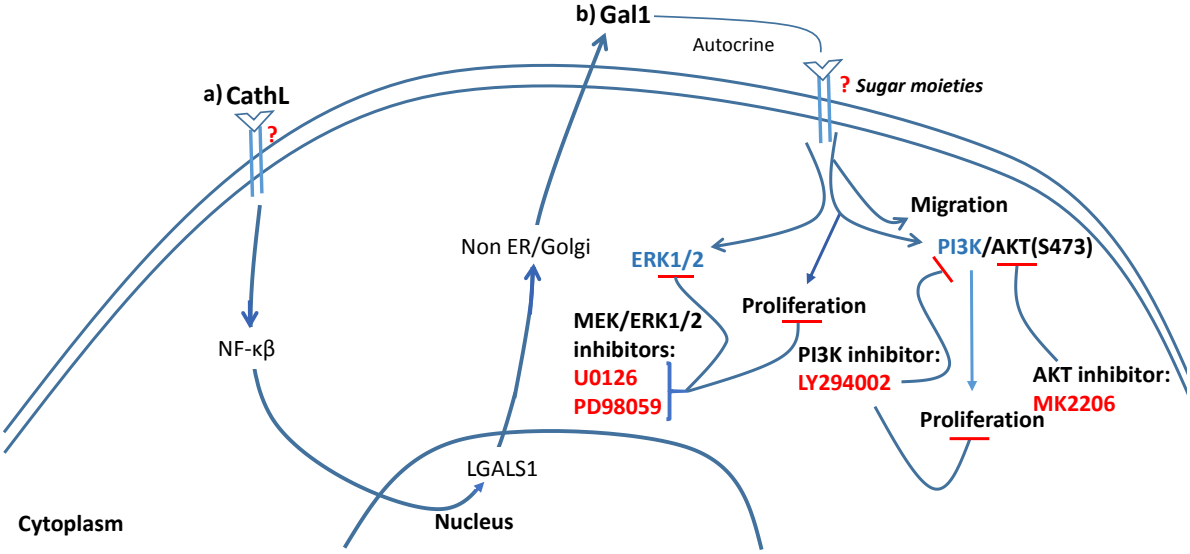

Figure 4.24: **A summary of secretion of Gal1 and subsequent activation of the ERK1/2 and AKT pathways, and cellular functions in HOMECs.** a) CathL induces increased expression of LGALS1 (Gal1 mRNA) possibly via NFκB activation, followed by protein production and secretion via a non ER/Golgi pathway. b) Secreted Gal1 binds to an unknown cell surface receptor in an autocrine manner and increases activation of EKR1/2, leading to the induction of cell proliferation. The MEK/ERK1/2 inhibitors U0126 and PD98059 significantly reduce this cellular function by inhibiting activation of ERK1/2. Both PI3K inhibitor LY294002 and AKT inhibitor MK2206 inhibit phosphorylation of AKT at Ser473 in Gal1-treated HOMECs. However, only LY294002 inhibits Gal1-induced cellular proliferation, suggesting activation of a pro-proliferative signalling cascade downstream of PI3K that is independent of AKT activation. Gal1 also acts as a pro-migratory factor, although the active intracellular kinases in this process remain unknown.

Chapter 5 Investigation into the proangiogenic role of cathepsin D (CathD) in ovarian cancer metastasis to the omentum

5.1 Introduction

The process of angiogenesis requires EC activation, proliferation, migration and sprouting towards the tumour which occurs via protease-mediated cleavage of extracellular matrix. Degradation of ECM is carried out by proteases secreted by ECs as well as tumour cells. Previously, a number of proteases were reported to be secreted by the EOC cells A2780 and SKOV3. A notable one with direct pro-migratory effect on HOMECs is CathD. CathD, just like CathL, is a lysosomal protease. However, unlike CathL it is an aspartic protease with an optimum pH of 3.5-4.5.

Although both CathL and CathD act in lysosomes, their optimum pH for proteolytic activity is slightly different. For instance, CathL is highly active between pH 5 and 6.5, whereas CathD has an optimum pH of 3.5-4.5. CathD has been found in the extracellular tumour microenvironment of several cancers (discussed in Chapter 1, Section 1.7.2.3) where it actively digests ECM components. However, reports also suggest that CathD may have a mitogenic role which it elicits in a non-proteolytic manner. Interestingly, CathD was found to be active at neutral pH in normal physiology. In ovarian cancer there is only one study indicating a role for CathD where it was shown to induce migration in HOMECs i.e. a potential angiogenic response (Winiarski et al., 2013). However, the underlying mechanisms remain unknown.

As proliferation is a key step in angiogenesis, a possible role for CathD in HOMEC proliferation was examined. Since CathD was found to be both proteolytically active and inactive in the extracellular microenvironment of several cancer models, and to induce a mitogenic effect, studies were carried out to explore its mechanism of action. Pepstatin A (pepA), a specific inhibitor of the proteolytic activity of CathD, was tested for its inhibitory effect on CathD-induced HOMEC proliferation. Subsequently, CathD activity at a range of pHs was examined to determine whether CathD was proteolytically active at its optimum versus at neutral pHs. As CathD has been reported to be proangiogenic in HOMECs, activated intracellular signalling pathways were also identified and tested in

subsequent functional studies such as cell proliferation and migration. Furthermore, CathD-induced EC sprouting and angiogenic tube-formation was tested in *in vitro* angiogenesis models. Finally, preliminary studies were also carried out to identify receptor targets of CathD.

5.1.1 Aims

The aims of this study were as follows:

- To investigate whether CathD induced HOMEC proliferation
- To examine the mechanism of action of CathD- whether it acts in a proteolytic manner or a non-proteolytic mechanism
- To identify potential cell signalling pathways activated in HOMECs
- To assess role of such pathways in HOMEC proliferation and migration induced by CathD
- To study angiogenic-tube formation of HOMECs by CathD
- To identify potential receptor target of CathD in HOMECs

5.2 Methods

HOMEC isolation: HOMECs were isolated according to previously published work (Winiarski et al., 2011) as described in the Method chapter section 2.3.1.

Cell proliferation: HOMEC proliferation was tested using both the WST-1 assay and CyQuant cell proliferation kit as described in the Method chapter sections 2.4.1 and 2.4.2.

CathD-proteolytic activity: The WST-1 assay was used to study CathD-induced HOMEC proliferation in the presence or absence of pepA, a specific inhibitor of CathD-proteolytic activity (Method section 2.4.1). An array of pHs were used to investigate proteolytic activity of CathD in the presence of a CathD-specific fluorogenic substrate and in the presence or absence of pepA, as has been described in the Method chapter sections 2.6 and 2.6.1. The pH of cultured media was also measured. These pHs were measured down to 2 decimal places in 100µl media/buffer using ABL800 FLEX blood gas analyser.

Activation of intracellular kinases: Commercially available proteome-profiler and cell-based ELISAs were used to detect and assess levels of phosphorylated intracellular kinases as described in the Method chapter sections 2.7.2 and 2.7.4.1.

Cell migration: A commercially available cultrex Boyden chamber kit was used to investigate the underlying mechanisms of CathD-induced HOMEC migration, as described in the Method chapter section 2.5.1.

3D *in vitro* angiogenesis: A 3D angiogenesis model was used to assess HOMEC sprouting as described in the Method chapter section 2.8.1.

2D Tube-formation: Angiogenic tube-formation was investigated in HOMECs treated with CathD using both a fibrin matrix assay and commercially available GFR-Matrigel, as described in the Method chapter section 2.8.2.

Identification of potential cell surface receptors: A commercially available human receptor-tyrosine kinase array was used as a screening to identify potential receptor as described in the Method section 2.7.3.

5.3 Results

5.3.1 CathD induces HOMEC proliferation

The first set of experiments examined the proliferative effect of CathD in HOMECs. As discussed in Chapter 2 (Section 2.4) and Chapter 3 (Section 3.4), both WST-1 and CyQUANT assays were chosen to test for cell proliferation. Initially, HOMECs were treated with increasing concentrations of CathD (20, 50 and 80 ng/ml) for 72 hours. No significant increase in cell proliferation was observed at 20ng/ml of CathD (108.28±23.0%, n=17, vs control (100%)), although at 50 ng/ml CathD significantly increased HOMEC proliferation (147.0±25.8%, n= 20, vs control (100%); Figure 5.1a). At 80ng/ml, a significant reduction in cell proliferation (83.4±11.5%, n=5 vs control (100%)) was observed (Figure 5.1a). On the basis of these data, subsequent experiments were carried out using 50ng/ml of CathD.

The initial cell proliferation data was complemented using a CyQUANT kit. HOMECs were treated with 50ng/ml of CathD for 72 hours. The data shows an increase in fluorescence intensity which correlates with an escalation of the

amount of DNA, and hence demonstrates proliferation of cells (109.1±10.4%, n= 0.01 vs control (100%); Figure 5.2a). This data confirmed the WST-1 proliferation data, and therefore only WST-1 was carried out in further experiments.

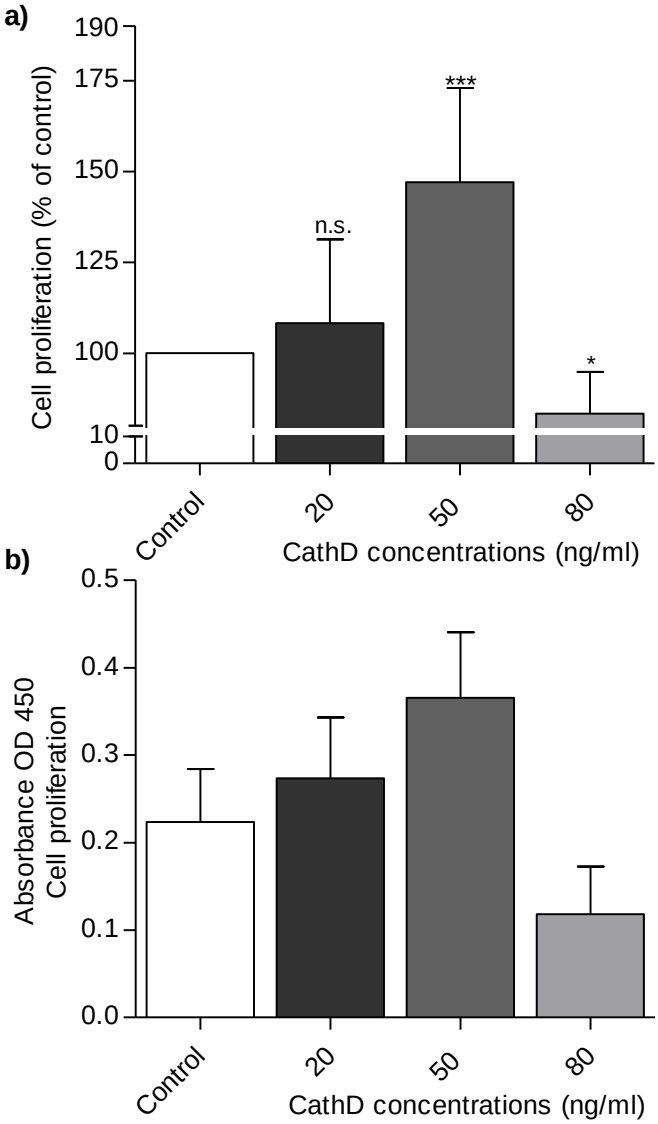

Figure 5.1: **Increased proliferation of HOMECs in media supplemented with CathD (WST-1 assay).** Cells were seeded in 2% gelatin pre-coated 96 well plates at a density of 10,000cells/well in starvation media containing 2% FCS. After overnight incubation, cells were treated with or without various concentrations of CathD and incubated for 72 hours. A commercially available WST-1 kit was used to assess cellular proliferation based on absorbance using a PHERAstar BMG plate-reader at 450nm. **a)** Results are mean ±SD and shown as percentage of the control, n.s., *p<0.05, ***p<0.001 vs control (100%), n=5-20. **b)** Raw data from representative experiment. n.s. denotes not significant.

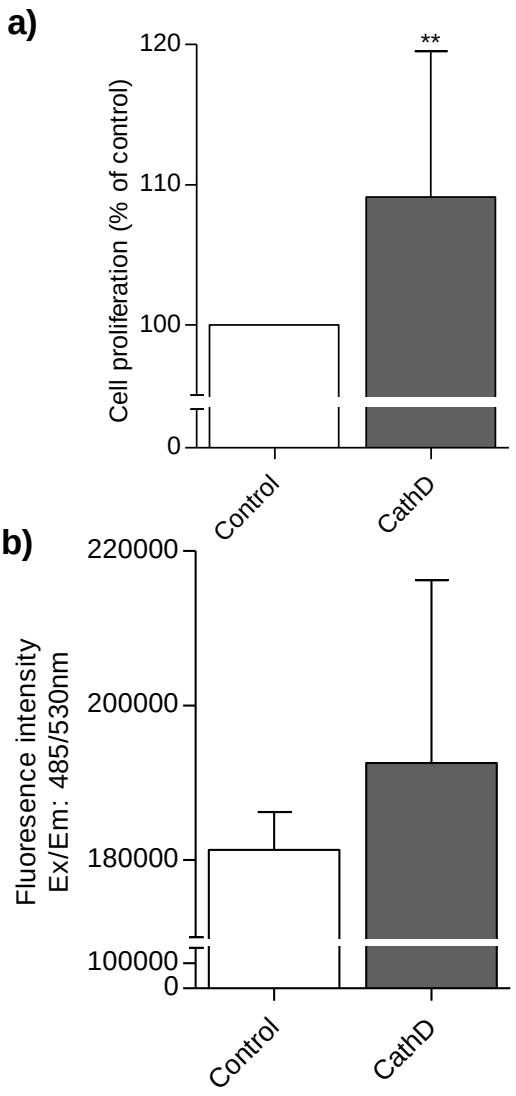

Figure 5.2: **Increased proliferation of HOMECs in media supplemented with CathD (CyQUANT).** Cells were seeded in 2% gelatin pre-coated 96 well plates at a density of 10,000cells/well in starvation media containing 2% FCS. After overnight incubation, cells were treated with or without 50ng/ml of CathD and incubated for 72 hours. A commercially available CyQUANT reagent was used to assess cell proliferation based on fluorescence intensity using a FLUOstar BMG plate-reader at Ex/Em: 485/530nm. **a)** Results are mean ±SD and shown as percentage of the control, **p<0.01, ***p<0.001 vs control (100%), n=20. **b)** Raw data from representative experiment.

5.3.2 CathD induces HOMECs proliferation in a non-proteolytic manner

CathD is an aspartic protease that resides in the lysosomes and therefore functions at acidic pHs between pH 3.5 and 4.5. Since CathD was found to be secreted by EOC cells and has now been shown to be proangiogenic, it was important to investigate whether CathD is acting in a proteolytic or non-proteolytic mechanism in HOMECs. Initially, CathD-induced cell proliferation was tested in the presence of pepA, an inhibitor of CathD proteolytic activity, at increasing concentrations over 24, 48 and 72 hours. The data demonstrated that pepA did not inhibit CathD-induced HOMEC proliferation at any concentration at any time point (Figure 5.3a, b, c; Table 5.1). Figure 5.3 b, d and f indicated that pepA-alone treatment did not induce toxicity or significantly alter proliferation in HOMECs over 24, 48 and 72 hour incubation.

The above data demonstrated that pepA did not inhibit CathD-induced HOMEC proliferation. These data suggested that either CathD is proteolytically active in these conditions and pepA does not act as an inhibitor or that CathD is acting via non-proteolytic mechanisms. Thus, this was investigated further. Initially, the pH of the cell culture media was tested over 24, 48 and 72 hours to confirm that the pH of the media remains unchanged overtime. In the presence of CathD, the pH of the basal media was initially 7.34 and did not reach a lower pH than 7.12 in all conditions tested over time (Table 5.2). Next, CathD's proteolytic activity at a range of pHs and the ability of the inhibitor to inhibit enzyme action at each pH was examined. Enzyme activity was tested using a CathD specific fluorogenic substrate Mca-Gly-Lys-Pro-Ile-Leu-Phe-Phe-Arg-Leu-Lys(Dnp)-D-Arg-NH2 (100 nM) and in the presence or absence of pepA (1 µM, concentration which was previously shown to not effect cell proliferation, (Figure 5.3; Table 5.1)). The experiment demonstrated that CathD was highly active at its optimum pH 3.6 to pH 4 (Figure 5.4a), with a gradual reduction in its proteolytic activity from pH 4.6 to 5.6. It was found that CathD was completely inactive above pH 6 to pH 7.6, including the pH of the culture media (Figure 5.4a). CathD was also inactive in the presence of pepA. PepA completely abolished enzymatic action at all pHs at which CathD demonstrated proteolytic activity i.e. pH 3.6 to pH 5.6 (Figure 5.4b). Figure 5.4c represents a summary of the proteolytic activity of CathD at pH 4 and

7 in the absence or presence of pepA. These combined data suggest that in cell culture media CathD is proteolytically inactive and induces HOMEC proliferation via an unknown non-proteolytic mechanism, possibly by acting as an extracellular ligand. Thus possible downstream signalling pathways were investigated.

5.3.3 Activation of intracellular signalling kinases in CathD-treated HOMECs

The induction of cell proliferation has been shown to involve activation of several intracellular signalling pathways including MAPK/ERK1/2 and PI3/AKT kinases (discussed in Chapter 3, Section 3.4). Since CathD induced proliferation, signalling cascades activated in CathD-treated HOMECs were examined. Initially, a commercially available proteome profiler was used to detect activation and phosphorylation of 43 kinases. It was found that after 4 minutes treatment CathD increased phosphorylation of p38-α, ERK1/2 and AKT (S473) by ~5-, 2.5- and 3-fold respectively, compared to control (Figure 5.5). The spots for ERK1/2 and AKT are shown in figure 2.2 (Chapter 2, Section 2.7.2). As for CathL (Chapter 3, Section 3.3.3), the ERK1/2 and AKT pathways were selected for further investigation as these two kinases have been shown to be significantly involved in cell proliferation, survival and cell migration in tumour angiogenesis.

The proteome profiler data was confirmed using commercially available cell-based ELISAs. CathD significantly induced ERK1/2 phosphorylation in HOMECs (>2-fold compared to control), similar to positive control VEGF (>2-fold compared to control), after 4 minutes treatment (Figure 5.6a). However, after 10 minutes treatment, levels of phosphorylated ERK1/2 reduced to the basal level (Figure 5.6b). Similar experiments were performed with AKT where AKT phosphorylation was induced (~1.6-fold compared to control) at 4 minutes after treatment (Figure 5.6c) and was back down to basal level after 10 minutes (Figure 5.6d). VEGF was used as positive control in all cell-based ELISAs.

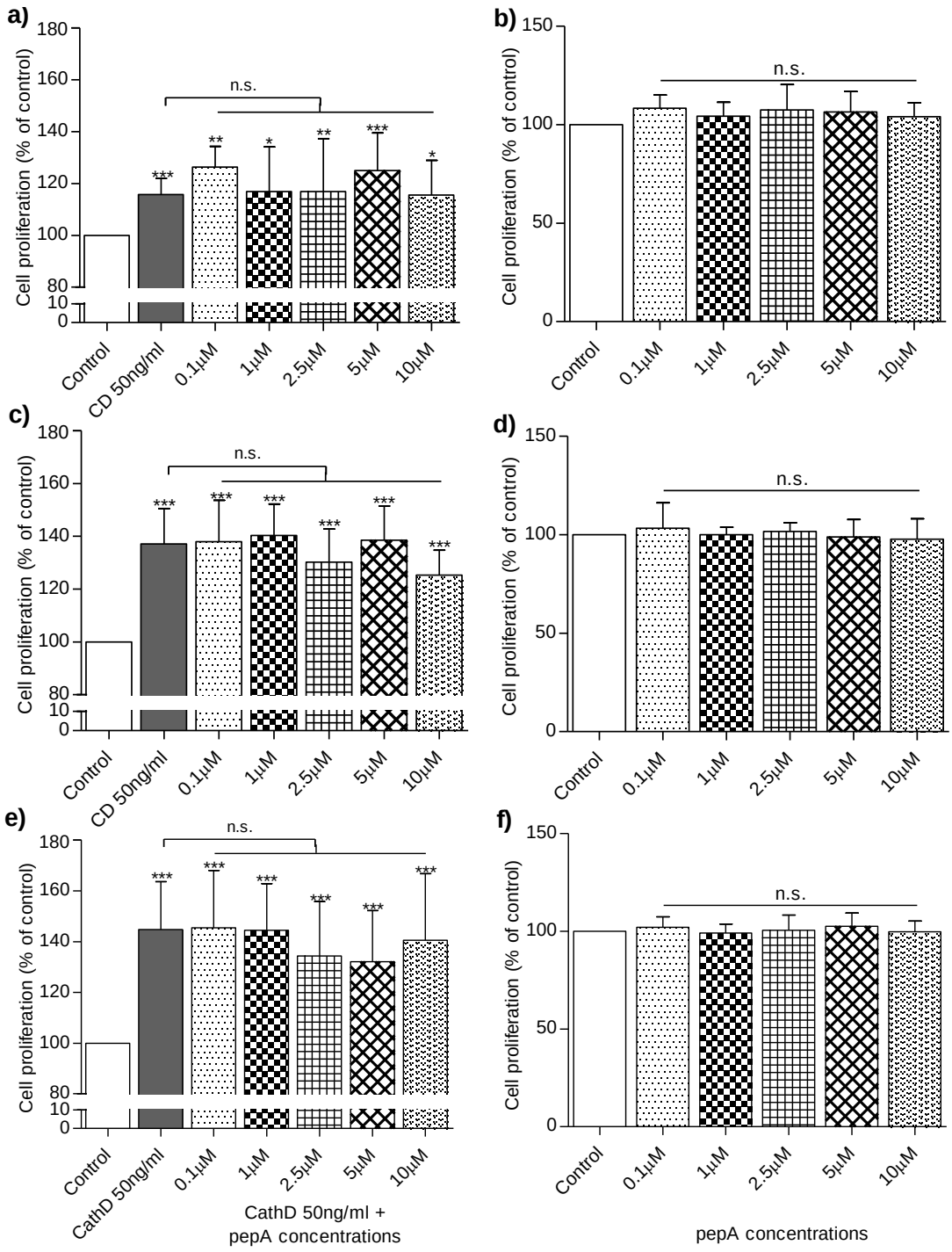

Figure 5.3: **PepA, an inhibitor of CathD proteolytic activity, does not inhibit CathD-induced HOMEC proliferation.** Cells were seeded in 2% gelatin pre-coated 96 well plates at a density of 10,000cells/well in starvation media containing 2% FCS. After overnight incubation, cells were treated with or without CathD (50ng/ml) in the presence or absence of various concentrations of pepA (as shown above- CathD + pepA a), c), e) or pepA alone b), d), f)) and incubated for **a), b)** 24, **c), d)** 48 and **e), f)** 72 hours. WST-1 assay was used to assess cellular proliferation based on absorbance using a PHERAstar BMG plate-reader at 450nm. Control wells contained 0.1% DMSO (carrier only). Results are mean ±SD and shown as percentage of the control, n.s., *p<0.05., **p<0.01, ***p<0.001 vs control (100%); n.s., ###p<0.001 vs CathD (expressed as % of control), n=8-16. n.s. denotes not significant.

Table 5.1: **Summary of effects of pepstatin A (pepA) on CathD-induced proliferation in HOMECs (shown in figure 5.3).** HOMECs were treated with or without CathD (50ng/ml) and in the presence or absence of increasing concentrations of pepA for 24, 48 and 72 hours. Results are mean ±SD and shown as percentage of control (100%). n.s. vs CathD (expressed as % of control), n=8-16. n.s. denotes not significant.

			CathD+ PepA (% of control)				
	Control (%)	CathD (% of control) (50ng/ml)	0.1 µM (n.s.)	1 µM (n.s.)	2.5 µM (n.s.)	5 µM (n.s.)	10 µM (n.s.)
24h	100	115.9±6.1	126.3±8.0	117.0±17.2	117.0±20.3	125.0±14.5	115.7±13.3
48h	100	137.1±13.4	138.0±15.7	140.3±11.9	130.2±12.6	138.5±13.0	125.3±9.5
72h	100	144.8±18.9	145.4±22.7	144.4±18.5	134.4±21.4	132.1±20.2	140.6±26.2

Table 5.2: **pH of cell culture media and supernatant overtime.** Cells were seeded in 6 well plates and treated with or without CathD (50ng/ml) for 24, 48 and 72 hours. Media were collected and their pH was measured by using Blood-gas analyser ABL800 flex. The pH of basal MV2 (starvation media) was analysed at 0 hour. n.d. denotes not determined.

	pH			
	0h	24h	48h	72h
Basal MV2	7.34	n.d.	n.d.	n.d.
Control	n.d.	7.19	7.13	7.12
CathD	n.d.	7.21	7.13	7.12

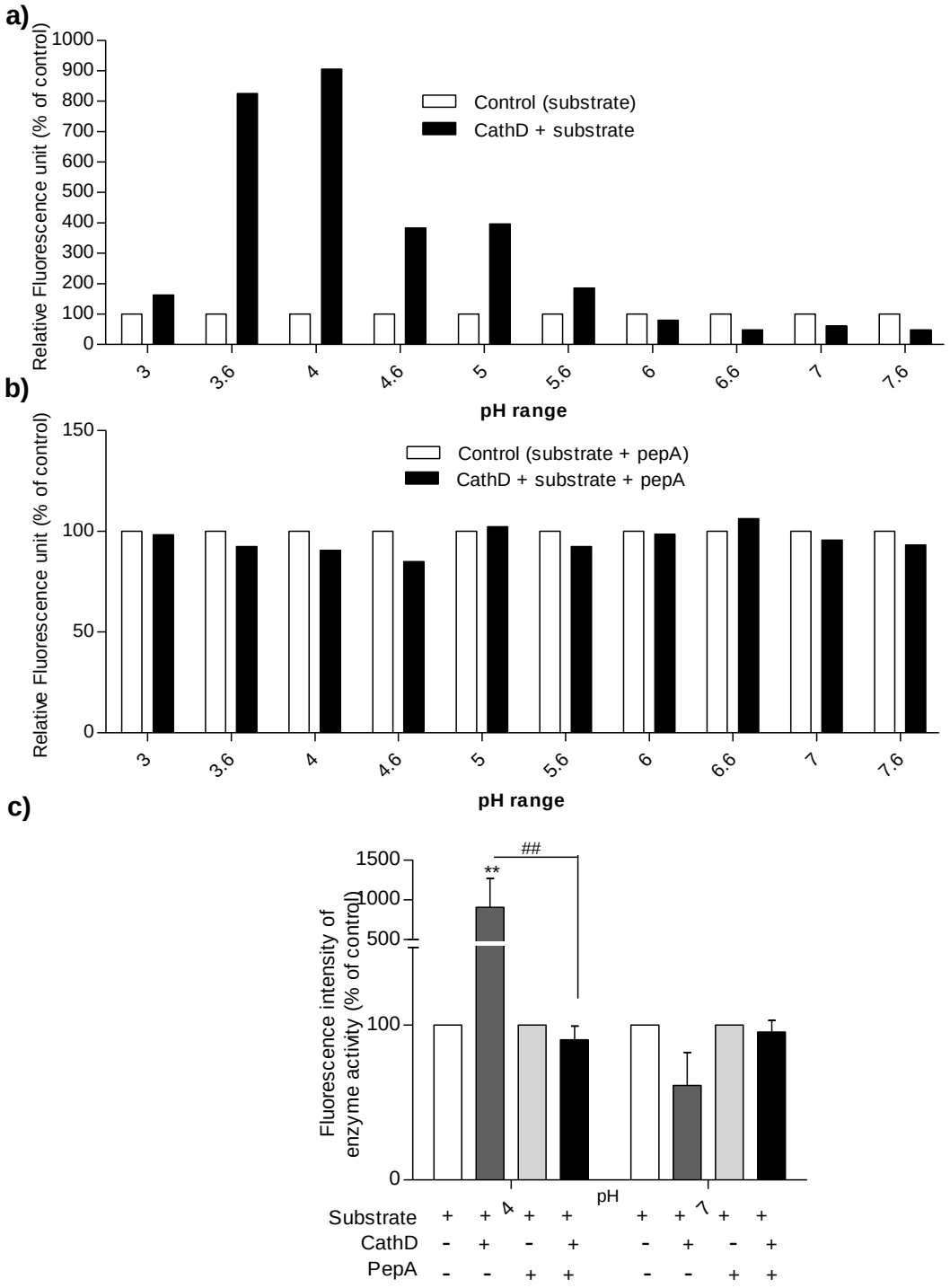

Figure 5.4: **CathD proteolytic activity is inhibited at an array of pHs by pepA, an inhibitor of CathD proteolytic activity.** A specific fluorogenic substrate (100 nM) was incubated with or without CathD (50ng/ml) and in the **a)** absence or **b)** presence of pepA (1 µM). **c)** A summary of data at pH 4 and 7 with or without CathD and in the presence of the substrate ± pepA. Fluorescence signals were measured immediately using a SpectraMax plate reader at Ex/Em: 320/393. Control wells contained pH buffer and substrate and/or inhibitor. The data are represented as percentage of control. **p<0.01 vs control (substrate) (100%); ##p<0.01 vs CathD+substrate (expressed as % of control), n=3. **a)** and **b)** Representative data from 1 of 3 independent experiments.

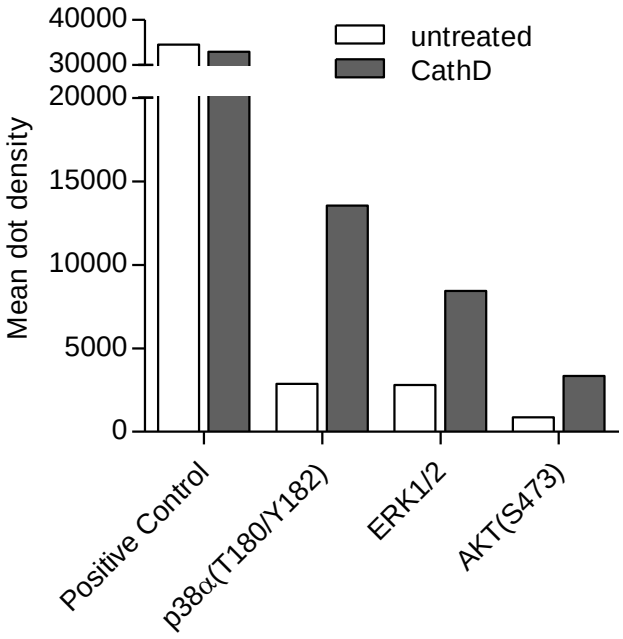

Figure 5.5: **CathD induces phosphorylation of p38α, ERK1/2 and AKT(S473) in HOMECs.** Phosphorylation statuses of the intracellular kinases were assessed in cell lysates from cells treated with or without CathD for 4 minutes. The results of 1 minute exposure are expressed as mean dot density (arbitrary units). The relative expression of specific phosphorylated proteins was determined following quantification of scanned images. A combination of 2 cell batches were used in this experiment. n= 2 (n=1).

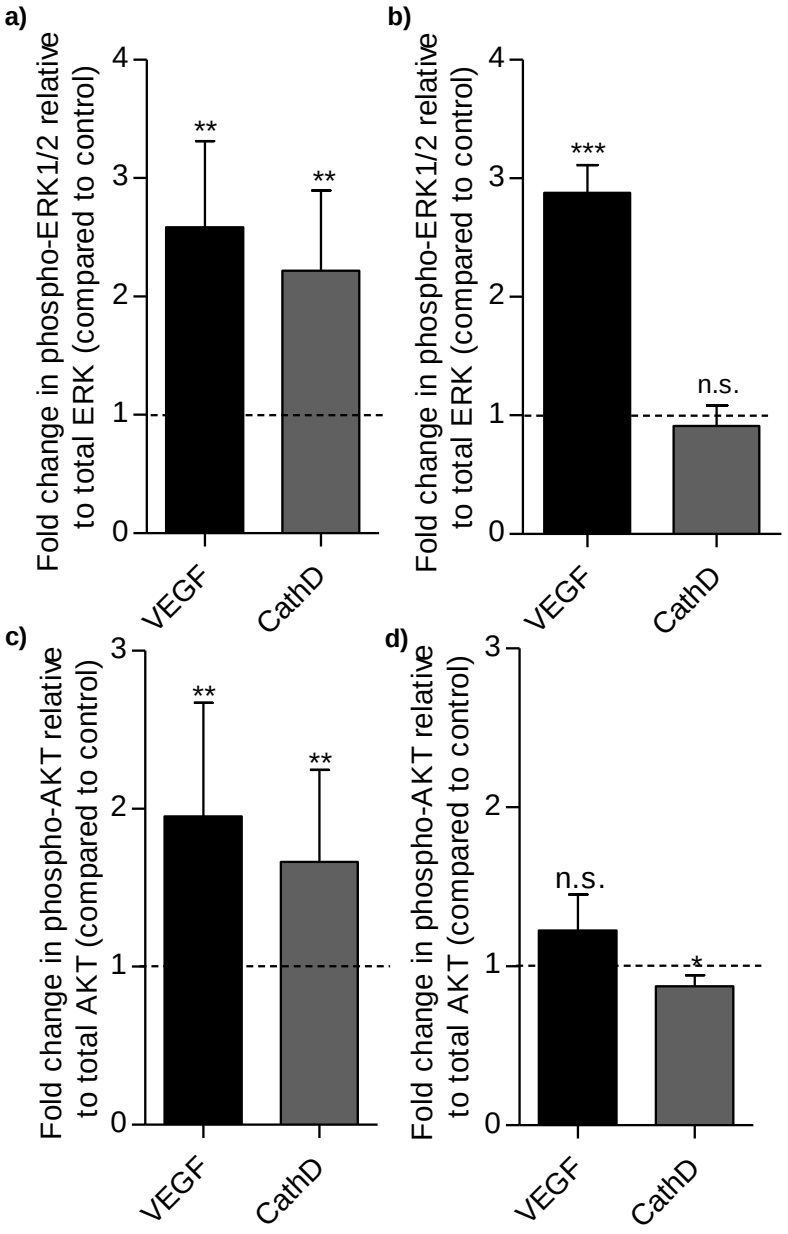

Figure 5.6: **CathD induces phosphorylation of ERK1/2 and AKT in HOMECs.** Cells were seeded in 2% gelatin pre-coated 96 well plates at a density of 10,000cells/well in starvation media containing 2% FCS. After overnight incubation, cells were treated with or without 50ng/ml of CathD or 20ng/ml of VEGF (positive control) and incubated for 4 or 10 minutes. ERK1/2 (a, b) and AKT (c, d) phosphorylation was examined after 4 minutes (a, c) and 10 minutes (b, d) treatments. Commercially available cell-based ELISAs were used for the determination ERK1/2 and AKT(S473) phosphorylation level. The ELISA experiments were carried out on two cell batches. The data is represented by fold change in phosho-ERK1/2/AKT relative to total ERK1/2/AKT (compared to control). Results are mean ±SD, n.s., *p<0.05, **p<0.01, ***p<0.001 vs control (dotted lines); n=4-6. n.s. denotes not significant.

5.3.4 CathD-induced HOMEC proliferation is mediated via the ERK1/2 pathway

Since CathD induces activation of the pro-proliferative kinase ERK1/2, it was hypothesised that ERK1/2 might be involved in the downstream signalling cascade in the induction of HOMEC proliferation and experiments were carried out to test this. Following initial toxicity assays using the ERK1/2 inhibitors U0126 and PD98059 (Figure 3.7, Chapter 3), the concentrations that were selected for further experiments were 1, 10 and 25 µM for both inhibitors. CathD-induced HOMEC proliferation was reduced significantly in the presence of all inhibitor concentrations compared to CathD treatment alone at 72 hour after incubation. For instance, at 1, 10 and 25 µM of U0126, cell proliferation decreased to 84.7±11.3% (n= 8; Figure 5.7a), 103.1±8.8% (n=8; Figure 5.7b) and 79.3±9.2% (n= 8; Figure 5.7c) respectively compared to CathD (140.6±17.9%, n=20), where both were expressed as percentage of control. In the case of PD98059, inhibition of proliferation was as follows: 122.2±6.1% (n= 8; Figure 5.7d), 101.4±6.2% (n= 8; Figure 5.7e) and 74.2±4.8 (n= 8; Figure 5.7f) at concentrations 1, 10 and 25 µM respectively, compared to CathD treatment alone (139.2±18.3%, n= 21), both were normalised to control. The inhibitors at all concentrations also reduced HOMEC proliferation at 72 hours in the absence of CathD (Figure 5.7).

As discussed in Chapter 3 (Section 3.3.4), the concentrations that were selected for further investigations were: 10 µM for U0126 and 25 µM for PD98059. At these concentrations of ERK1/2 inhibitors, CathD-induced HOMEC proliferation was significantly reduced compared to CathD treatment alone. A cell-based ELISA kit was performed to confirm the inhibitory effects of these inhibitors on cellular levels of phosphorylated ERK1/2. The data showed that CathD induced phosphorylation of ERK1/2 was abolished or reduced to 0.8-fold and 0.3-fold in HOMECs in the presence of U0126 (Figure 5.8a) and PD98059 (Figure 5.8b) respectively, compared to CathD treatment (1.6-fold). Together, these data suggest that CathD may induce HOMEC proliferation via activation of the ERK1/2 pathway.

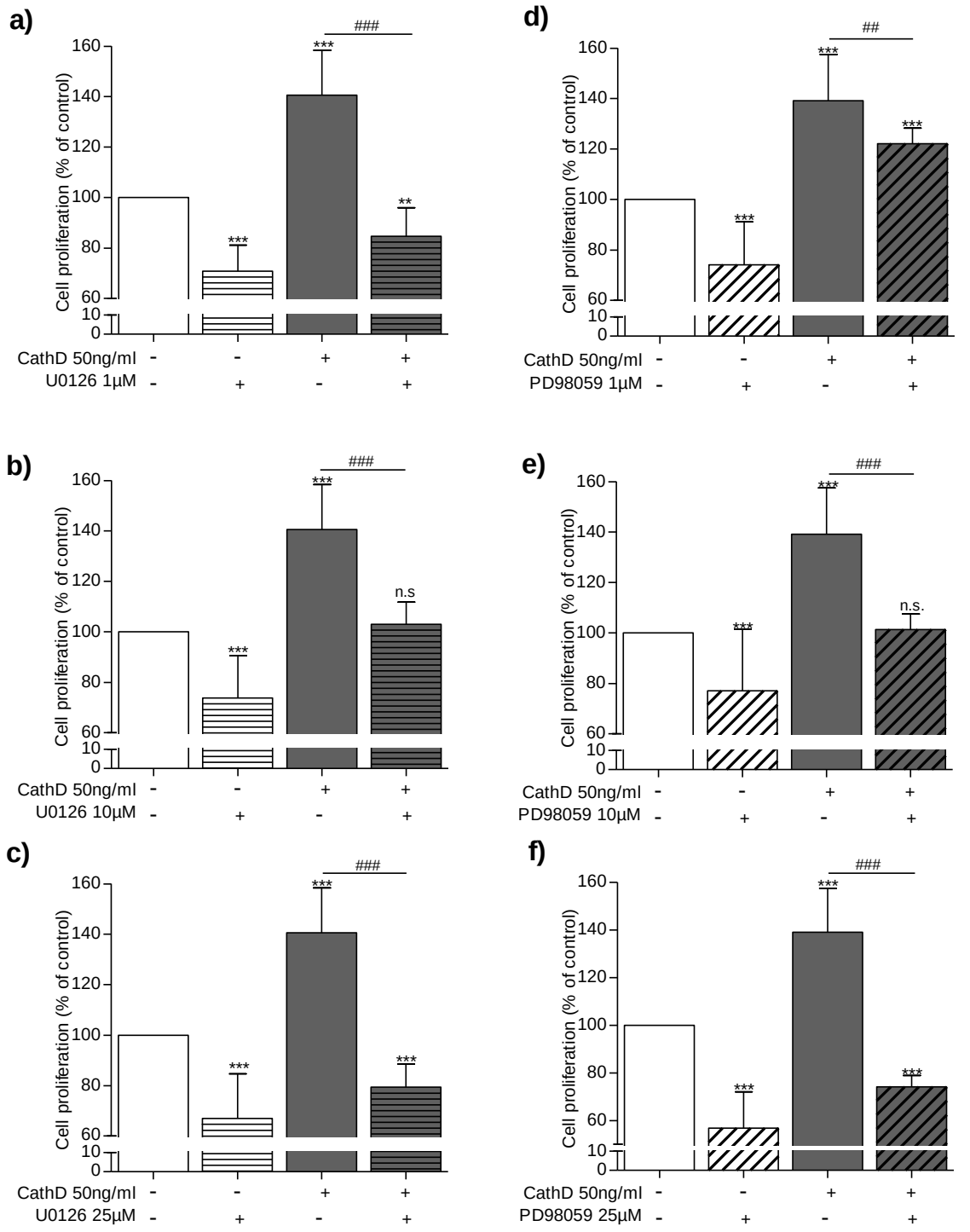

Figure 5.7: **Inhibition of ERK1/2 reduces CathD-induced HOMEC proliferation.** Cells were seeded in 2% gelatin pre-coated 96 well plates at a density of 10,000cells/well in starvation media containing 2% FCS. After overnight incubation, cells were treated with or without CathD (50ng/ml) and in the absence or presence of various concentrations of **a-c)** U0126 and **d-f)** PD98059 as indicated above and incubated for 72 hours. WST-1 assay was used to assess cellular proliferation. Results are mean ±SD and shown as percentage of the control, n.s., **p<0.01, ***p<0.001 vs control (100%), ##p<0.01, ###p<0.001 vs CathD (normalised to control 100%), n=7-13. n.s. denotes not significant.

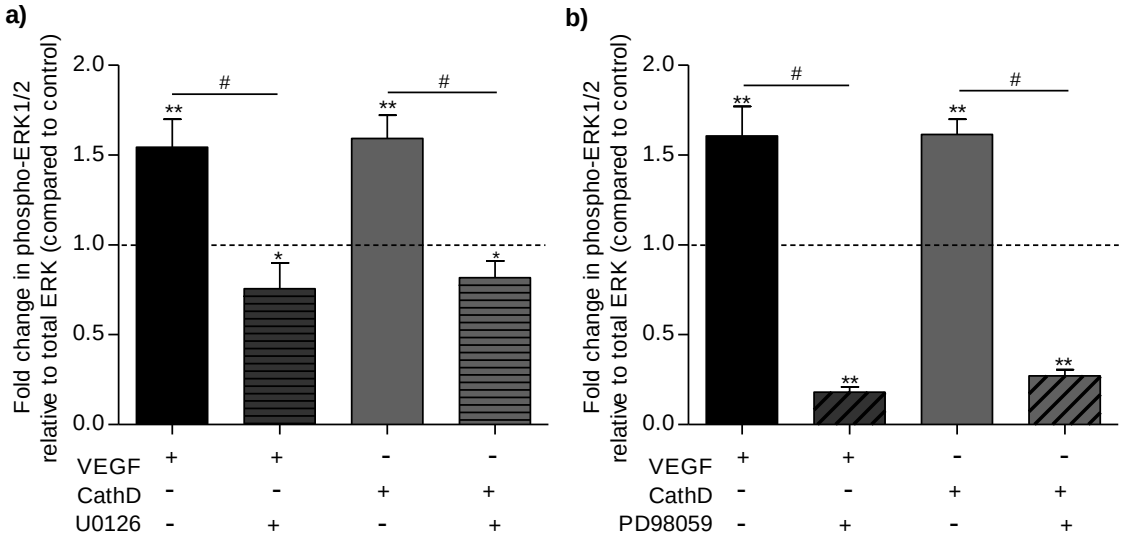

Figure 5.8: **CathD-induced ERK1/2 phosphorylation is inhibited in intact HOMECs treated with ERK1/2 inhibitors a) U0126 (10 µM) and b) PD98059 (25 µM)**. Cells were seeded in 2% gelatin pre-coated 96 well plates at a density of 10,000cells/well in starvation media containing 2% FCS. After overnight incubation, cells were pre-incubated with the inhibitors for 20-30 minutes, and then co-treated with or without 50ng/ml of CathD or 20ng/ml of VEGF in the absence or presence of the inhibitors for 4 minutes. Commercially available cell-based ELISAs were used for determination of ERK1/2 phosphorylation level. The data is represented as fold change in phosho-ERK1/2 relative to total ERK1/2 (compared to control). Results are mean ±SD, *p<0.05, **p<0.01 vs control (1-fold), #p<0.05 vs VEGF/CathD (normalised to control), n=4. The dotted lines represent basal level (control) of phosphorylation status in untreated HOMECs.

5.3.5 CathD-induced HOMEC proliferation is mediated via PI3K and not AKT activation

The PI3K/AKT signalling pathway plays a critical role in mediating survival signals in a wide range of cell types. Further to the data described and discussed in Chapter 3, the role of AKT was assessed in CathD-induced HOMEC proliferation using the PI3K inhibitor LY294002 (1, 25 and 50 µM) and AKT inhibitor MK2206 (1, 3 and 5 µM). Interestingly, although at 1 µM (157.6±12.0%, n=10; Figure 5.9a) there was no significant reduction in CathD-induced cell proliferation compared to CathD treatment alone (146.9±9.9%, n=10), LY294002 significantly reduced cell proliferation in a dose-dependent manner from 25 µM. For instance, cell proliferation at 25 µM and 50 µM of LY294002 were 108.9±7.6% (n=10; Figure 5.9b) and 78.7±3.9% (n=10; Figure 5.9c) respectively, compared to CathD treatment alone (146.9±9.9%, n=10), all expressed as percentage of control. Intriguingly, cell proliferation significantly increased in the presence of MK2206 at all concentrations. For example, cell proliferation at 1, 3 and 5 µM were 139.6±7.8% (n=6; Figure 5.9d), 144.0±7.1% (n=7; Figure 5.9e) and 140.3±8.9 (n=10; Figure 5.9f) respectively, compared to CathD treatment (130.3±7.9%, n=9), all expressed as percentage of control. Data from control wells for LY294002 demonstrated a significant reduction in cell proliferation over a 72 hour period (Figure 5.9 a, b, c). Interestingly, MK2206 did not show any reduction, rather a significant increase in proliferation was observed across all three concentrations (Figure 5.9 d, e, f). These data suggest that, similarly to CathL, CathD induces HOMEC proliferation by activating the PI3K pathway, but in an AKT-independent mechanism since the AKT-specific inhibitor did not reduce cell growth.

As discussed in Chapter 3 (Section 3.3.5), the concentrations that were selected for further investigation were: 25 µM for LY294002 and 5 µM for MK2206. The ELISA data with LY294002 and MK2206 confirmed that both drugs completely inhibit CathD-induced phosphorylation of AKT in intact HOMECs. In the presence of LY294002, CathD-induced levels of phosphorylated AKT reduced from ~1.7-fold to 0.4-fold (Figure 5.10a). In the case of MK2206, levels of phosphorylated AKT decreased from 1.6-fold to 0.5-fold (Figure 5.10b). This suggests that both drugs inhibit the PI3K/AKT pathway in HOMECs. However, a lack of inhibition in

cell proliferation suggests that activated PI3K, but not AKT(S473) is involved in the induction of CathD-mediated HOMEC proliferation.

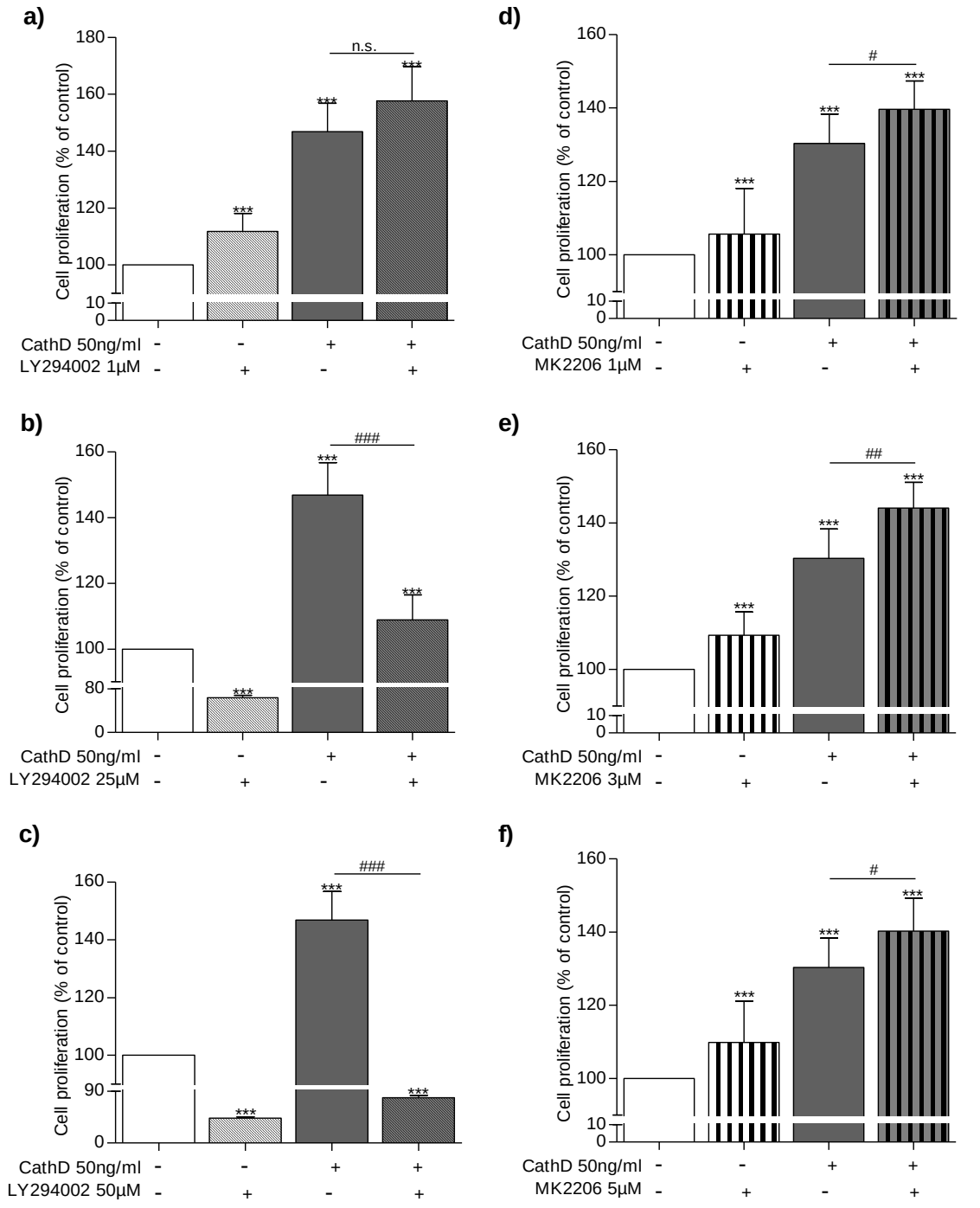

Figure 5.9: **PI3K inhibitor, but not AKT inhibitor, reduces CathD-induced HOMEC proliferation.** Cells were seeded in 2% gelatin pre-coated 96 well plates at a density of 10,000cells/well in starvation media containing 2% FCS. After overnight incubation, cells were treated with or without CathD (50ng/ml) and in the absence or presence of various concentrations of **a-c)** LY294002 (PI3K inhibitor) and **d-f)** MK2206 (AKT inhibitor) as indicated above and incubated for 72 hours. WST-1 assay was used to assess cellular proliferation. Results are mean ±SD and shown as percentage of the control, ***p<0.001 vs control (100%), n.s., #p<0.05, ##p<0.01, ###p<0.001 vs CathD, n=10-15 (normalised to control 100%). n.s. denotes not significant.

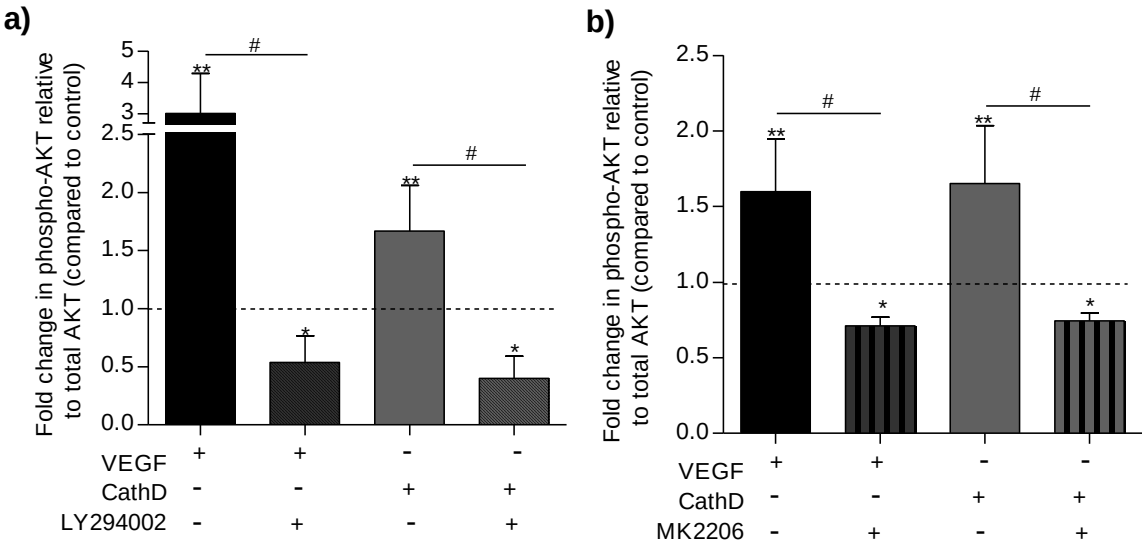

Figure 5.10: **CathD-induced AKT phosphorylation is inhibited in HOMECs treated with PI3K and AKT inhibitors a) LY294002 (25 µM) and b) MK2206 (5 µM)**, respectively. Cells were seeded in 2% gelatin pre-coated 96 well plates at a density of 10,000cells/well in starvation media containing 2% FCS. After overnight incubation, cells were pre-incubated with the inhibitors for 2.5 hours, and then co-treated with or without 50ng/ml of CathD or 20ng/ml of VEGF in the absence or presence of the inhibitors for 4 minutes. Commercially available cell-based ELISAs were used for determination of the levels of AKT phosphorylation. The ELISA experiments were carried out on two cell batches. The data is represented by fold change in phosho-AKT relative to total AKT (compared to control). Results are mean ±SD, *p<0.05, **p<0.01 vs control (1–fold), #p<0.05 vs VEGF/CathD (normalised to control), n=4. The dotted lines represent basal level (control) of phosphorylation status in untreated HOMECs.

5.3.6 CathD induces HOMEC migration via both the ERK1/2 and AKT pathways

A key component of angiogenesis is EC migration. Previous data suggested that CathD induces migration in HOMECs. However, the intracellular signalling mechanisms have not been examined. Also, previously, HOMEC migration was tested using Oris migration assay kit and as discussed in Chapter 3 (section 3.4) this was replaced by a Cultrex transwell migration Boyden chamber kit, with a reduction in incubation time from 48 hours to 6 hours. Therefore, initially, cell migration was tested using this system after 6 hour treatment with CathD, and it was revealed that CathD (174.9±52.9%, n= 10; Figure 5.11a) significantly induced HOMEC migration compared to control (100%). VEGF was used as positive control in cell migration experiments. This led to further investigation into the activation of potential downstream signalling pathways.

Since CathD was shown to activate the ERK1/2 and AKT pathways, their activation was examined in CathD-induced HOMEC migration. It was hypothesised that activated AKT may be involved in the induction of HOMEC migration of CathD as this role for AKT has been reported in several cell models (discussed in Chapter 3, Section 3.4). Therefore, the role of AKT in cell migration was examined in cells pre-treated with or without PI3K and AKT inhibitors and then co-treated with CathD in the absence or presence of the corresponding inhibitor for 6 hours. After 6 hour incubation, both inhibitors of PI3K and AKT kinase abolished HOMEC migration compared to CathD-treated cells. For instance, in the presence of LY294002 and MK2206, CathD-induced HOMEC migration was reduced to 92.9±46.3% (n=6; Figure 5.12a) and 105.6±45.8 (n=6; Figure 5.12b) respectively, compared to CathD treatment (180.0±65.6%, n=12), all expressed as percentage of control (100%). HOMECs treated with only LY294002 or MK2206 demonstrated a significant reduction in migration (Figure 5.12 a), b).

Cell migration was then examined in the presence of ERK1/2 inhibitors. HOMECs were pre-treated with U0126 (10 µM) or PD98059 (25 µM) and then co-treated with CathD. After 6 hour incubation, both inhibitors of ERK1/2 abolished HOMEC migration compared to CathD-treated cells. For instance, in the presence of U0126 and PD98059, CathD-induced HOMEC migration reduced to 91.8±7.9% (n=7; Figure 5.13a) and 99.2±9.9% (n=7; Figure 5.13b) respectively, compared

to CathD treatment alone (135.7±26.4%, n=12), all expressed as percentage of control (100%). U0126 treatment alone significantly reduced HOMEC migration (Figure 5.13a), however, although there was a slight reduction in migration by PD98059 alone, it was not significantly different to control (100%) (Figure 5.13b). These data combined with the ELISA data (Figure 3.9), suggest that CathD induces HOMEC migration via a pathway that requires activation of both the ERK1/2 and AKT(S473) pathways.

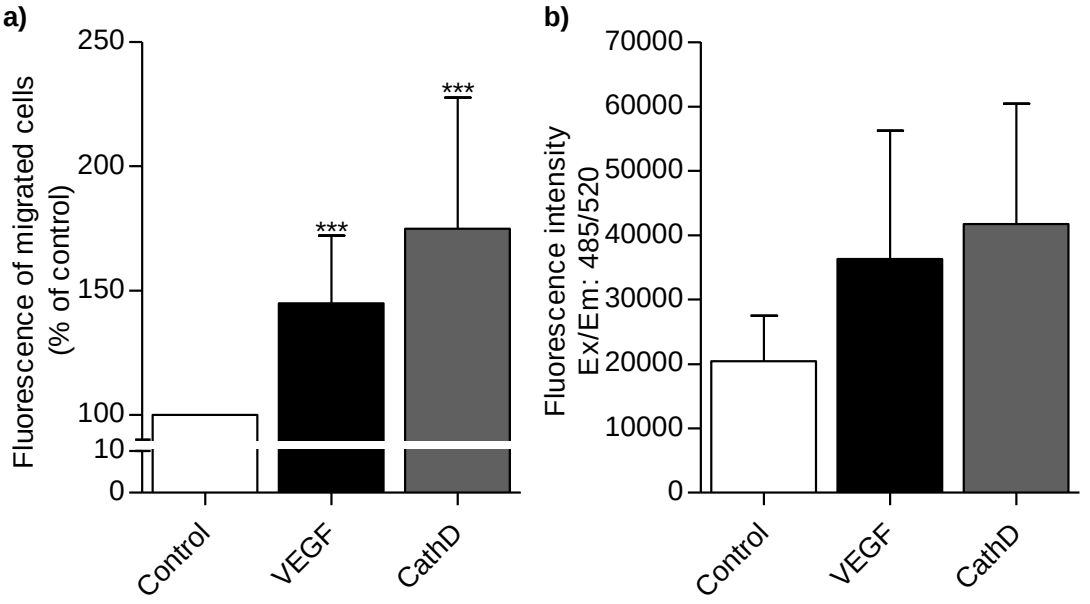

Figure 5.11: **CathD induces HOMEC migration.** HOMECs were seeded on the upper transwell insert and treated with or without CathD (50ng/ml) or VEGF (20ng/ml) supplementation of starvation media containing 0.5% FCS. The lower well contained correspondent treatment i.e. 0.5% FCS media, CathD (50ng/ml) or VEGF (20ng/ml). After 6 hours, migrated cells were stained with calcein AM and fluorescence was quantified using a FLUOstar plate reader at Ex/Em: 485/520. **a)** Results are mean ±SD and shown as percentage of the control, ***p<0.001 vs control (100%), n=10-15, **b)** Raw data from representative experiment.

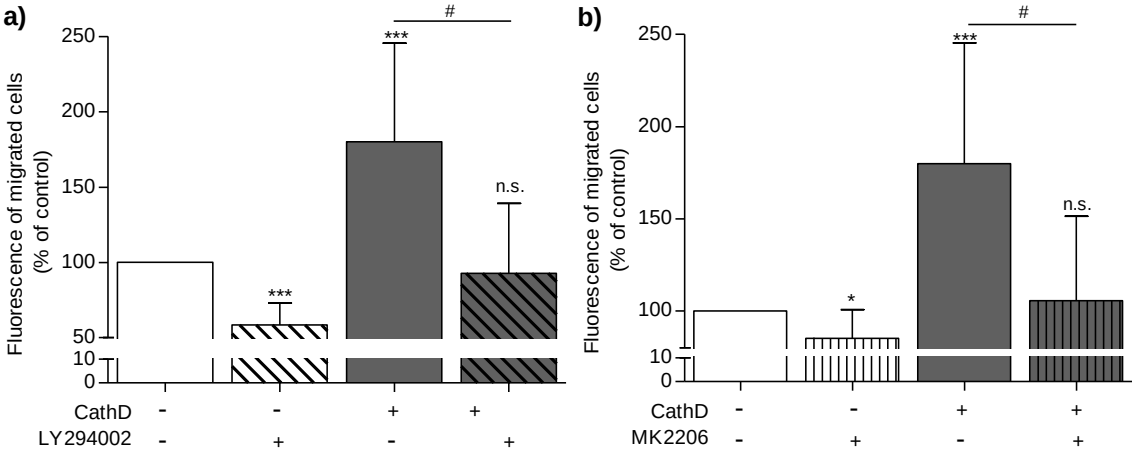

Figure 5.12: **CathD induces HOMEC migration via activation of the AKT pathway.** HOMECs were seeded in the upper transwell chamber and treated with or without CathD (50ng/ml) in the absence or presence of PI3K and AKT inhibitors **a)** LY294002 (25 µM) and **b)** MK2206 (5 µM) respectively in media containing 0.5% FCS. The lower well contained correspondent treatments. After 6 hours, migrated cells were stained with calcein AM and fluorescence was quantified using a FLUOstar plate reader at Ex/Em: 485/520. Results are mean ±SD and shown as percentage of the control, n.s., *p<0.05 ***p<0.001 vs control (100%), #p<0.05 vs CathD (normalised to control (100%)), n=6-12. n.s. denotes not significant.

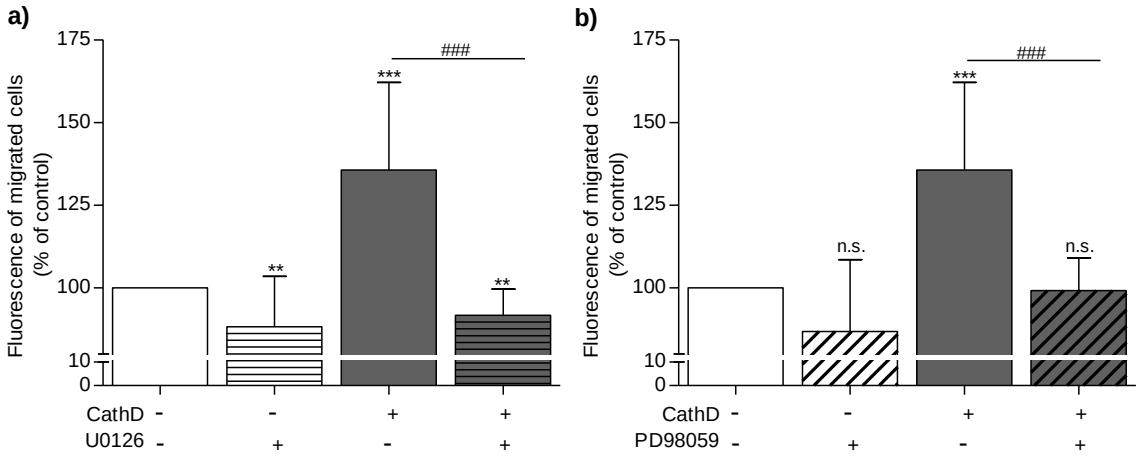

Figure 5.13: **CathD induced HOMEC migration via activation of the ERK1/2 pathway.** HOMECs were seeded in the upper transwell chamber and treated with or without CathD (50ng/ml) in the absence or presence of ERK1/2 inhibitors **a)** U0126 (10 µM) and **b)** PD98059 (25 µM) respectively in media containing 0.5% FCS. The lower well contained correspondent treatments. After 6 hours, migrated cells were stained with calcein AM and fluorescence was quantified using a FLUOstar plate reader at Ex/Em: 485/520. Results are mean ±SD and shown as percentage of the control, n.s., **p< 0.01, ***p<0.001 vs control (100%), ###p<0.001 vs CathD (normalised to control (100%)), n=6-12. n.s. denotes not significant.

5.3.7 Optimisation of 3D and 2D angiogenesis with CathD

The data described show that CathD has the potential to induce cell proliferation and migration in HOMECs, two critical steps of tumour-angiogenesis. To examine the ability of CathD to induce angiogenesis in HOMECs, a 3D *in vitro* model was established as described in Chapter 2 (Section 2.8) and Chapter 3 (section 3.3.7). As for CathL, initially, HCMECs were used to establish the model with different treatments: media supplemented with 2% FCS as basal control (Figure 5.14a), media supplemented with 5% FCS and manufacturer-provided growth factors as positive control (complete growth media) (Figure 5.14b), and 2% FCS media supplemented with 20ng/ml of VEGF (Figure 5.14c) or 50ng/ml of CathD (Figure 5.14d). Cell sprouting was observed in the positive control and in CathD- and VEGF-treated wells, but not in control wells (media with 2% FCS).

However, when the same conditions were applied using HOMECs, no sprouting was observed in any of the wells (data not shown). As described in Chapter 3 (Section 3.3.7), several modifications of the fibrin gel were applied and a variant of cytodex bead was used, but no difference was observed in cell growth or sprouting under those conditions, and therefore, it was decided to test CathD-induced angiogenesis tube-formation in HOMECs using a 2D *in vitro* model.

This second assay was performed as described in Chapter 2 (Section 2.8.2.1). After overnight incubation, cells were treated with media supplemented with 2% FCS (control media), VEGF (20ng/ml; positive control) or CathD (50ng/ml). At 72 hours after treatment, a complete monolayer formed in the control and VEGF-treated wells (data not shown). As for CathL, 2D assay based on the use of a fibrin matrix appeared to be a poor model to study CathD-induced angiogenesis in HOMECs. Therefore, commercially available growth factor-reduced (GFR) Matrigel was chosen to carry out further investigation on HOMECs angiogenesis.

Initially, cells were seeded on the Matrigel and treated 2 hours later with or without CathD and positive control VEGF for another 6 hours. After 6 hour incubation, it was found that although CathD induced an increase in tube formation, it was not significantly different (185.7±19.1, n=3; Figure 5.15) compared to control (145±15). This may be because with n= 3, there is not enough power to detect a significant difference and this may be worth investigating further. Positive control

VEGF significantly increased tube formation in HOMECs (210.3±22.4 vs control, n=3; Figure 5.15).

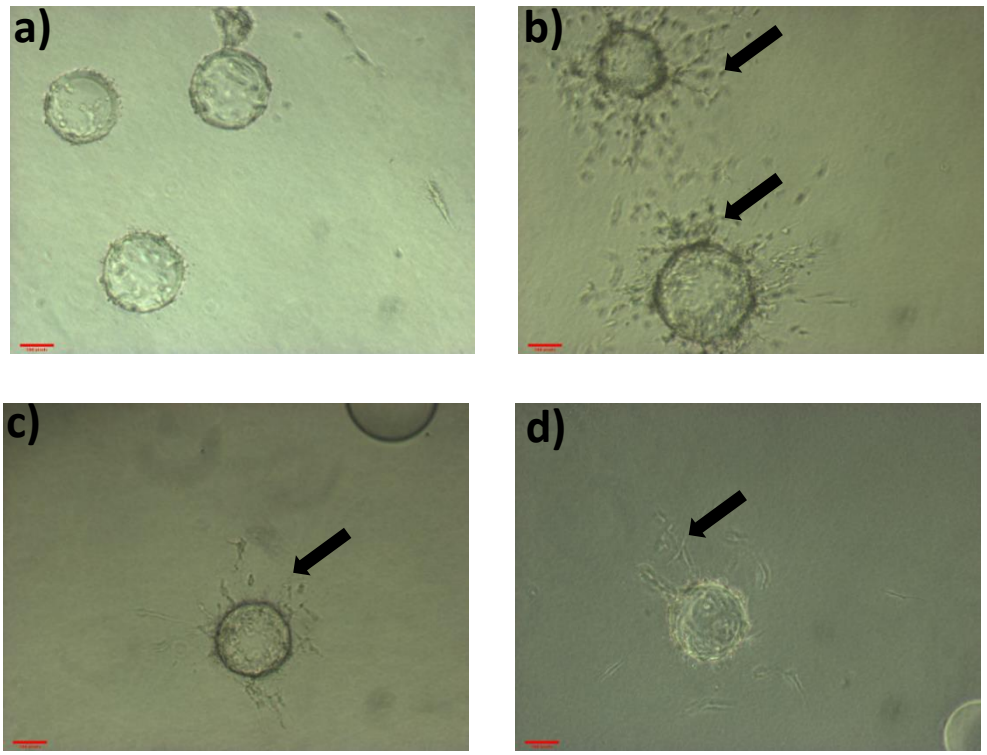

Figure 5.14: **Formation of angiogenic sprout in human cerebral microvascular endothelial cells (HCMECs) in 3D fibrin gel.** Cells were seeded on cytodex 3 microcarriers and embedded in fibrin matrix gel in media supplemented with 2% FCS **a)** Control, **b)** 5% FCS with added ECs growth factors (positive control), **c)** 20ng/ml of VEGF or **d)** 50ng/ml of CathD. Media/treatments were replaced every other day up to day 5. Photographs were taken on day 6 post-seeding using a Nikon phase-contrast microscope at 10X magnification. Arrow pointing to cell sprouting. Scale bar =100μM.

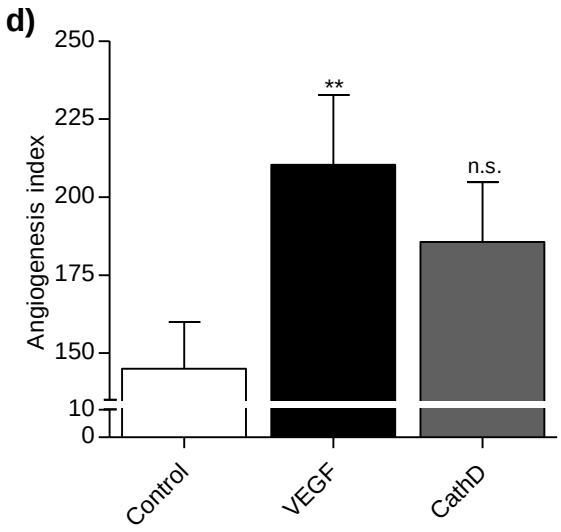

Figure 5.15: **CathD-induced tubule structure formation in HOMECs in 2D Matrigel.** HOMECs were plated onto growth factor reduced- (GFR) Matrigel in medium containing 2% FCS and treated with media supplemented with VEGF (20ng/ml) and/or CathD (50ng/ml) for 6 hours. Control wells contained HOMECs grown in medium containing 2% FCS alone. Photographs were taken at 6 hours after treatment using a Nikon phase contrast microscope camera and tubule-structure formation (including nascent tubule structures) was quantified as described in the method Section. The results are presented as an angiogenesis index, n.s., **p<0.01 vs control levels, n=3. n.s. denotes not significant.

5.3.8 Investigation of potential RTKs activated by CathD

Since CathD has been shown to induce proangiogenic changes in HOMECs via activation of ERK1/2 and AKT in a non-proteolytic manner, it is possible that the protein acts via an extracellular receptor. The possibility that CathD acts via a known tyrosine kinase receptor was investigated using a commercially available kit. After 10 minutes treatment with or without CathD or VEGF (positive control), it was found that CathD induced 4-fold activation of c-Ret (RET proto-oncogene) RTK compared to control (Figure 5.16). VEGF induced a 5-fold activation of this RTK in HOMECs. The results also revealed that VEGF strongly activated VEGFR2 as expected and slightly activated VEGFR3.

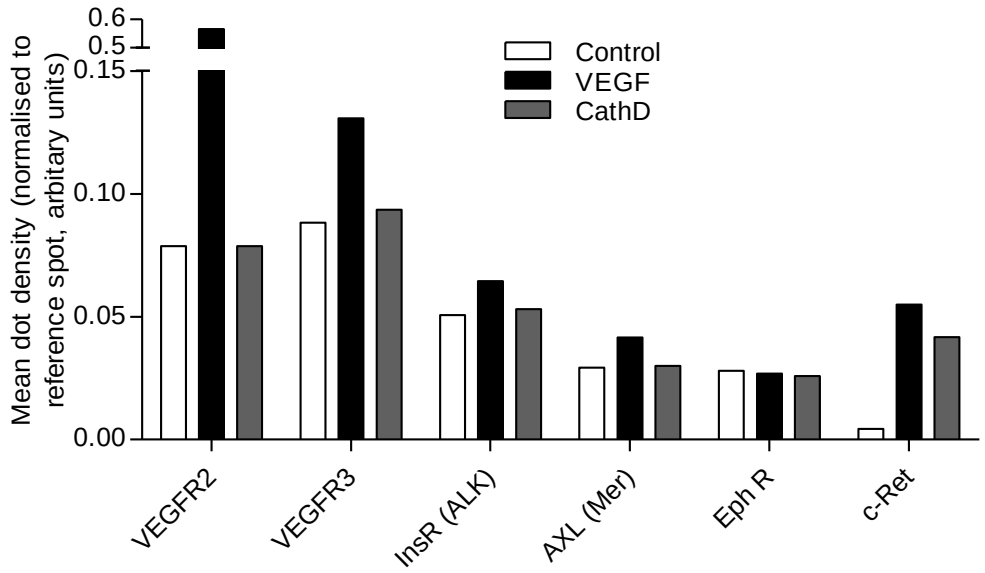

Figure 5.16: **CathD induces phosphorylation of RTK c-RET in HOMECs.** Phosphorylation statuses of RTKs were assessed in cell lysates treated with or without CathD or VEGF for 10 minutes. The results of 1 minute exposure are expressed as mean dot density. The relative expression of specific phosphorylated proteins was determined following quantification of scanned images of membrane using Azure software. n=1.

5.4 Discussion

In this Chapter CathD was shown to induce HOMEC proliferation via a non-proteolytic mechanism. Additionally, CathD was also observed to induce phosphorylation of ERK1/2, AKT and p38α in HOMECs. Studies investigating the downstream signalling involved in CathD-induced proliferation suggest that the activation of the pathway requires ERK1/2 and PI3K, but is independent of AKT phosphorylation. Interestingly, cell migration by CathD was shown to be induced via activation of both the ERK1/2 and AKT pathways. In a preliminary experiment, CathD was observed to activate c-Ret, a RTK.

CathD induced HOMEC proliferation in a non-proteolytic mechanism

Following activation by angiogenic factors secreted in the microenvironment, ECs undergo functional changes such as proliferation, migration and sprouting to make new blood vessels. Previous data suggested that CathD plays a role in inducing migration of HOMECs (Winiarski et al., 2013). However, its role in cell proliferation has not been elucidated. Therefore, in this study it was hypothesised that CathD induces HOMEC proliferation. Accordingly, WST-1 and CyQUANT assay were carried out to test for proliferation in CathD-treated cells at increasing concentrations. The results of the two independent techniques confirmed that CathD significantly induced HOMEC proliferation at 50ng/ml. The range of concentrations (20, 50 and 80ng/ml) was selected based on a concentration 58ng/ml that was detected in the peritoneal fluid of women with endometriosis (Suzumori et al., 2001). Additionally, previously a publication from our laboratory suggested that the EOC cell line SKOV3 secretes 14ng/ml in to the conditioned media. In this study, the concentration of CathD was optimised and selected to be 50ng/ml as it was within the physiological range and demonstrated a significant increase in HOMEC proliferation.

CathD has been reported to be proangiogenic in several EC and tumour cell models both *in vitro* and *in vivo* (Glondu et al., 2001, Berchem et al., 2002, Hu et al., 2008). However, its mechanism of action is not fully known. Since CathD was shown to be pro-proliferative in HOMECs, its mechanism of action was investigated. As CathD is a protease in normal physiology, it was possible that it induces HOMEC proliferation in a proteolytic manner. To investigate this further,

HOMECs were treated with CathD in the absence or presence of an increasing concentrations of pepA, an inhibitor of CathD-proteolytic activity, for 24, 48 and 72 hours. The results demonstrated that pepA did not inhibit CathD-induced HOMEC proliferation. These data primarily suggested that CathD induces HOMEC proliferation via a non-proteolytic mechanism.

PepA is a widely used potent inhibitor of CathD (Deiss et al., 1996, Hu et al., 2008). The range of concentrations of pepA (0.1, 1, 2.5, 5 and 10 μM) used in this experiment was based around its reported effective concentration (1 μM) (Farias and Manca de Nadra, 2000). The highest concentration that could be used in this experiment was 10 μM as a higher concentration would contain more than 0.1% DMSO which has been found to be toxic to HOMECs (data not shown).

Based on these data, the next set of experiments examined *in vitro* CathD-proteolytic activity at an array of pHs using a CathD-specific fluorogenic substrate. This revealed that CathD is proteolytic at its optimum pH 3.5 to 4.5, but proteolytically inactive from pH 6 up to pH 7.6, a range that includes the pH of the culture media. When added, pepA completely abolished this proteolytic activity of CathD at pHs where activity was observed. This demonstrates the validity of the inhibitor pepA in this experiment and further supports the conclusion that CathD induces HOMEC proliferation via a mechanism that is independent of its proteolytic activity.

This observation agrees with studies which have reported that the CathD-induced proangiogenic response is mediated via an as yet unknown non-proteolytic mechanism in other systems. For instance, *in vivo*, overexpression of CathD in xenografts in an athymic mice model correlated with increased vascular density (Berchem et al., 2002). The number of microvessels was significantly increased by 1.5-fold and 1.9-fold in the CathD and CathD-Asn 231(proteolytically inactive) groups respectively. This mutated version of CathD was also shown to induce proliferation of 3Y1-Ad12 rat cancer cells embedded in Matrigel or collagen 1 matrices, colony formation in soft agar and tumour growth in athymic nude mice (Berchem et al., 2002). Furthermore, Vignon *et al.* demonstrated that a precursor of CathD, pCathD, non-proteolytically induced growth of MCF7 breast cancer cells *in vitro* (Vignon et al., 1986). A significant increase in human skin CCD45K fibroblast proliferation, motility and invasive capacity was also observed to be induced by proteolytically inactive CathD (Laurent-Matha et al., 2005). Taken

together these data suggest that CathD induces proangiogenic and mitogenic responses via an unknown mechanism other than its proteolytic activity.

However, there are studies available which contest this observation. For example, Hu *et al.* reported that CathD-induced HUVEC proliferation via a proteolytic mechanism (Hu et al., 2008). CathD was also shown to be proteolytically active in inducing angiogenesis in the chick chorioallantoic membrane (CAM) model (Hu et al., 2008). These observations were completely inhibited by pepA, suggesting that CathD induces proangiogenic changes via its proteolytic mechanism. Moreover, Briozzo *et al.* demonstrated that proteolytically active CathD induced angiogenesis in MCF7 breast cancer cells by cleaving and releasing ECM-bound pro-angiogenic factor bFGF (Briozzo et al., 1991).

These reports suggest that CathD can act via a non-proteolytic or proteolytic manner to induce cellular changes. The fact that pepA does not alter CathD-induced proangiogenic changes in HOMECs and that CathD remains proteolytically inactive at cell culture media pH suggest that CathD acts via a novel proteolytic-independent mechanism to induce HOMEC proliferation. However, the exact mechanism via which CathD induces such effect should be investigated further in future experiments.

CathD-induced activation of intracellular signalling pathways and their role in cellular proliferation

As CathD induced HOMEC proliferation in a non-proteolytic manner, it was logical to assess the potential downstream intracellular signalling pathways. A proteome profiler which screens and detects levels of phosphorylated kinases revealed activation of the ERK1/2, AKT(S473) and p38α pathways. These pathways, as discussed in Chapter 3 (Section 3.4), are activated in cell survival, proliferation and migration. The ERK1/2 and AKT kinases were selected for further investigations primarily because both kinases have been shown to be involved in cell proliferation and cell migration, two critical steps of angiogenesis.

Subsequently, ELISAs were performed at two time points, 4 and 10 minutes after CathD treatment. These confirmed that CathD induced phosphorylation of both ERK1/2 and AKT 4 minutes after treatment. However, 10 minutes after treatment,

the level of phosphorylation reduced down to basal level (control), suggesting rapid and transient increase in phosphorylation in response to CathD. Interestingly, these data differed from those observed with VEGF (used as a positive control) where increases in ERK1/2 phosphorylation were sustained over 10 minutes.

Since CathD activates pro-proliferative kinases ERK1/2 and AKT, their role in CathD-induced HOMEC proliferation was examined. Firstly, two ERK1/2 inhibitors (U0126 and PD98059) were used. Both inhibitors demonstrated significant inhibition in cell proliferation compared to CathD treatment alone, suggesting that ERK1/2 may be involved in CathD-induced HOMEC proliferation. This observation was later confirmed by ELISA which showed that both inhibitors at their selected concentrations inhibited CathD-induced ERK1/2 phosphorylation. This agrees with a study where proteolytically inactive CathD was shown to induce human skin fibroblast proliferation via activation of the MAPK/ERK1/2 pathway (Laurent-Matha et al., 2005). This current study is the first report that demonstrates activation of ERK1/2 by CathD in an EC model. Activation of the ERK1/2 pathway in EC models and other cell models have been discussed in Chapter 3 (Section 3.4).

Based on the previously described role for PI3K/AKT in EC proliferation (Chapter 3, Section 3.4) and the fact that CathD treatment increased levels of phosphorylated AKT, the involvement of this pathway in HOMEC proliferation stimulated by CathD was tested. A PI3K (upstream of AKT) inhibitor LY294002 and selective AKT inhibitor MK2206 was used to examine this. LY294002 decreased HOMEC proliferation in a dose-dependent manner and ELISA data confirmed that LY294002 did inhibit phosphorylation of AKT in HOMECs. This suggested that the PI3K/AKT pathway is also involved in CathL-induced HOMEC proliferation.

To further investigate the above findings, a selective allosteric inhibitor of AKT was used. Intriguingly, MK2206 did not inhibit CathD-induced cell proliferation. Instead it increased cell proliferation in the absence or presence of CathD, although phosphorylated levels of AKT were maintained at basal level by the inhibitor (ELISA data). This may indicate that activation of AKT is not required CathD-induced HOMEC proliferation. It is possible that inhibition of AKT by

MK2206 may activate other kinases in a feedback loop which enhances cell proliferation, although there is no available literature to support this observation.

These data may also suggest that PI3K acts via an AKT-independent downstream pathway to mediate CathD-induced HOMEC proliferation. These results coincide with the reports discussed in Chapter 3 (Section 3.4). Previously, Sagulenko *et al.* reported an inhibition of CathD-induced AKT phosphorylation with LY294002 that resulted in apoptosis in the human neuroblastoma cell line Tet21N (Sagulenko et al., 2008). However, the authors, unlike in my study, did not test an AKT-selective inhibitor (e.g. MK2206) to verify whether it was PI3K or indeed AKT that was playing a role maintaining cell survival. To my knowledge, this current study is the first to report that CathD-induced activation of PI3K may enhance proliferation in an EC model in AKT-independent manner (discussed in Chapter 3, Section 3.4).

CathD induced HOMEC migration

EC migration is also a key element of angiogenesis. Previously CathD has been shown to be pro-migratory in HOMECs (Winiarski et al., 2013), although the downstream signalling pathways were not elucidated. In order to confirm the pro-migratory role of CathD in HOMECs, firstly, as discussed in Chapter 3 (Section 3.4), Cultrex transwell migration Boyden chamber assay kit was used to examine CathD-induced cell migration after 6 hour treatment. The data confirmed that CathD significantly induced cell migration compared to control.

Role of activated signalling pathways in CathD-induced HOMEC migration

The potential downstream signalling cascades were then examined. Based on the observation that CathD induces AKT phosphorylation and that AKT has a reported role in cell migration (discussed in Chapter 3, Section 3.4), it was hypothesised that AKT is involved in this process. Both the PI3K inhibitor LY294002 and AKT inhibitor MK2206 were used to assess CathD-induced cell migration. Interestingly, both inhibitors significantly inhibited CathD-induced HOMEC migration compared to control, suggesting that the PI3K/AKT pathway mediates this cellular function. The PI3K/AKT pathway has been shown to be

extensively linked to mammalian cell migration as discussed in Chapter 3, Section 3.4.

Since the ERK1/2 pathway has also been reported to be activated in migrating cells (discussed in Chapter 3, Section 3.4) and it was observed that CathD activates ERK1/2, a role for ERK1/2 was investigated in CathD-induced HOMEC migration. ERK1/2 inhibitors U0126 and PD98059 were used to examine this. Both inhibitors significantly inhibited CathD-induced cell migration, suggesting a pro-migratory role for ERK1/2. This agrees with a study where ERK1/2 activation was observed to play a key role in migration of human skin and mammary fibroblasts induced by CathD (Laurent-Matha et al., 2005).

CathD has been shown to induce migration in several cell models. Winiarski *et al.* demonstrated that CathD induced HOMEC migration *in vitro* (Winiarski et al., 2013). Also migration of HUVECs was increased when cells were treated with pure active CathD (Hu et al., 2008). In other studies pCathD and CathD have been reported to induce migration of breast cancer cells and human fibroblasts (Laurent-Matha et al., 2005, Ohri et al., 2008). Intriguingly, CathD has also been shown to selectively degrade macrophage inflammatory protein (MIP)-1α (CCL3), MIP-1β (CCL4), and SLC (CCL21) that, in turn, may affect the migration of human breast cancer cells (Wolf et al., 2003). However, no intracellular signalling cascade has been identified in CathD-induced EC migration in the available literature, although activation of the ERK1/2 pathway has been reported to be involved in inducing migration of human fibroblasts as discussed above (Laurent-Matha et al., 2005). This present study reports for the first time that CathD induces migration in HOMECs via both the PI3K/AKT and ERK1/2 pathways.

Examining angiogenesis in CathD-treated HOMECs

Since CathD induced HOMEC proliferation and migration, both key steps in angiogenesis, CathD-mediated induction of angiogenic sprouting in HOMECs was investigated. A 3D model was initially used to investigate this phenomenon. As discussed in Chapter 2 (Section 2.8) and 3 (Sections 3.3.7, 3.4), initially human brain microvascular endothelial cells (HCMECs) were used to verify this technique. When treated with CathD (50ng/ml), sprouting was observed in HCMECs. However, with HOMECs, no sprouting was observed. A number of

steps and constituents were altered to optimise the 3D model for HOMECs as discussed in Chapter 3 (Section 3.3.7 and 3.4), however, the outcome was unsuccessful and therefore, a 2D angiogenesis model was adopted using commercially available GFR-Matrigel (Chapter 3, Section 3.3.7).

Although there was an increase in angiogenesis index as shown in the figure, this was not statistically significant compared to control. As discussed in Section 5.3.7, this may be due to low replicate numbers and should be investigated further.

There are reports that CathD does induce angiogenesis in other models. For instance, CathD has been shown to form tubule-structures using HUVECs in Matrigel (Hu et al., 2008). The same study depicted blood vessel formation in CAM models treated with CathD. *In vivo*, overexpression of CathD in xenografts in an athymic mice model correlated with increased vascular density. The number of microvessels was significantly increased by 1.5-fold and 1.9-fold in the CathD and CathD-Asn 231(proteolytically inactive) groups respectively (Berchem et al., 2002). These combined data suggest that CathD is capable of inducing angiogenesis both *in vitro* and *in vivo*.

Although CathD did not show significant induction of tubule structure formation, it is possible that in the Matrigel, due to its constituents (i.e. presence of other growth factors), effects of CathD was not strongly elicited. This study should be taken further to establish a novel way to demonstrate angiogenesis- cell sprouting and tubule-structure formation. This should, in the future, allow in-depth research investigating critical and novel cell signalling pathways that aid the metastatic cascade in ovarian cancer.

CathD induced activation of RTK c-Ret

Since CathD activates intracellular kinases that promote cell survival and growth, it was hypothesised that a receptor tyrosine kinase (RTK) may be involved in mediating such cellular effects. A preliminary investigation was carried out to identify possible RTKs in HOMECs that might be activated by CathD. It was found that both positive control VEGF (VEGF-A 165) and CathD induced activation of c-RET in HOMECs. VEGF also induced phosphorylation and

activation of VEGFR2 and VEGFR3 in this experiment. The RET RTK is a single-pass transmembrane protein that is required for normal development, maturation and maintenance of several tissues and cell types such as the kidney and the nervous system (Coulpier et al., 2002, Jain et al., 2006). RET is the signalling receptor for the glial cell-derived neurotrophic factor (GDNF) family of ligands (GFLs): GDNF, Neurturin, Persephin and Artemin (Mulligan, 2014). Each of these ligands interacts with RET via a cell surface co-receptor of the GDNF family receptor-α (GFRα) family members. Once bound to the ligand–co-receptor complex, conformational changes facilitate RET monomer association via the cadherin homology domains and lead to receptor dimerization and autophosphorylation (Mulligan, 2014). This phosphorylation takes place on multiple tyrosine kinase residues which facilitate direct interactions with signalling molecules such as Src (proto-oncogene tyrosine-protein kinase) and phospholipase Cγ (PLCγ) or with any of a wide range of adaptor proteins, leading to the activation of multiple downstream signalling pathways. For instance, GDNF-stimulation induced phosphorylation of the MAPK/ERK1/2 and PI3K/AKT pathways in rat superior cervical ganglion cells (Creedon et al., 1997), mouse pro-B cell line Ba/F3 (Gu et al., 1998) and mouse fibroblast cell line MG87 (Besset et al., 2000) which are known to promote cell growth, proliferation, survival or differentiation.

There is no evidence that CathD may induce RET phosphorylation in any cell model in the current literature. However, VEGF was shown to induce activation of RET in addition to VEGFR2 autophosphorylation in ureteric bud cells which in turn led to branching of these cells (Tufro et al., 2007). Also, interestingly, cabozantinib, an inhibitor of VEGFR2, has been shown to elicit significant activity against the RET receptor in medullary cancer cells (Grullich, 2014), suggesting that the RET receptor may display a similar homology to that of VEGFR2 and that VEGF may interact with RET RTK. In contrast, a recent study suggested that in HUVECs, VEGF-independent activation of RET is responsible for angiogenesis (Zhong et al., 2016). GDNF (a physiological activator of RET) secreted from adipose-derived stem cells induced *in vitro* angiogenesis, via RET activation in HUVECs which remained unchanged on blocking VEGF activity (Zhong et al., 2016). The current study agrees with the former findings which demonstrate activation of RET RTK in VEGF-treated cells.

This current study suggests that CathD induced proliferation and migration in HOMECs via activation of the ERK1/2 and AKT pathways. Since RET RTK has been shown to be involved in the induction of angiogenesis in HUVECs, it is possible that RET may be responsible for CathD-induced proangiogenic changes in HOMECs. As discussed above, VEGF is able to induce phosphorylation of RET in ureteric bud cells and in HOMECs (in our study). Also, pro-proliferative, pro-migratory and pro-survival pathways ERK1/2 and AKT are downstream of RET activation. The fact that CathD induces these proangiogenic changes through activation of these pathways, it is reasonable to speculate that RET may be a receptor that CathD interacts with to produce such functional outcomes in HOMECs. At present the only receptor that CathD is known to interact with is M6P/IGF2 receptor, which has a well-defined function in the transport of various proteins via the endosomal pathway (Benes et al., 2008). It has been suggested that the M6P moieties of extracellular CathD may interact with the M6P receptor which then induces mitogenic responses in human skin fibroblasts (Laurent-Matha et al., 2005). However, Glondu *et al.* contradicted this observation and showed that the M6P receptor was not responsible for mitogenic responses induced by CathD in 3Y1-Ad12 rat cancer cells (Glondu et al., 2001), rather the presence of an unknown receptor, other than the M6P receptor, was strongly suggested. Therefore, the RET RTK may be a possible candidate which is responsible for inducing such proangiogenic effects in HOMECs by both VEGF and CathD. However, as this was a brief investigation, further research needs to be carried out in order to verify this finding by performing immunocytochemistry and immunoprecipitation to investigate the presence of RET receptor in HOMECs, followed by functional studies using inhibitors of RET to examine proliferation and migration in HOMECs treated with both CathD and VEGF.

A summary of CathD-induced proangiogenic responses in HOMECs are described in figure 5.17.

5.5 Conclusion

In this study, CathD, a factor secreted by ovarian cancer cell lines, has been demonstrated to induce proangiogenic changes in HOMECs via activation of the

ERK1/2 and AKT pathways. The fact that anti-VEGF therapies targeting VEGF-induced angiogenesis have not shown great success indicated that factors, other than VEGF, may be involved in aiding the transition process of ovarian tumour cells becoming metastatic. CathD, despite being a lysosomal protease, is a potential pro-angiogenic factor which may be inducing such changes in HOMECs. This may indicate that CathD can be targeted as a novel anti-tumourigenic/anti-angiogenic therapeutic target in the treatment of ovarian cancer.

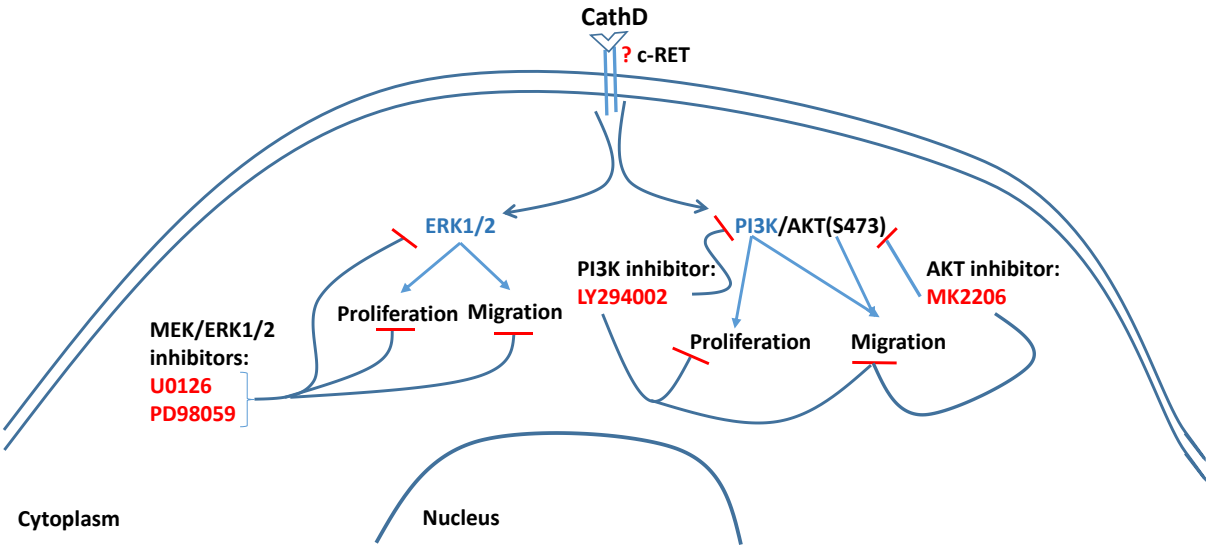

Figure 5.17: **A summary of CathD -induced activation of the ERK1/2 and AKT pathways, and cellular functions in HOMECs.** CathD possibly activates c-RET receptor tyrosine kinase on the cell surface membrane of HOMECs which leads to an increase in phosphorylation of ERK1/2 and AKT. The MEK/ERK1/2 inhibitors U0126 and PD98059 significantly reduce these cellular functions by inhibiting ERK1/2 phosphorylation. Both PI3K inhibitor LY294002 and AKT inhibitor MK2206 inhibit phosphorylation of AKT at Ser473 (S473) in CathD-treated HOMECs. However, only LY294002 inhibits CathL-induced HOMEC proliferation, suggesting activation of a pro-proliferative signalling cascade downstream of PI3K that is independent of AKT activation. Interestingly, both PI3K and AKT kinases are activated in CathD-induced HOMEC migration, which was reduced in the presence of both LY294002 and MK2206.

Chapter 6

Investigation into potential proangiogenic roles of IGFBP7 in human omental microvascular endothelial cells (HOMECs)

6.1 Introduction

In the establishment of secondary tumour foci, angiogenesis is a vital component. Previously, EOC cells secreted factors CathL and CathD have been shown to induce proangiogenic changes in HOMECs. IGFBP7, also known as angiomodulin, is an IGF binding protein that is also secreted from EOC cells (Winiarski et al., 2013). Numerous reports suggest that IGFBP7 plays an important role in inducing proangiogenic responses such as increased EC proliferation, migration and capillary like tube formation. However, IGFBP7 has also been shown to inhibit angiogenesis in several studies (see below- Section 6.4).

In HOMECs, IGFBP7 has been shown to be pro-proliferative, pro-migratory and induce angiogenic tube formation *in vitro* (Winiarski et al., 2013), although the activated signalling cascades involved in inducing such responses have not been examined. In this study, IGFBP7-induced proliferation was confirmed using two different methods. To identify activation of downstream phosphokinases, a proteome profiler and cell-based ELISAs were carried out. Subsequently, activation of these potential kinases were assessed in IGFBP7-induced HOMEC migration. In addition, tubule-structure formation was investigated using Matrigel in HOMECs. Finally, potential cell surface receptor targets of IGFBP7 was also assessed in a brief investigation.

6.1.2 Aims

The aims of this chapter are:

- To investigate whether IGFBP7 induces HOMEC proliferation
- To examine IGFBP7-induced migration in HOMECs
- To study potential cell signalling pathways involved in inducing HOMEC migration by IGFBP7

- To assess HOMEC angiogenic tube-formation induced by IGFBP7
- To identify potential cell surface receptor targets of IGFBP7 in HOMECs

6.2 Methods

HOMEC isolation: HOMECs were isolated according to (Winiarski et al., 2011) as described in the Method chapter section 2.3.1

Cell proliferation: HOMEC proliferation was tested using both the WST-1 assay and CyQuant cell proliferation kit as described in the Method chapter sections 2.4.1 and 2.4.2.

Cell migration: A commercially available cultrex Boyden chamber kit was used to investigate the underlying mechanisms of IGFBP7-induced HOMEC migration, as described in the Method chapter section 2.5.1.

Activation of intracellular kinases: A commercially available proteome-profiler and cell-based ELISAs were used to detect and assess levels of phosphorylated intracellular kinases as described in the Method chapter sections 2.7.2 and 2.7.4.1.

3D *in vitro* angiogenesis: A 3D angiogenesis model was used to assess HOMEC sprouting as described in the Method chapter section 2.8.1.

2D tube-formation: Angiogenic tube-formation was investigated in HOMECs treated with IGFBP7 using both a fibrin matrix assay and commercially available GFR-Matrigel, as described in the Method chapter section 2.8.2.

Identification of potential cell surface receptors: A commercially available human receptor-tyrosine kinase array was used as a screening tool to identify potential receptor as described in the Method chapter section 2.7.3.

6.3 Results

6.3.1 IGFBP7 induces HOMEC proliferation

Previously IGFBP7 has been shown to induce HOMEC proliferation. However, due to the presence of conflicting data in the literature on IGFBP7-induced

cellular response, it was essential to confirm the pro-proliferative role of IGFBP7 in HOMECs. In the current study, HOMEC proliferation was tested using both the WST-1 and CyQUANT assays. Initially, increasing concentrations (10, 20 and 50 ng/ml) of IGFBP7 were tested which revealed a significant increase in cell proliferation after 72 hour treatment. At 10, 20 and 50 ng/ml of IGFBP7 cell proliferation was 153±32.1% (n=18), 144.3±36.1% (n=18) and 141.3±21.5% (n=25) respectively compared to control (100%; Figure 6.1a). The range of concentrations were selected based around the secreted concentration (27 ng/ml) of IGFBP7 in SKOV3 tumour-conditioned media in our laboratory (unpublished data). These data confirmed the previous results published by the group that identified that IGFBP7 is a pro-proliferative factor for HOMECs (Winiarski et al., 2013). Since all three concentrations of IGFBP7 induced significant cell proliferation, a concentration of 50ng/ml was selected for further experiments.

Cell proliferation was then tested by CyQUANT assay which also revealed a significant increase in cell proliferation induced by IGFBP7. For example, at 50ng/ml IGFBP7, cell proliferation increased to 108.2±8.1% ($p<0.001$, n=20) compared to control (100%). These data confirm that IGFBP7 induces proliferation in HOMECs.

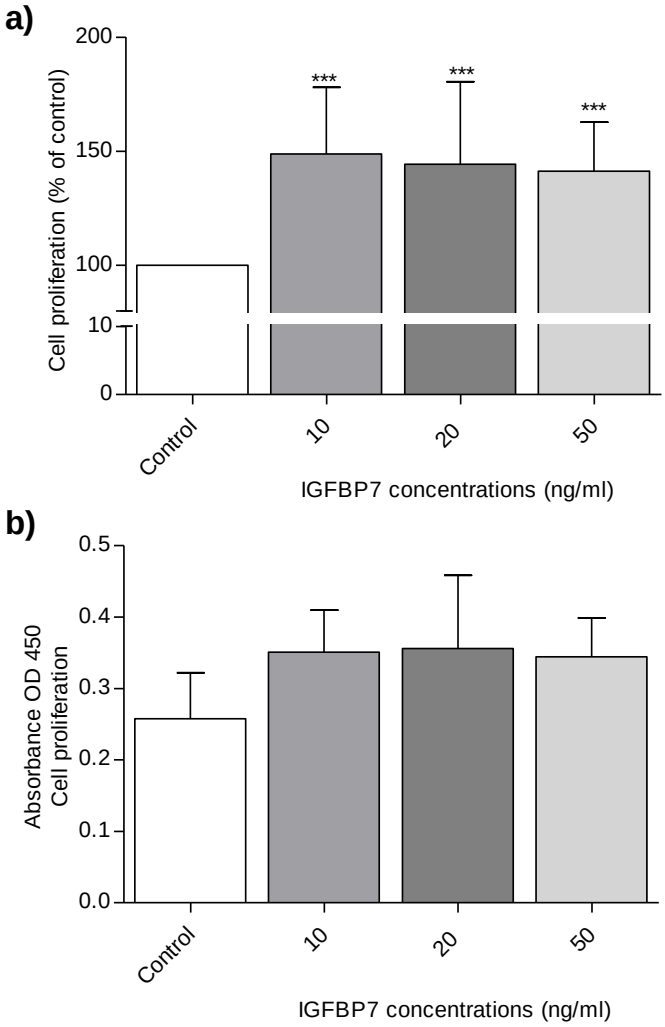

Figure 6.1: **Increased proliferation of HOMECs in media supplemented with IGFBP7 (WST-1 assay).** Cells were seeded in 2% gelatin pre-coated 96 well plates at a density of 10,000cells/well in starvation media containing 2% FCS. After overnight incubation, cells were treated with or without various concentrations of IGFBP7 and incubated for 72 hours. A commercially available WST-1 kit was used to assess cellular proliferation based on absorbance using a PHERAstar BMG plate-reader at 450nm. **a)** Results are mean ±SD and shown as percentage of the control, ***p<0.001 vs control (100%), n=18-25. **b)** Raw data from representative experiment.

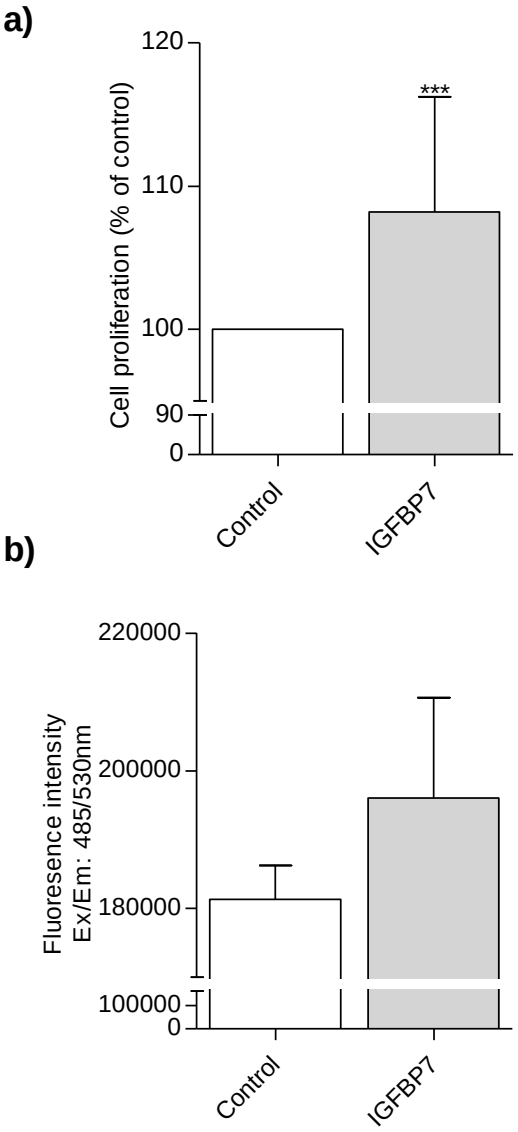

Figure 6.2: **Increased proliferation of HOMECs in media supplemented with IGFBP7 (CyQUANT).** Cells were seeded in 2% gelatin pre-coated 96 well plates at a density of 10,000cells/well in starvation media containing 2% FCS. After overnight incubation, cells were treated with or without 50ng/ml of IGFBP7 and incubated for 72 hours. A commercially available CyQUANT reagent was used to assess cell proliferation based on fluorescence intensity using a FLUOstar BMG plate-reader at Ex/Em: 485/530nm. **a)** Results are mean ±SD and shown as percentage of the control, ***$p<0.001$ vs control (100%), n=20. **b)** Raw data from representative experiment.

6.3.2 IGFBP7 induces HOMEC migration

IGFBP7 has been shown to induce migration in HOMECs a using Oris migration assay kit (Winiarski et al., 2013). As discussed Chapter 3 (section 3.4), a Cultrex transwell Boyden chamber was used to assess IGFBP7-induced HOMEC migration at a reduced time point. After 6 hour incubation IGFBP7 induced significant cell migration (168.6±40.9%, n=11) compared to control (100%; Figure 6.3a). Positive control VEGF also induced significant migration compared to control. These data confirm that IGFBP7 also has a pro-migratory role in HOMECs. Thus, the signalling pathways activated during IGFBP7 treatment were investigated.

6.3.3 IGFBP7 induces activation of ERK1/2 and AKT kinases

Based on the previous proliferation and migration data, it was hypothesised that IGFBP7 induces activation of pro-proliferative and pro-migratory pathways as identified in several cell models, including HOMECs as discussed in Chapter 3, 4 and 5. Therefore, to investigate potential downstream signalling pathways, initially, IGFBP7-treated HOMECs were tested using a proteome profiler that simultaneously detects activation of 43 kinases. It was revealed that after 4 minutes treatment IGFBP7 increases phosphorylation of the p38α (~3.5-fold), ERK1/2 (~3.4-fold), AKT (4-fold) kinases in HOMECs compared to control (Figure 6.4). The ERK1/2 and AKT kinases were selected for further investigation as these two kinases have been shown to significantly induce migration in several cell models as previously described in Chapter 3, section 3.4.

The proteome profiler data was confirmed using cell-based ELISAs. After 4 minutes treatment, IGFBP7 significantly induced phosphorylation of ERK1/2 in HOMECs (2.33-fold vs control; Figure 6.5a). A similar increase in ERK1/2 phosphorylation (2.6-fold vs control) was also observed in the positive control VEGF-treated (4 minute treatment) HOMECs (Figure 6.5a). However, after 10 minutes treatment with IGFBP7, levels of phosphorylated ERK1/2 reduced to the basal level, although this remained unchanged with VEGF treatment (Figure 6.5b). Similar experiments were performed with AKT where AKT phosphorylation was induced (2.1-fold compared to control) at 4 minutes after treatment (Figure

6.5c) and was reduced to the basal level after 10 minutes (Figure 6.5d). VEGF was used as positive control in all cell-based ELISA experiments.

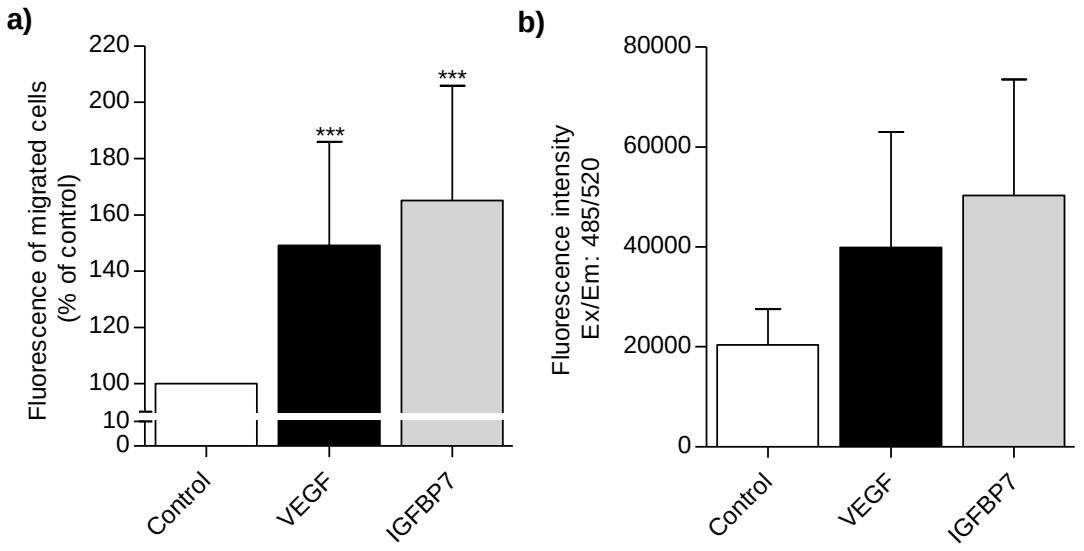

Figure 6.3: **IGFBP7 induces HOMEC migration.** HOMECs were seeded on the upper transwell insert and treated with or without IGFBP7 (50ng/ml) or VEGF (20ng/ml) supplementation of starvation media containing 0.5% FCS. The lower well contained corresponding treatment i.e. 0.5% FCS media, IGFBP7 (50ng/ml) or VEGF (20ng/ml). After 6 hours, migrated cells were stained with calcein AM and fluorescence was quantified by using a FLUOstar plate reader at Ex/Em: 485/520. **a)** Results are mean ±SD and shown as percentage of the control, ***p<0.001 vs control (100%), n=11, **b)** Raw data from representative experiment.

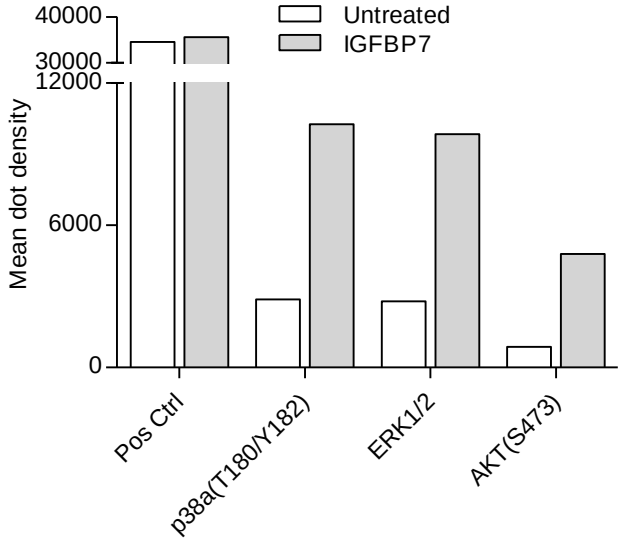

Figure 6.4: **IGFBP7 induces phosphorylation of p38α, ERK1/2 and AKT(S473) in HOMECs.** Phosphorylation status of the intracellular kinases was assessed in cell lysates from cells treated with or without IGFBP7 for 4 minutes. The results of 1 minute exposure are expressed as mean dot density (arbitrary units). The relative expression of specific phosphorylated proteins was determined following quantification of scanned images. A combination of 2 cell batches were used in this experiment. n= 2 (n=1).

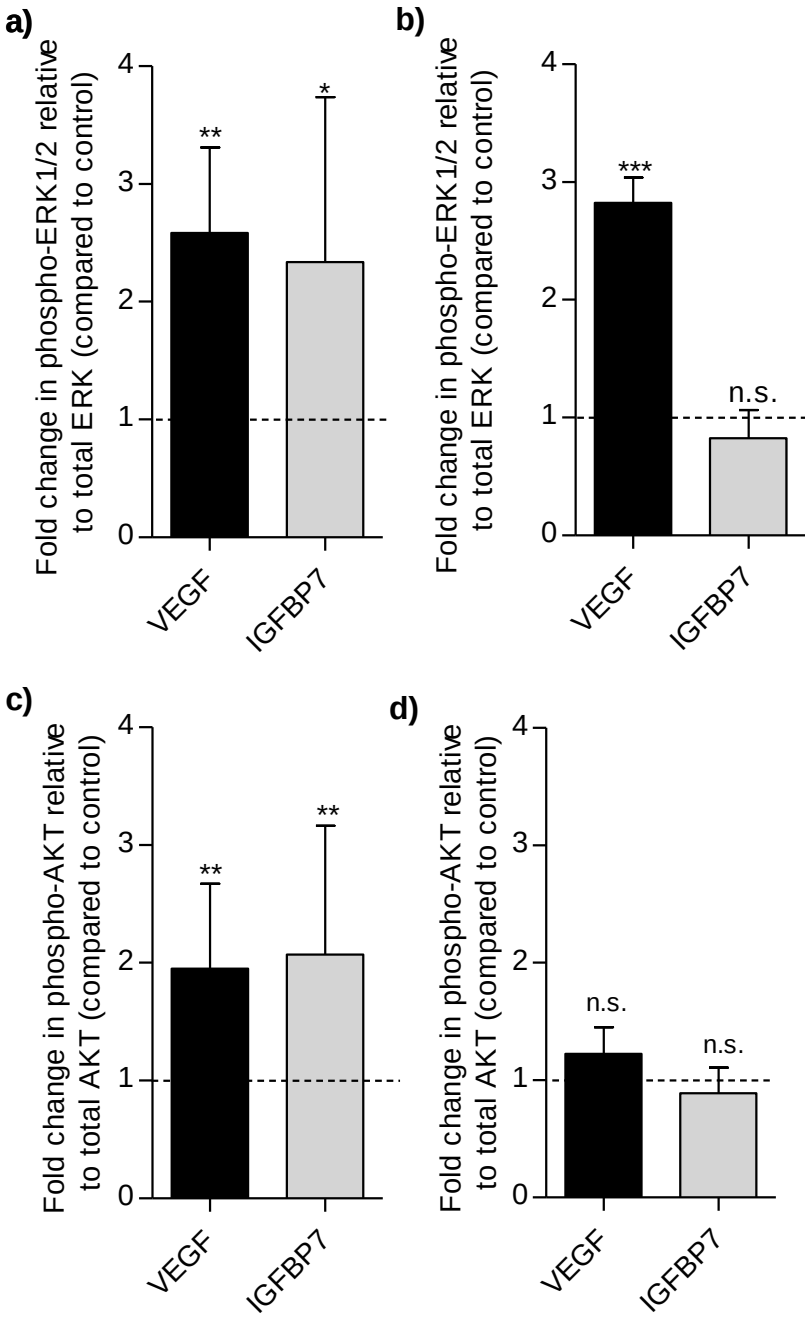

Figure 6.5: **IGFBP7 induces phosphorylation of ERK1/2 and AKT in HOMECs.** Cells were seeded in 2% gelatin pre-coated 96 well plates at a density of 10,000cells/well in starvation media containing 2% FCS. After overnight incubation, cells were treated with or without 50ng/ml of IGFBP7 or 20ng/ml of VEGF. ERK1/2 **(a, b)** and AKT **(c, d)** phosphorylation was examined after 4 minutes **(a, c)** and 10 minutes **(b, d)** treatments. Commercially available cell-based ELISAs were used for the determination of ERK1/2 and AKT(S473) phosphorylation level. The ELISA experiments were carried out in quadruplets on two cell batches. The data is represented as fold change in phosho-ERK1/2/AKT relative to total ERK1/2/AKT (compared to control). Results are mean ±SD, n.s., *p<0.05, **p<0.01, ***p<0.001 vs control; n=4-6. The dotted lines represent basal level (control) of phosphorylation status in untreated HOMECs. n.s. denotes not significant.

6.3.4 IGFBP7 induces HOMEC migration via activation of ERK1/2, but not AKT

Previous data showed that IGFBP7 plays a pro-migratory role and that it induces activation of ERK1/2 and AKT in HOMECs. Both the activated ERK1/2 and AKT pathways have been shown to induce cell proliferation in several models (discussed in Chapter 3, section 3.4), with AKT being the most common pathway known in this process. Therefore, it was hypothesised that IGFBP7 induces HOMEC migration via activation of AKT. Thus, the role of AKT in cell migration was examined in cells pre-treated with or without PI3K and AKT inhibitors LY294002 (25 µM) and MK2206 (5 µM) (concentrations previously determined in Chapter 3, Section 3.3.5) respectively, and then co-treated with IGFBP7 in the absence or presence of the corresponding inhibitor for 6 hours. Although both inhibitors inhibited IGFBP7-induced migration, this was not a significant reduction. For instance, migration of IGFBP7-treated cells in the presence of LY294002 was 127.8±46.9% (n= 6) with no significant difference compared to IGFBP7-induced migration (165±40.1%, n= 12), both were expressed as percentage of control (100%; Figure 6.6a). In the case of MK2206 and IGFBP7 treatment, cell migration was 128.8±62.0% (n= 6), which was not significantly different to IGFBP7-induced migration (165±40.1%, n= 12), both were normalised to control (100%; Figure 6.6b). HOMECs treated with only LY294002 and/or MK2206 demonstrated a significant reduction in migration (Figure 6.6 a),b).

The ELISA data with LY294002 (25 µM) and MK2206 (5 µM) confirmed that both drugs do inhibit IGFBP7-induced phosphorylation of AKT in intact HOMECs. In the presence of LY294002, IGFBP7-induced levels of phosphorylated AKT reduced from 1.8-fold to 0.9-fold (Figure 6.7a). In the case of MK2206, levels of phosphorylated AKT decreased from 1.8-fold to 0.85-fold (Figure 6.7b). This suggests that both drugs inhibit the PI3K/AKT pathway in HOMECs. However, a lack of statistically significant inhibition of cell migration suggests that activation of AKT(S473) may not be solely involved in the induction of IGFBP7-mediated HOMEC migration.

Cell migration was then tested in the presence of the ERK1/2 inhibitors U0126 and PD98059. Cells were pre-treated with U0126 (10 µM) or PD98059 (25 µM) (as determined in Chapter 3, Section 3.3.4) and then were co-treated with IGFBP7 in the presence or absence of the inhibitors. After 6 hours incubation,

both inhibitors of ERK1/2 abolished HOMEC migration compared to IGFBP7-alone treated cells. In the presence of U0126 and PD98059, IGFBP7-induced HOMEC migration reduced to 86.6±28.9% (n=7; Figure 6.8a) and 85.6±18.1% (n=6; Figure 6.8b) respectively, compared to IGFBP7-treatment alone (139.8±24.2%, n=9), both data were expressed as percentage of control (100%). U0126 treatment alone significantly reduced HOMEC migration (Figure 6.8a), however, although there was a slight reduction in migration by PD98059 only treatment, it was not significantly different compared to control (Figure 6.8b).

Cell-based ELISAs confirmed that the levels of phosphorylated ERK1/2 abolished or reduced in HOMECs to 0.3-fold and 0.4-fold in the presence of U0126 (Figure 6.9a) and PD98059 (Figure 6.9b) respectively when compared with IGFBP7-alone (1.4-fold). These data, along with inhibition of cell migration data suggest that IGFBP7 induces HOMEC migration via activation of ERK1/2.

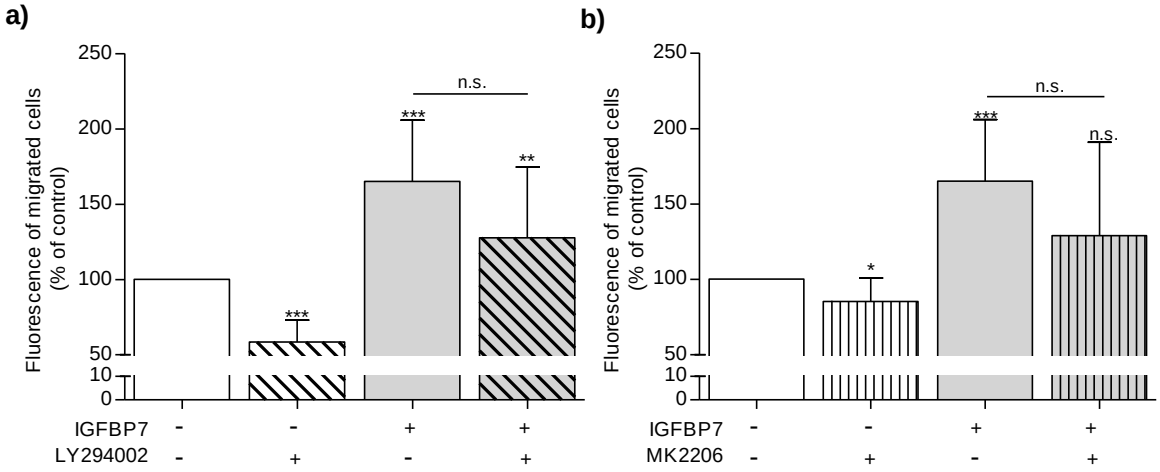

Figure 6.6: **IGFBP7 does not induce HOMEC migration via the AKT pathway.** HOMECs were seeded in the upper transwell chamber and treated with or without IGFBP7 (50ng/ml) in the absence or presence of PI3K and AKT inhibitors **a)** LY294002 (25 µM) and **b)** MK2206 (5 µM) respectively in media containing 0.5% FCS. The lower well contained corresponding treatments. After 6 hours, migrated cells were stained with calcein AM and fluorescence was quantified using a FLUOstar plate reader at Ex/Em: 485/520. Results are mean ±SD and shown as percentage of the control (100%), *p<0.05, **p<0.01, ***p<0.001 vs control (100%), n=6-12. n.s. denotes not significant vs IGFBP7.

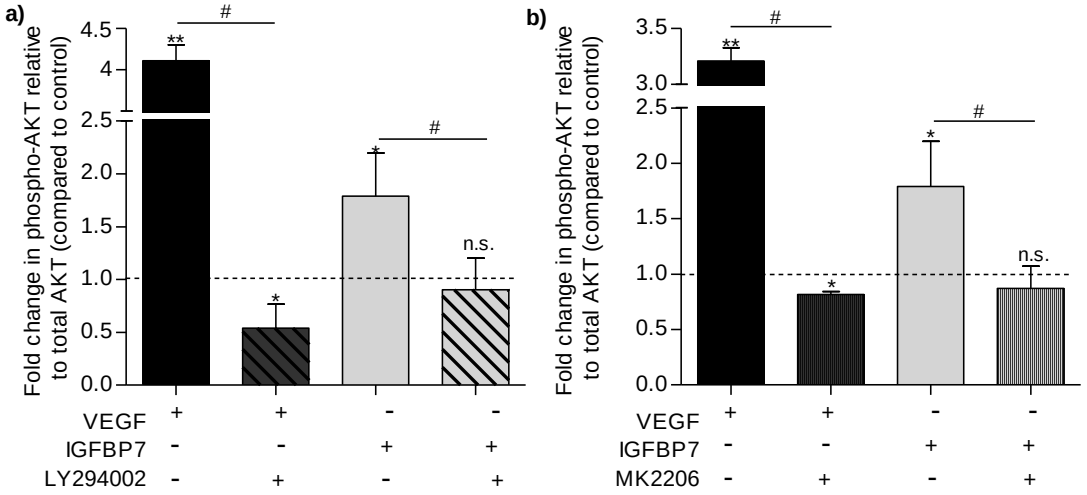

Figure 6.7: **IGFBP7-induced AKT phosphorylation is inhibited in HOMECs treated with PI3K and AKT inhibitors a) LY294002 (25 µM) and b) MK2206 (5 µM)**, respectively. Cells were seeded in 2% gelatin pre-coated 96 well plates at a density of 10,000cells/well in starvation media containing 2% FCS. After overnight incubation, cells were pre-incubated with the inhibitors for 2.5 hours, and then co-treated with or without 50ng/ml of IGFBP7 or 20ng/ml of VEGF in the absence or presence of the inhibitors for 4 minutes. Commercially available cell-based ELISAs were used to determine the level of AKT phosphorylation. The ELISA experiments were performed on two cell batches. The data is represented by fold change in phospho-AKT relative to total AKT (compared to control). Results are mean ±SD, n.s., *p<0.05, **p<0.01 vs control (1-fold), #p<0.05 vs VEGF/IGFBP7 (normalised to control), n=4. The dotted lines represent basal level (control) of phosphorylation status in untreated HOMECs. n.s. denotes not significant.

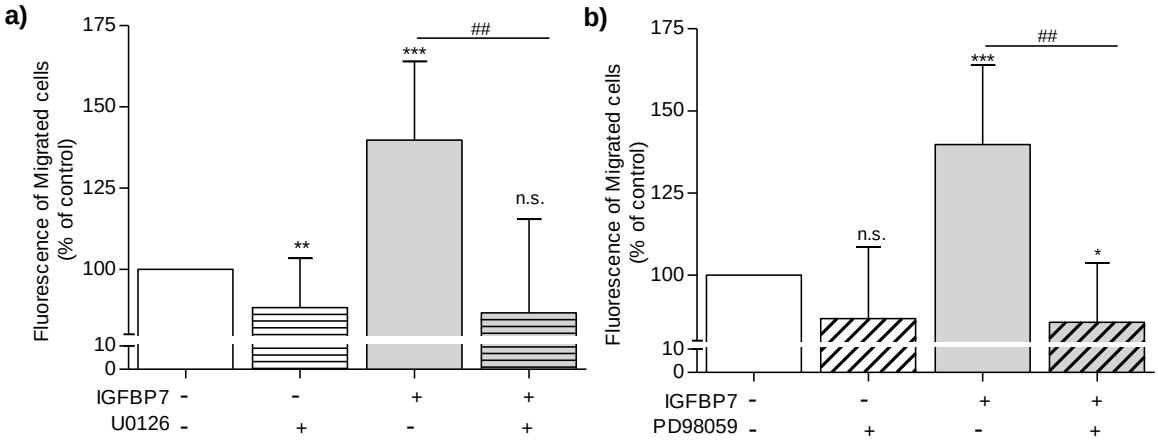

Figure 6.8: **IGFBP7 induces HOMEC migration via the ERK1/2 pathway.** HOMECs were seeded in the upper transwell chamber and treated with or without IGFBP7 (50ng/ml) in the absence or presence of ERK1/2 inhibitors **a)** U0126 (10 µM) and **b)** PD98059 (25 µM) respectively in media containing 0.5% FCS. The lower well contained correspondent treatments. After 6 hours, migrated cells were stained with calcein AM and fluorescence was quantified using a FLUOstar plate reader at Ex/Em: 485/520. Results are mean ±SD and shown as percentage of the control, n.s., *p<0.05, **p<0.01, ***p<0.001 vs control (100%), ##p<0.01 vs IGFBP7, n=7-9. n.s. denotes not significant.

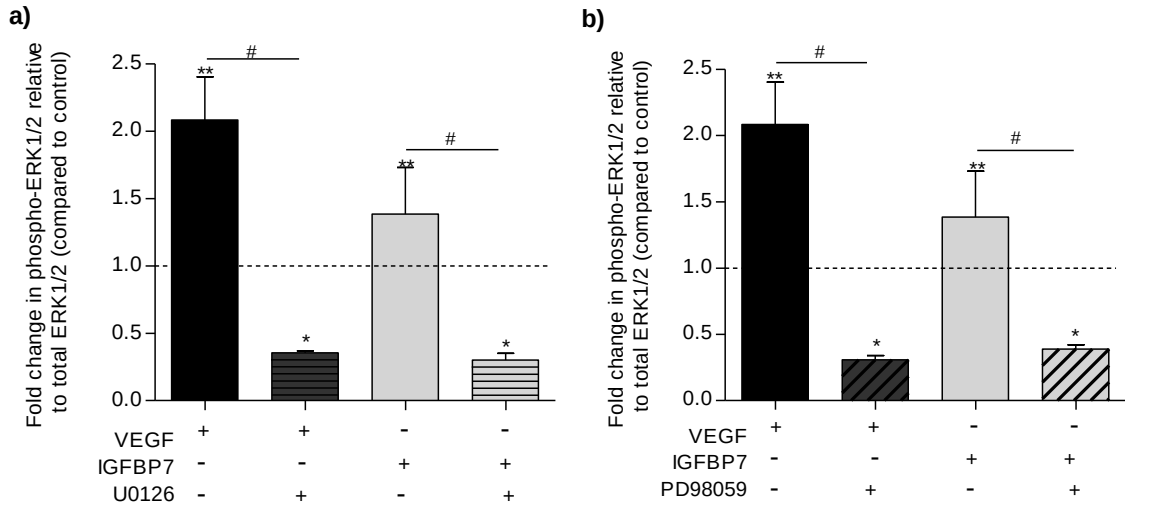

Figure 6.9: **IGFBP7-induced ERK1/2 phosphorylation is inhibited in intact HOMECs treated with ERK1/2 inhibitors a) U0126 (10 µM) and b) PD98059 (25 µM)**. Cells were seeded in 2% gelatin pre-coated 96 well plates at a density of 10,000cells/well in starvation media containing 2% FCS. After overnight incubation, cells were pre-incubated with the inhibitors for 20-30 minutes, and then co-treated with or without 50ng/ml of IGFBP7 or 20ng/ml of VEGF in the absence or presence of the inhibitors for 4 minutes. Commercially available cell-based ELISAs were used for determination of ERK1/2 phosphorylation levels. The data is represented by fold change in phosho-ERK1/2 relative to total ERK1/2 (compared to control). Results are mean ±SD, *p<0.05, **p<0.01 vs control (1-fold), #p<0.05 vs VEGF/IGFBP7 (normalised to control). The dotted lines represent basal level (control) of phosphorylation status in untreated HOMECs. n=4.

6.3.5 Optimisation of 3D and 2D *in vitro* angiogenesis models with IGFBP7

The data described show that IGFBP7 has the potential to induce cell proliferation and migration in HOMECs, two critical steps of tumour-angiogenesis. To examine the ability of IGFBP7 to induce angiogenesis in HOMECs, a 3D *in vitro* model was established as described before in Chapter 2 (Section 2.8) and Chapter 3 (Section 3.3.7). Initially, HCMECs were used to establish the model with different treatments: media supplemented with 2% FCS as basal control (Figure 6.10a), media supplemented with 5% FCS and manufacturer-provided growth factors as positive control (complete growth media) (Figure 6.10b), and 2% FCS media supplemented with 20ng/ml of VEGF (Figure 6.10c) or 50ng/ml of IGFBP7 (Figure 6.10d). Cell sprouting was observed in the positive control, IGFBP7 and in VEGF-treated wells, but not in cells containing media with 2% FCS (control).

However, when the same conditions were applied using HOMECs, no sprouting was observed in any of the wells (data not shown). As described and discussed in the previous chapters, further optimisation led to the investigation of angiogenesis in growth factor-reduced Matrigel (GFR-Matrigel). Therefore, initially, cells were seeded and treated 2 hours later with or without IGFBP7 and positive control VEGF for another 6 hours. After 6 hour incubation, it was found that IGFBP7 induced a significant increase in tube formation (213±12.0, n=4; Figure 6.11) compared to control (145±15). Positive control VEGF significantly increased tube formation in HOMECs (210.3±22.4, n=4). These data, along with proliferation and migration data, suggest that IGFBP7 plays a role in inducing 2D angiogenic tube-formation in HOMECs.

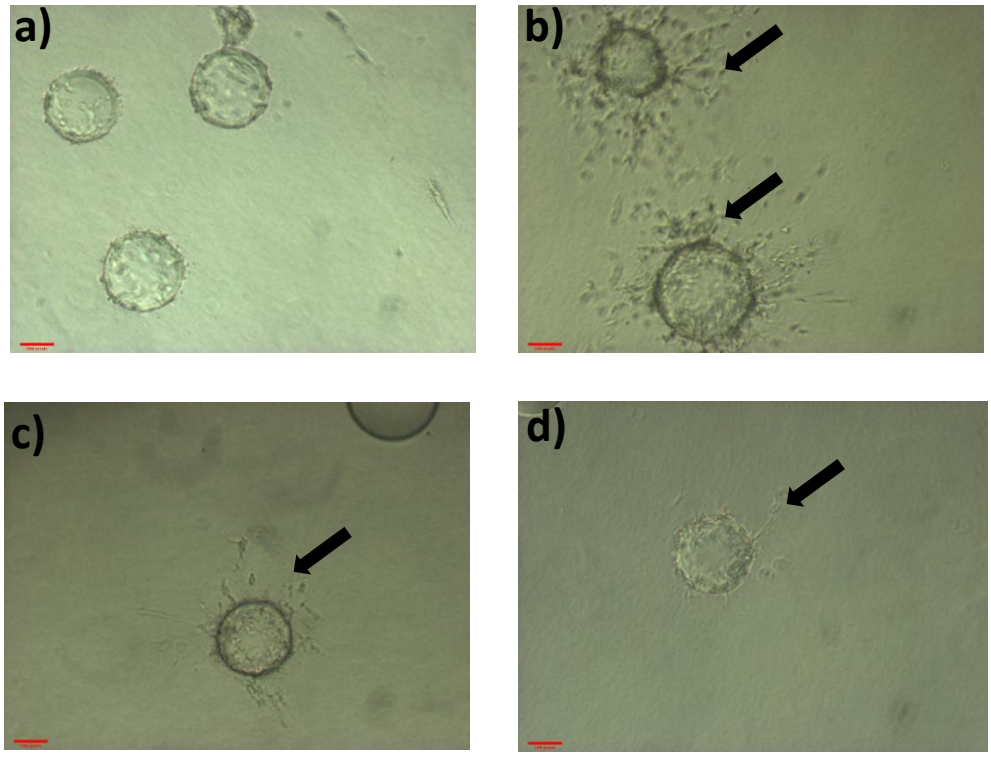

Figure 6.10: **Formation of angiogenic sprout in human cerebral microvascular ECs (HCMECs) in 3D fibrin gel.** Cells were seeded on cytodex 3 microcarriers and embedded in fibrin matrix gel in media supplemented with 2% FCS **a)** Control, **b)** 5% FCS with added ECs growth factors (positive control), **c)** 20ng/ml of VEGF or **d)** 50ng/ml of IGFBP7. Media/treatments were replaced every other day up to day 5. Photographs were taken on day 6 post-seeding using a Nikon phase-contrast microscope at 10X magnification. Arrow pointing at cell sprouting. Scale bar =100 µm.

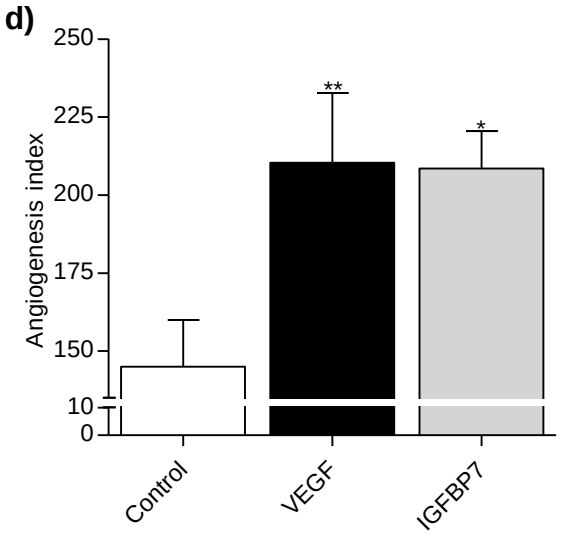

Figure 6.11: **IGFBP7-induced tubule structure formation in HOMECs in 2D Matrigel.** HOMECs were plated onto growth factor reduced- (GFR) Matrigel in medium containing 2% FCS and treated with media supplemented with VEGF (20ng/ml) and/or IGFBP7 (50ng/ml) for 8 hours. Controls contained HOMECs grown in medium containing 2% FCS alone. Photographs were taken at 8 hours after treatment using a Nikon phase contrast microscope camera and tubule-structure formation (including nascent tubule structures) was quantified as described in method section. The results are presented as an angiogenesis index. *p<0.05, **p<0.01 vs control levels, n=4.

6.3.6 Investigation into the activation of receptor tyrosine kinases by IGFBP7 in HOMECs

The previous data suggested that IGFBP7 plays a role in inducing proangiogenic changes in HOMECs via ERK1/2, and activating important intracellular kinases. This raised the possibility that IGFBP7 may act via a known tyrosine kinase receptor which was investigated using a commercially available RTK array kit. Cells were treated for 10 minutes with starvation media (2% FCS MV2), media supplemented with IGFBP7 (50ng/ml) or VEGF (20ng/ml; positive control). The results revealed that VEGF strongly activated VEGFR2 and slightly activated VEGFR3 (Figure 6.12). Intriguingly, IGFBP7 increased activation of c-RET receptor by ~16 fold compared to control. An increase in activation of VEGFR2 and a slight increase in phosphorylation of InsR (ALK) and Axl (Mer) receptor tyrosine kinases by IGFBP7 was also observed (Figure 6.12).

Since VEGFR2 is an important element of VEGF signalling and IGFBP7 induced activation of this receptor and the ERK1/2 and AKT kinases, its role in IGFBP7-induced cell proliferation was examined. To test this, IGFBP7-induced HOMEC proliferation was assessed in the presence of SU5416 (10 μM), a potent inhibitor of VEGFR2 tyrosine kinase (Huss et al., 2003). Initially, cells were pre-treated with or without SU5416 for 1 hour at a concentration previously determined in our laboratory (Winiarski et al., 2013), followed by co-treatment with or without IGFBP7 or positive control VEGF. After 72 hour incubation it was found that IGFBP7-induced HOMEC proliferation (145.3±26.7%, n= 9) was partially, but significantly reduced in the presence of SU5416 (115.9±13.4%, n=8), both were expressed as percentage of control (Figure 6.13). Positive control VEGF-induced cell proliferation was reduced to basal level in the presence of SU5416 as shown. These data suggest that activation of VEGFR2 by IGFBP7 may be involved in the induction of HOMEC proliferation.

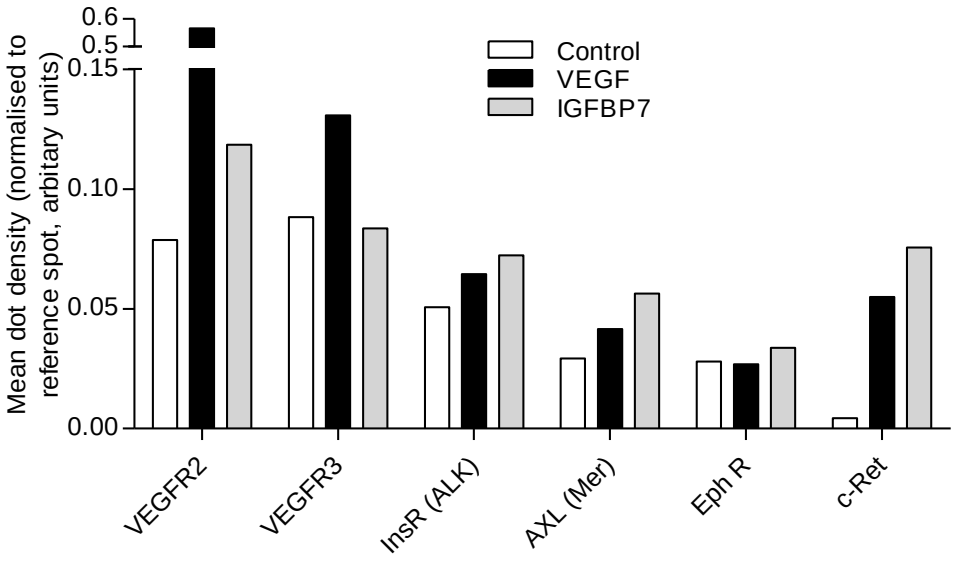

Figure 6.12: **IGFBP7 induces phosphorylation and activation of receptor tyrosine kinase (RTK) VEGFR2 and c-RET.** Phosphorylation status of RTKs was assessed in cell lysates treated with or without IGFBP7 or VEGF for 10 minutes. The results of 1 minute exposure are expressed as mean dot density. The relative expression of specific phosphorylated proteins was determined following quantification of scanned images of membrane using Azure software. n=1.

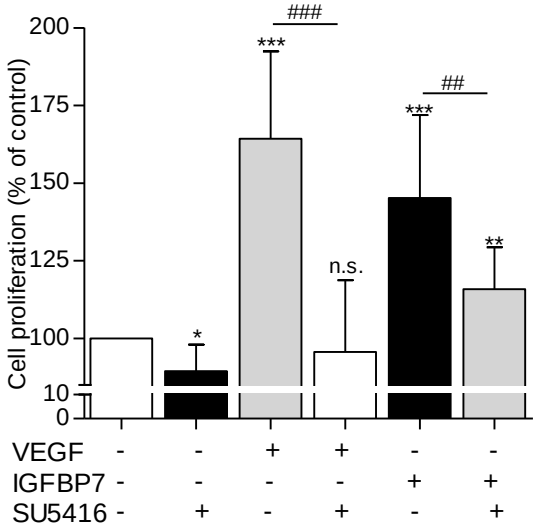

Figure 6.13: **IGFBP7 induces HOMEC proliferation via activation of VEGFR2.** Cells were seeded in 2% gelatin pre-coated 96 well plates at a density of 10,000cells/well in starvation media containing 2% FCS. After overnight incubation, cells were pre-treated with or without SU5416 (10 μM) in the presence of 0.1% BSA media for 1 hour, then co-treated with or without VEGF (20ng/ml; positive control) or IGFBP7 (50ng/ml) for 72 hours. WST-1 assay was used to assess cellular proliferation. Control wells contained 0.1% DMSO (vehicle) and 0.1% BSA. Results are mean ±SD and shown as percentage of the control, *p<0.05, **p<0.01, ***p<0.001 vs control (100%); ##p<0.01, ###p<0.001 vs IGFBP7/VEGF, n=8-10. n.s. denotes not significant vs control.

6.4 Discussion

In early angiogenic responses, tumour-secreted factors activate EC to proliferate, migrate and sprout out to generate new blood vessels. IGFBP7, an EOC secreted factor, was previously found to induce proliferation, migration and tube-formation in HOMECs (Winiarski et al., 2013). However, the underlying mechanisms which mediate these proangiogenic responses had not been elucidated. In this study, roles of IGFBP7 were confirmed in inducing HOMEC proliferation, migration and angiogenic tube-formation. Furthermore, activated downstream signalling cascades were also assessed and it was revealed that IGFBP7 induces HOMEC migration via activation of the ERK1/2 pathway. In a preliminary investigation, IGFBP7 was found to increase activation of c-RET, VEGFR2 and Mer (Axl) RTKs in HOMECs.

IGFBP7 induced HOMEC proliferation

Although IGFBP7 was previously shown to induce HOMEC proliferation, the contradictory data in the current literature (discussed below) meant that it was essential to repeat and confirm the finding in this study. Two independent techniques WST1 and CyQuant assay were utilised to verify the previous findings and both confirmed that IGFBP7 significantly induces HOMEC proliferation. This agrees with several studies that indicates a role for IGFBP7 in inducing cellular proliferation. For instance, exogenous IGFBP7 treatment significantly induced proliferation of LN18 and LN443 glioma cell lines *in vitro* (Jiang et al., 2008). Additionally, a recent study on haemocytes of small abalone *Haliotis diversivolor* reported a pro-proliferative role for IGFBP7 (Wang et al., 2015). When tested, IGFBP7 was found to increase cell density of these cells. IGFBP7 was also shown to induce growth of the mouse fibroblast cell line BALB/c3T3 *in vitro* (Akaogi et al., 1996b). These studies suggest that exogenous IGFBP7 can induce proliferation in cells. However, there are numerous studies available that contrast these findings. For instance, IGFBP7 was shown to inhibit VEGF-induced EC proliferation (Tamura et al., 2009). Also, apoptosis was induced in several cancer cell lines, particularly colorectal cancer and melanoma both *in vitro* and *in vivo* when treated with IGFBP7 (Wajapeyee et al., 2008, Wajapeyee et al., 2009). IGFBP7 has also been shown to strongly supress activation of the MAPK/ERK1/2

pathway, thereby reducing proliferation of the breast cancer cell line MDA-MB-468 and human melanoma cell lines (mutation BRAF V600e-positive SK-MEL-28 and SK-MEL-31) both *in vitro* and *in vivo* (Wajapeyee et al., 2008, Amemiya et al., 2011). When added exogenously, IGFBP7 significantly suppressed growth of human cervical carcinoma cells (HeLa), osteosarcoma cells (Saos-2), and murine embryonic carcinoma cells (Kato, 2000). These studies strongly suggest an inhibitory role of IGFBP7 on cell proliferation and survival. However in this current study, IGFBP7 was shown to induce HOMEC proliferation, and to my knowledge this is the only report that demonstrates such pro-proliferative response in an EC model.

Although IGFBP7 has been shown to be pro-proliferative in HOMECs, the underlying signalling mechanisms involved in the proliferative response were not examined in this study. In the future, an in-depth investigation (using human phosphokinase array and ELISAs) should be carried out to identify pathways involved in mediating the induction of proliferation in HOMECs.

IGFBP7 induced HOMEC migration

IGFBP7 also significantly induced HOMEC migration. There is very little available literature on the role of IGFBP7 in migration. The data presented here confirmed previously published data (Winiarski et al., 2013). Also, IGFBP7 has been shown to interact with various ECM proteins such as collagen type IV to stimulate adhesion and induce migration/invasion of HUVECs *in vitro* (Sato et al., 1999, Kishibe et al., 2000).

Signalling pathways involved in IGFBP7-induced HOMEC migration

As IGFBP7 induced HOMEC migration, the activation of downstream signalling pathways was examined. A proteome profiler and cell-based ELISAs were used to detect activated signalling kinases in HOMECs treated with IGFBP7 and revealed activation of two pro-proliferative and pro-migratory kinases ERK1/2 and AKT. It was hypothesised that AKT plays a key role in inducing IGFBP7-induced HOMEC migration since this kinase has been shown in numerous studies to

mediate such cellular function (as previously described in Chapter 3, Section 3.4). PI3K and AKT inhibitors LY294002 and MK2206 respectively were used to investigate the role of these in IGFBP7-induced migration. Intriguingly, inhibition of the PI3K/AKT pathway reduced cellular migration in control wells, however, no significant difference was observed between IGFBP7-induced migration and with co-treatment with the inhibitors, although both inhibitors (alone) significantly inhibited phosphorylation of AKT by IGFBP7 in HOMECs as demonstrated by ELISA data. Interestingly, both ERK1/2 inhibitors U0126 and PD98059 significantly reduced IGFBP7-induced HOMEC migration and reduced levels of phosphorylated ERK1/2 in IGFBP7-treated cells. This suggests that ERK1/2 may play a role in IGFBP7-induced HOMEC migration.

This observation is supported by the literature showing IGFBP7-mediated cell growth and migration via ERK1/2 and AKT phosphorylation. Jiang *et al.* reported that IGFBP7 induced migration by regulating levels of phosphorylated ERK1/2 and AKT in glioblastoma (GBM) cell lines LN 18 and LN443 (Jiang et al., 2008). Interestingly, it was shown that the level of phosphorylated AKT decreased in a time-dependent manner (0-6 hours) although the level of phosphorylated ERK1/2 remained higher in IGFBP7-treated cells compared to untreated cells. Thus, it was suggested that IGFBP7 induces cell migration by increasing ERK1/2 phosphorylation and decreasing levels of activated AKT. In the current study, although activation of ERK1/2 played a key role in inducing migration in HOMECs, level of AKT phosphorylation was also increased in IGFBP7-treated cells compared to control. Perhaps, in the future, levels of both ERK1/2 and AKT should be examined over a longer incubation to assess whether there is any downregulation of phosphorylated AKT as observed (up to 6 hours) previously in GBM cell lines (Jiang et al., 2008).

Although IGFBP7 has been shown to induce migration in HOMECs and in GBM cell lines, there are reports that contest these findings. For instance, IGFBP7 was shown to inhibit VEGF-induced migration and angiogenesis of HUVECs in a dose-dependent manner by downregulating the activation of COX-2 (an enzyme involved in the biosynthetic pathway of prostaglandin E2) and phosphorylated ERK1/2 induced by VEGF treatment (Tamura et al., 2009). When treated alone, IGFBP7 did not induce any proangiogenic changes in HUVECs. Sun *et al.* also

reported a significant inhibition in VEGF-induced migration of the retinal EC line RF/6A when co-treated with an increasing concentration of IGFBP7. Although the authors did not test cellular migration with IGFBP7-alone, the inhibition of VEGF-induced migration by IGFBP7 was shown to be mediated via an inhibition of the B-RAF/MEK/ERK1/2 pathway that subsequently induced apoptosis in these ECs (Sun et al., 2011), suggesting that IGFBP7 may elicit an anti-angiogenic response in certain ECs, although this was not the case in HOMECs.

Examining angiogenesis in IGFBP7-treated HOMECs

The observation that IGFBP7 induces HOMEC proliferation and migration suggested a role for this protein in angiogenesis and so angiogenic sprouting and tube-formation in these cells was assessed. A significant increase in tube-like structure formation was seen compared to control. Indeed, Winiarski *et al.* also demonstrated that IGFBP7 induced angiogenic tube-formation in HOMECs (Winiarski et al., 2013). Additionally, Zhao *et al.* has shown that IGFBP7 plays an important role in inducing tube like structure in lymphatic ECs which may stimulate tumour progression in non-small cell lung carcinoma (Zhao et al., 2016b). IGFBP7 was also shown to induce capillary-like tube formation in HCMECs in the pathogenesis of GBM (Pen et al., 2008). Together these data strongly suggest that IGFBP7 may play a pro-angiogenic role in tumour progression and metastasis.

However, again there are studies that contradict the above findings. For instance, IGFBP7 was shown to inhibit VEGF-induced *in vitro* angiogenesis in HUVECs (Tamura et al., 2009) and in vascular ECs of rat corpus luteum (Tamura et al., 2014). The authors demonstrated a dose-dependent reduction in tube-formation in ECs when treated with increasing concentrations of IGFBP7 in the presence of VEGF. Interestingly, Hooper *et al.* contradicted this latter finding and claimed that IGFBP7 interacts with VEGF by providing an extracellular scaffold to which VEGF can bind within the ECM milieu resulting in VEGF-induced pro-angiogenic responses during embryogenesis in a zebra fish model (Hooper et al., 2009). Although, these data suggest that IGFBP7 induces both anti- and pro-angiogenic responses in different EC models, the fact that this study confirms previously published data on the induction of tubule-structure formation in HOMECs

(Winiarski et al., 2013), indicates that IGFBP7 may be a potential proangiogenic factor in this cell model of ovarian cancer metastasis.

IGFBP7 induced phosphorylation of RTKs: ALK, cRET, AXL (Mer) and VEGFR2

Since IGFBP7 increased activation of ERK1/2 and AKT and induced proangiogenic changes in HOMECs, it was hypothesised that a RTK may be involved in mediating such cellular effects. In a brief investigation it was found that IGFBP7 induced activation of c-RET, and to a lesser extent activation of VEGFR2, anaplastic lymphoma kinase (ALK, insulin receptor superfamily) and Axl (Mer, member of Tyro3-Axl-MER family). This preliminary data suggests, for the first time in any cell model, that IGFBP7 induces activation of RET RTK. A role for RET has been discussed in Chapter 4 (Section 4.4). Briefly, RET has been reported to be activated by VEGF-VEGFR2 signalling in ureteric bud cells which in turn led to branching of these cells (Tufro et al., 2007). Furthermore, VEGF-independent activation of RET has also been suggested to induce angiogenesis in HUVECs (Zhong et al., 2016). Phosphorylation of signalling cascades such as the MAPK and PI3K/AKT pathways via RET RTK has also been reported in several cell models as described before (Chapter 4, Section 4.4). The fact that IGFBP7 induces proliferation, migration and angiogenesis in HOMECs, raises the possibility that RET RTK plays a key role in inducing such functions in HOMECs. Further research is required to verify these findings, which may shed light on the regulation of angiogenesis in IGFBP7-treated HOMECs.

ALK is a novel RTK that was discovered in the brain and specific neurones in the nervous system. It was originally identified as an oncogene activated in anaplastic large cell lymphomas (ALCL) (Shiota et al., 1995, Shiota et al., 1994). Subsequent cDNA cloning of the full-length proto-*alk* have shown that it encodes a novel, putative RTK of the insulin receptor family (Iwahara et al., 1997, Morris et al., 1997). This RTK was recently shown to be involved in the activation of several cellular functions. For instance, nucleophosmin (a nuclear protein involved in the biogenesis of ribosomes) was shown to interact with ALK RTKs in ALK-positive ALCL cell lines (SUDHL-1, Ki-JK, Karpas 299 and SR786) that induced significant phosphorylation of STAT3, ERK1/2 and AKT, whereby ERK1/2 was observed to be responsible for inducing cellular proliferation

(Anastasov et al., 2010). In another study, a monoclonal antibody (mAb16-39) targeting the extracellular domain of ALK demonstrated an increase in the level of endogenous ALK-phosphorylation in neuroblastoma cell line SK-N-SH (Motegi et al., 2004). Interestingly, ALK activation led to increased phosphorylation of ERK1/2 and subsequent cellular proliferation which was completely abolished by the ERK1/2 inhibitor PD98059 (Motegi et al., 2004). Armstrong *et al.* reported that overexpression of ALK in mouse fibroblasts (NIH3T3) induced proliferation and Matrigel invasion via activation of the PI3K/AKT pathway (Armstrong et al., 2004). Together, these data suggest that ALK may be responsible for induction of cellular proliferation via activation of ERK1/2. In the current study, IGFBP7 was demonstrated to be pro-proliferative in HOMECs. Although the activated signalling pathways have not yet been investigated in IGFBP7-induced HOMEC-proliferation, ALK would be an interesting RTK candidate to be examined in future studies.

ALK has also been reported to be involved in the induction of cellular migration via pathways that contrast with the present study. For example, Seo *et al.* demonstrated that overexpression of ALK induced activation of p55γ (a subunit of PI3K) that in turn resulted in migration of NIH3T3 cells (Seo et al., 2016). This was mediated by ALK-stimulated phosphorylation of the PI3K/AKT pathway, which was not observed in HOMECs when treated with IGFBP7. Interestingly, in another study, the phosphorylated p55γ subunit of PI3K was shown to stimulate angiogenesis in colorectal cancer cells by activating the NFκB pathway, via an AKT or ERK1/2-independent pathway (Wang et al., 2013). These data perhaps shed light on the role of ALK in mediating cellular migration, although in this study IGFBP7 has been shown to induce HOMEC migration via the ERK1/2 but not the AKT pathway. However, the fact that ALK has been observed to play significant roles in cellular proliferation and migration, suggests that these preliminary findings could be taken further in future experiments to investigate IGFBP7-induced ALK activation and downstream cellular functions. It is also important to note that ALK activation has never been reported in an EC model, and therefore it would be very important to investigate expression of ALK in HOMECs further.

Since IGFBP7 induced activation of VEGFR2 tyrosine kinase in HOMECs, the role of this receptor in inducing HOMEC proliferation was examined. IGFBP7-induced HOMEC proliferation was partially but significantly reduced in the

presence of the VEGFR2 tyrosine kinase inhibitor SU5416. This may suggest that VEGFR2 activation plays an important role in IGFBP7-induced HOMEC proliferation. However, since SU5416 did not completely abolish IGFBP7-induced cell proliferation, unlike in VEGF-treated cells (positive control), it may indicate that other receptors might also have been activated in HOMECs, as shown in figure 6.13.

Although IGFBP7 induced activation of VEGFR2 in HOMECs, there are reports that contradict the current finding. For instance, IGFBP7 was shown to inhibit VEGF-induced proliferation and tube-formation in HUVECs (Tamura et al., 2009). IGFBP7 was not shown to bind to VEGFR2 or VEGF itself, but it was suggested that this inhibition may be induced by IGFBP7-mediated blocking of the MEK-ERK signalling pathway. In addition, Hooper *et al.* suggested that in neoangiogenesis, ECM-bound IGFBP7 plays an inhibitory role by directly binding to VEGF in the extracellular milieu and thereby blocking VEGF-induced vascular patterning in mice (Hooper et al., 2009). To my knowledge, there are no other reports of IGFBP7 binding to and activating VEGFR2 in any cell model.

The data in the current study suggested that IGFBP7 induced phosphorylation of ERK1/2 and AKT in HOMECs. In the VEGF-VEGFR2 signalling axis, these two kinases are commonly activated during proliferation, migration and angiogenesis. The fact that IGFBP7 also induces activation of these intracellular kinases and also phosphorylates VEGFR2 tyrosine kinase, may indicate a role for VEGFR2 activation in IGFBP7-induced cellular functions. Although these are only preliminary data, it will be very interesting to examine this further in future studies.

IGFBP7 also induced activation of Mer, another RTK that was initially discovered in human leukaemia cells and cancer cells such as lung cancer, breast cancer, GBM, epidermoid carcinoma, colon cancer, and normal human fibroblasts. (Graham and Peng, 2006). Mer is a member of the TAM (*T*yro3, *A*xl and *M*ertk) family of RTKs that has not been fully characterised. Interestingly, there are striking similarities between the tyrosine kinase domain amino acid sequences of family members Axl and Mer RTKs. Overall, the protein sequences of the human TAM receptors share 31–36% identical (52–57% similar) amino acids within the extracellular region. The intracellular domains share 54–59% sequence identity

(72–75% similarity) with higher homology in the tyrosine kinase domain (Graham and Peng, 2006), and hence it is believed that these RTKs, particularly Axl and Mer are involved in inducing similar cellular responses (Linger et al., 2008).

A role for Mer RTK has been reported recently to be involved in the progression of GBM. This study demonstrated that Mer and Axl RTKs are highly expressed and often co-expressed in astrocytic and glioblastoma cell lines (Keating et al., 2010), which may be important clinically given the correlation of TAM RTK coexpression and poor prognosis in gastric carcinoma. Keating *et al.* observed that downregulation of Mer or Axl RTK resulted in increased apoptosis, decreased short- and long-term survival, and increased chemosensitivity of GBM cells *in vitro* (Keating et al., 2010), suggesting a prosurvival role for Mer RTK, which has been shown to be mediated via activation of the AKT pathway (Krause et al., 2015). Recently, a study reported that both shRNA-knockdown of Mer RTK and a monoclonal antibody against Mer RTK can significantly inhibit GBM cell migration, which was rescued by re-introducing Mer RTK expression in these cells (Rogers et al., 2012). The authors observed an alteration in FAK signalling and suggested that an intact Mer RTK signalling is necessary for appropriate levels of FAK activation, and that this altered FAK signalling may be responsible in part for the aberrant migration of Mer-inhibited GBM cells (Rogers et al., 2012). Since IGFBP7 induces HOMEC migration, it is possible that Mer RTK contributes to this response. Interestingly, Keating and colleagues reported a reduction in the activation of the PI3K and ERK1/2 pathways when Mer or Axl were blocked in serum-treated astrocytoma cells *in vitro* (Keating et al., 2010). Previous reports have shown that the PI3K/AKT survival pathway is critical for normal CNS cell survival signalling (Shankar et al., 2006, Shankar et al., 2003). Several groups have published data implicating the PI3K and MAPK pathways in astrocytoma proliferation. Hlobilkova *et al.* have shown that aberrant activation of AKT is found in both low-grade and high-grade astrocytoma patient samples (Hlobilkova et al., 2007), whereas Mizoguchi *et al.* showed that the PI3K/AKT and MAPK pathways were abnormally activated in high-grade astrocytomas (Mizoguchi et al., 2006). Interestingly, Keating *et al.* found that inhibition of either RTK (Axl or Mer) resulted in a similar phenotype with increased apoptosis and apoptotic biochemical markers as well as decreased astrocytoma cell survival in functional assays

(Keating et al., 2010). Together, these data suggest that upon activation, Mer RTK may induce phosphorylation of the PI3K/AKT and MAPK pathways, which, as described earlier, are involved in cell proliferation and migration. Since IGFBP7 induced proliferation and migration in HOMECs, it is possible that Mer RTK may be involved in these processes. However, these exciting preliminary experiments need to be repeated in the future and tested using functional studies to verify a role for Mer RTK in IGFBP7-treated HOMECs.

Although a role for Mer RTK in angiogenesis has not been reported yet, Axl RTK (family member of Mer) has been found to be activated in the induction of angiogenesis. Holland *et al.* 2005 reported that Axl knockdown significantly reduced growth arrest-specific protein 6- (Gas6, a ligand for Axl RTK)-induced HUVEC proliferation and impaired EC-tube formation when co-cultured with pulmonary artery smooth muscle cells. A similar observation was also found in mice where severe immunodeficient mice transplanted with Axl knockdown human dermal microvascular ECs failed to undergo neoangiogenesis (Holland et al., 2005). VEGF-A-induced corneal neovascularisation in mice was significantly reduced in Axl-knockout mice compared to wild-type mice, suggesting a role for Axl in VEGFA-dependent angiogenesis (Ruan and Kazlauskas, 2012). In another study, glioblastoma (GBM) xenografts containing a mutant Axl exhibited reduced gliomagenesis (Vajkoczy et al., 2006). *In vitro* experiments demonstrated a significant reduction in proliferation and migration of glioma cells U1242, U373, U118, and SF126 containing a mutant form of Axl compared to wild-type Axl RTK (Vajkoczy et al., 2006). These results suggest that Axl kinase activity is important for regulating both EC and tumour cell growth, migration and angiogenesis.

Interestingly, Axl activation has been shown to induce activation of the PI3K/AKT and ERK1/2 in several cell lines. Ruan and Kazlauskas reported Axl RTK to be a contributor to VEGF-A-dependent activation of the PI3K/AKT pathway in HUVECs (Ruan and Kazlauskas, 2012). The Gas6/Axl/PI3K/AKT pathway was shown to protect mouse embryonic fibroblast NIH3T3 cells from apoptosis by phosphorylating and inactivating a pro-apoptotic protein BCL2-associated agonist of cell death (Bad) (Goruppi et al., 1999). Gas6-Axl-mediated activation of AKT has been reported to inhibit pro-apoptotic caspase-3 and induce phosphorylation of NF-kB that increases expression of the anti-apoptotic proteins B-cell lymphoma 2 and B-cell lymphoma-extra-large in primary HUVECs

(Hasanbasic et al., 2004). Axl activation has also been shown to induce cell proliferation via activation of the ERK1/2 pathway. Stimulation of ERK and p38 kinases by Axl is attributed, in part, to its ability to bind to the adapter protein Grb2 (Fridell et al., 1996). However, there is no report of activation of RTK Axl by IGFBP7 in any cell model. In this study, the data indicate that IGFBP7 induces proliferation, migration and tube-formation in HOMECs, and migration is mediated via activation of the ERK1/2 pathway. This may indicate a role of active Axl and/or Mer RTK in IGFBP7-induced cellular functions in HOMECs. Therefore, this preliminary data should be investigated further using immunocytochemistry and immunoprecipitation to detect the presence of Axl and/or Mer RTKs and identify and assess their role in functional studies such as proliferation, migration and angiogenesis. Taken together, these preliminary data may suggest that each RTK may act individually or in combination with other RTKs in mediating the induction of proangiogenic responses in HOMECs treated with IGFBP7.

A summary of the data from this chapter are described in figure 6.14.

6.5 Conclusion

As the current literature has conflicting data on the role of IGFBP7 in tumour progression, it was necessary to identify its role in HOMECs. In this study, IGFBP7, a factor secreted by ovarian cancer cell lines, has been demonstrated to induce proangiogenic changes in HOMECs via activation of the ERK1/2 pathway. Interestingly, the preliminary data suggest that IGFBP7 induced activation of several RTKs including VEGFR2, c-RET, Mer (TAM) and ALK, which need to be examined further. This may shed light on novel receptors of IGFBP7 in HOMECs that may be utilised as potential targets in anti-angiogenic therapy in ovarian cancer metastasis.

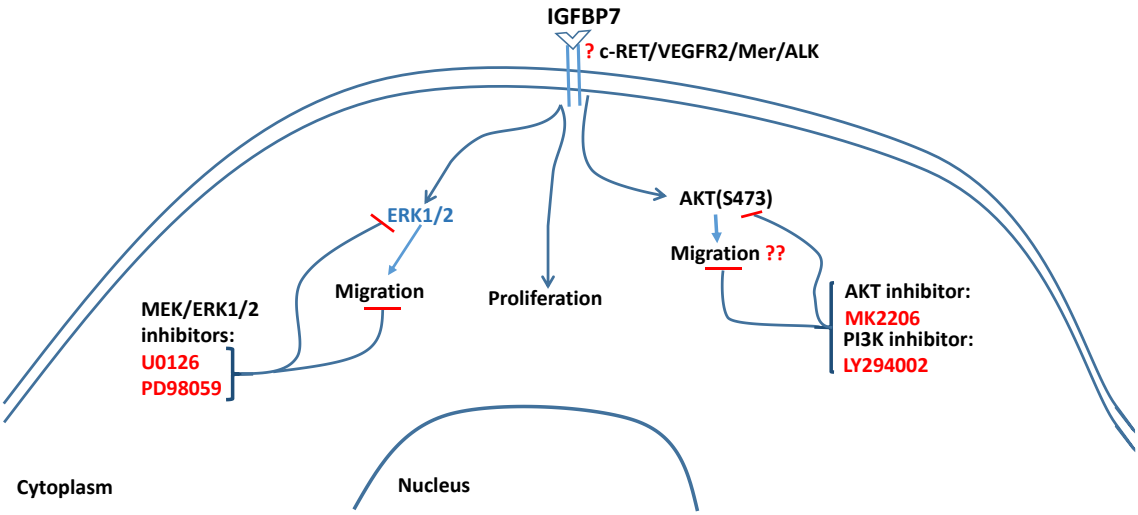

Figure 6.14: **A summary of IGFBP7-induced activation of the ERK1/2 and AKT pathways, and their potential role in mediating cellular functions in HOMECs.** IGFBP7 possibly activates receptor tyrosine kinases: c-RET, VEGFR2, Mer and ALK on the cell surface membrane of HOMECs which leads to phosphorylation of ERK1/2 and AKT. The ERK1/2 activation may mediate cellular migration in HOMECs in response to IGFBP7, since the MEK/ERK1/2 inhibitors U0126 and PD98059 significantly reduce cell migration and activation of ERK1/2. Both PI3K inhibitor LY294002 and AKT inhibitor MK2206 inhibited phosphorylation of AKT at Ser473 (S473) in IGFBP7-treated HOMECs. However, the role of AKT in mediating IGFBP7-induced migration is not clear in HOMECs. IGFBP7 also induces proliferation, although the activating signalling cascades have not yet been investigated.

Chapter 7 General Discussion

Angiogenesis is vital in tumour metastasis. A lack of oxygen in the local tumour microenvironment due to increased demand by tumour cells elicits a pro-angiogenic response in the local microvasculature of the affected organ. Although both pro- and anti-angiogenic factors are secreted by both local cells and tumour cells, the ratio is in favour of the proangiogenic factors such as VEGF and bFGF. This cohort of proangiogenic factors triggers activation of ECs from existing local microvasculature, inducing secretion of proteases that aid matrix digestion, allowing ECs to migrate towards the secondary tumour foci. These proangiogenic factors also induce EC proliferation and enhance migration, forming sprouts or branches of neovessels, feeding the tumour cells to grow and invade further.

EOC cells have been shown to secrete VEGF and hence the monoclonal anti-VEGF antibody bevacizumab was developed to block angiogenesis at advanced disease stage. However, due to severe toxicity and side effects, this treatment has significant drawbacks. Also, recently Winiarski *et al.* reported that despite blocking the VEGF/VEGFR axis, significant angiogenesis was observed in HOMECs when treated with EOC conditioned media, suggesting that there are factors, other than VEGF, that might be involved in this process (Winiarski et al., 2013). Subsequent studies revealed that EOC cells secrete proteases CathL and CathD, and IGFBP7 all of which have a potential role in angiogenesis. This current study hypothesised that these EOC-secreted factors play a role in tumour angiogenesis during metastasis of EOC to the omentum, and therefore examined the effects of these proteins on HOMEC proliferation, migration and the signalling pathways involved.

CathL, a cysteine protease, has been shown to increase HOMEC proliferation. This is an interesting observation as CathL is a protease that works at an acidic pH inside cellular lysosomes. However, CathL has been reported to be present at a higher concentration in the plasma of ovarian cancer patients compared to normal patients. Published data from our lab also demonstrated increased

expression of CathL in the omental tissue and the microvasculature in advanced EOC patients, compared to EOC with benign tumour or healthy participants.

Since CathL was detected in the tumour conditioned media and in ascites, it was thought that this protease may have a proangiogenic role in HOMECs. Intriguingly, CathL was found to induce HOMEC proliferation. This phenomenon was initially thought to occur via CathL-proteolytic activity. Indeed, CathL-proteolytic activity was observed at a range of pHs including pHs 4 (optimum) and 7 (pH of cell culture media) and the CathL-proteolytic specific inhibitor FY-CHO completely abolished proteolytic activity at all pHs (3-7.6). However, in the presence of FY-CHO, no inhibition of proliferation was observed, suggesting that CathL is acting in a way that is independent of its proteolytic activity. This suggestion was supported by the observation that CathL induced phosphorylation of MAP kinase ERK1/2 and p38α, and AKT (S473) at 4 minutes after treatment. These kinases are downstream of RTKs, which are known to be activated by growth factors such as EGF and VEGF. Interestingly CathL was shown to activate RTK Tie-1, part of the angiopoietin/Tie-1 axis, which often plays an important role in angiogenesis, as discussed before. This suggests for the first time that CathL may play a mitogenic role in a non-proteolytic manner, possibly via yet an unidentified allosteric site.

Since CathL induced activation of ERK1/2, it was thought that this MAPK may play a role in CathL-induced HOMECs proliferation. Indeed, activation of ERK1/2 was found to mediate CathL-induced cellular proliferation. Interestingly, PI3K, but not AKT, activation was also shown to play a role in CathL-induced HOMEC proliferation. As discussed before, activation of PI3K and, particularly, ERK1/2 are well-known signalling events in cellular proliferation. Additionally, activated ERK1/2 was also shown to mediate cellular migration. Although the PI3K/AKT pathway is known to be activated in cellular migration in other systems, in CathL-induced HOMEC migration, this was not the case. In recent years, activated ERK1/2 has been highlighted as a pro-migratory kinase in several cell models. The study in this thesis is the first to demonstrate a role for CathL in inducing both proliferation and migration of microvascular ECs in a non-proteolytic manner.

The cell surface receptor target for this protein remains unconfirmed. Although Tie-1 was observed to be phosphorylated, it is essential to validate this

preliminary detection and identify other possible receptors involved in mediating the activation of downstream signalling pathways in HOMECs, inducing pro-angiogenic changes. This may reveal potential novel targets for anti-angiogenic therapies. To test this, initially, a commercially available Human Receptor Tyrosine Kinase Array (R&D) could be performed, along with immunoprecipitation and immunocytochemistry. This could be followed by subsequent functional studies (e.g. proliferation and migration of HOMECs) whereby specific receptors will be targeted either by using a competitive blocker of the receptor or a receptor- kinase inhibitor. This data may then be complemented by knockdown studies, utilising siRNAs to knockdown expression of identified receptor-specific genes, followed by testing cell proliferation and migration with corresponding protein treatments.

In these future studies, cellular proliferation could be examined using other techniques. For example, HOMECs can be stained with BrdU or fluorescently labelled anti-Ki-67 (cell proliferation marker) antibody and cell proliferation could be measured using flow cytometry. This is a more reliable method as it allows quantitative analysis of number of cells increased in a treatment. Cellular migration could also be examined using other techniques such as wound-healing assays, which allows visualisation of migratory cells and hence a more direct measurement of cell migration.

Work investigating a role of CathL in HOMEC angiogenesis led to the identification of another potential proangiogenic candidate Gal1. Previously, unpublished data from gene sequencing experiments suggested a differential expression of Gal1 mRNA (LGALS1) in HOMECs when treated with CathL. This raised the question whether CathL induces an increase in the expression and/or production of Gal1 in HOMECs. A commercially available ELISA was used to test for secreted levels of Gal1 from HOMECs when treated with CathL. Interestingly, an increase in Gal1 secretion was observed in CathL-treated HOMECs (compared to control), which was later found to be transcriptionally-regulated. To our knowledge, this is the first study to report Gal1 production and secretion in CathL-treated cells.

According to the literature, Gal1 has been found to be secreted from different cell types (discussed before) and also in mice models when oxidative stress or hypoxia is applied. However, in this study, exogenous CathL increased this

secretion, which could mean that CathL activates yet an unknown signalling pathway that induces upregulation of Gal1 mRNA, followed by its secretion. One possible signalling pathway that may be involved upstream of LGALS1 expression is p38α. p38α has been shown to be activated by both intracellular (mitochondrial reactive oxygen species) and extracellular (e.g. hypoxia) stress, and Gal1 has been shown to be secreted by induced-stress in mice and *in vitro* cell models. Also, NFκB activation has been detected in the upstream of LGALS1 expression, both in the current studies and other published works, as discussed above. Since CathL activates p38α, it could be possible that this kinase is responsible for the activation of NFκB and hence an increase in LGALS1 expression and subsequent Gal1 secretion. However, this needs to be further verified by ELISA or western blotting technique with inclusion of inhibitors of p38α.

The secretion process of Gal1 also remains a mystery. It had been shown that Gal1 is not secreted via the conventional ER/Golgi secretory pathway. In this current study, a significant level of Gal1 was secreted despite breakdown of the Golgi body, suggesting that in HOMECs, Gal1 secretory pathway is independent of the classical route, agreeing with the previous reports. However, this should be investigated further. Firstly, the intracellular localisation of Gal1 should be examined by immunocytochemistry. If it reveals an area concentrated with Gal1 proteins, it may indicate that Gal1 is produced/stored within that particular compartment. For example, it has been shown that glycoproteins (integrins) are internalised and recycled in the perinuclear recycling endosomal compartments (Caswell et al., 2009). Since Gal1 is a glycoprotein that interacts with integrins and also is expressed at cell surface membrane, it could be possible that trafficking and subsequent secretion of Gal1 is regulated in a similar manner as cellular integrins. This requires further research such as immunochemical detection of Gal1 within HOMECs. Following visualisation of Gal1, co-localisation studies can be performed combining specific antibodies targeting particular organelles or compartments and Gal1. Once identified, the pathway can be inhibited or the organelle can be destabilised using a pharmacological inhibitor, followed by measurement of the secreted levels of Gal1 in the cell supernatant. This may unveil a new area of focus in the future.

As Gal1 was found to be secreted from HOMECs by CathL treatment, it was thought that Gal1 may induce a proangiogenic response in these cells. Firstly, proliferation assays were carried out, which revealed that Gal1 induced HOMEC proliferation via both ERK1/2 and PI3K, but not AKT, pathways. Additionally, Gal1 was also found to induce HOMEC migration. These functional studies suggested an autocrine mechanism which Gal1 utilises to induce such proangiogenic responses. This begged a question whether CathL-induced proangiogenic responses are dependent on Gal1. To test this, HOMEC proliferation was examined in the presence of L-glucose (binds to Gal1) and CathL or Gal1. Intriguingly, Gal1-induced HOMEC proliferation was inhibited in the presence of L-glucose, however, no inhibition was observed in CathL-treated cells. This suggested, for the first time, that CathL may induce HOMEC proliferation in a manner that is independent of Gal1 activity. However, both proteins (exogenously added) may produce an additive effect in inducing cell proliferation which has not been tested yet. Also, CathL-induced cell migration in HOMECs was not tested in the presence of L-glu, which should be examined in the future to determine whether CathL-induced HOMEC migration is dependent on Gal1.

Since L-glu inhibited both Gal1-induced HOMEC proliferation and migration, it may be suggested that Gal1 interacts with a cell surface receptor displaying a sugar residue in its N-terminal domain. Indeed there are a number of studies (cited in Chapter 4) that demonstrated interaction of Gal1 with integrins and neuropilin-1 (a co-receptor of VEGFR2), activating proangiogenic pathways. This could be further investigated in HOMECs by repeating the RTK array kit (as discussed above), followed by immunoprecipitation and immunocytochemistry. Additionally, enzymes that break down glucose residues on the cell surface membrane, such as hyaluronidase and neuraminidase, could be used to examine Gal1-induced proangiogenic events in HOMECs. This may reveal whether Gal1 acts on a cell surface receptor containing a sugar residue in HOMECs.

Although Gal1 induced HOMEC migration, neither ERK1/2 nor AKT activation was observed to play a role in this, suggesting that other signalling pathways may be involved in this process and/or a combination of activated kinases may play a role. This could be further investigated using a commercially available phosphokinase array kit, which will allow identification of activated kinases in

Gal1-treated HOMECs, followed by ELISAs to validate the array data. Subsequent migration experiments may be carried out in the presence of pharmacological inhibitors to test for the role of activated signalling kinases.

The unique relationship between CathL and Gal1 could be researched further as both of these proteins have been shown, for the first time, to be involved in proangiogenic responses in HOMECs and therefore may be involved in EOC metastasis. Gal1 has already been reported to induce tumour angiogenesis in several cancer models. However, a non-proteolytic proangiogenic role for CathL along with it eliciting Gal1 production and secretion, is exclusive in this study. Therefore, both CathL and Gal1 could be further examined as discussed above and explored with regards to identifying novel anti-angiogenic therapies in EOC metastasis in near future.

Another potential proangiogenic factor that was investigated in this study was CathD, an aspartic protease that resides in the acidic milieu of lysosomes. This thesis investigated its role in inducing proangiogenic responses in HOMECs. Interestingly, CathD was found to induce both proliferation and migration in HOMECs, possibly via a mechanism that is independent of its proteolytic activity. Whether CathD acts via its native proteolytic mechanisms or not was tested at a range of pHs in the presence of an inhibitor, pepA. Interestingly, CathD was found to be inactive at pHs similar to that of the cell culture conditions, suggesting that CathD is also acting in a non-proteolytic manner, an important observation that agrees with the current literature. However, further work is needed to examine and identify an as yet unknown non-proteolytic, mitogenic mechanism.

Additionally, CathD was found to activate both ERK1/2 and AKT pathways in HOMECs. To my knowledge, this is the first study to demonstrate such as observation in a vascular EC model. Further investigation demonstrated that these pathways are activated in CathD-induced HOMEC proliferation and migration. Additionally, investigation of the activated RTK by CathD revealed an increased level of phosphorylated RET RTK in HOMECs. As discussed previously, this RTK is upstream of ERK1/2 and PI3K/AKT kinases which are known to be involved in mediating cell proliferation and migration, and hence it

may be suggested, for the first time, that CathD mitogenically induces a proangiogenic response in HOMECs via activation of RET RTK. However, the receptor target for CathD should be further investigated in future studies to confirm and validate this observation.

In the current study, ovarian tumour-secreted factor IGFBP7 was also examined for its potential role in proangiogenic changes in HOMECs. IGFBP7 has been found to increase HOMEC proliferation and migration. Due to time constraints, the signalling pathways involved in IGFBP7-induced cellular proliferation have not been elucidated in this study, however, cellular migration was observed to occur via activation of the ERK1/2 pathway. As discussed above, the activated ERK1/2 kinase plays a key role in cellular migration. However, IGFBP7-activated signalling pathways could be investigated further in both HOMEC proliferation and migration as the current literature has conflicting data on its role in angiogenesis.

Interestingly, when tested, IGFBP7 was found to activate VEGFR2 in HOMECs. This was further tested using WST1 proliferation assay in the presence of SU5416, a potent inhibitor of VEGFR2 tyrosine kinase. Intriguingly, SU5416 significantly reduced IGFBP7-induced HOMEC proliferation, suggesting, for the first time, that IGFBP7 may act on VEGFR2 to induce proangiogenic changes in HOMECs. However, the receptor target should be examined further as discussed above.

Development of an appropriate *in vitro* angiogenesis model

Since angiogenesis plays a significant role in aiding tumour metastasis, an attempt was made to investigate sprouting (3D model) or tube-forming (2D model) capabilities of HOMECs when treated with the selected tumour secreted factors. Unfortunately, it was not possible to optimise the right model to study HOMEC angiogenesis in this report. However, when tested with human brain microvascular ECs, sprouting was observed in the 3D model using a fibrin matrix, which was completely absent in HOMECs. This could be explained by the heterogeneity that exists between ECs from different vascular beds and organs, which suggests that an EC type requires a particular niche that suits their normal

functions. A commercially available growth factor reduced-matrigel was also used to test tube-formation. However, it was shown to be an ineffective method to test for proangiogenesis as the gel contains, albeit in very low concentrations, potent growth factors which enhanced tube-like structures in basal media in HOMECs in the 2D assay.

The 3D *in vitro* model used to study angiogenesis in this report was mainly constituted of fibrin matrix. This is a well-known matrix used in the angiogenic studies of different EC models. Since this model failed to establish angiogenesis in HOMECs, a different model will need to be proposed in the future. Alterations that could be made are addition of laminin and/or fibronectin in the matrix mix.

Laminins are multifunctional matrix molecules that are widely expressed, forming the major scaffold of the basement membrane. There are different types of laminins which display organ, site and developmental specificity (Simon-Assmann et al., 2011). For example, in most tissues, only laminin-411 (α4 chain) and -511 (α5 chain) are found in the endothelial basement membrane. However, formation of new blood vessels during angiogenesis requires degradation of the BM, a process in which ECs are exposed to other laminin isoforms such as laminin-111 (α1 chain), reviewed in (Simon-Assmann et al., 2011). Laminin-411 is a specific high affinity ligand for αvB3 and α3β1 integrins, which enhance EC-ECM interactions aiding cell adhesion and migration. Using dermal microvascular EC, Li *et al.* reported that laminin-411 promoted cell spreading and migration in a scratch wound assay and accelerated angiogenic tube formation in collagen gel overlay assays (Li et al., 2006). Therefore, a mixture of laminin-411, -511 and a low concentrations of -111 isoforms could be used to constitute a fibrin-based gel to test for both 2D (tube formation) and 3D *in vitro* sprouting angiogenesis assay using HOMECs.

As developing microvessels enter different stages of maturation, the ECM around them undergoes complex structural and compositional changes that may influence the ability of ECs to respond to growth factors and organise into capillary tubes. One of the major components of the provisional ECM of developing microvessels is fibronectin (Nicosia et al., 1993). As a result of its

multiple binding sites for ECs and other ECM proteins, fibronectin functions as an adhesive scaffold for the migration of ECs. Fibronectin has been shown to bind VEGF-A and support directed migration of EC tip cells (Mettouchi, 2012). In the presence of both fibrin and fibronectin, cells with actin filament stress fibres were more spreading than those in fibrin (Fournier and Doillon, 1992). In an *ex vivo* study using rat aorta, fibronectin incorporated in the collagen gel promoted a selective dose-dependent elongation of the newly formed microvessels without stimulating vascular proliferation. The fibronectin-treated microvessels were longer due to a proportional increase in the number of microvascular cells (Nicosia et al., 1993). However, fibronectin had no effect on microvascular DNA synthesis and mitotic activity. Therefore, a 2D or 3D *in vitro* angiogenesis model could be developed by incorporating fibrin matrix and fibronectin to examine angiogenic tube formation or sprouting of microvessels in HOMECs. Currently there is no method available to test for angiogenic tube-formation or sprouting in HOMECs, and hence it is a potential project for future studies.

Further work and potential projects

As discussed before, metastasis of EOC cells to the omentum requires a microenvironment that aids their attachment to the mesothelium of the omentum and enhances invasion and metastasis. Cancer cells secrete factors that activate surrounding cells within the stroma which actively support tumour progression such as fibroblasts, pericytes, ECs, diverse immune cells and adipocytes. Although the focus of this thesis was to investigate roles of tumour-secreted factors on omental angiogenesis, it should be noted that proangiogenic effects of local fibroblasts or, in this case, cancer activated fibroblasts (CAFs) may significantly contribute to the pathogenesis process. For example, it has been shown that CAFs possess high contractile ability, promote angiogenesis, and stimulate epithelial cell growth via production of ECM and secretion of growth factors and cytokines such insulin-like growth factor 1, VEGF and hepatocyte growth factor 1 (Mueller and Fusenig, 2004). CAFs have also been shown to increase proliferation and migration of tumour cells. These functions of CAFs are observed in breast, colon, oral, pancreatic, bile duct, prostate, skin cancers and ovarian (primary) tumour (Yeung et al., 2015). However, there is a lack of

understanding of how CAFs may interact with migrant ovarian tumour cells and microvascular ECs at the metastatic site- omentum. Since angiogenesis in the metastatic site is key to metastasis, CAF-induced tumour angiogenesis could also be examined, possibly by combining tumour conditioned media and CAFs in co-cultured HOMECs. This may reveal a more physiological scenario of the omental microenvironment that aids advanced ovarian cancer progression.

Another key cell type within the omentum is adipocytes. EOC cells preferably metastasise to the omentum, a pad of fat cells, in 80% of serous ovarian carcinoma patients, suggesting that this is not a random event. The adipocytes which are in close proximity to cancer cells are called cancer-associated adipocytes (CAAs). A number of studies have investigated potential cross-talks between CAAs and ovarian tumour cells. For example, Nieman and colleagues reported that CAAs promote homing, migration, and invasion of ovarian cancer cells, possibly by secreting soluble factors such as tumour necrosis factor-α, IL6, IL8 and monocyte chemoattractant factor-1 (Nieman et al., 2011). Also, CAAs were shown to provide energy for the tumour cells to grow via stimulating mitochondrial metabolism in these cells (Yeung et al., 2015).

Although research has been carried out on investigating the interaction between ovarian cancer cells and omental adipocytes, very little is known about the cross-talk events between HOMECs and the host adipocytes. As adipocytes provide energy to cells and promote tumour cell proliferation and migration, it is reasonable to speculate that the omental fat cell-secreted factors could also induce angiogenesis. Therefore, it would be very interesting to investigate the role of adipocytes (or their secreted adipokines and free fatty acids) on HOMEC survival, migration, proliferation, and hence angiogenesis, in future studies. This could be followed by further studies whereby EC function in angiogenesis could be tested in a combination of tumour conditioned media as well CAFs conditioned media along with CAAs, which should produce a more physiological *in vitro* model of metastatic EOC microenvironment within the omentum.

Another potential study that could be carried out using HOMECs is to examine the effects of pericytes. Tumour microvessels tend to be leaky due to an unstable basement membrane and lack of organised pericytes surrounding the endothelium (Cooke et al., 2012). These “leaky” vessels allow tumour cells to enter the circulation and hence aid tumour invasion and metastasis. Therefore, transendothelial electrical resistance could be used to measure the integrity of tight junction dynamics in HOMEC monolayers treated with tumour secreted factors such VEGF, CathL, CathD and IGFBP7, or HOMEC-secreted proangiogenic factor Gal1. This experiment could also be carried out in a transwell co-culture system with pericytes (from omentum) growing on the underside and HOMECs on the top chamber of the transwell, which will create a more physiological milieu of the microvessels. This could be combined with ovarian tumour cell conditioned media or individual secreted factors to test for induced permeability in EC monolayer under different conditions. As not much is known about the secreted factors in the angiogenic process of ovarian cancer metastasis involving the microenvironment at the secondary site, a combination of the aforementioned studies could shed light in the gap of information that currently exists.

Despite ongoing efforts to develop effective surgery and treatment regimens for advanced EOC, the overall survival rate (5 year) remains a dismal 45%, which in large part results from diagnosis at a late stage. When ovarian cancer is detected at an early stage (tumour tissue is confined to one or both ovaries), the cure rate with conventional therapies such as cytoreductive surgery and chemotherapy, is as high as 90%. However, after the disease has spread to peritoneal organs, particularly the omentum, the cure rate decreases substantially owing to the limited efficacy of optimal debulking and tumour management. Also, chemoresistance poses a greater challenge, limiting the overall treatment efficacy. Therefore, understanding the molecular mechanisms that enhance tumour progression and metastasis at the secondary site is crucial, so that therapeutic interventions may be developed against the components of the tumour microenvironment. Although anti-VEGF therapy bevacizumab was developed to block angiogenesis in advanced disease, it was shown that VEGF is not solely responsible for the proangiogenic response in omental metastasis. Therefore, this thesis investigated potential proangiogenic factors (CathL, Gal1,

CathD and IGFBP7) and their roles in tumour-angiogenesis. This work may explain the lack of success in treating advanced ovarian cancer, as these novel factors have been clearly shown to induce proangiogenic responses in HOMECs *in vitro*. However, a greater understanding of the processes involved in omental angiogenesis and metastatic tumour growth could lead to improvements in the treatment and prognosis of ovarian cancer patients.

A summary diagram depicting the overall data are described in figure 7.1:

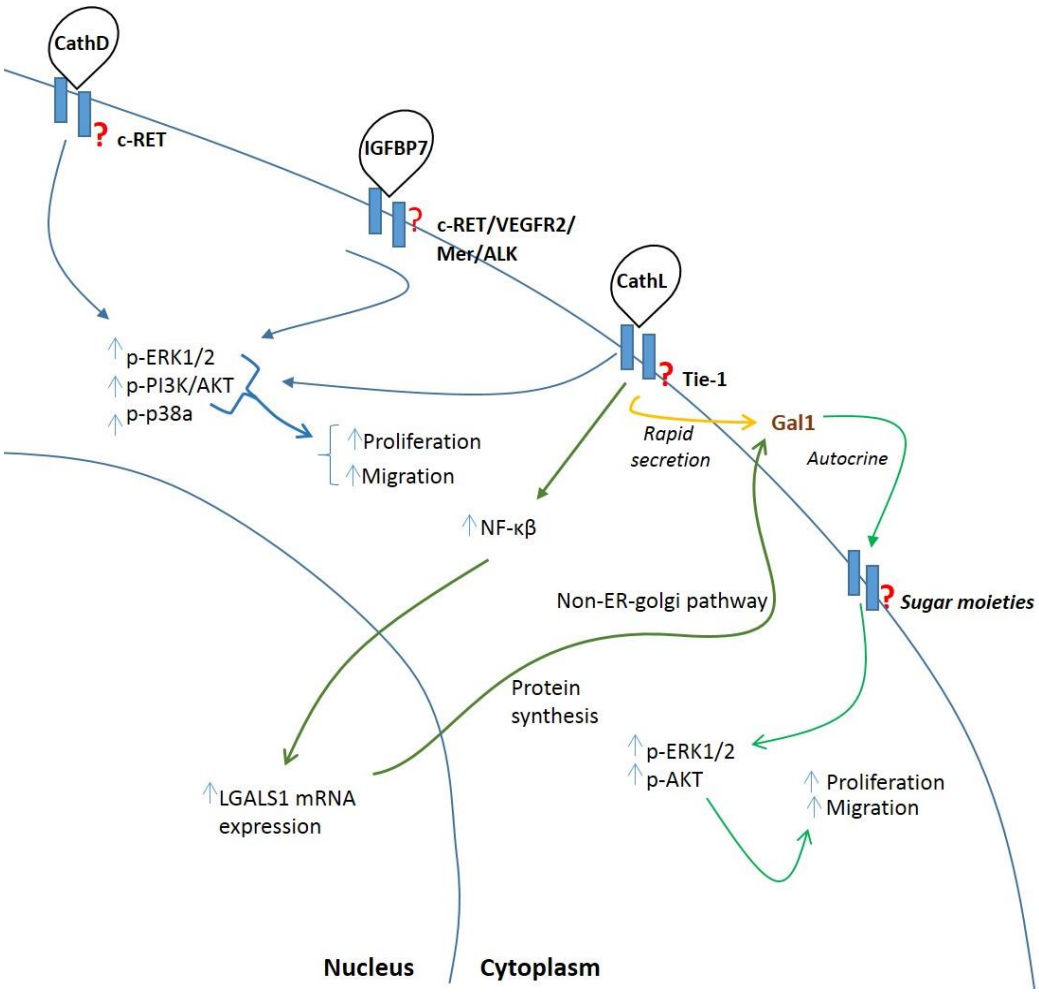

Figure 7.1: **A summary of ovarian cancer secreted factors (CathL, CathD and IGFBP7) and CathL-induced HOMEC-secreted factor Gal1, and their potential role in mediating cellular functions in HOMECs.** Ovarian tumour-secreted factors CathL, CathD and IGFBP7 induce HOMEC proliferation and migration, possibly via activation of the ERK1/2 and/or AKT pathways. This thesis suggest that both proteases (e.g. CathL and CathD) act via an unknown mechanism that is independent of their proteolytic activity. Preliminary investigation suggested an activation of receptor tyrosine kinases (e.g. c-RET, Tie-1, VEGFR2, Mer and ALK; as shown) by these tumour-secreted factors in the upstream of the aforementioned cellular responses. Interestingly, CathL was found to induce secretion of Gal1 over 30 mins and 8 hours. After 30 mins, CathL was thought to induce a rapid secretion of Gal1 from HOMECs via an unknown mechanism (yellow arrow). However, Gal1 secretion at the latter time-point (8 hours) was thought to be transcriptionally regulated. Indeed, CathL was found to induce an increase in the expression of Gal1 mRNA (LGALS1) via activation of NFκB, which led to the secretion of Gal1 via a non-ER-Golgi pathway from HOMECs (olive arrow). Interestingly, secreted Gal1 was found to be pro-proliferative and pro-migratory in HOMECs via an autocrine mechanism, probably by acting through a receptor with extracellular sugar moieties. Gal1-induced phosphorylation of ERK1/2 and AKT kinases was shown to mediate these cellular responses in HOMECs. Overall, this thesis suggests an increased proangiogenic responses in HOMECs, induced by CathL, Gal1, CathD and IGFBP7. ER; endoplasmic reticulum, ALK; anaplastic lymphoma kinase.

Appendix 1

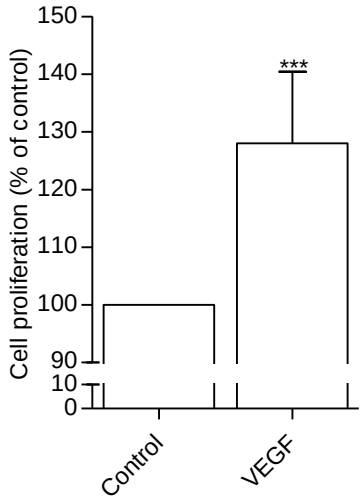

Figure A1.1: **Increased proliferation of HOMECs in media supplemented with VEGF (positive control) (WST-1 assay).** Cells were seeded in 2% gelatin pre-coated 96 well plates at a density of 10,000cells/well in starvation media containing 2% FCS. After overnight incubation, cells were treated with or without VEGF (20ng/ml) and incubated for 72 hours. A commercially available WST-1 kit was used to assess cellular proliferation based on absorbance using PHERAstar BMG plate-reader at 450nm. Results are mean ±SD and shown as percentage of the control, ***p<0.001 vs control (100%), n=18.

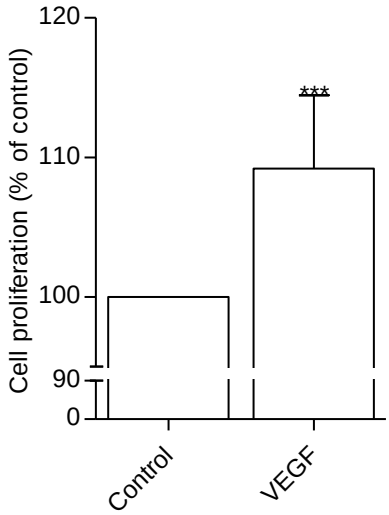

Figure A1.2: **Increased proliferation of HOMECs in media supplemented with VEGF (positive control) (CyQUANT).** Cells were seeded in 2% gelatin pre-coated 96 well plates at a density of 10,000cells/well in starvation media containing 2% FCS. After overnight incubation, cells were treated with or without 20ng/ml of VEGF and incubated for 72 hours. A commercially available CyQUANT reagent was used to assess cell proliferation based on fluorescence intensity using FLUOstar BMG plate-reader at Ex/Em: 485/530nm. Results are mean ±SD and shown as percentage of the control, ***p<0.001 vs control (100%), n=20.

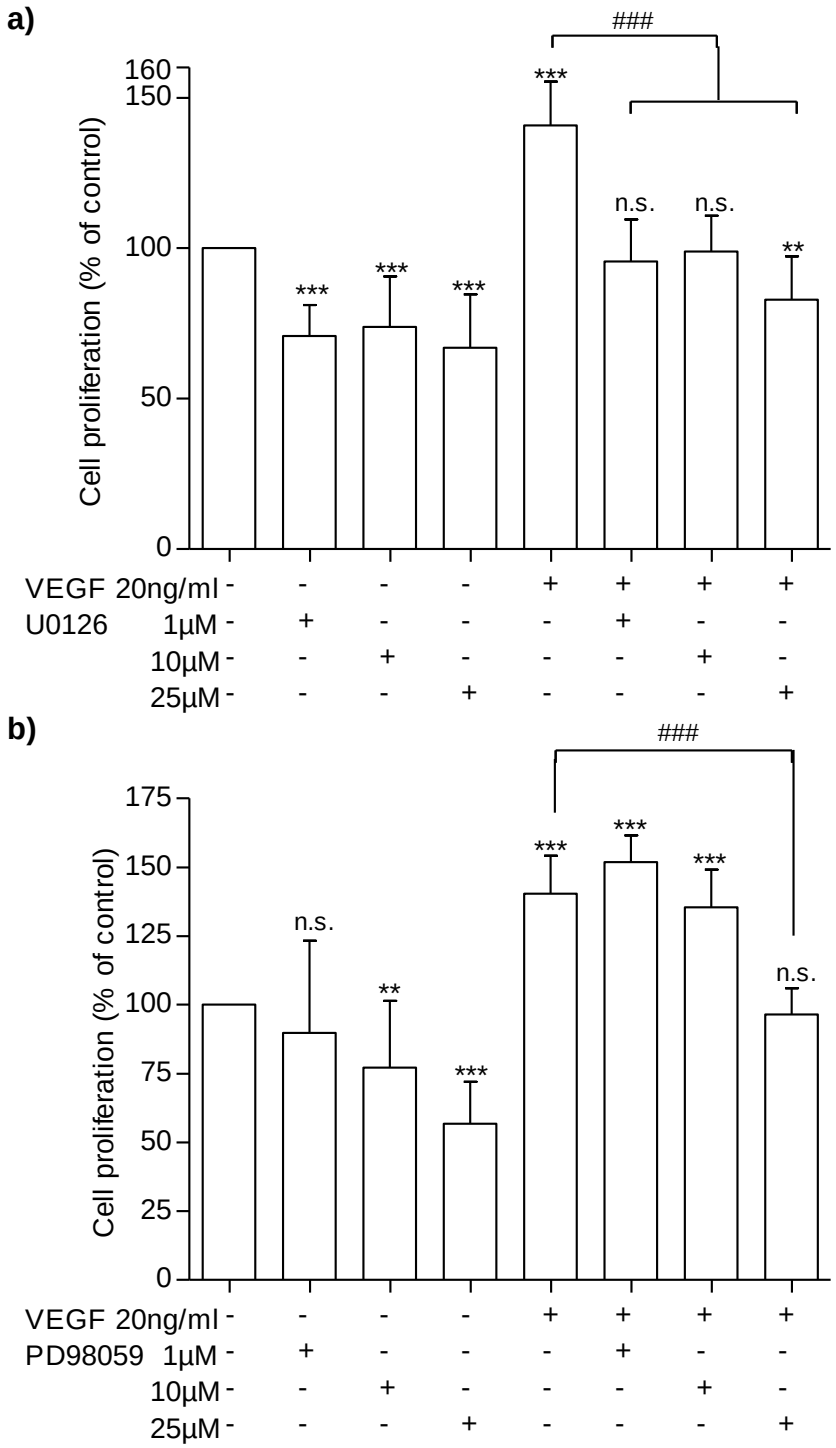

Figure A1.3: **Inhibition of ERK1/2 reduces positive control VEGF-induced HOMEC proliferation.** Cells were seeded in 2% gelatin pre-coated 96 well plates at a density of 10,000cells/well in starvation media containing 2% FCS. After overnight incubation, cells were treated with or without VEGF (20ng/ml) and in the absence or presence of various concentrations of ERK1/2 inhibitors **a)** U0126 and **b)** PD98059 as indicated above and incubated for 72 hours. WST-1 assay was used to assess cellular proliferation. Results are mean ±SD and shown as percentage of the control, n.s., **p<0.01, ***p<0.001 vs control (100%), ###p<0.001 vs VEGF (normalised to control 100%), n=7-13. n.s. denotes not significant.

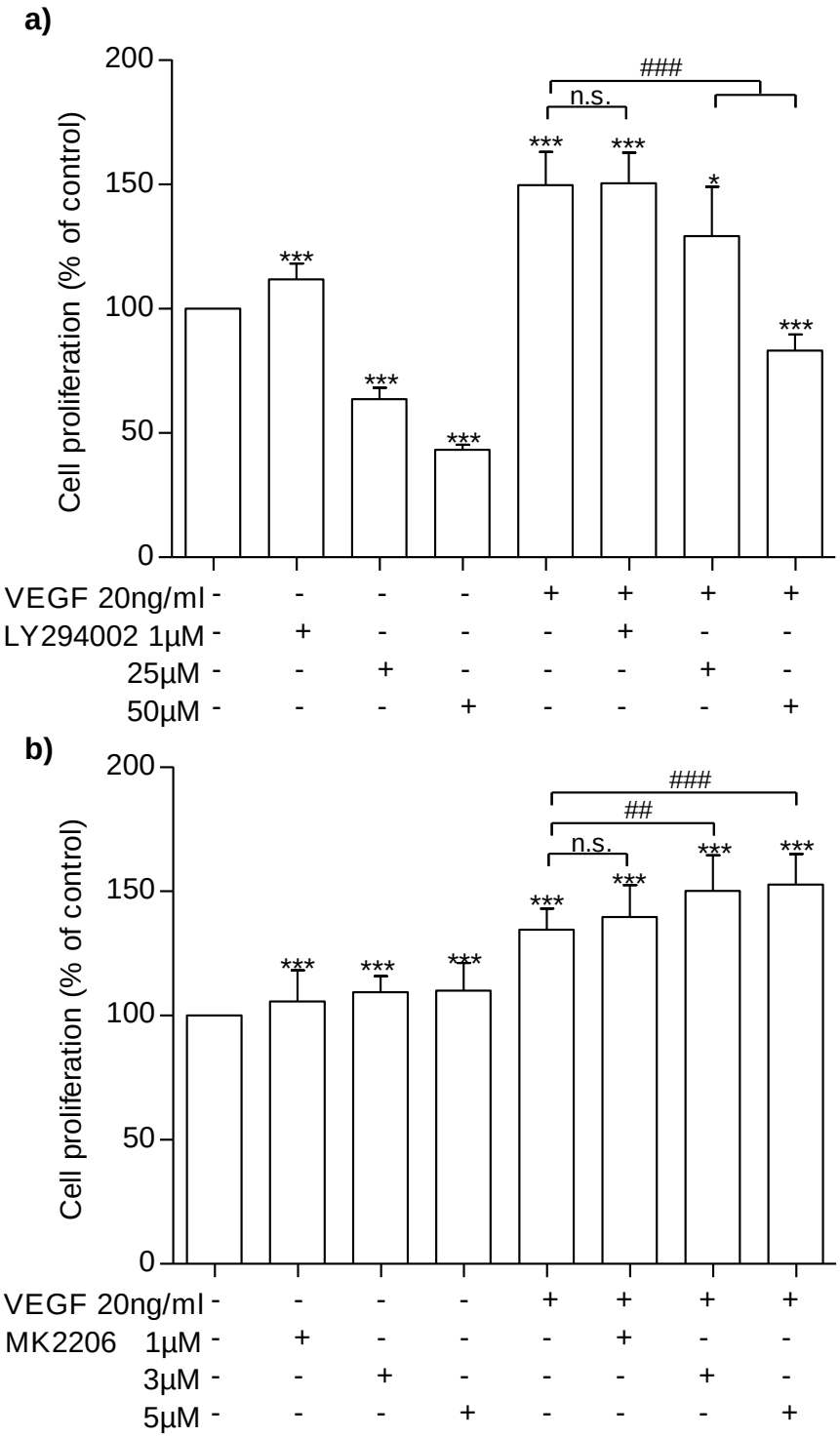

Figure A1.4: **PI3K inhibitor, but not AKT inhibitor, reduces positive control VEGF-induced HOMEC proliferation.** Cells were seeded in 2% gelatin pre-coated 96 well plates at a density of 10,000cells/well in starvation media containing 2% FCS. After overnight incubation, cells were treated with or without VEGF (20ng/ml) and in the absence or presence of various concentrations of **a)** LY294002 (PI3K inhibitor) and **b)** MK2206 (AKT inhibitor) as indicated above and incubated for 72 hours. WST-1 assay was used to assess cellular proliferation. Results are mean ±SD and shown as percentage of the control, *p<0.05, ***p<0.001 vs control (100%), n.s., ##p<0.01, ###p<0.001 vs VEGF, n=10-15 (normalised to control 100%). n.s. denotes not significant.

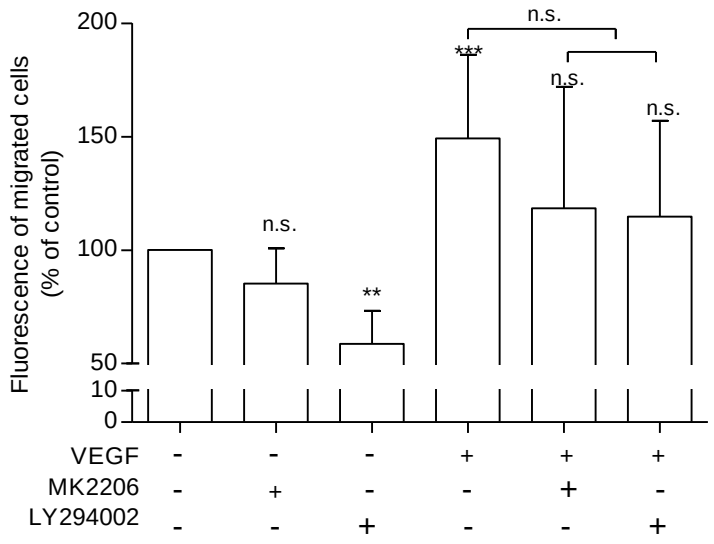

Figure A1.5: **Positive control VEGF does not induce HOMEC migration via the AKT pathway.** HOMECs were seeded in the upper transwell chamber and treated with or without VEGF (20ng/ml) in the absence or presence of PI3K and AKT inhibitors LY294002 (25 µM) and MK2206 (5 µM) respectively in media containing 0.5% FCS. The lower well contained correspondent treatments. After 6 hours, migrated cells were stained with calcein AM and fluorescence was quantified using a FLUOstar plate reader at Ex/Em: 485/520. Results are mean ±SD and shown as percentage of the control, n.s., **p<0.05, ***p<0.001 vs control (100%), n.s. vs VEGF (normalised to control), n=6-12. n.s. denotes not significant.

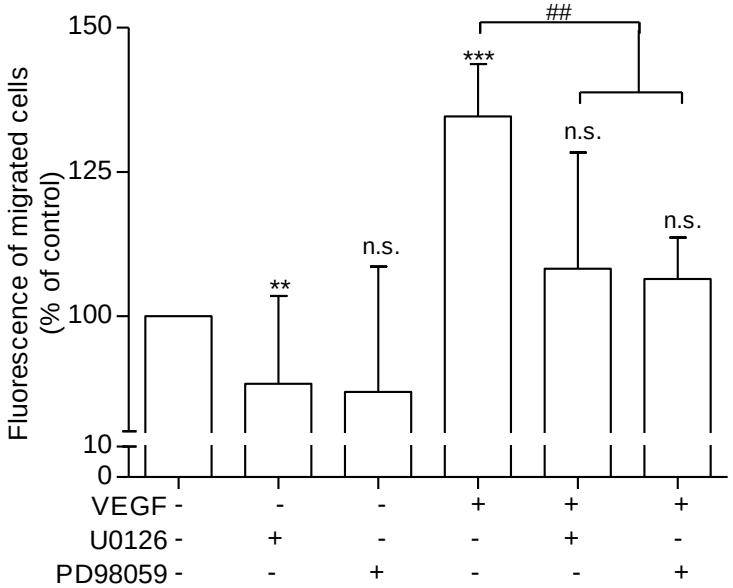

Figure A1.6: **Positive control VEGF induces HOMEC migration via the ERK1/2 pathway.** HOMECs were seeded in the upper transwell chamber and treated with or without VEGF (20ng/ml) in the absence or presence of ERK1/2 inhibitors U0126 (10 µM) and PD98059 (25 µM) respectively in media containing 0.5% FCS. The lower well contained correspondent treatments. After 6 hours, migrated cells were stained with calcein AM and fluorescence was quantified using a FLUOstar plate reader at Ex/Em: 485/520. Results are mean ±SD and shown as percentage of the control, n.s., **p< 0.01, ***p<0.001 vs control (100%), ##p<0.001 vs VEGF, n=7-9. n.s. denotes not significant.

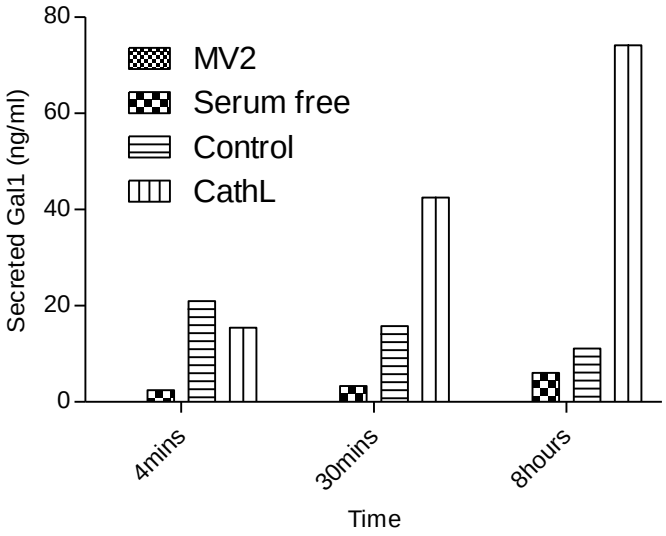

Figure A1.7: **CathL induces secretion of Gal1 in HOMECs.** Cells were seeded in 2% gelatin pre-coated 24-well plates at a density of 35,000 cells/well in starvation media containing 2% FCS. After overnight incubation, cells were treated with or without CathL (50ng/ml) and supernatants were collected after 4 minutes, 30 minutes and 8 hours treatment. A commercially available ELISA kit was used to assess the levels of secreted Gal1 using a SpectraMax plate reader. Results are represented as secreted Gal1 (ng/ml) (raw data from representative experiment). Gal1 was also measure in media only (without cells) (MV2) and in supernatant from serum-free media treatment.

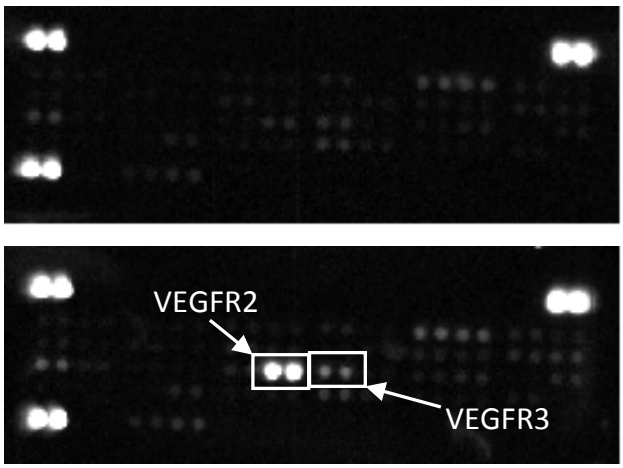

Figure A1.8: **Activation of RTK VEGFR2 and VEGFR3 in VEGF-treated HOMECs.** Representation of developed membrane using AzureSpot.

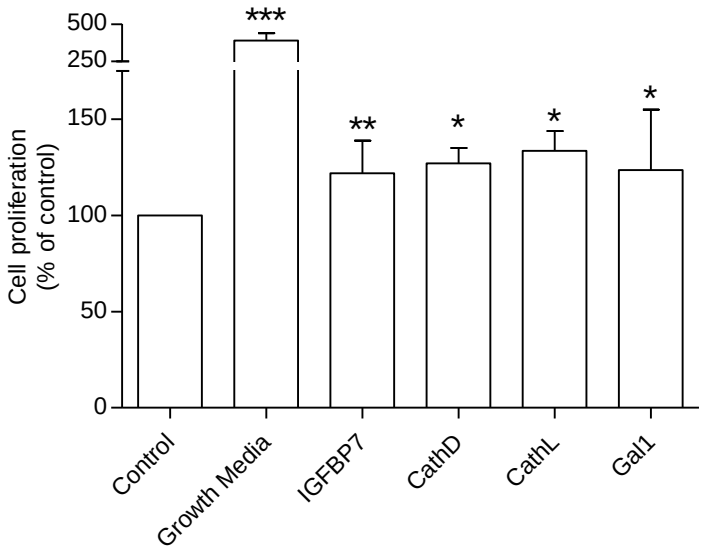

Figure A1.9: **Increased proliferation of HOMECs in media supplemented with treatments (BrdU assay).** Cells were seeded in 2% gelatin pre-coated 96 well plates at a density of 10,000cells/well in starvation media containing 2% FCS. After overnight incubation, cells were treated with or without growth media (positive control), IGFBP7 (50 ng/ml), CathD (50 ng/ml), CathL (50 ng/ml) and Gal1 (50ng/ml) and incubated for 48 hours. A commercially available BrdU reagent was added to the wells for the last 24 hour incubation and cellular proliferation was assessed (according to the manufacturer's instructions) based on fluorescence intensity using a SpectraMax plate-reader at Ex/Em of 450/550 nm. Results are mean ±SD and shown as percentage of the control, *p<0.05, **p<0.01, ***p<0.001 vs control (100%), n= 4-7.

Appendix 2

A2.1 Publication

Journal article

Pranjol, M. Z., Gutowski, N., Hannemann, M. & Whatmore, J. 2015. *The Potential Role of the Proteases Cathepsin D and Cathepsin L in the Progression and Metastasis of Epithelial Ovarian Cancer.* Biomolecules, 5, 3260-79.

Conference papers

Pranjol, M.Z.I., Gutowski, N. J., Hannemann, M. and Whatmore, J.L. 2017. *Cathepsins D and L Induce Proangiogenic Changes in Human Omental Microvascular Endothelial Cells.* The British Microcirculation Society Abstracts of the 66th annual meeting in University of Newcastle. Microcirculation, 24, 4.

Pranjol, Z., Gutowski, N., Hannemann, M. & Whatmore, J. 2015. *Tumour secreted factors cathepsins D and L induce pro-angiogenic changes in human omental microvascular endothelial cells (HOMECs) in ovarian cancer metastasis.* T26. European Journal of Cancer Supplements, 13(1), 44.

A2.2 Key presentations and achievements during PhD studies

Oral presentations

- "*Cathepsins D and L induce pro-angiogenic changes in human omental microvascular endothelial cells in epithelial ovarian cancer metastasis*"- 66th Annual **British Microcirculation Society** Meeting- Microvessels of the Heart, Newcastle, UK, 2016.

- "*Tumour secreted factors cathepsins D and L induce pro-angiogenic changes in human omental microvascular endothelial cells (HOMECs) in ovarian cancer metastasis*"- Conference on "Cellular and molecular mechanism of tumour–microenvironment crosstalk", **European Molecular Biology Organization (EMBO)**, Tomsk, Russia, 2015.

Poster presentations

- "*Cathepsin D induces migration in human omental microvascular endothelial cells (HOMECs)*"- 67th Annual British Microcirculation Society meeting, Birmingham, UK, 2017.

- "*Cathepsins D and L induce proangiogenic changes in human omental microvascular endothelial cells (HOMECs)*"- 65th Annual British Microcirculation Society meeting, Manchester, UK, 2015.

Travel awards

- Student Assisted Scheme Travel Award at 65th, 66th and 67th Annual British Microcirculation Society Meetings, UK.
- EMBO Travel Grant award, Tomsk, Russia.

References

ABEDI, H. & ZACHARY, I. 1997. Vascular endothelial growth factor stimulates tyrosine phosphorylation and recruitment to new focal adhesions of focal adhesion kinase and paxillin in endothelial cells. *J Biol Chem,* 272**,** 15442-51.

ABROUN, S., OTSUYAMA, K., SHAMSASENJAN, K., ISLAM, A., AMIN, J., IQBAL, M. S., GONDO, T., ASAOKU, H. & KAWANO, M. M. 2008. Galectin-1 supports the survival of CD45RA(-) primary myeloma cells in vitro. *Br J Haematol,* 142**,** 754-65.

ABU-SAFIEH, L., ABBOUD, E. B., ALKURAYA, H., SHAMSELDIN, H., AL-ENZI, S., AL-ABDI, L., HASHEM, M., COLAK, D., JARALLAH, A., AHMAD, H., BOBIS, S., NEMER, G., BITAR, F. & ALKURAYA, F. S. 2011. Mutation of IGFBP7 causes upregulation of BRAF/MEK/ERK pathway and familial retinal arterial macroaneurysms. *Am J Hum Genet,* 89**,** 313-9.

ABULAFIA, O., TRIEST, W. E. & SHERER, D. M. 1997. Angiogenesis in primary and metastatic epithelial ovarian carcinoma. *Am J Obstet Gynecol,* 177**,** 541-7.

ACHKAR, C., GONG, Q. M., FRANKFATER, A. & BAJKOWSKI, A. S. 1990. Differences in targeting and secretion of cathepsins B and L by BALB/3T3 fibroblasts and Moloney murine sarcoma virus-transformed BALB/3T3 fibroblasts. *J Biol Chem,* 265**,** 13650-4.

ADAIR, T. H. & MONTANI, J. P. 2010. *Angiogenesis.* San Rafael (CA).

ADAMS, L., SCOTT, G. K. & WEINBERG, C. S. 1996. Biphasic modulation of cell growth by recombinant human galectin-1. *Biochim Biophys Acta,* 1312**,** 137-44.

AGHAJANIAN, C., BLANK, S. V., GOFF, B. A., JUDSON, P. L., TENERIELLO, M. G., HUSAIN, A., SOVAK, M. A., YI, J. & NYCUM, L. R. 2012. OCEANS: a randomized, double-blind, placebo-controlled phase III trial of chemotherapy with or without bevacizumab in patients with platinum-sensitive recurrent epithelial ovarian, primary peritoneal, or fallopian tube cancer. *Journal of clinical oncology : official journal of the American Society of Clinical Oncology,* 30**,** 2039-45.

AHMAD, A., SCHAACK, J. B., WHITE, C. W. & AHMAD, S. 2013. Adenosine A2A receptor-dependent proliferation of pulmonary endothelial cells is mediated through calcium mobilization, PI3-kinase and ERK1/2 pathways. *Biochem Biophys Res Commun,* 434**,** 566-71.

AHMED, N., THOMPSON, E. W. & QUINN, M. A. 2007. Epithelial-mesenchymal interconversions in normal ovarian surface epithelium and ovarian carcinomas: an exception to the norm. *J Cell Physiol,* 213**,** 581-8.

AIRD, W. C. 2007a. Phenotypic heterogeneity of the endothelium: I. Structure, function, and mechanisms. *Circ Res,* 100**,** 158-73.

AIRD, W. C. 2007b. Phenotypic heterogeneity of the endothelium: II. Representative vascular beds. *Circ Res,* 100**,** 174-90.

AKAOGI, K., OKABE, Y., SATO, J., NAGASHIMA, Y., YASUMITSU, H., SUGAHARA, K. & MIYAZAKI, K. 1996a. Specific accumulation of tumor-derived adhesion factor in tumor blood vessels and in capillary tube-like structures of cultured vascular endothelial cells. *Proc Natl Acad Sci U S A,* 93**,** 8384-9.

AKAOGI, K., SATO, J., OKABE, Y., SAKAMOTO, Y., YASUMITSU, H. & MIYAZAKI, K. 1996b. Synergistic growth stimulation of mouse fibroblasts by tumor-derived adhesion factor with insulin-like growth factors and insulin. *Cell Growth Differ,* 7**,** 1671-7.

AKIEL, M., RAJASEKARAN, D., GREDLER, R., SIDDIQ, A., SRIVASTAVA, J., ROBERTSON, C., JARIWALA, N. H., FISHER, P. B. & SARKAR, D. 2014. Emerging role of insulin-like growth factor-binding protein 7 in hepatocellular carcinoma. *J Hepatocell Carcinoma,* 1**,** 9-19.

ALVAREZ, C. & SZTUL, E. S. 1999. Brefeldin A (BFA) disrupts the organization of the microtubule and the actin cytoskeletons. *Eur J Cell Biol,* 78**,** 1-14.

AMEMIYA, Y., YANG, W., BENATAR, T., NOFECH-MOZES, S., YEE, A., KAHN, H., HOLLOWAY, C. & SETH, A. 2011. Insulin like growth factor binding protein-7 reduces growth of human breast cancer cells and xenografted tumors. *Breast Cancer Res Treat,* 126**,** 373-84.

ANASTASOV, N., BONZHEIM, I., RUDELIUS, M., KLIER, M., DAU, T., ANGERMEIER, D., DUYSTER, J., PITTALUGA, S., FEND, F., RAFFELD, M. & QUINTANILLA-MARTINEZ, L. 2010. C/EBPbeta expression in ALK-positive anaplastic large cell lymphomas is required for cell proliferation and is induced by the STAT3 signaling pathway. *Haematologica,* 95**,** 760-7.

ANDJELKOVIC, M., MAIRA, S. M., CRON, P., PARKER, P. J. & HEMMINGS, B. A. 1999. Domain swapping used to investigate the mechanism of protein kinase B regulation by 3-phosphoinositide-dependent protein kinase 1 and Ser473 kinase. *Mol Cell Biol,* 19**,** 5061-72.

APTE, S. M., FAN, D., KILLION, J. J. & FIDLER, I. J. 2004. Targeting the platelet-derived growth factor receptor in antivascular therapy for human ovarian carcinoma. *Clin Cancer Res,* 10**,** 897-908.

ARMSTRONG, F., DUPLANTIER, M. M., TREMPAT, P., HIEBLOT, C., LAMANT, L., ESPINOS, E., RACAUD-SULTAN, C., ALLOUCHE, M., CAMPO, E., DELSOL, G. & TOURIOL, C. 2004. Differential effects of X-ALK fusion proteins on proliferation, transformation, and invasion properties of NIH3T3 cells. *Oncogene,* 23**,** 6071-82.

ASTORGUES-XERRI, L., RIVEIRO, M. E., TIJERAS-RABALLAND, A., SEROVA, M., NEUZILLET, C., ALBERT, S., RAYMOND, E. & FAIVRE, S. 2014. Unraveling galectin-1 as a novel therapeutic target for cancer. *Cancer Treat Rev,* 40**,** 307-19.

AUGUSTE, P., LEMIERE, S., LARRIEU-LAHARGUE, F. & BIKFALVI, A. 2005. Molecular mechanisms of tumor vascularization. *Crit Rev Oncol Hematol,* 54**,** 53-61.

AWANO, T., KATZ, M. L., O'BRIEN, D. P., TAYLOR, J. F., EVANS, J., KHAN, S., SOHAR, I., LOBEL, P. & JOHNSON, G. S. 2006. A mutation in the cathepsin D gene (CTSD) in American Bulldogs with neuronal ceroid lipofuscinosis. *Mol Genet Metab,* 87**,** 341-8.

BAECHLE, D., FLAD, T., CANSIER, A., STEFFEN, H., SCHITTEK, B., TOLSON, J., HERRMANN, T., DIHAZI, H., BECK, A., MUELLER, G. A., MUELLER, M., STEVANOVIC, S., GARBE, C., MUELLER, C. A. & KALBACHER, H. 2006. Cathepsin D is present in human eccrine sweat and involved in the postsecretory processing of the antimicrobial peptide DCD-1L. *J Biol Chem,* 281**,** 5406-15.

BAEKELANDT, M., HOLM, R., TROPE, C. G., NESLAND, J. M. & KRISTENSEN, G. B. 1999. The significance of metastasis-related factors cathepsin-D and nm23 in advanced ovarian cancer. *Ann Oncol,* 10**,** 1335-41.

BALA, K., GOMES, J. & GOHIL, N. K. 2011. Interaction of glycated human serum albumin with endothelial cells in a hemodynamic environment: structural and functional correlates. *Mol Biosyst,* 7**,** 3036-41.

BAMBERGER, E. S. & PERRETT, C. W. 2002. Angiogenesis in epithelian ovarian cancer. *Mol Pathol,* 55**,** 348-59.

BANERJEE, S. & KAYE, S. 2011. The role of targeted therapy in ovarian cancer. *Eur J Cancer,* 47 Suppl 3**,** S116-30.

BARONDES, S. H., CASTRONOVO, V., COOPER, D. N., CUMMINGS, R. D., DRICKAMER, K., FEIZI, T., GITT, M. A., HIRABAYASHI, J., HUGHES, C., KASAI, K. & ET AL. 1994a. Galectins: a family of animal beta-galactoside-binding lectins. *Cell,* 76**,** 597-8.

BARONDES, S. H., COOPER, D. N., GITT, M. A. & LEFFLER, H. 1994b. Galectins. Structure and function of a large family of animal lectins. *J Biol Chem,* 269**,** 20807-10.

BARTON, M., BARETELLA, O. & MEYER, M. R. 2012. Obesity and risk of vascular disease: importance of endothelium-dependent vasoconstriction. *Br J Pharmacol,* 165**,** 591-602.

BAUM, L. G., SEILHAMER, J. J., PANG, M., LEVINE, W. B., BEYNON, D. & BERLINER, J. A. 1995. Synthesis of an endogeneous lectin, galectin-1, by human endothelial cells is up-regulated by endothelial cell activation. *Glycoconj J,* 12**,** 63-8.

BAZZONI, G. & DEJANA, E. 2004. Endothelial cell-to-cell junctions: molecular organization and role in vascular homeostasis. *Physiol Rev,* 84**,** 869-901.

BEAUJOUIN, M., BAGHDIGUIAN, S., GLONDU-LASSIS, M., BERCHEM, G. & LIAUDET-COOPMAN, E. 2006. Overexpression of both catalytically active and -inactive cathepsin D by cancer cells enhances apoptosis-dependent chemo-sensitivity. *Oncogene,* 25**,** 1967-73.

BELLOU, S., HINK, M. A., BAGLI, E., PANOPOULOU, E., BASTIAENS, P. I., MURPHY, C. & FOTSIS, T. 2009. VEGF autoregulates its proliferative and migratory ERK1/2 and p38 cascades by enhancing the expression of DUSP1 and DUSP5 phosphatases in endothelial cells. *Am J Physiol Cell Physiol,* 297**,** C1477-89.

BEN-ARI, Y., BRODY, Y., KINOR, N., MOR, A., TSUKAMOTO, T., SPECTOR, D. L., SINGER, R. H. & SHAV-TAL, Y. 2010. The life of an mRNA in space and time. *J Cell Sci,* 123**,** 1761-74.

BENATAR, T., YANG, W., AMEMIYA, Y., EVDOKIMOVA, V., KAHN, H., HOLLOWAY, C. & SETH, A. 2012. IGFBP7 reduces breast tumor growth by induction of senescence and apoptosis pathways. *Breast Cancer Res Treat,* 133**,** 563-73.

BENES, P., KOELSCH, G., DVORAK, B., FUSEK, M. & VETVICKA, V. 2002. Detection of procathepsin D in rat milk. *Comp Biochem Physiol B Biochem Mol Biol,* 133**,** 113-8.

BENES, P., VETVICKA, V. & FUSEK, M. 2008. Cathepsin D--many functions of one aspartic protease. *Crit Rev Oncol Hematol,* 68**,** 12-28.

BERAL, V., MILLION WOMEN STUDY, C., BULL, D., GREEN, J. & REEVES, G. 2007. Ovarian cancer and hormone replacement therapy in the Million Women Study. *Lancet,* 369**,** 1703-10.

BERCHEM, G., GLONDU, M., GLEIZES, M., BROUILLET, J. P., VIGNON, F., GARCIA, M. & LIAUDET-COOPMAN, E. 2002. Cathepsin-D affects multiple tumor progression steps in vivo: proliferation, angiogenesis and apoptosis. *Oncogene,* 21**,** 5951-5.

BESSET, V., SCOTT, R. P. & IBANEZ, C. F. 2000. Signaling complexes and protein-protein interactions involved in the activation of the Ras and phosphatidylinositol 3-kinase pathways by the c-Ret receptor tyrosine kinase. *J Biol Chem,* 275**,** 39159-66.

BIKFALVI, A., ALTERIO, J., INYANG, A. L., DUPUY, E., LAURENT, M., HARTMANN, M. P., VIGNY, L., RAULAIS, D., COURTOIS, Y. & TOBELEM, G. 1990. Basic fibroblast growth factor expression in human omental microvascular endothelial cells and the effect of phorbol ester. *J Cell Physiol,* 144**,** 151-8.

BLANCO, R. & GERHARDT, H. 2013. VEGF and Notch in Tip and Stalk Cell Selection. *Cold Spring Harbor Perspectives in Medicine,* 3.

BLOMGRAN, R., ZHENG, L. & STENDAHL, O. 2007. Cathepsin-cleaved Bid promotes apoptosis in human neutrophils via oxidative stress-induced lysosomal membrane permeabilization. *J Leukoc Biol,* 81**,** 1213-23.

BRIOZZO, P., BADET, J., CAPONY, F., PIERI, I., MONTCOURRIER, P., BARRITAULT, D. & ROCHEFORT, H. 1991. MCF7 mammary cancer cells respond to bFGF and internalize it following its release from extracellular matrix: a permissive role of cathepsin D. *Exp Cell Res,* 194**,** 252-9.

BRIOZZO, P., MORISSET, M., CAPONY, F., ROUGEOT, C. & ROCHEFORT, H. 1988. In vitro degradation of extracellular matrix with Mr 52,000 cathepsin D secreted by breast cancer cells. *Cancer Res,* 48**,** 3688-92.

BROOKS, S. A., LOMAX-BROWNE, H. J., CARTER, T. M., KINCH, C. E. & HALL, D. M. 2010. Molecular interactions in cancer cell metastasis. *Acta Histochem,* 112**,** 3-25.

BROUILLET, J. P., DUFOUR, F., LEMAMY, G., GARCIA, M., SCHLUP, N., GRENIER, J., MANI, J. C. & ROCHEFORT, H. 1997. Increased cathepsin D level in the serum of patients with metastatic breast carcinoma detected with a specific pro-cathepsin D immunoassay. *Cancer,* 79**,** 2132-6.

BROWN, L. F., DETMAR, M., CLAFFEY, K., NAGY, J. A., FENG, D., DVORAK, A. M. & DVORAK, H. F. 1997. Vascular permeability factor/vascular endothelial growth factor: a multifunctional angiogenic cytokine. *EXS,* 79**,** 233-69.

BRUDNO, Y., ENNETT-SHEPARD, A. B., CHEN, R. R., AIZENBERG, M. & MOONEY, D. J. 2013. Enhancing microvascular formation and vessel maturation through temporal control over multiple pro-angiogenic and pro-maturation factors. *Biomaterials,* 34**,** 9201-9.

BURRI, P. H., HLUSHCHUK, R. & DJONOV, V. 2004. Intussusceptive angiogenesis: its emergence, its characteristics, and its significance. *Dev Dyn,* 231**,** 474-88.

CAMBY, I., BELOT, N., LEFRANC, F., SADEGHI, N., DE LAUNOIT, Y., KALTNER, H., MUSETTE, S., DARRO, F., DANGUY, A., SALMON, I., GABIUS, H. J. & KISS, R. 2002. Galectin-1 modulates

human glioblastoma cell migration into the brain through modifications to the actin cytoskeleton and levels of expression of small GTPases. *J Neuropathol Exp Neurol,* 61**,** 585-96.

CAMBY, I., LE MERCIER, M., LEFRANC, F. & KISS, R. 2006. Galectin-1: a small protein with major functions. *Glycobiology,* 16**,** 137R-157R.

CARY, L. A., CHANG, J. F. & GUAN, J. L. 1996. Stimulation of cell migration by overexpression of focal adhesion kinase and its association with Src and Fyn. *J Cell Sci,* 109 (Pt 7)**,** 1787-94.

CASWELL, P. T., VADREVU, S. & NORMAN, J. C. 2009. Integrins: masters and slaves of endocytic transport. *Nat Rev Mol Cell Biol,* 10**,** 843-53.

CHAI, Y., WU, W., ZHOU, C. & ZHOU, J. 2012. The potential prognostic value of cathepsin D protein in serous ovarian cancer. *Arch Gynecol Obstet,* 286**,** 465-71.

CHAMBERS, A. F., COLELLA, R., DENHARDT, D. T. & WILSON, S. M. 1992. Increased expression of cathepsins L and B and decreased activity of their inhibitors in metastatic, ras-transformed NIH 3T3 cells. *Mol Carcinog,* 5**,** 238-45.

CHANG, Y. S., DI TOMASO, E., MCDONALD, D. M., JONES, R., JAIN, R. K. & MUNN, L. L. 2000. Mosaic blood vessels in tumors: frequency of cancer cells in contact with flowing blood. *Proc Natl Acad Sci U S A,* 97**,** 14608-13.

CHEN, B. H., TZEN, J. T., BRESNICK, A. R. & CHEN, H. C. 2002. Roles of Rho-associated kinase and myosin light chain kinase in morphological and migratory defects of focal adhesion kinase-null cells. *J Biol Chem,* 277**,** 33857-63.

CHEN, C. H., HUNG, H. S. & HSU, S. H. 2008. Low-energy laser irradiation increases endothelial cell proliferation, migration, and eNOS gene expression possibly via PI3K signal pathway. *Lasers Surg Med,* 40**,** 46-54.

CHEN, D., SIDDIQ, A., EMDAD, L., RAJASEKARAN, D., GREDLER, R., SHEN, X. N., SANTHEKADUR, P. K., SRIVASTAVA, J., ROBERTSON, C. L., DMITRIEV, I., KASHENTSEVA, E. A., CURIEL, D. T., FISHER, P. B. & SARKAR, D. 2013. Insulin-like Growth Factor-binding Protein-7 (IGFBP7); A Promising Gene Therapeutic for Hepatocellular Carcinoma (HCC). *Mol Ther,* 21**,** 758-766.

CHEN, H. C. 2005. Boyden chamber assay. *Methods Mol Biol,* 294**,** 15-22.

CHEN, L., LI, H., LIU, W., ZHU, J., ZHAO, X., WRIGHT, E., CAO, L., DING, I. & RODGERS, G. P. 2011. Olfactomedin 4 suppresses prostate cancer cell growth and metastasis via negative interaction with cathepsin D and SDF-1. *Carcinogenesis,* 32**,** 986-94.

CHEN, L., YAO, Y., SUN, L., ZHOU, J., LIU, J., WANG, J., LI, J. & TANG, J. 2015. Clinical implication of the serum galectin-1 expression in epithelial ovarian cancer patients. *J Ovarian Res,* 8**,** 78.

CHEN, Y., PACYNA-GENGELBACH, M., YE, F., KNOSEL, T., LUND, P., DEUTSCHMANN, N., SCHLUNS, K., KOTB, W. F., SERS, C., YASUMOTO, H., USUI, T. & PETERSEN, I. 2007. Insulin-like growth factor binding protein-related protein 1 (IGFBP-rP1) has potential tumour-suppressive activity in human lung cancer. *J Pathol,* 211**,** 431-8.

CHIARIOTTI, L., BERLINGIERI, M. T., BATTAGLIA, C., BENVENUTO, G., MARTELLI, M. L., SALVATORE, P., CHIAPPETTA, G., BRUNI, C. B. & FUSCO, A. 1995. Expression of galectin-1 in normal human thyroid gland and in differentiated and poorly differentiated thyroid tumors. *Int J Cancer,* 64**,** 171-5.

CHIEN, S. 2007. Mechanotransduction and endothelial cell homeostasis: the wisdom of the cell. *Am J Physiol Heart Circ Physiol,* 292**,** H1209-24.

CHIN, Y. R. & TOKER, A. 2010. Akt2 regulates expression of the actin-bundling protein palladin. *FEBS Lett,* 584**,** 4769-74.

CHIU, W. C., LIN, J. Y., LEE, T. S., YOU, L. R. & CHIANG, A. N. 2013. beta(2)-glycoprotein I inhibits VEGF-induced endothelial cell growth and migration via suppressing phosphorylation of VEGFR2, ERK1/2, and Akt. *Mol Cell Biochem,* 372**,** 9-15.

CHO, M. & CUMMINGS, R. D. 1995. Galectin-1, a beta-galactoside-binding lectin in Chinese hamster ovary cells. II. Localization and biosynthesis. *J Biol Chem,* 270**,** 5207-12.

CHO, S. Y. & KLEMKE, R. L. 2000. Extracellular-regulated kinase activation and CAS/Crk coupling regulate cell migration and suppress apoptosis during invasion of the extracellular matrix. *J Cell Biol,* 149**,** 223-36.

CHUNG, J. H., IM, E. K., JIN, T. W., LEE, S. M., KIM, S. H., CHOI, E. Y., SHIN, M. J., LEE, K. H. & JANG, Y. 2011. Cathepsin L derived from skeletal muscle cells transfected with bFGF promotes endothelial cell migration. *Exp Mol Med,* 43**,** 179-88.

CHUNG, L. Y., TANG, S. J., SUN, G. H., CHOU, T. Y., YEH, T. S., YU, S. L. & SUN, K. H. 2012. Galectin-1 promotes lung cancer progression and chemoresistance by upregulating p38 MAPK, ERK, and cyclooxygenase-2. *Clin Cancer Res,* 18**,** 4037-47.

CINES, D. B., POLLAK, E. S., BUCK, C. A., LOSCALZO, J., ZIMMERMAN, G. A., MCEVER, R. P., POBER, J. S., WICK, T. M., KONKLE, B. A., SCHWARTZ, B. S., BARNATHAN, E. S., MCCRAE, K. R., HUG, B. A., SCHMIDT, A. M. & STERN, D. M. 1998. Endothelial cells in physiology and in the pathophysiology of vascular disorders. *Blood,* 91**,** 3527-61.

CLEVES, A. E., COOPER, D. N., BARONDES, S. H. & KELLY, R. B. 1996. A new pathway for protein export in Saccharomyces cerevisiae. *J Cell Biol,* 133**,** 1017-26.

COLEMAN, M. P., ESTEVE, J., DAMIECKI, P., ARSLAN, A. & RENARD, H. 1993. Trends in cancer incidence and mortality. *IARC Sci Publ***,** 1-806.

COOKE, V. G., LEBLEU, V. S., KESKIN, D., KHAN, Z., O'CONNELL, J. T., TENG, Y., DUNCAN, M. B., XIE, L., MAEDA, G., VONG, S., SUGIMOTO, H., ROCHA, R. M., DAMASCENA, A., BRENTANI, R. R. & KALLURI, R. 2012. Pericyte depletion results in hypoxia-associated epithelial-to-mesenchymal transition and metastasis mediated by met signaling pathway. *Cancer Cell,* 21**,** 66-81.

COOPER, D. N. & BARONDES, S. H. 1990. Evidence for export of a muscle lectin from cytosol to extracellular matrix and for a novel secretory mechanism. *J Cell Biol,* 110**,** 1681-91.

COULPIER, M., ANDERS, J. & IBANEZ, C. F. 2002. Coordinated activation of autophosphorylation sites in the RET receptor tyrosine kinase: importance of tyrosine 1062 for GDNF mediated neuronal differentiation and survival. *J Biol Chem,* 277**,** 1991-9.

CRAMER, D. W., KUPER, H., HARLOW, B. L. & TITUS-ERNSTOFF, L. 2001. Carotenoids, antioxidants and ovarian cancer risk in pre- and postmenopausal women. *Int J Cancer,* 94**,** 128-34.

CREEDON, D. J., TANSEY, M. G., BALOH, R. H., OSBORNE, P. A., LAMPE, P. A., FAHRNER, T. J., HEUCKEROTH, R. O., MILBRANDT, J. & JOHNSON, E. M., JR. 1997. Neurturin shares receptors and signal transduction pathways with glial cell line-derived neurotrophic factor in sympathetic neurons. *Proc Natl Acad Sci U S A,* 94**,** 7018-23.

CROCI, D. O., SALATINO, M., RUBINSTEIN, N., CERLIANI, J. P., CAVALLIN, L. E., LEUNG, H. J., OUYANG, J., ILARREGUI, J. M., TOSCANO, M. A., DOMAICA, C. I., CROCI, M. C., SHIPP, M. A., MESRI, E. A., ALBINI, A. & RABINOVICH, G. A. 2012. Disrupting galectin-1 interactions with N-glycans suppresses hypoxia-driven angiogenesis and tumorigenesis in Kaposi's sarcoma. *J Exp Med,* 209**,** 1985-2000.

CROWE, D. L. & SHULER, C. F. 1999. Regulation of tumor cell invasion by extracellular matrix. *Histol Histopathol,* 14**,** 665-71.

CUEVAS, B. D., ABELL, A. N., WITOWSKY, J. A., YUJIRI, T., JOHNSON, N. L., KESAVAN, K., WARE, M., JONES, P. L., WEED, S. A., DEBIASI, R. L., OKA, Y., TYLER, K. L. & JOHNSON, G. L. 2003. MEKK1 regulates calpain-dependent proteolysis of focal adhesion proteins for rear-end detachment of migrating fibroblasts. *EMBO J,* 22**,** 3346-55.

CUI, L., JOHKURA, K., LIANG, Y., TENG, R., OGIWARA, N., OKOUCHI, Y., ASANUMA, K. & SASAKI, K. 2002. Biodefense function of omental milky spots through cell adhesion molecules and leukocyte proliferation. *Cell Tissue Res,* 310**,** 321-30.

CULLEN, V., LINDFORS, M., NG, J., PAETAU, A., SWINTON, E., KOLODZIEJ, P., BOSTON, H., SAFTIG, P., WOULFE, J., FEANY, M. B., MYLLYKANGAS, L., SCHLOSSMACHER, M. G. & TYYNELA, J. 2009. Cathepsin D expression level affects alpha-synuclein processing, aggregation, and toxicity in vivo. *Mol Brain,* 2**,** 5.

CUVIER, C., JANG, A. & HILL, R. P. 1997. Exposure to hypoxia, glucose starvation and acidosis: effect on invasive capacity of murine tumor cells and correlation with cathepsin (L + B) secretion. *Clin Exp Metastasis,* 15**,** 19-25.

D'AMICO, G., KORHONEN, E. A., ANISIMOV, A., ZARKADA, G., HOLOPAINEN, T., HAGERLING, R., KIEFER, F., EKLUND, L., SORMUNEN, R., ELAMAA, H., BREKKEN, R. A., ADAMS, R. H., KOH, G. Y., SAHARINEN, P. & ALITALO, K. 2014. Tie1 deletion inhibits tumor growth and improves angiopoietin antagonist therapy. *J Clin Invest,* 124**,** 824-34.

D'HAENE, N., SAUVAGE, S., MARIS, C., ADANJA, I., LE MERCIER, M., DECAESTECKER, C., BAUM, L. & SALMON, I. 2013. VEGFR1 and VEGFR2 involvement in extracellular galectin-1- and galectin-3-induced angiogenesis. *PLoS One,* 8**,** e67029.

DAHMS, N. M., LOBEL, P. & KORNFELD, S. 1989. Mannose 6-phosphate receptors and lysosomal enzyme targeting. *J Biol Chem,* 264**,** 12115-8.

DANIILIDIS, A. & KARAGIANNIS, V. 2007. Epithelial ovarian cancer. Risk factors, screening and the role of prophylactic oophorectomy. *Hippokratia,* 11**,** 63-6.

DE GAETANO, G., DONATI, M. B. & CERLETTI, C. 2003. Prevention of thrombosis and vascular inflammation: benefits and limitations of selective or combined COX-1, COX-2 and 5-LOX inhibitors. *Trends Pharmacol Sci,* 24**,** 245-52.

DEHRMANN, F. M., COETZER, T. H., PIKE, R. N. & DENNISON, C. 1995. Mature cathepsin L is substantially active in the ionic milieu of the extracellular medium. *Arch Biochem Biophys,* 324**,** 93-8.

DEISS, L. P., GALINKA, H., BERISSI, H., COHEN, O. & KIMCHI, A. 1996. Cathepsin D protease mediates programmed cell death induced by interferon-gamma, Fas/APO-1 and TNF-alpha. *EMBO J,* 15**,** 3861-70.

DOKLADDA, K., GREEN, K. A., PAN, D. A. & HARDIE, D. G. 2005. PD98059 and U0126 activate AMP-activated protein kinase by increasing the cellular AMP:ATP ratio and not via inhibition of the MAP kinase pathway. *FEBS Lett,* 579**,** 236-40.

DONG, J. M., PRENCE, E. M. & SAHAGIAN, G. G. 1989. Mechanism for selective secretion of a lysosomal protease by transformed mouse fibroblasts. *J Biol Chem,* 264**,** 7377-83.

DONG, J. M. & SAHAGIAN, G. G. 1990. Basis for low affinity binding of a lysosomal cysteine protease to the cation-independent mannose 6-phosphate receptor. *J Biol Chem,* 265**,** 4210-7.

DONOVAN, D., BROWN, N. J., BISHOP, E. T. & LEWIS, C. E. 2001. Comparison of three in vitro human 'angiogenesis' assays with capillaries formed in vivo. *Angiogenesis,* 4**,** 113-21.

DOUFEKAS, K. & OLAITAN, A. 2014. Clinical epidemiology of epithelial ovarian cancer in the UK. *Int J Womens Health,* 6**,** 537-45.

DOURDIN, N., BHATT, A. K., DUTT, P., GREER, P. A., ARTHUR, J. S., ELCE, J. S. & HUTTENLOCHER, A. 2001. Reduced cell migration and disruption of the actin cytoskeleton in calpain-deficient embryonic fibroblasts. *J Biol Chem,* 276**,** 48382-8.

DUFOUR, M., DORMOND-MEUWLY, A., PYTHOUD, C., DEMARTINES, N. & DORMOND, O. 2013. Reactivation of AKT signaling following treatment of cancer cells with PI3K inhibitors attenuates their antitumor effects. *Biochem Biophys Res Commun,* 438**,** 32-7.

DUNN, G. P., BRUCE, A. T., IKEDA, H., OLD, L. J. & SCHREIBER, R. D. 2002. Cancer immunoediting: from immunosurveillance to tumor escape. *Nat Immunol,* 3**,** 991-8.

DVORAK, H. F. 2005. Angiogenesis: update 2005. *J Thromb Haemost,* 3**,** 1835-42.

EBI, H., COSTA, C., FABER, A. C., NISHTALA, M., KOTANI, H., JURIC, D., DELLA PELLE, P., SONG, Y., YANO, S., MINO-KENUDSON, M., BENES, C. H. & ENGELMAN, J. A. 2013. PI3K regulates MEK/ERK signaling in breast cancer via the Rac-GEF, P-Rex1. *Proc Natl Acad Sci U S A,* 110**,** 21124-9.

ENOMOTO, A., MURAKAMI, H., ASAI, N., MORONE, N., WATANABE, T., KAWAI, K., MURAKUMO, Y., USUKURA, J., KAIBUCHI, K. & TAKAHASHI, M. 2005. Akt/PKB regulates actin organization and cell motility via Girdin/APE. *Dev Cell,* 9**,** 389-402.

FAES, S. & DORMOND, O. 2015. PI3K and AKT: Unfaithful Partners in Cancer. *Int J Mol Sci,* 16**,** 21138-52.

FARIAS, M. E. & MANCA DE NADRA, M. C. 2000. Purification and partial characterization of Oenococcus oeni exoprotease. *FEMS Microbiol Lett,* 185**,** 263-6.

FELBOR, U., DREIER, L., BRYANT, R. A., PLOEGH, H. L., OLSEN, B. R. & MOTHES, W. 2000. Secreted cathepsin L generates endostatin from collagen XVIII. *EMBO J,* 19**,** 1187-94.

FERLAY, J., PARKIN, D. M. & STELIAROVA-FOUCHER, E. 2010. Estimates of cancer incidence and mortality in Europe in 2008. *Eur J Cancer,* 46**,** 765-81.

FERRANDINA, G., SCAMBIA, G., BARDELLI, F., BENEDETTI PANICI, P., MANCUSO, S. & MESSORI, A. 1997. Relationship between cathepsin-D content and disease-free survival in node-negative breast cancer patients: a meta-analysis. *Br J Cancer,* 76**,** 661-6.

FERRANDINA, G., SCAMBIA, G., FAGOTTI, A., D'AGOSTINO, G., BENEDETTI PANICI, P., CARBONE, A. & MANCUSO, S. 1998. Immunoradiometric and immunohistochemical analysis of Cathepsin D in ovarian cancer: lack of association with clinical outcome. *Br J Cancer,* 78**,** 1645-52.

FERRARA, N. 2002. Role of vascular endothelial growth factor in physiologic and pathologic angiogenesis: therapeutic implications. *Semin Oncol,* 29**,** 10-4.

FIEBIGER, E., MAEHR, R., VILLADANGOS, J., WEBER, E., ERICKSON, A., BIKOFF, E., PLOEGH, H. L. & LENNON-DUMENIL, A. M. 2002. Invariant chain controls the activity of extracellular cathepsin L. *J Exp Med,* 196**,** 1263-9.

FILIPPA, N., SABLE, C. L., FILLOUX, C., HEMMINGS, B. & VAN OBBERGHEN, E. 1999. Mechanism of protein kinase B activation by cyclic AMP-dependent protein kinase. *Mol Cell Biol,* 19**,** 4989-5000.

FISCHER, C., SANCHEZ-RUDERISCH, H., WELZEL, M., WIEDENMANN, B., SAKAI, T., ANDRE, S., GABIUS, H. J., KHACHIGIAN, L., DETJEN, K. M. & ROSEWICZ, S. 2005. Galectin-1 interacts with the {alpha}5{beta}1 fibronectin receptor to restrict carcinoma cell growth via induction of p21 and p27. *J Biol Chem,* 280**,** 37266-77.

FOEKENS, J. A., LOOK, M. P., BOLT-DE VRIES, J., MEIJER-VAN GELDER, M. E., VAN PUTTEN, W. L. & KLIJN, J. G. 1999. Cathepsin-D in primary breast cancer: prognostic evaluation involving 2810 patients. *Br J Cancer,* 79**,** 300-7.

FOURNIER, N. & DOILLON, C. J. 1992. In vitro angiogenesis in fibrin matrices containing fibronectin or hyaluronic acid. *Cell Biol Int Rep,* 16**,** 1251-63.

FRADE, R., RODRIGUES-LIMA, F., HUANG, S., XIE, K., GUILLAUME, N. & BAR-ELI, M. 1998. Procathepsin-L, a proteinase that cleaves human C3 (the third component of complement), confers high tumorigenic and metastatic properties to human melanoma cells. *Cancer Res,* 58**,** 2733-6.

FRIDELL, Y. W., JIN, Y., QUILLIAM, L. A., BURCHERT, A., MCCLOSKEY, P., SPIZZ, G., VARNUM, B., DER, C. & LIU, E. T. 1996. Differential activation of the Ras/extracellular-signal-regulated protein kinase pathway is responsible for the biological consequences induced by the Axl receptor tyrosine kinase. *Mol Cell Biol,* 16**,** 135-45.

FRIEDLANDER, M., HANCOCK, K., BENIGNO, B. & AL, E. 2007. Pazopanib (GW786034) is active in women with advanced epithelial ovarian, fallopian tube and peritoneal cancers: initial results of a phase II study. *Journal of Clinical Oncology*.

FRITCHIE, K., SIINTOLA, E., ARMAO, D., LEHESJOKI, A. E., MARINO, T., POWELL, C., TENNISON, M., BOOKER, J. M., KOCH, S., PARTANEN, S., SUZUKI, K., TYYNELA, J. & THORNE, L. B. 2009. Novel mutation and the first prenatal screening of cathepsin D deficiency (CLN10). *Acta Neuropathol,* 117**,** 201-8.

FUKUDA, M. E., IWADATE, Y., MACHIDA, T., HIWASA, T., NIMURA, Y., NAGAI, Y., TAKIGUCHI, M., TANZAWA, H., YAMAURA, A. & SEKI, N. 2005. Cathepsin D is a potential serum marker for poor prognosis in glioma patients. *Cancer Res,* 65**,** 5190-4.

FUNG-KEE-FUNG, M., OLIVER, T., ELIT, L., OZA, A., HIRTE, H. W. & BRYSON, P. 2007. Optimal chemotherapy treatment for women with recurrent ovarian cancer. *Curr Oncol,* 14**,** 195-208.

FUSEK, M. & VETVICKA, V. 1994. Mitogenic function of human procathepsin D: the role of the propeptide. *Biochem J,* 303 (Pt 3)**,** 775-80.

GAGLIARDI, P. A., DI BLASIO, L., ORSO, F., SEANO, G., SESSA, R., TAVERNA, D., BUSSOLINO, F. & PRIMO, L. 2012. 3-phosphoinositide-dependent kinase 1 controls breast tumor growth in a kinase-dependent but Akt-independent manner. *Neoplasia,* 14**,** 719-31.

GARCIA, M., DEROCQ, D., PUJOL, P. & ROCHEFORT, H. 1990. Overexpression of transfected cathepsin D in transformed cells increases their malignant phenotype and metastatic potency. *Oncogene,* 5**,** 1809-14.

GAYTHER, S. A. & PHAROAH, P. D. 2010. The inherited genetics of ovarian and endometrial cancer. *Curr Opin Genet Dev,* 20**,** 231-8.

GEIGER, P., MAYER, B., WIEST, I., SCHULZE, S., JESCHKE, U. & WEISSENBACHER, T. 2016. Binding of galectin-1 to breast cancer cells MCF7 induces apoptosis and inhibition of proliferation in vitro in a 2D- and 3D- cell culture model. *BMC Cancer,* 16**,** 870.

GERHARDT, H. 2008. VEGF and endothelial guidance in angiogenic sprouting. *Organogenesis,* 4**,** 241-6.

GIESELMANN, V., HASILIK, A. & VON FIGURA, K. 1985. Processing of human cathepsin D in lysosomes in vitro. *J Biol Chem,* 260**,** 3215-20.

GIL, C. D., COOPER, D., ROSIGNOLI, G., PERRETTI, M. & OLIANI, S. M. 2006. Inflammation-induced modulation of cellular galectin-1 and -3 expression in a model of rat peritonitis. *Inflamm Res,* 55**,** 99-107.

GLADING, A., BODNAR, R. J., REYNOLDS, I. J., SHIRAHA, H., SATISH, L., POTTER, D. A., BLAIR, H. C. & WELLS, A. 2004. Epidermal growth factor activates m-calpain (calpain II), at least in part, by extracellular signal-regulated kinase-mediated phosphorylation. *Mol Cell Biol,* 24**,** 2499-512.

GLONDU, M., COOPMAN, P., LAURENT-MATHA, V., GARCIA, M., ROCHEFORT, H. & LIAUDET-COOPMAN, E. 2001. A mutated cathepsin-D devoid of its catalytic activity stimulates the growth of cancer cells. *Oncogene,* 20**,** 6920-9.

GOCHEVA, V., ZENG, W., KE, D., KLIMSTRA, D., REINHECKEL, T., PETERS, C., HANAHAN, D. & JOYCE, J. A. 2006. Distinct roles for cysteine cathepsin genes in multistage tumorigenesis. *Genes Dev,* 20**,** 543-56.

GOETZE, S., BUNGENSTOCK, A., CZUPALLA, C., EILERS, F., STAWOWY, P., KINTSCHER, U., SPENCER-HANSCH, C., GRAF, K., NURNBERG, B., LAW, R. E., FLECK, E. & GRAFE, M. 2002. Leptin induces endothelial cell migration through Akt, which is inhibited by PPARgamma-ligands. *Hypertension,* 40**,** 748-54.

GOPALAKRISHNAN, M. M., GROSCH, H. W., LOCATELLI-HOOPS, S., WERTH, N., SMOLENOVA, E., NETTERSHEIM, M., SANDHOFF, K. & HASILIK, A. 2004. Purified recombinant human prosaposin forms oligomers that bind procathepsin D and affect its autoactivation. *Biochem J,* 383**,** 507-15.

GORUPPI, S., RUARO, E., VARNUM, B. & SCHNEIDER, C. 1999. Gas6-mediated survival in NIH3T3 cells activates stress signalling cascade and is independent of Ras. *Oncogene,* 18**,** 4224-36.

GOUT, S., TREMBLAY, P. L. & HUOT, J. 2008. Selectins and selectin ligands in extravasation of cancer cells and organ selectivity of metastasis. *Clin Exp Metastasis,* 25**,** 335-44.

GRAHAM, H. & PENG, C. 2006. Activin receptor-like kinases: structure, function and clinical implications. *Endocr Metab Immune Disord Drug Targets,* 6**,** 45-58.

GRIFFITHS, C. T. 1975. Surgical resection of tumor bulk in the primary treatment of ovarian carcinoma. *Natl Cancer Inst Monogr,* 42**,** 101-4.

GRULLICH, C. 2014. Cabozantinib: a MET, RET, and VEGFR2 tyrosine kinase inhibitor. *Recent Results Cancer Res,* 201**,** 207-14.

GU, H., PRATT, J. C., BURAKOFF, S. J. & NEEL, B. G. 1998. Cloning of p97/Gab2, the major SHP2-binding protein in hematopoietic cells, reveals a novel pathway for cytokine-induced gene activation. *Mol Cell,* 2**,** 729-40.

GUO, Z., HUO, J., DI, J., ZENG, S., LIU, J. & XING, F. 2014. PI3K pathway inhibitor LY294002 alters Jurkat T cell biobehaviours via ERK1/2-ICBP90 mediation. *Central European Journal of Biology,* 9**,** 739-748.

HAINSWORTH, J. D., THOMPSON, D. S., BISMAYER, J. A., GIAN, V. G., MERRITT, W. M., WHORF, R. C., FINNEY, L. H. & DUDLEY, B. S. 2015. Paclitaxel/carboplatin with or without sorafenib in the first-line treatment of patients with stage III/IV epithelial ovarian cancer: a randomized phase II study of the Sarah Cannon Research Institute. *Cancer Med,* 4**,** 673-81.

HANAHAN, D. & WEINBERG, R. A. 2000. The hallmarks of cancer. *Cell,* 100**,** 57-70.

HASANBASIC, I., CUERQUIS, J., VARNUM, B. & BLOSTEIN, M. D. 2004. Intracellular signaling pathways involved in Gas6-Axl-mediated survival of endothelial cells. *Am J Physiol Heart Circ Physiol,* 287**,** H1207-13.

HAWKINS, P. T., EGUINOA, A., QIU, R. G., STOKOE, D., COOKE, F. T., WALTERS, R., WENNSTROM, S., CLAESSON-WELSH, L., EVANS, T., SYMONS, M. & ET AL. 1995. PDGF stimulates an increase in GTP-Rac via activation of phosphoinositide 3-kinase. *Curr Biol,* 5**,** 393-403.

HEINRICH, M., NEUMEYER, J., JAKOB, M., HALLAS, C., TCHIKOV, V., WINOTO-MORBACH, S., WICKEL, M., SCHNEIDER-BRACHERT, W., TRAUZOLD, A., HETHKE, A. & SCHUTZE, S. 2004. Cathepsin D links TNF-induced acid sphingomyelinase to Bid-mediated caspase-9 and -3 activation. *Cell Death Differ,* 11**,** 550-63.

HENNESSY, B. T., COLEMAN, R. L. & MARKMAN, M. 2009. Ovarian cancer. *Lancet,* 374**,** 1371-82.

HENZEN-LOGMANS, S. C., FIERET, E. J., BERNS, E. M., VAN DER BURG, M. E., KLIJN, J. G. & FOEKENS, J. A. 1994. Ki-67 staining in benign, borderline, malignant primary and metastatic ovarian tumors: correlation with steroid receptors, epidermal-growth-factor receptor and cathepsin D. *Int J Cancer,* 57**,** 468-72.

HERZOG, B., PELLET-MANY, C., BRITTON, G., HARTZOULAKIS, B. & ZACHARY, I. C. 2011. VEGF binding to NRP1 is essential for VEGF stimulation of endothelial cell migration, complex formation between NRP1 and VEGFR2, and signaling via FAK Tyr407 phosphorylation. *Mol Biol Cell,* 22**,** 2766-76.

HILFIKER-KLEINER, D., KAMINSKI, K., PODEWSKI, E., BONDA, T., SCHAEFER, A., SLIWA, K., FORSTER, O., QUINT, A., LANDMESSER, U., DOERRIES, C., LUCHTEFELD, M., POLI, V., SCHNEIDER, M. D., BALLIGAND, J. L., DESJARDINS, F., ANSARI, A., STRUMAN, I., NGUYEN, N. Q., ZSCHEMISCH, N. H., KLEIN, G., HEUSCH, G., SCHULZ, R., HILFIKER, A. & DREXLER, H. 2007. A cathepsin D-cleaved 16 kDa form of prolactin mediates postpartum cardiomyopathy. *Cell,* 128**,** 589-600.

HLOBILKOVA, A., EHRMANN, J., SEDLAKOVA, E., KREJCI, V., KNIZETOVA, P., FIURASKOVA, M., KALA, M., KALITA, O. & KOLAR, Z. 2007. Could changes in the regulation of the PI3K/PKB/Akt signaling pathway and cell cycle be involved in astrocytic tumor pathogenesis and progression? *Neoplasma,* 54**,** 334-41.

HOLASH, J., MAISONPIERRE, P. C., COMPTON, D., BOLAND, P., ALEXANDER, C. R., ZAGZAG, D., YANCOPOULOS, G. D. & WIEGAND, S. J. 1999. Vessel cooption, regression, and growth in tumors mediated by angiopoietins and VEGF. *Science,* 284**,** 1994-8.

HOLLAND, S. J., POWELL, M. J., FRANCI, C., CHAN, E. W., FRIERA, A. M., ATCHISON, R. E., MCLAUGHLIN, J., SWIFT, S. E., PALI, E. S., YAM, G., WONG, S., LASAGA, J., SHEN, M. R., YU, S., XU, W., HITOSHI, Y., BOGENBERGER, J., NOR, J. E., PAYAN, D. G. & LORENS, J. B. 2005. Multiple roles for the receptor tyrosine kinase axl in tumor formation. *Cancer Res,* 65**,** 9294-303.

HOLLINGSWORTH, H. C., KOHN, E. C., STEINBERG, S. M., ROTHENBERG, M. L. & MERINO, M. J. 1995. Tumor angiogenesis in advanced stage ovarian carcinoma. *Am J Pathol,* 147**,** 33-41.

HOOPER, A. T., SHMELKOV, S. V., GUPTA, S., MILDE, T., BAMBINO, K., GILLEN, K., GOETZ, M., CHAVALA, S., BALJEVIC, M., MURPHY, A. J., VALENZUELA, D. M., GALE, N. W., THURSTON, G., YANCOPOULOS, G. D., VAHDAT, L., EVANS, T. & RAFII, S. 2009. Angiomodulin is a specific marker of vasculature and regulates vascular endothelial growth factor-A-dependent neoangiogenesis. *Circ Res,* 105**,** 201-8.

HSIEH, C. S., DEROOS, P., HONEY, K., BEERS, C. & RUDENSKY, A. Y. 2002. A role for cathepsin L and cathepsin S in peptide generation for MHC class II presentation. *J Immunol,* 168**,** 2618-25.

HSIEH, S. H., YING, N. W., WU, M. H., CHIANG, W. F., HSU, C. L., WONG, T. Y., JIN, Y. T., HONG, T. M. & CHEN, Y. L. 2008. Galectin-1, a novel ligand of neuropilin-1, activates VEGFR-2 signaling and modulates the migration of vascular endothelial cells. *Oncogene,* 27**,** 3746-53.

HSU, Y. L., WU, C. Y., HUNG, J. Y., LIN, Y. S., HUANG, M. S. & KUO, P. L. 2013. Galectin-1 promotes lung cancer tumor metastasis by potentiating integrin alpha6beta4 and Notch1/Jagged2 signaling pathway. *Carcinogenesis,* 34**,** 1370-81.

HU, L., ROTH, J. M., BROOKS, P., LUTY, J. & KARPATKIN, S. 2008. Thrombin up-regulates cathepsin D which enhances angiogenesis, growth, and metastasis. *Cancer research,* 68**,** 4666-73.

HU, Y. L., TEE, M. K., GOETZL, E. J., AUERSPERG, N., MILLS, G. B., FERRARA, N. & JAFFE, R. B. 2001. Lysophosphatidic acid induction of vascular endothelial growth factor expression in human ovarian cancer cells. *Journal of the National Cancer Institute,* 93**,** 762-768.

HUANG, C., JACOBSON, K. & SCHALLER, M. D. 2004. MAP kinases and cell migration. *J Cell Sci,* 117**,** 4619-28.

HUANG, C., RAJFUR, Z., BORCHERS, C., SCHALLER, M. D. & JACOBSON, K. 2003. JNK phosphorylates paxillin and regulates cell migration. *Nature,* 424**,** 219-23.

HUANG, Z., YAN, D. P. & GE, B. X. 2008. JNK regulates cell migration through promotion of tyrosine phosphorylation of paxillin. *Cell Signal,* 20**,** 2002-12.

HUNGER-GLASER, I., SALAZAR, E. P., SINNETT-SMITH, J. & ROZENGURT, E. 2003. Bombesin, lysophosphatidic acid, and epidermal growth factor rapidly stimulate focal adhesion kinase phosphorylation at Ser-910: requirement for ERK activation. *J Biol Chem,* 278**,** 22631-43.

HUSS, W. J., BARRIOS, R. J. & GREENBERG, N. M. 2003. SU5416 selectively impairs angiogenesis to induce prostate cancer-specific apoptosis. *Mol Cancer Ther,* 2**,** 611-6.

HUTTENLOCHER, A., PALECEK, S. P., LU, Q., ZHANG, W., MELLGREN, R. L., LAUFFENBURGER, D. A., GINSBERG, M. H. & HORWITZ, A. F. 1997. Regulation of cell migration by the calcium-dependent protease calpain. *J Biol Chem,* 272**,** 32719-22.

HWA, V., OH, Y. & ROSENFELD, R. G. 1999. The insulin-like growth factor-binding protein (IGFBP) superfamily. *Endocr Rev,* 20**,** 761-87.

HWA, V., TOMASINI-SPRENGER, C., BERMEJO, A. L., ROSENFELD, R. G. & PLYMATE, S. R. 1998. Characterization of insulin-like growth factor-binding protein-related protein-1 in prostate cells. *J Clin Endocrinol Metab,* 83**,** 4355-62.

ILINA, O. & FRIEDL, P. 2009. Mechanisms of collective cell migration at a glance. *J Cell Sci,* 122**,** 3203-8.

ISHIBE, S., JOLY, D., ZHU, X. & CANTLEY, L. G. 2003. Phosphorylation-dependent paxillin-ERK association mediates hepatocyte growth factor-stimulated epithelial morphogenesis. *Mol Cell,* 12**,** 1275-85.

ISHIDOH, K. & KOMINAMI, E. 1995. Procathepsin L degrades extracellular matrix proteins in the presence of glycosaminoglycans in vitro. *Biochem Biophys Res Commun,* 217**,** 624-31.

ISHIDOH, K. & KOMINAMI, E. 1998. Gene regulation and extracellular functions of procathepsin L. *Biol Chem,* 379**,** 131-5.

ISHIDOH, K., MUNO, D., SATO, N. & KOMINAMI, E. 1991. Molecular cloning of cDNA for rat cathepsin C. Cathepsin C, a cysteine proteinase with an extremely long propeptide. *J Biol Chem,* 266**,** 16312-7.

ITO, K. & RALPH, S. J. 2012. Inhibiting galectin-1 reduces murine lung metastasis with increased CD4(+) and CD8 (+) T cells and reduced cancer cell adherence. *Clin Exp Metastasis,* 29**,** 561-72.

ITO, K., SCOTT, S. A., CUTLER, S., DONG, L. F., NEUZIL, J., BLANCHARD, H. & RALPH, S. J. 2011. Thiodigalactoside inhibits murine cancers by concurrently blocking effects of galectin-1

on immune dysregulation, angiogenesis and protection against oxidative stress. *Angiogenesis,* 14**,** 293-307.

IVANOVIC, Z. 2009. Hypoxia or in situ normoxia: The stem cell paradigm. *J Cell Physiol,* 219**,** 271-5.

IWAHARA, T., FUJIMOTO, J., WEN, D., CUPPLES, R., BUCAY, N., ARAKAWA, T., MORI, S., RATZKIN, B. & YAMAMOTO, T. 1997. Molecular characterization of ALK, a receptor tyrosine kinase expressed specifically in the nervous system. *Oncogene,* 14**,** 439-49.

JAIN, S., ENCINAS, M., JOHNSON, E. M., JR. & MILBRANDT, J. 2006. Critical and distinct roles for key RET tyrosine docking sites in renal development. *Genes Dev,* 20**,** 321-33.

JENSEN, A., SHARIF, H., FREDERIKSEN, K. & KJAER, S. K. 2009. Use of fertility drugs and risk of ovarian cancer: Danish Population Based Cohort Study. *BMJ,* 338**,** b249.

JIANG, W., XIANG, C., CAZACU, S., BRODIE, C. & MIKKELSEN, T. 2008. Insulin-like growth factor binding protein 7 mediates glioma cell growth and migration. *Neoplasia,* 10**,** 1335-42.

JIN, J., YUAN, F., SHEN, M. Q., FENG, Y. F. & HE, Q. L. 2013. Vascular endothelial growth factor regulates primate choroid-retinal endothelial cell proliferation and tube formation through PI3K/Akt and MEK/ERK dependent signaling. *Mol Cell Biochem,* 381**,** 267-72.

JOHANSSON, A. C., STEEN, H., OLLINGER, K. & ROBERG, K. 2003. Cathepsin D mediates cytochrome c release and caspase activation in human fibroblast apoptosis induced by staurosporine. *Cell Death Differ,* 10**,** 1253-9.

JOUVE, N., DESPOIX, N., ESPELI, M., GAUTHIER, L., CYPOWYJ, S., FALLAGUE, K., SCHIFF, C., DIGNAT-GEORGE, F., VELY, F. & LEROYER, A. S. 2013. The involvement of CD146 and its novel ligand Galectin-1 in apoptotic regulation of endothelial cells. *J Biol Chem,* 288**,** 2571-9.

JUNG, E. J., MOON, H. G., CHO, B. I., JEONG, C. Y., JOO, Y. T., LEE, Y. J., HONG, S. C., CHOI, S. K., HA, W. S., KIM, J. W., LEE, C. W., LEE, J. S. & PARK, S. T. 2007. Galectin-1 expression in cancer-associated stromal cells correlates tumor invasiveness and tumor progression in breast cancer. *Int J Cancer,* 120**,** 2331-8.

KAGEDAL, K., JOHANSSON, U. & OLLINGER, K. 2001. The lysosomal protease cathepsin D mediates apoptosis induced by oxidative stress. *FASEB J,* 15**,** 1592-4.

KAGEYAMA, T., TATEMATSU, M., ICHINOSE, M., YAHAGI, N., MIKI, K., MORIYAMA, A. & YONEZAWA, S. 1998. Development-dependent expression of cathepsins d and e in various rat tissues, with special reference to the high expression of cathepsin e in fetal liver. *Zoolog Sci,* 15**,** 517-23.

KAKINUMA, N., ROY, B. C., ZHU, Y., WANG, Y. & KIYAMA, R. 2008. Kank regulates RhoA-dependent formation of actin stress fibers and cell migration via 14-3-3 in PI3K-Akt signaling. *J Cell Biol,* 181**,** 537-49.

KANNO, S., ODA, N., ABE, M., TERAI, Y., ITO, M., SHITARA, K., TABAYASHI, K., SHIBUYA, M. & SATO, Y. 2000. Roles of two VEGF receptors, Flt-1 and KDR, in the signal transduction of VEGF effects in human vascular endothelial cells. *Oncogene,* 19**,** 2138-46.

KATO, M. V. 2000. A secreted tumor-suppressor, mac25, with activin-binding activity. *Mol Med,* 6**,** 126-35.

KAUFF, N. D., DOMCHEK, S. M., FRIEBEL, T. M., ROBSON, M. E., LEE, J., GARBER, J. E., ISAACS, C., EVANS, D. G., LYNCH, H., EELES, R. A., NEUHAUSEN, S. L., DALY, M. B., MATLOFF, E., BLUM, J. L., SABBATINI, P., BARAKAT, R. R., HUDIS, C., NORTON, L., OFFIT, K. & REBBECK, T. R. 2008. Risk-reducing salpingo-oophorectomy for the prevention of BRCA1- and BRCA2-associated breast and gynecologic cancer: a multicenter, prospective study. *J Clin Oncol,* 26**,** 1331-7.

KAWASAKI, K., SMITH, R. S., JR., HSIEH, C. M., SUN, J., CHAO, J. & LIAO, J. K. 2003. Activation of the phosphatidylinositol 3-kinase/protein kinase Akt pathway mediates nitric oxide-induced endothelial cell migration and angiogenesis. *Mol Cell Biol,* 23**,** 5726-37.

KEATING, A. K., KIM, G. K., JONES, A. E., DONSON, A. M., WARE, K., MULCAHY, J. M., SALZBERG, D. B., FOREMAN, N. K., LIANG, X., THORBURN, A. & GRAHAM, D. K. 2010. Inhibition of

Mer and Axl receptor tyrosine kinases in astrocytoma cells leads to increased apoptosis and improved chemosensitivity. *Mol Cancer Ther,* 9**,** 1298-307.

KENESSEY, A., NACHARAJU, P., KO, L. W. & YEN, S. H. 1997. Degradation of tau by lysosomal enzyme cathepsin D: implication for Alzheimer neurofibrillary degeneration. *J Neurochem,* 69**,** 2026-38.

KIM, B. R., SEO, S. H., PARK, M. S., LEE, S. H., KWON, Y. & RHO, S. B. 2015. sMEK1 inhibits endothelial cell proliferation by attenuating VEGFR-2-dependent-Akt/eNOS/HIF-1alpha signaling pathways. *Oncotarget,* 6**,** 31830-43.

KIM, S., BELL, K., MOUSA, S. A. & VARNER, J. A. 2000. Regulation of angiogenesis in vivo by ligation of integrin alpha5beta1 with the central cell-binding domain of fibronectin. *Am J Pathol,* 156**,** 1345-62.

KIRSCHKE, H., LANGNER, J., WIEDERANDERS, B., ANSORGE, S. & BOHLEY, P. 1977. Cathepsin L. A new proteinase from rat-liver lysosomes. *Eur J Biochem,* 74**,** 293-301.

KISHIBE, J., YAMADA, S., OKADA, Y., SATO, J., ITO, A., MIYAZAKI, K. & SUGAHARA, K. 2000. Structural requirements of heparan sulfate for the binding to the tumor-derived adhesion factor/angiomodulin that induces cord-like structures to ECV-304 human carcinoma cells. *J Biol Chem,* 275**,** 15321-9.

KLINT, P., KANDA, S., KLOOG, Y. & CLAESSON-WELSH, L. 1999. Contribution of Src and Ras pathways in FGF-2 induced endothelial cell differentiation. *Oncogene,* 18**,** 3354-64.

KOMINAMI, E., TSUKAHARA, T., HARA, K. & KATUNUMA, N. 1988. Biosyntheses and processing of lysosomal cysteine proteinases in rat macrophages. *FEBS Lett,* 231**,** 225-8.

KOMINAMI, E., UENO, T., MUNO, D. & KATUNUMA, N. 1991. The selective role of cathepsins B and D in the lysosomal degradation of endogenous and exogenous proteins. *FEBS Lett,* 287**,** 189-92.

KONNO, S., CHERRY, J. P., MORDENTE, J. A., CHAPMAN, J. R., CHOUDHURY, M. S., MALLOUH, C. & TAZAKI, H. 2001. Role of cathepsin D in prostatic cancer cell growth and its regulation by brefeldin A. *World J Urol,* 19**,** 234-9.

KONOPATSKAYA, O., SHORE, A. C., TOOKE, J. E. & WHATMORE, J. L. 2005. A role for heterotrimeric GTP-binding proteins and ERK1/2 in insulin-mediated, nitric-oxide-dependent, cyclic GMP production in human umbilical vein endothelial cells. *Diabetologia,* 48**,** 595-604.

KOPITZ, J., VON REITZENSTEIN, C., ANDRE, S., KALTNER, H., UHL, J., EHEMANN, V., CANTZ, M. & GABIUS, H. J. 2001. Negative regulation of neuroblastoma cell growth by carbohydrate-dependent surface binding of galectin-1 and functional divergence from galectin-3. *J Biol Chem,* 276**,** 35917-23.

KOPITZ, J., VON REITZENSTEIN, C., BURCHERT, M., CANTZ, M. & GABIUS, H. J. 1998. Galectin-1 is a major receptor for ganglioside GM1, a product of the growth-controlling activity of a cell surface ganglioside sialidase, on human neuroblastoma cells in culture. *J Biol Chem,* 273**,** 11205-11.

KORNFELD, S. 1986. Trafficking of lysosomal enzymes in normal and disease states. *J Clin Invest,* 77**,** 1-6.

KOVACS-SOLYOM, F., BLASKO, A., FAJKA-BOJA, R., KATONA, R. L., VEGH, L., NOVAK, J., SZEBENI, G. J., KRENACS, L., UHER, F., TUBAK, V., KISS, R. & MONOSTORI, E. 2010. Mechanism of tumor cell-induced T-cell apoptosis mediated by galectin-1. *Immunol Lett,* 127**,** 108-18.

KRAUSE, S., PFEIFFER, C., STRUBE, S., ALSADEQ, A., FEDDERS, H., VOKUHL, C., LOGES, S., WAIZENEGGER, J., BEN-BATALLA, I., CARIO, G., MORICKE, A., STANULLA, M., SCHRAPPE, M. & SCHEWE, D. M. 2015. Mer tyrosine kinase promotes the survival of t(1;19)-positive acute lymphoblastic leukemia (ALL) in the central nervous system (CNS). *Blood,* 125**,** 820-30.

KURIAN, A. W., BALISE, R. R., MCGUIRE, V. & WHITTEMORE, A. S. 2005. Histologic types of epithelial ovarian cancer: have they different risk factors? *Gynecol Oncol,* 96**,** 520-30.

KUTSUKAKE, M., ISHIHARA, R., YOSHIE, M., KOGO, H. & TAMURA, K. 2007. Involvement of insulin-like growth factor-binding protein-related protein 1 in decidualization of human endometrial stromal cells. *Mol Hum Reprod,* 13**,** 737-43.

LAFLEUR, M. A., HANDSLEY, M. M., KNAUPER, V., MURPHY, G. & EDWARDS, D. R. 2002. Endothelial tubulogenesis within fibrin gels specifically requires the activity of membrane-type-matrix metalloproteinases (MT-MMPs). *J Cell Sci,* 115**,** 3427-38.

LANG, L., REITMAN, M., TANG, J., ROBERTS, R. M. & KORNFELD, S. 1984. Lysosomal enzyme phosphorylation. Recognition of a protein-dependent determinant allows specific phosphorylation of oligosaccharides present on lysosomal enzymes. *J Biol Chem,* 259**,** 14663-71.

LARSEN, L. B. & PETERSEN, T. E. 1995. Identification of five molecular forms of cathepsin D in bovine milk. *Adv Exp Med Biol,* 362**,** 279-83.

LAURENT-MATHA, V., DEROCQ, D., PREBOIS, C., KATUNUMA, N. & LIAUDET-COOPMAN, E. 2006. Processing of human cathepsin D is independent of its catalytic function and auto-activation: involvement of cathepsins L and B. *J Biochem,* 139**,** 363-71.

LAURENT-MATHA, V., MARUANI-HERRMANN, S., PREBOIS, C., BEAUJOUIN, M., GLONDU, M., NOEL, A., ALVAREZ-GONZALEZ, M. L., BLACHER, S., COOPMAN, P., BAGHDIGUIAN, S., GILLES, C., LONCAREK, J., FREISS, G., VIGNON, F. & LIAUDET-COOPMAN, E. 2005. Catalytically inactive human cathepsin D triggers fibroblast invasive growth. *J Cell Biol,* 168**,** 489-99.

LAWLEY, T. J. & KUBOTA, Y. 1989. Induction of morphologic differentiation of endothelial cells in culture. *J Invest Dermatol,* 93**,** 59S-61S.

LAWLOR, M. A. & ALESSI, D. R. 2001. PKB/Akt: a key mediator of cell proliferation, survival and insulin responses? *J Cell Sci,* 114**,** 2903-10.

LE MERCIER, M., MATHIEU, V., HAIBE-KAINS, B., BONTEMPI, G., MIJATOVIC, T., DECAESTECKER, C., KISS, R. & LEFRANC, F. 2008. Knocking down galectin 1 in human hs683 glioblastoma cells impairs both angiogenesis and endoplasmic reticulum stress responses. *J Neuropathol Exp Neurol,* 67**,** 456-69.

LEE, H., SHIN, N., SONG, M., KANG, U. B., YEOM, J., LEE, C., AHN, Y. H., YOO, J. S., PAIK, Y. K. & KIM, H. 2010. Analysis of nuclear high mobility group box 1 (HMGB1)-binding proteins in colon cancer cells: clustering with proteins involved in secretion and extranuclear function. *J Proteome Res,* 9**,** 4661-70.

LEE, J., PARK, S. Y., LEE, E. K., PARK, C. G., CHUNG, H. C., RHA, S. Y., KIM, Y. K., BAE, G. U., KIM, B. K., HAN, J. W. & LEE, H. Y. 2006. Activation of hypoxia-inducible factor-1 alpha is necessary for lysophosphatidic acid-induced vascular endothelial growth factor expression. *Clinical Cancer Research,* 12**,** 6351-6358.

LEE, M. Y., LEE, S. H., PARK, J. H. & HAN, H. J. 2009. Interaction of galectin-1 with caveolae induces mouse embryonic stem cell proliferation through the Src, ERas, Akt and mTOR signaling pathways. *Cell Mol Life Sci,* 66**,** 1467-78.

LENGYEL, E. 2010. Ovarian cancer development and metastasis. *Am J Pathol,* 177**,** 1053-64.

LEPPANEN, A., STOWELL, S., BLIXT, O. & CUMMINGS, R. D. 2005. Dimeric galectin-1 binds with high affinity to alpha2,3-sialylated and non-sialylated terminal N-acetyllactosamine units on surface-bound extended glycans. *J Biol Chem,* 280**,** 5549-62.

LI, J., ZHOU, L., TRAN, H. T., CHEN, Y., NGUYEN, N. E., KARASEK, M. A. & MARINKOVICH, M. P. 2006. Overexpression of laminin-8 in human dermal microvascular endothelial cells promotes angiogenesis-related functions. *J Invest Dermatol,* 126**,** 432-40.

LIAUDET, E., DEROCQ, D., ROCHEFORT, H. & GARCIA, M. 1995. Transfected cathepsin D stimulates high density cancer cell growth by inactivating secreted growth inhibitors. *Cell Growth Differ,* 6**,** 1045-52.

LIAUDET, E., GARCIA, M. & ROCHEFORT, H. 1994. Cathepsin D maturation and its stimulatory effect on metastasis are prevented by addition of KDEL retention signal. *Oncogene,* 9**,** 1145-54.

LIN, Z., LIU, Y., SUN, Y. & HE, X. 2011. Expression of Ets-1, Ang-2 and maspin in ovarian cancer and their role in tumor angiogenesis. *J Exp Clin Cancer Res,* 30**,** 31.

LINGER, R. M., KEATING, A. K., EARP, H. S. & GRAHAM, D. K. 2008. TAM receptor tyrosine kinases: biologic functions, signaling, and potential therapeutic targeting in human cancer. *Adv Cancer Res,* 100**,** 35-83.

LIPPINCOTT-SCHWARTZ, J., YUAN, L., TIPPER, C., AMHERDT, M., ORCI, L. & KLAUSNER, R. D. 1991. Brefeldin A's effects on endosomes, lysosomes, and the TGN suggest a general mechanism for regulating organelle structure and membrane traffic. *Cell,* 67**,** 601-16.

LIU, Z. X., YU, C. F., NICKEL, C., THOMAS, S. & CANTLEY, L. G. 2002. Hepatocyte growth factor induces ERK-dependent paxillin phosphorylation and regulates paxillin-focal adhesion kinase association. *J Biol Chem,* 277**,** 10452-8.

LOKSHIN, A. E., WINANS, M., LANDSITTEL, D., MARRANGONI, A. M., VELIKOKHATNAYA, L., MODUGNO, F., NOLEN, B. M. & GORELIK, E. 2006. Circulating IL-8 and anti-IL-8 autoantibody in patients with ovarian cancer. *Gynecol Oncol,* 102**,** 244-51.

LOPEZ-LUCENDO, M. F., SOLIS, D., ANDRE, S., HIRABAYASHI, J., KASAI, K., KALTNER, H., GABIUS, H. J. & ROMERO, A. 2004. Growth-regulatory human galectin-1: crystallographic characterisation of the structural changes induced by single-site mutations and their impact on the thermodynamics of ligand binding. *J Mol Biol,* 343**,** 957-70.

LOSCH, A., KOHLBERGER, P., GITSCH, G., KAIDER, A., BREITENECKER, G. & KAINZ, C. 1996. Lysosomal protease cathepsin D is a prognostic marker in endometrial cancer. *Br J Cancer,* 73**,** 1525-8.

LOSCH, A., SCHINDL, M., KOHLBERGER, P., LAHODNY, J., BREITENECKER, G., HORVAT, R. & BIRNER, P. 2004. Cathepsin D in ovarian cancer: prognostic value and correlation with p53 expression and microvessel density. *Gynecol Oncol,* 92**,** 545-52.

LUTOMSKI, D., FOUILLIT, M., BOURIN, P., MELLOTTEE, D., DENIZE, N., PONTET, M., BLADIER, D., CARON, M. & JOUBERT-CARON, R. 1997. Externalization and binding of galectin-1 on cell surface of K562 cells upon erythroid differentiation. *Glycobiology,* 7**,** 1193-9.

LYDEN, D., HATTORI, K., DIAS, S., COSTA, C., BLAIKIE, P., BUTROS, L., CHADBURN, A., HEISSIG, B., MARKS, W., WITTE, L., WU, Y., HICKLIN, D., ZHU, Z., HACKETT, N. R., CRYSTAL, R. G., MOORE, M. A., HAJJAR, K. A., MANOVA, K., BENEZRA, R. & RAFII, S. 2001. Impaired recruitment of bone-marrow-derived endothelial and hematopoietic precursor cells blocks tumor angiogenesis and growth. *Nat Med,* 7**,** 1194-201.

MACIEWICZ, R. A. & WOTTON, S. F. 1991. Degradation of cartilage matrix components by the cysteine proteinases, cathepsins B and L. *Biomed Biochim Acta,* 50**,** 561-4.

MACIEWICZ, R. A., WOTTON, S. F., ETHERINGTON, D. J. & DUANCE, V. C. 1990. Susceptibility of the cartilage collagens types II, IX and XI to degradation by the cysteine proteinases, cathepsins B and L. *FEBS Lett,* 269**,** 189-93.

MAHAJAN, K. & MAHAJAN, N. P. 2012. PI3K-independent AKT activation in cancers: a treasure trove for novel therapeutics. *J Cell Physiol,* 227**,** 3178-84.

MAHDY, A. M. & WEBSTER, N. R. 2004. Perioperative systemic haemostatic agents. *Br J Anaesth,* 93**,** 842-58.

MANDACHE, E., MOLDOVEANU, E. & SAVI, G. 1985. The involvement of omentum and its milky spots in the dynamics of peritoneal macrophages. *Morphol Embryol (Bucur),* 31**,** 137-42.

MANIOTIS, A. J., FOLBERG, R., HESS, A., SEFTOR, E. A., GARDNER, L. M., PE'ER, J., TRENT, J. M., MELTZER, P. S. & HENDRIX, M. J. 1999. Vascular channel formation by human melanoma cells in vivo and in vitro: vasculogenic mimicry. *Am J Pathol,* 155**,** 739-52.

MANNING, B. D. & CANTLEY, L. C. 2007. AKT/PKB signaling: navigating downstream. *Cell,* 129**,** 1261-74.

MARCINKOWSKA, E. & WIEDLOCHA, A. 2003. Phosphatidylinositol-3 kinase-dependent activation of Akt does not correlate with either high mitogenicity or cell migration induced by FGF-1. *Anticancer Res,* 23**,** 4071-7.

MARQUEZ-ROSADO, L., SOLAN, J. L., DUNN, C. A., NORRIS, R. P. & LAMPE, P. D. 2012. Connexin43 phosphorylation in brain, cardiac, endothelial and epithelial tissues. *Biochim Biophys Acta,* 1818**,** 1985-92.

MARRON, M. B., HUGHES, D. P., EDGE, M. D., FORDER, C. L. & BRINDLE, N. P. 2000. Evidence for heterotypic interaction between the receptor tyrosine kinases TIE-1 and TIE-2. *J Biol Chem,* 275**,** 39741-6.

MASON, R. W., GAL, S. & GOTTESMAN, M. M. 1987. The identification of the major excreted protein (MEP) from a transformed mouse fibroblast cell line as a catalytically active precursor form of cathepsin L. *Biochem J,* 248**,** 449-54.

MASON, R. W., JOHNSON, D. A., BARRETT, A. J. & CHAPMAN, H. A. 1986. Elastinolytic activity of human cathepsin L. *Biochem J,* 233**,** 925-7.

MASON, R. W. & MASSEY, S. D. 1992. Surface activation of pro-cathepsin L. *Biochem Biophys Res Commun,* 189**,** 1659-66.

MATEI, D., SILL, M., DEGEEST, K. & AL, E. 2008. Phase II trial of sorafenib in persistent or recurrent epithelial ovarian cancer (EOC) or primary peritoneal cancer (PPC). *A Gynecologic Oncology Group*.

MATHIEU, M., VIGNON, F., CAPONY, F. & ROCHEFORT, H. 1991. Estradiol down-regulates the mannose-6-phosphate/insulin-like growth factor-II receptor gene and induces cathepsin-D in breast cancer cells: a receptor saturation mechanism to increase the secretion of lysosomal proenzymes. *Mol Endocrinol,* 5**,** 815-22.

MATOBA, Y., KATAYAMA, H. & OHAMI, H. 1996. Evaluation of omental implantation for perforated gastric ulcer therapy: findings in a rat model. *J Gastroenterol,* 31**,** 777-84.

MATULONIS, U., BERLIN, S., IVY, P. & AL, E. 2009. Cediranib, an oral inhibitor of vascular endothelial growth factor receptor kinases, is an active drug in recurrent epithelial ovarian, fallopian tube, and peritoneal cancer. *Journal of clinical oncology,* 27.

MCLAUGHLIN, J. R., RISCH, H. A., LUBINSKI, J., MOLLER, P., GHADIRIAN, P., LYNCH, H., KARLAN, B., FISHMAN, D., ROSEN, B., NEUHAUSEN, S. L., OFFIT, K., KAUFF, N., DOMCHEK, S., TUNG, N., FRIEDMAN, E., FOULKES, W., SUN, P., NAROD, S. A. & HEREDITARY OVARIAN CANCER CLINICAL STUDY, G. 2007. Reproductive risk factors for ovarian cancer in carriers of BRCA1 or BRCA2 mutations: a case-control study. *Lancet Oncol,* 8**,** 26-34.

MEBRATU, Y. & TESFAIGZI, Y. 2009. How ERK1/2 activation controls cell proliferation and cell death: Is subcellular localization the answer? *Cell Cycle,* 8**,** 1168-75.

MESCHER, A. 2010. *Junqueira's basic histology : text & atlas,* New York

London, McGraw-Hill Medical ;

McGraw-Hill distributor.

METTOUCHI, A. 2012. The role of extracellular matrix in vascular branching morphogenesis. *Cell Adh Migr,* 6**,** 528-34.

MIZOGUCHI, M., BETENSKY, R. A., BATCHELOR, T. T., BERNAY, D. C., LOUIS, D. N. & NUTT, C. L. 2006. Activation of STAT3, MAPK, and AKT in malignant astrocytic gliomas: correlation with EGFR status, tumor grade, and survival. *J Neuropathol Exp Neurol,* 65**,** 1181-8.

MOORE, M. A. 2002. Putting the neo into neoangiogenesis. *J Clin Invest,* 109**,** 313-5.

MORALES-RUIZ, M., FULTON, D., SOWA, G., LANGUINO, L. R., FUJIO, Y., WALSH, K. & SESSA, W. C. 2000. Vascular endothelial growth factor-stimulated actin reorganization and migration of endothelial cells is regulated via the serine/threonine kinase Akt. *Circ Res,* 86**,** 892-6.

MORIKAWA, W., YAMAMOTO, K., ISHIKAWA, S., TAKEMOTO, S., ONO, M., FUKUSHI, J., NAITO, S., NOZAKI, C., IWANAGA, S. & KUWANO, M. 2000. Angiostatin generation by cathepsin D secreted by human prostate carcinoma cells. *J Biol Chem,* 275**,** 38912-20.

MOROTTI, M., BECKER, C. M., MENADA, M. V. & FERRERO, S. 2013. Targeting tyrosine-kinases in ovarian cancer. *Expert Opin Investig Drugs,* 22**,** 1265-79.

MORRIS, S. W., NAEVE, C., MATHEW, P., JAMES, P. L., KIRSTEIN, M. N., CUI, X. & WITTE, D. P. 1997. ALK, the chromosome 2 gene locus altered by the t(2;5) in non-Hodgkin's

lymphoma, encodes a novel neural receptor tyrosine kinase that is highly related to leukocyte tyrosine kinase (LTK). *Oncogene,* 14**,** 2175-88.

MORROW, C. J., GRAY, A. & DIVE, C. 2005. Comparison of phosphatidylinositol-3-kinase signalling within a panel of human colorectal cancer cell lines with mutant or wild-type PIK3CA. *FEBS Lett,* 579**,** 5123-8.

MOTEGI, A., FUJIMOTO, J., KOTANI, M., SAKURABA, H. & YAMAMOTO, T. 2004. ALK receptor tyrosine kinase promotes cell growth and neurite outgrowth. *J Cell Sci,* 117**,** 3319-29.

MUELLER, M. M. & FUSENIG, N. E. 2004. Friends or foes - bipolar effects of the tumour stroma in cancer. *Nat Rev Cancer,* 4**,** 839-49.

MULLER, A. M., HERMANNS, M. I., CRONEN, C. & KIRKPATRICK, C. J. 2002. Comparative study of adhesion molecule expression in cultured human macro- and microvascular endothelial cells. *Exp Mol Pathol,* 73**,** 171-80.

MULLER, W. A. 2011. Mechanisms of leukocyte transendothelial migration. *Annu Rev Pathol,* 6**,** 323-44.

MULLIGAN, L. M. 2014. RET revisited: expanding the oncogenic portfolio. *Nat Rev Cancer,* 14**,** 173-86.

NAGY, J. A., CHANG, S. H., DVORAK, A. M. & DVORAK, H. F. 2009. Why are tumour blood vessels abnormal and why is it important to know? *Br J Cancer,* 100**,** 865-9.

NAKAGAWA, T., ROTH, W., WONG, P., NELSON, A., FARR, A., DEUSSING, J., VILLADANGOS, J. A., PLOEGH, H., PETERS, C. & RUDENSKY, A. Y. 1998. Cathepsin L: critical role in Ii degradation and CD4 T cell selection in the thymus. *Science,* 280**,** 450-3.

NAKATSU, M. N., DAVIS, J. & HUGHES, C. C. 2007. Optimized fibrin gel bead assay for the study of angiogenesis. *J Vis Exp***,** 186.

NAZEER, T., MALFETANO, J. H., ROSANO, T. G. & ROSS, J. S. 1992. Correlation of tumor cytosol cathepsin D with differentiation and invasiveness of endometrial adenocarcinoma. *Am J Clin Pathol,* 97**,** 764-9.

NGUYEN, Q., MORT, J. S. & ROUGHLEY, P. J. 1990. Cartilage proteoglycan aggregate is degraded more extensively by cathepsin L than by cathepsin B. *Biochem J,* 266**,** 569-73.

NICKEL, W. 2005. Unconventional secretory routes: direct protein export across the plasma membrane of mammalian cells. *Traffic,* 6**,** 607-14.

NICOSIA, R. F., BONANNO, E. & SMITH, M. 1993. Fibronectin promotes the elongation of microvessels during angiogenesis in vitro. *J Cell Physiol,* 154**,** 654-61.

NIEMAN, K. M., KENNY, H. A., PENICKA, C. V., LADANYI, A., BUELL-GUTBROD, R., ZILLHARDT, M. R., ROMERO, I. L., CAREY, M. S., MILLS, G. B., HOTAMISLIGIL, G. S., YAMADA, S. D., PETER, M. E., GWIN, K. & LENGYEL, E. 2011. Adipocytes promote ovarian cancer metastasis and provide energy for rapid tumor growth. *Nat Med,* 17**,** 1498-503.

NILSSON, M. B., LANGLEY, R. R. & FIDLER, I. J. 2005. Interleukin-6, secreted by human ovarian carcinoma cells, is a potent proangiogenic cytokine. *Cancer Res,* 65**,** 10794-800.

NISHIDA, Y., KOHNO, K., KAWAMATA, T., MORIMITSU, K., KUWANO, M. & MIYAKAWA, I. 1995. Increased cathepsin L levels in serum in some patients with ovarian cancer: comparison with CA125 and CA72-4. *Gynecol Oncol,* 56**,** 357-61.

NISHIMURA, Y., FURUNO, K. & KATO, K. 1988. Biosynthesis and processing of lysosomal cathepsin L in primary cultures of rat hepatocytes. *Arch Biochem Biophys,* 263**,** 107-16.

NORLING, L. V., SAMPAIO, A. L., COOPER, D. & PERRETTI, M. 2008. Inhibitory control of endothelial galectin-1 on in vitro and in vivo lymphocyte trafficking. *FASEB J,* 22**,** 682-90.

NOSAKA, A. Y., KANAORI, K., TENO, N., TOGAME, H., INAOKA, T., TAKAI, M. & KOKUBO, T. 1999. Conformational studies on the specific cleavage site of Type I collagen (alpha-1) fragment (157-192) by cathepsins K and L by proton NMR spectroscopy. *Bioorg Med Chem,* 7**,** 375-9.

NOSKOVA, V., AHMADI, S., ASANDER, E. & CASSLEN, B. 2009. Ovarian cancer cells stimulate uPA gene expression in fibroblastic stromal cells via multiple paracrine and autocrine mechanisms. *Gynecol Oncol,* 115**,** 121-6.

OH, Y., NAGALLA, S. R., YAMANAKA, Y., KIM, H. S., WILSON, E. & ROSENFELD, R. G. 1996. Synthesis and characterization of insulin-like growth factor-binding protein (IGFBP)-7. Recombinant human mac25 protein specifically binds IGF-I and -II. *J Biol Chem,* 271**,** 30322-5.

OHRI, S. S., VASHISHTA, A., PROCTOR, M., FUSEK, M. & VETVICKA, V. 2008. The propeptide of cathepsin D increases proliferation, invasion and metastasis of breast cancer cells. *Int J Oncol,* 32**,** 491-8.

OKADA, M., BLOMBACK, B., CHANG, M. D. & HOROWITZ, B. 1985. Fibronectin and fibrin gel structure. *J Biol Chem,* 260**,** 1811-20.

OLLINGER, K. 2000. Inhibition of cathepsin D prevents free-radical-induced apoptosis in rat cardiomyocytes. *Arch Biochem Biophys,* 373**,** 346-51.

OOSTERLING, S. J., VAN DER BIJ, G. J., BOGELS, M., VAN DER SIJP, J. R., BEELEN, R. H., MEIJER, S. & VAN EGMOND, M. 2006. Insufficient ability of omental milky spots to prevent peritoneal tumor outgrowth supports omentectomy in minimal residual disease. *Cancer Immunol Immunother,* 55**,** 1043-51.

PALECEK, S. P., LOFTUS, J. C., GINSBERG, M. H., LAUFFENBURGER, D. A. & HORWITZ, A. F. 1997. Integrin-ligand binding properties govern cell migration speed through cell-substratum adhesiveness. *Nature,* 385**,** 537-40.

PAPADOPOULOS, I., GIATROMANOLAKI, A., KOUKOURAKIS, M. I. & SIVRIDIS, E. 2004. Tumour angiogenic activity and vascular survival ability in bladder carcinoma. *J Clin Pathol,* 57**,** 250-5.

PARTANEN, J., PURI, M. C., SCHWARTZ, L., FISCHER, K. D., BERNSTEIN, A. & ROSSANT, J. 1996. Cell autonomous functions of the receptor tyrosine kinase TIE in a late phase of angiogenic capillary growth and endothelial cell survival during murine development. *Development,* 122**,** 3013-21.

PASALICH, M., SU, D., BINNS, C. W. & LEE, A. H. 2013. Reproductive factors for ovarian cancer in southern Chinese women. *J Gynecol Oncol,* 24**,** 135-40.

PASSALIDOU, E., TRIVELLA, M., SINGH, N., FERGUSON, M., HU, J., CESARIO, A., GRANONE, P., NICHOLSON, A. G., GOLDSTRAW, P., RATCLIFFE, C., TETLOW, M., LEIGH, I., HARRIS, A. L., GATTER, K. C. & PEZZELLA, F. 2002. Vascular phenotype in angiogenic and non-angiogenic lung non-small cell carcinomas. *Br J Cancer,* 86**,** 244-9.

PEN, A., MORENO, M. J., DUROCHER, Y., DEB-RINKER, P. & STANIMIROVIC, D. B. 2008. Glioblastoma-secreted factors induce IGFBP7 and angiogenesis by modulating Smad-2-dependent TGF-beta signaling. *Oncogene,* 27**,** 6834-44.

PERILLO, N. L., PACE, K. E., SEILHAMER, J. J. & BAUM, L. G. 1995. Apoptosis of T cells mediated by galectin-1. *Nature,* 378**,** 736-9.

PERREN, T. J., SWART, A. M., PFISTERER, J., LEDERMANN, J. A., PUJADE-LAURAINE, E., KRISTENSEN, G., CAREY, M. S., BEALE, P., CERVANTES, A., KURZEDER, C., DU BOIS, A., SEHOULI, J., KIMMIG, R., STAHLE, A., COLLINSON, F., ESSAPEN, S., GOURLEY, C., LORTHOLARY, A., SELLE, F., MIRZA, M. R., LEMINEN, A., PLANTE, M., STARK, D., QIAN, W., PARMAR, M. K., OZA, A. M. & INVESTIGATORS, I. 2011. A phase 3 trial of bevacizumab in ovarian cancer. *N Engl J Med,* 365**,** 2484-96.

PLATELL, C., COOPER, D., PAPADIMITRIOU, J. M. & HALL, J. C. 2000. The omentum. *World J Gastroenterol,* 6**,** 169-176.

POTTS, W., BOWYER, J., JONES, H., TUCKER, D., FREEMONT, A. J., MILLEST, A., MARTIN, C., VERNON, W., NEERUNJUN, D., SLYNN, G., HARPER, F. & MACIEWICZ, R. 2004. Cathepsin L-deficient mice exhibit abnormal skin and bone development and show increased resistance to osteoporosis following ovariectomy. *Int J Exp Pathol,* 85**,** 85-96.

PRANJOL, M. Z., GUTOWSKI, N., HANNEMANN, M. & WHATMORE, J. 2015. The Potential Role of the Proteases Cathepsin D and Cathepsin L in the Progression and Metastasis of Epithelial Ovarian Cancer. *Biomolecules,* 5**,** 3260-79.

PRENCE, E. M., DONG, J. M. & SAHAGIAN, G. G. 1990. Modulation of the transport of a lysosomal enzyme by PDGF. *J Cell Biol,* 110**,** 319-26.

PRUDOVSKY, I., MANDINOVA, A., SOLDI, R., BAGALA, C., GRAZIANI, I., LANDRISCINA, M., TARANTINI, F., DUARTE, M., BELLUM, S., DOHERTY, H. & MACIAG, T. 2003. The non-classical export routes: FGF1 and IL-1alpha point the way. *J Cell Sci,* 116**,** 4871-81.

PRUITT, F. L., HE, Y., FRANCO, O. E., JIANG, M., CATES, J. M. & HAYWARD, S. W. 2013. Cathepsin D acts as an essential mediator to promote malignancy of benign prostatic epithelium. *Prostate,* 73**,** 476-88.

PURDIE, D. M., BAIN, C. J., SISKIND, V., WEBB, P. M. & GREEN, A. C. 2003. Ovulation and risk of epithelial ovarian cancer. *Int J Cancer,* 104**,** 228-32.

QIAN, Y., CORUM, L., MENG, Q., BLENIS, J., ZHENG, J. Z., SHI, X., FLYNN, D. C. & JIANG, B. H. 2004. PI3K induced actin filament remodeling through Akt and p70S6K1: implication of essential role in cell migration. *Am J Physiol Cell Physiol,* 286**,** C153-63.

RAJENDRAN, P., RENGARAJAN, T., THANGAVEL, J., NISHIGAKI, Y., SAKTHISEKARAN, D., SETHI, G. & NISHIGAKI, I. 2013. The vascular endothelium and human diseases. *Int J Biol Sci,* 9**,** 1057-69.

REES, D. C., JOHNSON, E. & LEWINSON, O. 2009. ABC transporters: the power to change. *Nat Rev Mol Cell Biol,* 10**,** 218-27.

REK, A., KRENN, E. & KUNGL, A. J. 2009. Therapeutically targeting protein-glycan interactions. *Br J Pharmacol,* 157**,** 686-94.

REN, X. D., KIOSSES, W. B., SIEG, D. J., OTEY, C. A., SCHLAEPFER, D. D. & SCHWARTZ, M. A. 2000. Focal adhesion kinase suppresses Rho activity to promote focal adhesion turnover. *J Cell Sci,* 113 (Pt 20)**,** 3673-8.

RIMAN, T., DICKMAN, P. W., NILSSON, S., NORDLINDER, H., MAGNUSSON, C. M. & PERSSON, I. R. 2004a. Some life-style factors and the risk of invasive epithelial ovarian cancer in Swedish women. *Eur J Epidemiol,* 19**,** 1011-9.

RIMAN, T., NILSSON, S. & PERSSON, I. R. 2004b. Review of epidemiological evidence for reproductive and hormonal factors in relation to the risk of epithelial ovarian malignancies. *Acta Obstet Gynecol Scand,* 83**,** 783-95.

RITONJA, A., POPOVIC, T., KOTNIK, M., MACHLEIDT, W. & TURK, V. 1988. Amino acid sequences of the human kidney cathepsins H and L. *FEBS Lett,* 228**,** 341-5.

RIZQIAWAN, A., TOBIUME, K., OKUI, G., YAMAMOTO, K., SHIGEISHI, H., ONO, S., SHIMASUE, H., TAKECHI, M., HIGASHIKAWA, K. & KAMATA, N. 2013. Autocrine galectin-1 promotes collective cell migration of squamous cell carcinoma cells through up-regulation of distinct integrins. *Biochem Biophys Res Commun,* 441**,** 904-10.

ROBERG, K., JOHANSSON, U. & OLLINGER, K. 1999. Lysosomal release of cathepsin D precedes relocation of cytochrome c and loss of mitochondrial transmembrane potential during apoptosis induced by oxidative stress. *Free Radic Biol Med,* 27**,** 1228-37.

ROCHEFORT, H. 1992. Cathepsin D in breast cancer: a tissue marker associated with metastasis. *Eur J Cancer,* 28A**,** 1780-3.

ROCHEFORT, H., CAPONY, F., GARCIA, M., CAVAILLES, V., FREISS, G., CHAMBON, M., MORISSET, M. & VIGNON, F. 1987. Estrogen-induced lysosomal proteases secreted by breast cancer cells: a role in carcinogenesis? *J Cell Biochem,* 35**,** 17-29.

ROCHEFORT, H., GARCIA, M., GLONDU, M., LAURENT, V., LIAUDET, E., REY, J. M. & ROGER, P. 2000. Cathepsin D in breast cancer: mechanisms and clinical applications, a 1999 overview. *Clin Chim Acta,* 291**,** 157-70.

RODRIGUEZ, M. 2013. Ziv-aflibercept use in metastatic colorectal cancer. *J Adv Pract Oncol,* 4**,** 348-52.

ROGERS, A. E., LE, J. P., SATHER, S., PERNU, B. M., GRAHAM, D. K., PIERCE, A. M. & KEATING, A. K. 2012. Mer receptor tyrosine kinase inhibition impedes glioblastoma multiforme migration and alters cellular morphology. *Oncogene,* 31**,** 4171-81.

ROTH, W., DEUSSING, J., BOTCHKAREV, V. A., PAULY-EVERS, M., SAFTIG, P., HAFNER, A., SCHMIDT, P., SCHMAHL, W., SCHERER, J., ANTON-LAMPRECHT, I., VON FIGURA, K., PAUS, R. & PETERS, C. 2000. Cathepsin L deficiency as molecular defect of furless:

hyperproliferation of keratinocytes and pertubation of hair follicle cycling. *FASEB J,* 14**,** 2075-86.

ROUSSEAU, S., HOULE, F., KOTANIDES, H., WITTE, L., WALTENBERGER, J., LANDRY, J. & HUOT, J. 2000. Vascular endothelial growth factor (VEGF)-driven actin-based motility is mediated by VEGFR2 and requires concerted activation of stress-activated protein kinase 2 (SAPK2/p38) and geldanamycin-sensitive phosphorylation of focal adhesion kinase. *J Biol Chem,* 275**,** 10661-72.

ROUSSELET, N., MILLS, L., JEAN, D., TELLEZ, C., BAR-ELI, M. & FRADE, R. 2004. Inhibition of tumorigenicity and metastasis of human melanoma cells by anti-cathepsin L single chain variable fragment. *Cancer Res,* 64**,** 146-51.

ROYAL, I., LAMARCHE-VANE, N., LAMORTE, L., KAIBUCHI, K. & PARK, M. 2000. Activation of cdc42, rac, PAK, and rho-kinase in response to hepatocyte growth factor differentially regulates epithelial cell colony spreading and dissociation. *Mol Biol Cell,* 11**,** 1709-25.

RUAN, G. X. & KAZLAUSKAS, A. 2012. Axl is essential for VEGF-A-dependent activation of PI3K/Akt. *EMBO J,* 31**,** 1692-703.

RUBINFELD, H. & SEGER, R. 2005. The ERK cascade: a prototype of MAPK signaling. *Mol Biotechnol,* 31**,** 151-74.

RUDNEY, H. 1940. The Utilization of L-Glucose by Mammalian Tissues and Bacteria. *Science,* 92**,** 112-3.

SACCHI, V., MITTERMAYR, R., HARTINGER, J., MARTINO, M. M., LORENTZ, K. M., WOLBANK, S., HOFMANN, A., LARGO, R. A., MARSCHALL, J. S., GROPPA, E., GIANNI-BARRERA, R., EHRBAR, M., HUBBELL, J. A., REDL, H. & BANFI, A. 2014. Long-lasting fibrin matrices ensure stable and functional angiogenesis by highly tunable, sustained delivery of recombinant VEGF164. *Proc Natl Acad Sci U S A,* 111**,** 6952-7.

SAGULENKO, V., MUTH, D., SAGULENKO, E., PAFFHAUSEN, T., SCHWAB, M. & WESTERMANN, F. 2008. Cathepsin D protects human neuroblastoma cells from doxorubicin-induced cell death. *Carcinogenesis,* 29**,** 1869-77.

SAHARINEN, P., KERKELA, K., EKMAN, N., MARRON, M., BRINDLE, N., LEE, G. M., AUGUSTIN, H., KOH, G. Y. & ALITALO, K. 2005. Multiple angiopoietin recombinant proteins activate the Tie1 receptor tyrosine kinase and promote its interaction with Tie2. *J Cell Biol,* 169**,** 239-43.

SALEHI, F., DUNFIELD, L., PHILLIPS, K. P., KREWSKI, D. & VANDERHYDEN, B. C. 2008. Risk factors for ovarian cancer: an overview with emphasis on hormonal factors. *J Toxicol Environ Health B Crit Rev,* 11**,** 301-21.

SAMIE, M. A. & XU, H. 2014. Lysosomal exocytosis and lipid storage disorders. *J Lipid Res,* 55**,** 995-1009.

SANCHEZ-RUDERISCH, H., DETJEN, K. M., WELZEL, M., ANDRE, S., FISCHER, C., GABIUS, H. J. & ROSEWICZ, S. 2011. Galectin-1 sensitizes carcinoma cells to anoikis via the fibronectin receptor alpha5beta1-integrin. *Cell Death Differ,* 18**,** 806-16.

SANDER, E. E., VAN DELFT, S., TEN KLOOSTER, J. P., REID, T., VAN DER KAMMEN, R. A., MICHIELS, F. & COLLARD, J. G. 1998. Matrix-dependent Tiam1/Rac signaling in epithelial cells promotes either cell-cell adhesion or cell migration and is regulated by phosphatidylinositol 3-kinase. *J Cell Biol,* 143**,** 1385-98.

SATO, J., HASEGAWA, S., AKAOGI, K., YASUMITSU, H., YAMADA, S., SUGAHARA, K. & MIYAZAKI, K. 1999. Identification of cell-binding site of angiomodulin (AGM/TAF/Mac25) that interacts with heparan sulfates on cell surface. *J Cell Biochem,* 75**,** 187-95.

SATO, S., FUJITA, N. & TSURUO, T. 2004. Involvement of 3-phosphoinositide-dependent protein kinase-1 in the MEK/MAPK signal transduction pathway. *J Biol Chem,* 279**,** 33759-67.

SAVANT, S., LA PORTA, S., BUDNIK, A., BUSCH, K., HU, J., TISCH, N., KORN, C., VALLS, A. F., BENEST, A. V., TERHARDT, D., QU, X., ADAMS, R. H., BALDWIN, H. S., RUIZ DE ALMODOVAR, C., RODEWALD, H. R. & AUGUSTIN, H. G. 2015. The Orphan Receptor Tie1 Controls Angiogenesis and Vascular Remodeling by Differentially Regulating Tie2 in Tip and Stalk Cells. *Cell Rep,* 12**,** 1761-73.

SCAPPATICCI, F. A., SKILLINGS, J. R., HOLDEN, S. N., GERBER, H. P., MILLER, K., KABBINAVAR, F., BERGSLAND, E., NGAI, J., HOLMGREN, E., WANG, J. & HURWITZ, H. 2007. Arterial thromboembolic events in patients with metastatic carcinoma treated with chemotherapy and bevacizumab. *J Natl Cancer Inst,* 99**,** 1232-9.

SCHAFER, T., ZENTGRAF, H., ZEHE, C., BRUGGER, B., BERNHAGEN, J. & NICKEL, W. 2004. Unconventional secretion of fibroblast growth factor 2 is mediated by direct translocation across the plasma membrane of mammalian cells. *J Biol Chem,* 279**,** 6244-51.

SCOTT, K. & ZHANG, J. 2002. Partial identification by site-directed mutagenesis of a cell growth inhibitory site on the human galectin-1 molecule. *BMC Cell Biol,* 3**,** 3.

SECCHIERO, P., GONELLI, A., CARNEVALE, E., MILANI, D., PANDOLFI, A., ZELLA, D. & ZAULI, G. 2003. TRAIL promotes the survival and proliferation of primary human vascular endothelial cells by activating the Akt and ERK pathways. *Circulation,* 107**,** 2250-6.

SEELENMEYER, C., STEGMAYER, C. & NICKEL, W. 2008. Unconventional secretion of fibroblast growth factor 2 and galectin-1 does not require shedding of plasma membrane-derived vesicles. *FEBS Lett,* 582**,** 1362-8.

SEELENMEYER, C., WEGEHINGEL, S., LECHNER, J. & NICKEL, W. 2003. The cancer antigen CA125 represents a novel counter receptor for galectin-1. *J Cell Sci,* 116**,** 1305-18.

SEELENMEYER, C., WEGEHINGEL, S., TEWS, I., KUNZLER, M., AEBI, M. & NICKEL, W. 2005. Cell surface counter receptors are essential components of the unconventional export machinery of galectin-1. *J Cell Biol,* 171**,** 373-81.

SEO, M., KIM, J. H. & SUK, K. 2016. Role of the p55-gamma subunit of PI3K in ALK-induced cell migration: RNAi-based selection of cell migration regulators. *Cell Adh Migr***,** 1-6.

SHANKAR, S. L., O'GUIN, K., CAMMER, M., MCMORRIS, F. A., STITT, T. N., BASCH, R. S., VARNUM, B. & SHAFIT-ZAGARDO, B. 2003. The growth arrest-specific gene product Gas6 promotes the survival of human oligodendrocytes via a phosphatidylinositol 3-kinase-dependent pathway. *J Neurosci,* 23**,** 4208-18.

SHANKAR, S. L., O'GUIN, K., KIM, M., VARNUM, B., LEMKE, G., BROSNAN, C. F. & SHAFIT-ZAGARDO, B. 2006. Gas6/Axl signaling activates the phosphatidylinositol 3-kinase/Akt1 survival pathway to protect oligodendrocytes from tumor necrosis factor alpha-induced apoptosis. *J Neurosci,* 26**,** 5638-48.

SHEIKH, A. M., LI, X., WEN, G., TAUQEER, Z., BROWN, W. T. & MALIK, M. 2010. Cathepsin D and apoptosis related proteins are elevated in the brain of autistic subjects. *Neuroscience,* 165**,** 363-70.

SHIMADA, N., OHNO-MATSUI, K., ISEKI, S., KOIKE, M., UCHIYAMA, Y., WANG, J., YOSHIDA, T., SATO, T., PETERS, C., MOCHIZUKI, M. & MORITA, I. 2010. Cathepsin L in bone marrow-derived cells is required for retinal and choroidal neovascularization. *Am J Pathol,* 176**,** 2571-80.

SHIOTA, M., FUJIMOTO, J., SEMBA, T., SATOH, H., YAMAMOTO, T. & MORI, S. 1994. Hyperphosphorylation of a novel 80 kDa protein-tyrosine kinase similar to Ltk in a human Ki-1 lymphoma cell line, AMS3. *Oncogene,* 9**,** 1567-74.

SHIOTA, M., NAKAMURA, S., ICHINOHASAMA, R., ABE, M., AKAGI, T., TAKESHITA, M., MORI, N., FUJIMOTO, J., MIYAUCHI, J., MIKATA, A., NANBA, K., TAKAMI, T., YAMABE, H., TAKANO, Y., IZUMO, T., NAGATANI, T., MOHRI, N., NASU, K., SATOH, H., KATANO, H., FUJIMOTO, J., YAMAMOTO, T. & MORI, S. 1995. Anaplastic large cell lymphomas expressing the novel chimeric protein p80NPM/ALK: a distinct clinicopathologic entity. *Blood,* 86**,** 1954-60.

SHONO, T., KANETAKE, H. & KANDA, S. 2001. The role of mitogen-activated protein kinase activation within focal adhesions in chemotaxis toward FGF-2 by murine brain capillary endothelial cells. *Exp Cell Res,* 264**,** 275-83.

SIINTOLA, E., PARTANEN, S., STROMME, P., HAAPANEN, A., HALTIA, M., MAEHLEN, J., LEHESJOKI, A. E. & TYYNELA, J. 2006. Cathepsin D deficiency underlies congenital human neuronal ceroid-lipofuscinosis. *Brain,* 129**,** 1438-45.

SIMON-ASSMANN, P., OREND, G., MAMMADOVA-BACH, E., SPENLE, C. & LEFEBVRE, O. 2011. Role of laminins in physiological and pathological angiogenesis. *Int J Dev Biol,* 55**,** 455-65.

SMALL, J. V., STRADAL, T., VIGNAL, E. & ROTTNER, K. 2002. The lamellipodium: where motility begins. *Trends Cell Biol,* 12**,** 112-20.

SOOD, A. K., SEFTOR, E. A., FLETCHER, M. S., GARDNER, L. M., HEIDGER, P. M., BULLER, R. E., SEFTOR, R. E. & HENDRIX, M. J. 2001. Molecular determinants of ovarian cancer plasticity. *Am J Pathol,* 158**,** 1279-88.

STEENHUIS, P., FROEMMING, J., REINHECKEL, T. & STORCH, S. 2012. Proteolytic cleavage of the disease-related lysosomal membrane glycoprotein CLN7. *Biochim Biophys Acta,* 1822**,** 1617-28.

STEINFELD, R., REINHARDT, K., SCHREIBER, K., HILLEBRAND, M., KRAETZNER, R., BRUCK, W., SAFTIG, P. & GARTNER, J. 2006. Cathepsin D deficiency is associated with a human neurodegenerative disorder. *Am J Hum Genet,* 78**,** 988-98.

STEMKE-HALE, K., GONZALEZ-ANGULO, A. M., LLUCH, A., NEVE, R. M., KUO, W. L., DAVIES, M., CAREY, M., HU, Z., GUAN, Y., SAHIN, A., SYMMANS, W. F., PUSZTAI, L., NOLDEN, L. K., HORLINGS, H., BERNS, K., HUNG, M. C., VAN DE VIJVER, M. J., VALERO, V., GRAY, J. W., BERNARDS, R., MILLS, G. B. & HENNESSY, B. T. 2008. An integrative genomic and proteomic analysis of PIK3CA, PTEN, and AKT mutations in breast cancer. *Cancer Res,* 68**,** 6084-91.

STERN, D. M., ESPOSITO, C., GERLACH, H., GERLACH, M., RYAN, J., HANDLEY, D. & NAWROTH, P. 1991. Endothelium and regulation of coagulation. *Diabetes Care,* 14**,** 160-6.

STONE, R. L., SOOD, A. K. & COLEMAN, R. L. 2010. Collateral damage: toxic effects of targeted antiangiogenic therapies in ovarian cancer. *Lancet Oncol,* 11**,** 465-75.

STOWELL, S. R., QIAN, Y., KARMAKAR, S., KOYAMA, N. S., DIAS-BARUFFI, M., LEFFLER, H., MCEVER, R. P. & CUMMINGS, R. D. 2008. Differential roles of galectin-1 and galectin-3 in regulating leukocyte viability and cytokine secretion. *J Immunol,* 180**,** 3091-102.

SUBAUSTE, M. C., PERTZ, O., ADAMSON, E. D., TURNER, C. E., JUNGER, S. & HAHN, K. M. 2004. Vinculin modulation of paxillin-FAK interactions regulates ERK to control survival and motility. *J Cell Biol,* 165**,** 371-81.

SUDHAN, D. R. & SIEMANN, D. W. 2013. Cathepsin L inhibition by the small molecule KGP94 suppresses tumor microenvironment enhanced metastasis associated cell functions of prostate and breast cancer cells. *Clin Exp Metastasis,* 30**,** 891-902.

SUEBLINVONG, T. & CARNEY, M. E. 2009. Current understanding of risk factors for ovarian cancer. *Curr Treat Options Oncol,* 10**,** 67-81.

SUN, T., CAO, H., XU, L., ZHU, B., GU, Q. & XU, X. 2011. Insulin-like growth factor binding protein-related protein 1 mediates VEGF-induced proliferation, migration and tube formation of retinal endothelial cells. *Curr Eye Res,* 36**,** 341-9.

SUZUMORI, N., OZAKI, Y., OGASAWARA, M. & SUZUMORI, K. 2001. Increased concentrations of cathepsin D in peritoneal fluid from women with endometriosis. *Mol Hum Reprod,* 7**,** 459-62.

SWISSHELM, K., RYAN, K., TSUCHIYA, K. & SAGER, R. 1995. Enhanced expression of an insulin growth factor-like binding protein (mac25) in senescent human mammary epithelial cells and induced expression with retinoic acid. *Proc Natl Acad Sci U S A,* 92**,** 4472-6.

TAKADA, Y., MUKHOPADHYAY, A., KUNDU, G. C., MAHABELESHWAR, G. H., SINGH, S. & AGGARWAL, B. B. 2003. Hydrogen peroxide activates NF-kappa B through tyrosine phosphorylation of I kappa B alpha and serine phosphorylation of p65: evidence for the involvement of I kappa B alpha kinase and Syk protein-tyrosine kinase. *J Biol Chem,* 278**,** 24233-41.

TAKESHIMA, H., SAKAGUCHI, M., MIHARA, K., MURAKAMI, K. & OMURA, T. 1995. Intracellular targeting of lysosomal cathepsin D in COS cells. *J Biochem,* 118**,** 981-8.

TAMURA, K., HASHIMOTO, K., SUZUKI, K., YOSHIE, M., KUTSUKAKE, M. & SAKURAI, T. 2009. Insulin-like growth factor binding protein-7 (IGFBP7) blocks vascular endothelial cell

growth factor (VEGF)-induced angiogenesis in human vascular endothelial cells. *Eur J Pharmacol,* 610**,** 61-7.

TAMURA, K., YOSHIE, M., HASHIMOTO, K. & TACHIKAWA, E. 2014. Inhibitory effect of insulin-like growth factor-binding protein-7 (IGFBP7) on in vitro angiogenesis of vascular endothelial cells in the rat corpus luteum. *J Reprod Dev,* 60**,** 447-53.

TANAKA, K., BABIC, I., NATHANSON, D., AKHAVAN, D., GUO, D., GINI, B., DANG, J., ZHU, S., YANG, H., DE JESUS, J., AMZAJERDI, A. N., ZHANG, Y., DIBBLE, C. C., DAN, H., RINKENBAUGH, A., YONG, W. H., VINTERS, H. V., GERA, J. F., CAVENEE, W. K., CLOUGHESY, T. F., MANNING, B. D., BALDWIN, A. S. & MISCHEL, P. S. 2011. Oncogenic EGFR signaling activates an mTORC2-NF-kappaB pathway that promotes chemotherapy resistance. *Cancer Discov,* 1**,** 524-38.

TANAKA, Y., MIYAMOTO, S., SUZUKI, S. O., OKI, E., YAGI, H., SONODA, K., YAMAZAKI, A., MIZUSHIMA, H., MAEHARA, Y., MEKADA, E. & NAKANO, H. 2005. Clinical significance of heparin-binding epidermal growth factor-like growth factor and a disintegrin and metalloprotease 17 expression in human ovarian cancer. *Clin Cancer Res,* 11**,** 4783-92.

TARDY, C., TYYNELA, J., HASILIK, A., LEVADE, T. & ANDRIEU-ABADIE, N. 2003. Stress-induced apoptosis is impaired in cells with a lysosomal targeting defect but is not affected in cells synthesizing a catalytically inactive cathepsin D. *Cell Death Differ,* 10**,** 1090-100.

TATEO, S., MEREU, L., SALAMANO, S., KLERSY, C., BARONE, M., SPYROPOULOS, A. C. & PIOVELLA, F. 2005. Ovarian cancer and venous thromboembolic risk. *Gynecol Oncol,* 99**,** 119-25.

TEBBEN, P. J., KALLI, K. R., CLIBY, W. A., HARTMANN, L. C., GRANDE, J. P., SINGH, R. J. & KUMAR, R. 2005. Elevated fibroblast growth factor 23 in women with malignant ovarian tumors. *Mayo Clin Proc,* 80**,** 745-51.

THIBAULT, B., CASTELLS, M., DELORD, J. P. & COUDERC, B. 2014. Ovarian cancer microenvironment: implications for cancer dissemination and chemoresistance acquisition. *Cancer Metastasis Rev,* 33**,** 17-39.

THIEMANN, S., MAN, J. H., CHANG, M. H., LEE, B. & BAUM, L. G. 2015. Galectin-1 regulates tissue exit of specific dendritic cell populations. *J Biol Chem,* 290**,** 22662-77.

THIJSSEN, V. L., BARKAN, B., SHOJI, H., ARIES, I. M., MATHIEU, V., DELTOUR, L., HACKENG, T. M., KISS, R., KLOOG, Y., POIRIER, F. & GRIFFIOEN, A. W. 2010. Tumor cells secrete galectin-1 to enhance endothelial cell activity. *Cancer Res,* 70**,** 6216-24.

THIJSSEN, V. L., POSTEL, R., BRANDWIJK, R. J., DINGS, R. P., NESMELOVA, I., SATIJN, S., VERHOFSTAD, N., NAKABEPPU, Y., BAUM, L. G., BAKKERS, J., MAYO, K. H., POIRIER, F. & GRIFFIOEN, A. W. 2006. Galectin-1 is essential in tumor angiogenesis and is a target for antiangiogenesis therapy. *Proc Natl Acad Sci U S A,* 103**,** 15975-80.

TINARI, N., KUWABARA, I., HUFLEJT, M. E., SHEN, P. F., IACOBELLI, S. & LIU, F. T. 2001. Glycoprotein 90K/MAC-2BP interacts with galectin-1 and mediates galectin-1-induced cell aggregation. *Int J Cancer,* 91**,** 167-72.

TOSCANO, M. A., CAMPAGNA, L., MOLINERO, L. L., CERLIANI, J. P., CROCI, D. O., ILARREGUI, J. M., FUERTES, M. B., NOJEK, I. M., FEDEDA, J. P., ZWIRNER, N. W., COSTAS, M. A. & RABINOVICH, G. A. 2011. Nuclear factor (NF)-kappaB controls expression of the immunoregulatory glycan-binding protein galectin-1. *Mol Immunol,* 48**,** 1940-9.

TOUTIRAIS, O., CHARTIER, P., DUBOIS, D., BOUET, F., LEVEQUE, J., CATROS-QUEMENER, V. & GENETET, N. 2003. Constitutive expression of TGF-beta1, interleukin-6 and interleukin-8 by tumor cells as a major component of immune escape in human ovarian carcinoma. *Eur Cytokine Netw,* 14**,** 246-55.

TOYOKAWA, K., CARLING, S. J. & OTT, T. L. 2007. Cellular localization and function of the antiviral protein, ovine Mx1 (oMx1): I. Ovine Mx1 is secreted by endometrial epithelial cells via an 'unconventional' secretory pathway. *Am J Reprod Immunol,* 57**,** 13-22.

TUFRO, A., TEICHMAN, J., BANU, N. & VILLEGAS, G. 2007. Crosstalk between VEGF-A/VEGFR2 and GDNF/RET signaling pathways. *Biochem Biophys Res Commun,* 358**,** 410-6.

TWOROGER, S. S., FAIRFIELD, K. M., COLDITZ, G. A., ROSNER, B. A. & HANKINSON, S. E. 2007. Association of oral contraceptive use, other contraceptive methods, and infertility with ovarian cancer risk. *Am J Epidemiol,* 166**,** 894-901.

TYYNELA, J., SOHAR, I., SLEAT, D. E., GIN, R. M., DONNELLY, R. J., BAUMANN, M., HALTIA, M. & LOBEL, P. 2000. A mutation in the ovine cathepsin D gene causes a congenital lysosomal storage disease with profound neurodegeneration. *EMBO J,* 19**,** 2786-92.

TYYNELA, J., SOHAR, I., SLEAT, D. E., GIN, R. M., DONNELLY, R. J., BAUMANN, M., HALTIA, M. & LOBEL, P. 2001. Congenital ovine neuronal ceroid lipofuscinosis--a cathepsin D deficiency with increased levels of the inactive enzyme. *Eur J Paediatr Neurol,* 5 Suppl A**,** 43-5.

UNGARI, S., KATARI, R. S., ALESSANDRI, G. & GULLINO, P. M. 1985. Cooperation between fibronectin and heparin in the mobilization of capillary endothelium. *Invasion Metastasis,* 5**,** 193-205.

URBICH, C., HEESCHEN, C., AICHER, A., SASAKI, K., BRUHL, T., FARHADI, M. R., VAJKOCZY, P., HOFMANN, W. K., PETERS, C., PENNACCHIO, L. A., ABOLMAALI, N. D., CHAVAKIS, E., REINHECKEL, T., ZEIHER, A. M. & DIMMELER, S. 2005. Cathepsin L is required for endothelial progenitor cell-induced neovascularization. *Nat Med,* 11**,** 206-13.

USHIJIMA, K. 2009. Current status of gynecologic cancer in Japan. *J Gynecol Oncol,* 20**,** 67-71.

VAJKOCZY, P., KNYAZEV, P., KUNKEL, A., CAPELLE, H. H., BEHRNDT, S., VON TENGG-KOBLIGK, H., KIESSLING, F., EICHELSBACHER, U., ESSIG, M., READ, T. A., ERBER, R. & ULLRICH, A. 2006. Dominant-negative inhibition of the Axl receptor tyrosine kinase suppresses brain tumor cell growth and invasion and prolongs survival. *Proc Natl Acad Sci U S A,* 103**,** 5799-804.

VAN BUUL, J. D., MUL, F. P., VAN DER SCHOOT, C. E. & HORDIJK, P. L. 2004. ICAM-3 activation modulates cell-cell contacts of human bone marrow endothelial cells. *J Vasc Res,* 41**,** 28-37.

VAN DEN BRULE, F., CALIFICE, S., GARNIER, F., FERNANDEZ, P. L., BERCHUCK, A. & CASTRONOVO, V. 2003. Galectin-1 accumulation in the ovary carcinoma peritumoral stroma is induced by ovary carcinoma cells and affects both cancer cell proliferation and adhesion to laminin-1 and fibronectin. *Lab Invest,* 83**,** 377-86.

VAN DEN BRULE, F. A., WALTREGNY, D. & CASTRONOVO, V. 2001. Increased expression of galectin-1 in carcinoma-associated stroma predicts poor outcome in prostate carcinoma patients. *J Pathol,* 193**,** 80-7.

VAN HINSBERGH, V. W. & KOOLWIJK, P. 2008. Endothelial sprouting and angiogenesis: matrix metalloproteinases in the lead. *Cardiovasc Res,* 78**,** 203-12.

VAN RY, P. M., WUEBBLES, R. D., KEY, M. & BURKIN, D. J. 2015. Galectin-1 Protein Therapy Prevents Pathology and Improves Muscle Function in the mdx Mouse Model of Duchenne Muscular Dystrophy. *Mol Ther,* 23**,** 1285-97.

VAN VUGT, E., VAN RIJTHOVEN, E. A., KAMPERDIJK, E. W. & BEELEN, R. H. 1996. Omental milky spots in the local immune response in the peritoneal cavity of rats. *Anat Rec,* 244**,** 235-45.

VAN ZIJL, F., KRUPITZA, G. & MIKULITS, W. 2011. Initial steps of metastasis: cell invasion and endothelial transmigration. *Mutat Res,* 728**,** 23-34.

VAS, V., FAJKA-BOJA, R., ION, G., DUDICS, V., MONOSTORI, E. & UHER, F. 2005. Biphasic effect of recombinant galectin-1 on the growth and death of early hematopoietic cells. *Stem Cells,* 23**,** 279-87.

VASUDEVAN, K. M., BARBIE, D. A., DAVIES, M. A., RABINOVSKY, R., MCNEAR, C. J., KIM, J. J., HENNESSY, B. T., TSENG, H., POCHANARD, P., KIM, S. Y., DUNN, I. F., SCHINZEL, A. C., SANDY, P., HOERSCH, S., SHENG, Q., GUPTA, P. B., BOEHM, J. S., REILING, J. H., SILVER, S., LU, Y., STEMKE-HALE, K., DUTTA, B., JOY, C., SAHIN, A. A., GONZALEZ-ANGULO, A. M., LLUCH, A., RAMEH, L. E., JACKS, T., ROOT, D. E., LANDER, E. S., MILLS, G. B., HAHN, W. C., SELLERS, W. R. & GARRAWAY, L. A. 2009. AKT-independent signaling downstream of oncogenic PIK3CA mutations in human cancer. *Cancer Cell,* 16**,** 21-32.

VETVICKA, V., VAGNER, J., BAUDYS, M., TANG, J., FOUNDLING, S. I. & FUSEK, M. 1993. Human breast milk contains procathepsin D--detection by specific antibodies. *Biochem Mol Biol Int,* 30**,** 921-8.

VETVICKA, V., VEKTVICKOVA, J. & FUSEK, M. 1994. Effect of human procathepsin D on proliferation of human cell lines. *Cancer Lett,* 79**,** 131-5.

VETVICKA, V., VETVICKOVA, J. & BENES, P. 2004. Role of enzymatically inactive procathepsin D in lung cancer. *Anticancer Res,* 24**,** 2739-43.

VETVICKA, V., VETVICKOVA, J. & FUSEK, M. 1998. Effect of procathepsin D and its activation peptide on prostate cancer cells. *Cancer Lett,* 129**,** 55-9.

VETVICKA, V., VETVICKOVA, J. & FUSEK, M. 1999. Anti-human procathepsin D activation peptide antibodies inhibit breast cancer development. *Breast Cancer Res Treat,* 57**,** 261-9.

VETVICKA, V., VETVICKOVA, J. & FUSEK, M. 2000. Role of procathepsin D activation peptide in prostate cancer growth. *Prostate,* 44**,** 1-7.

VETVICKA, V., VETVICKOVA, J., HILGERT, I., VOBURKA, Z. & FUSEK, M. 1997. Analysis of the interaction of procathepsin D activation peptide with breast cancer cells. *Int J Cancer,* 73**,** 403-9.

VIGNON, F., CAPONY, F., CHAMBON, M., FREISS, G., GARCIA, M. & ROCHEFORT, H. 1986. Autocrine growth stimulation of the MCF 7 breast cancer cells by the estrogen-regulated 52 K protein. *Endocrinology,* 118**,** 1537-45.

VON FIGURA, K. & HASILIK, A. 1986. Lysosomal enzymes and their receptors. *Annu Rev Biochem,* 55**,** 167-93.

WAJAPEYEE, N., KAPOOR, V., MAHALINGAM, M. & GREEN, M. R. 2009. Efficacy of IGFBP7 for treatment of metastatic melanoma and other cancers in mouse models and human cell lines. *Mol Cancer Ther,* 8**,** 3009-14.

WAJAPEYEE, N., SERRA, R. W., ZHU, X., MAHALINGAM, M. & GREEN, M. R. 2008. Oncogenic BRAF induces senescence and apoptosis through pathways mediated by the secreted protein IGFBP7. *Cell,* 132**,** 363-74.

WANDJI, S. A., GADSBY, J. E., BARBER, J. A. & HAMMOND, J. M. 2000. Messenger ribonucleic acids for MAC25 and connective tissue growth factor (CTGF) are inversely regulated during folliculogenesis and early luteogenesis. *Endocrinology,* 141**,** 2648-57.

WANG, G., CHEN, C., YANG, R., CAO, X., LAI, S., LUO, X., FENG, Y., XIA, X., GONG, J. & HU, J. 2013. p55PIK-PI3K stimulates angiogenesis in colorectal cancer cell by activating NF-kappaB pathway. *Angiogenesis,* 16**,** 561-73.

WANG, G., LI, N., ZHANG, L., ZHANG, L., ZHANG, Z. & WANG, Y. 2015. IGFBP7 promotes hemocyte proliferation in small abalone Haliotis diversicolor, proved by dsRNA and cap mRNA exposure. *Gene,* 571**,** 65-70.

WANG, K., JIANG, Y. Z., CHEN, D. B. & ZHENG, J. 2009. Hypoxia enhances FGF2- and VEGF-stimulated human placental artery endothelial cell proliferation: roles of MEK1/2/ERK1/2 and PI3K/AKT1 pathways. *Placenta,* 30**,** 1045-51.

WATSON, P., VASEN, H. F., MECKLIN, J. P., BERNSTEIN, I., AARNIO, M., JARVINEN, H. J., MYRHOJ, T., SUNDE, L., WIJNEN, J. T. & LYNCH, H. T. 2008. The risk of extra-colonic, extra-endometrial cancer in the Lynch syndrome. *Int J Cancer,* 123**,** 444-9.

WELCH, H. C., COADWELL, W. J., STEPHENS, L. R. & HAWKINS, P. T. 2003. Phosphoinositide 3-kinase-dependent activation of Rac. *FEBS Lett,* 546**,** 93-7.

WEN, J., LI, H. Z., JI, Z. G., GANG-YAN, W. & SHI, B. B. 2013. Simultaneous renal clear cell carcinoma and gastrointestinal stromal tumor in one case. *Urol Ann,* 5**,** 122-3.

WESTLEY, B. R. & MAY, F. E. 1996. Cathepsin D and breast cancer. *Eur J Cancer,* 32A**,** 15-24.

WHITE, N. M., MASUI, O., NEWSTED, D., SCORILAS, A., ROMASCHIN, A. D., BJARNASON, G. A., SIU, K. W. & YOUSEF, G. M. 2014. Galectin-1 has potential prognostic significance and is implicated in clear cell renal cell carcinoma progression through the HIF/mTOR signaling axis. *Br J Cancer,* 110**,** 1250-9.

WHITTEMORE, A. S., BALISE, R. R., PHAROAH, P. D., DICIOCCIO, R. A., OAKLEY-GIRVAN, I., RAMUS, S. J., DALY, M., USINOWICZ, M. B., GARLINGHOUSE-JONES, K., PONDER, B. A.,

BUYS, S., SENIE, R., ANDRULIS, I., JOHN, E., HOPPER, J. L. & PIVER, M. S. 2004. Oral contraceptive use and ovarian cancer risk among carriers of BRCA1 or BRCA2 mutations. *Br J Cancer,* 91**,** 1911-5.

WINIARSKI, B. K., ACHESON, N., GUTOWSKI, N. J., MCHARG, S. & WHATMORE, J. L. 2011. An improved and reliable method for isolation of microvascular endothelial cells from human omentum. *Microcirculation,* 18**,** 635-45.

WINIARSKI, B. K., COPE, N., ALEXANDER, M., PILLING, L. C., WARREN, S., ACHESON, N., GUTOWSKI, N. J. & WHATMORE, J. L. 2014. Clinical Relevance of Increased Endothelial and Mesothelial Expression of Proangiogenic Proteases and VEGFA in the Omentum of Patients with Metastatic Ovarian High-Grade Serous Carcinoma. *Transl Oncol,* 7**,** 267-276 e4.

WINIARSKI, B. K., WOLANSKA, K. I., RAI, S., AHMED, T., ACHESON, N., GUTOWSKI, N. J. & WHATMORE, J. L. 2013. Epithelial ovarian cancer-induced angiogenic phenotype of human omental microvascular endothelial cells may occur independently of VEGF signaling. *Transl Oncol,* 6**,** 703-14.

WOLF, M., CLARK-LEWIS, I., BURI, C., LANGEN, H., LIS, M. & MAZZUCCHELLI, L. 2003. Cathepsin D specifically cleaves the chemokines macrophage inflammatory protein-1 alpha, macrophage inflammatory protein-1 beta, and SLC that are expressed in human breast cancer. *Am J Pathol,* 162**,** 1183-90.

WOO, J. T., YAMAGUCHI, K., HAYAMA, T., KOBORI, T., SIGEIZUMI, S., SUGIMOTO, K., KONDO, K., TSUJI, T., OHBA, Y., TAGAMI, K. & SUMITANI, K. 1996. Suppressive effect of N-(benzyloxycarbonyl)-L-phenylalanyl-L-tyrosinal on bone resorption in vitro and in vivo. *Eur J Pharmacol,* 300**,** 131-5.

WYMANN, M. P., ZVELEBIL, M. & LAFFARGUE, M. 2003. Phosphoinositide 3-kinase signalling--which way to target? *Trends Pharmacol Sci,* 24**,** 366-76.

XIE, H., PALLERO, M. A., GUPTA, K., CHANG, P., WARE, M. F., WITKE, W., KWIATKOWSKI, D. J., LAUFFENBURGER, D. A., MURPHY-ULLRICH, J. E. & WELLS, A. 1998. EGF receptor regulation of cell motility: EGF induces disassembly of focal adhesions independently of the motility-associated PLCgamma signaling pathway. *J Cell Sci,* 111 (Pt 5)**,** 615-24.

XU, L., YONEDA, J., HERRERA, C. & AL, E. 2000. Inhibition of malignant ascites and growth of human ovarian carcinoma by oral administration of a potent inhibitor of the vascular endothelial growth factor receptor tyrosine kinases. *International journal of clinical oncology,* 16**,** 445-454.

XU, X., GREENLAND, J., BALUK, P., ADAMS, A., BOSE, O., MCDONALD, D. M. & CAUGHEY, G. H. 2013. Cathepsin L protects mice from mycoplasmal infection and is essential for airway lymphangiogenesis. *Am J Respir Cell Mol Biol,* 49**,** 437-44.

XUE, G. & HEMMINGS, B. A. 2013. PKB/Akt-dependent regulation of cell motility. *J Natl Cancer Inst,* 105**,** 393-404.

YAMANAKA, Y., WILSON, E. M., ROSENFELD, R. G. & OH, Y. 1997. Inhibition of insulin receptor activation by insulin-like growth factor binding proteins. *J Biol Chem,* 272**,** 30729-34.

YANG, J., CRON, P., GOOD, V. M., THOMPSON, V., HEMMINGS, B. A. & BARFORD, D. 2002. Crystal structure of an activated Akt/protein kinase B ternary complex with GSK3-peptide and AMP-PNP. *Nat Struct Biol,* 9**,** 940-4.

YANG, J., WU, Z., RENIER, N., SIMON, D. J., URYU, K., PARK, D. S., GREER, P. A., TOURNIER, C., DAVIS, R. J. & TESSIER-LAVIGNE, M. 2015. Pathological axonal death through a MAPK cascade that triggers a local energy deficit. *Cell,* 160**,** 161-76.

YANG, X. F., YIN, Y. & WANG, H. 2008. VASCULAR INFLAMMATION AND ATHEROGENESIS ARE ACTIVATED VIA RECEPTORS FOR PAMPs AND SUPPRESSED BY REGULATORY T CELLS. *Drug Discov Today Ther Strateg,* 5**,** 125-142.

YANG, Z. & COX, J. L. 2007. Cathepsin L increases invasion and migration of B16 melanoma. *Cancer Cell Int,* 7**,** 8.

YASUDA, Y., TSUKUBA, T., OKAMOTO, K., KADOWAKI, T. & YAMAMOTO, K. 2005. The role of the cathepsin E propeptide in correct folding, maturation and sorting to the endosome. *J Biochem,* 138**,** 621-30.

YAU, J. W., TEOH, H. & VERMA, S. 2015. Endothelial cell control of thrombosis. *BMC Cardiovasc Disord,* 15**,** 130.

YEUNG, T. L., LEUNG, C. S., YIP, K. P., AU YEUNG, C. L., WONG, S. T. & MOK, S. C. 2015. Cellular and molecular processes in ovarian cancer metastasis. A Review in the Theme: Cell and Molecular Processes in Cancer Metastasis. *Am J Physiol Cell Physiol,* 309**,** C444-56.

YOON, Y. J., KIM, D. K., YOON, C. M., PARK, J., KIM, Y. K., ROH, T. Y. & GHO, Y. S. 2014. Egr-1 activation by cancer-derived extracellular vesicles promotes endothelial cell migration via ERK1/2 and JNK signaling pathways. *PLoS One,* 9**,** e115170.

YOSHINARI, M. & TAUROG, A. 1985. Lysosomal digestion of thyroglobulin: role of cathepsin D and thiol proteases. *Endocrinology,* 117**,** 1621-31.

YUAN, H. T., VENKATESHA, S., CHAN, B., DEUTSCH, U., MAMMOTO, T., SUKHATME, V. P., WOOLF, A. S. & KARUMANCHI, S. A. 2007. Activation of the orphan endothelial receptor Tie1 modifies Tie2-mediated intracellular signaling and cell survival. *FASEB J,* 21**,** 3171-83.

ZENG, X., XU, H. & GLAZER, R. I. 2002. Transformation of mammary epithelial cells by 3-phosphoinositide-dependent protein kinase-1 (PDK1) is associated with the induction of protein kinase Calpha. *Cancer Res,* 62**,** 3538-43.

ZHANG, L., WEI, L., SHEN, G., HE, B., GONG, W., MIN, N., ZHANG, L., DUAN, Y., XIE, J., LUO, H. & GAO, X. 2015. Cathepsin L is involved in proliferation and invasion of ovarian cancer cells. *Mol Med Rep,* 11**,** 468-74.

ZHANG, P., ZHANG, P., SHI, B., ZHOU, M., JIANG, H., ZHANG, H., PAN, X., GAO, H., SUN, H. & LI, Z. 2014a. Galectin-1 overexpression promotes progression and chemoresistance to cisplatin in epithelial ovarian cancer. *Cell Death Dis,* 5**,** e991.

ZHANG, P. F., LI, K. S., SHEN, Y. H., GAO, P. T., DONG, Z. R., CAI, J. B., ZHANG, C., HUANG, X. Y., TIAN, M. X., HU, Z. Q., GAO, D. M., FAN, J., KE, A. W. & SHI, G. M. 2016. Galectin-1 induces hepatocellular carcinoma EMT and sorafenib resistance by activating FAK/PI3K/AKT signaling. *Cell Death Dis,* 7**,** e2201.

ZHANG, Q. X., MAGOVERN, C. J., MACK, C. A., BUDENBENDER, K. T., KO, W. & ROSENGART, T. K. 1997. Vascular endothelial growth factor is the major angiogenic factor in omentum: mechanism of the omentum-mediated angiogenesis. *J Surg Res,* 67**,** 147-54.

ZHANG, W., WANG, S., WANG, Q., YANG, Z., PAN, Z. & LI, L. 2014b. Overexpression of cysteine cathepsin L is a marker of invasion and metastasis in ovarian cancer. *Oncol Rep,* 31**,** 1334-42.

ZHAO, B., LIU, J. Q., ZHENG, Z., ZHANG, J., WANG, S. Y., HAN, S. C., ZHOU, Q., GUAN, H., LI, C., SU, L. L. & HU, D. H. 2016a. Human amniotic epithelial stem cells promote wound healing by facilitating migration and proliferation of keratinocytes via ERK, JNK and AKT signaling pathways. *Cell Tissue Res,* 365**,** 85-99.

ZHAO, W., WANG, J., ZHU, B., DUAN, Y., CHEN, F., NIAN, W., SUN, J., ZHANG, B., TONG, Z. & CHEN, Z. 2016b. IGFBP7 functions as a potential lymphangiogenesis inducer in non-small cell lung carcinoma. *Oncol Rep,* 35**,** 1483-92.

ZHENG, Z. & LIU, Z. 2006. CD151 gene delivery activates PI3K/Akt pathway and promotes neovascularization after myocardial infarction in rats. *Mol Med,* 12**,** 214-20.

ZHONG, Z., GU, H., PENG, J., WANG, W., JOHNSTONE, B. H., MARCH, K. L., FARLOW, M. R. & DU, Y. 2016. GDNF secreted from adipose-derived stem cells stimulates VEGF-independent angiogenesis. *Oncotarget,* 7**,** 36829-36841.

ZHOU, B. P., LIAO, Y., XIA, W., SPOHN, B., LEE, M. H. & HUNG, M. C. 2001. Cytoplasmic localization of p21Cip1/WAF1 by Akt-induced phosphorylation in HER-2/neu-overexpressing cells. *Nat Cell Biol,* 3**,** 245-52.

ZHOU, Y., TU, C., ZHAO, Y., LIU, H. & ZHANG, S. 2016. Placental growth factor enhances angiogenesis in human intestinal microvascular endothelial cells via PI3K/Akt pathway:

Potential implications of inflammation bowel disease. *Biochem Biophys Res Commun,* 470**,** 967-74.

ZHU, L., WADA, M., USAGAWA, Y., YASUKOCHI, Y., YOKOYAMA, A., WADA, N., SAKAMOTO, M., MAEKAWA, T., MIYAZAKI, R., YONENAGA, E., KIYOMATSU, M., MURATA, M. & FURUE, M. 2013. Overexpression of cathepsin D in malignant melanoma. *Fukuoka Igaku Zasshi,* 104**,** 370-5.

ZUHLSDORF, M., IMORT, M., HASILIK, A. & VON FIGURA, K. 1983. Molecular forms of beta-hexosaminidase and cathepsin D in serum and urine of healthy subjects and patients with elevated activity of lysosomal enzymes. *Biochem J,* 213**,** 733-40.

ZUZARTE-LUIS, V., MONTERO, J. A., KAWAKAMI, Y., IZPISUA-BELMONTE, J. C. & HURLE, J. M. 2007a. Lysosomal cathepsins in embryonic programmed cell death. *Dev Biol,* 301**,** 205-17.

ZUZARTE-LUIS, V., MONTERO, J. A., TORRE-PEREZ, N., GARCIA-PORRERO, J. A. & HURLE, J. M. 2007b. Cathepsin D gene expression outlines the areas of physiological cell death during embryonic development. *Dev Dyn,* 236**,** 880-5.